

Lawrence Berkeley National Laboratory

Recent Work

Title

ABSTRACTS. 5TH INTERNATIONAL CONFERENCE ON SOLID STATE IONICS, LAKE TAHOE, AUGUST 18-24, 1985.

Permalink

<https://escholarship.org/uc/item/98b0n83x>

Author

Lawrence Berkeley National Laboratory

Publication Date

1985-09-09

LBL-20000
August 1985

ABSTRACTS

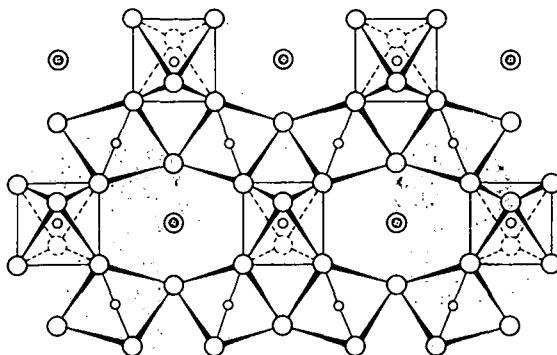
RECEIVED
LAWRENCE
BERKELEY LABORATORY

SEP 9 1985

LIBRARY AND
DOCUMENTS SECTION



5TH INTERNATIONAL CONFERENCE ON SOLID STATE IONICS



Lake Tahoe
USA
AUGUST 18-24, 1985



Lawrence Berkeley Laboratory
University of California
Berkeley, California 94720

TWO-WEEK LOAN COPY
This is a Library Circulating Copy
which may be borrowed for two weeks.

LBL-20000
e-2

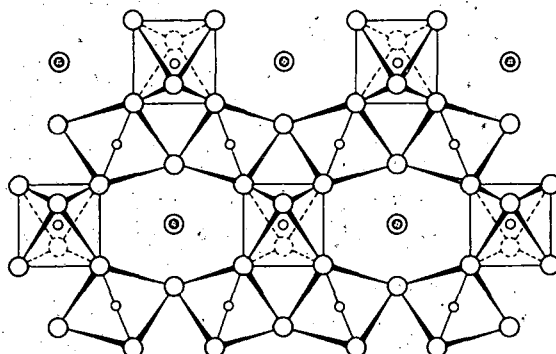
DISCLAIMER

This document was prepared as an account of work sponsored by the United States Government. While this document is believed to contain correct information, neither the United States Government nor any agency thereof, nor the Regents of the University of California, nor any of their employees, makes any warranty, express or implied, or assumes any legal responsibility for the accuracy, completeness, or usefulness of any information, apparatus, product, or process disclosed, or represents that its use would not infringe privately owned rights. Reference herein to any specific commercial product, process, or service by its trade name, trademark, manufacturer, or otherwise, does not necessarily constitute or imply its endorsement, recommendation, or favoring by the United States Government or any agency thereof, or the Regents of the University of California. The views and opinions of authors expressed herein do not necessarily state or reflect those of the United States Government or any agency thereof or the Regents of the University of California.

ABSTRACTS



**5TH
INTERNATIONAL
CONFERENCE ON
SOLID STATE
IONICS**



**Lake Tahoe
USA
AUGUST 18-24, 1985**



Lawrence Berkeley Laboratory
University of California
Berkeley, California 94720

**INTERNATIONAL
SCIENTIFIC COMMITTEE**

- J. B. Bates** - Oak Ridge National Laboratory, USA
E. Budevski - Central Laboratory of Electrochemical
Power Sources, Bulgaria
S. Chandra - Banaras Hindu University, India
W. Dieterich - Konstanz University, W. Germany
G. C. Farrington - University of Pennsylvania, USA
P. Hagenmuller - CNRS Bordeaux, France
M. Kleitz - INP. CNRS Grenoble, France
B. B. Owens - Medtronix, Inc., USA
B. Sapoval - Ecole Polytechnique, Palaiseau, France
J. Schoonman - Utrecht University, Netherlands
H. Schulz - University of Munchen, W. Germany
B. Scrosati - University of Rome, Italy
B. C. H. Steele - Imperial College, London, UK
T. Takahashi - Nagoya, Japan
U. Von Alpen - Varta Batteries AG., W. Germany
C. A. Vincent - St. Andrews University, UK
W. Weppner - Max Planck, Stuttgart, W. Germany

CO-CHAIRMEN

James B. Boyce, Xerox Palo Alto
Research Center
Palo Alto, CA 94394, USA

Lutgard C. De Jonghe
Materials and Molecular Research Division
Lawrence Berkeley Laboratory
Berkeley, CA 94720, USA

Robert A. Huggins
Department of Materials Science and Engineering
Stanford University
Stanford, CA 94305, USA

LBL CONFERENCE COORDINATOR

Peggy Little
Lawrence Berkeley Laboratory
Berkeley, CA 94720, USA
(415) 486-6386; FTS: 451-6386

ABSTRACTS OF PLENARY LECTURES

PS/A-1	D.W. Murphy	Insertion Reaction Electrode Materials
PS/A-2	H. Schulz	Application of Diffraction Methods to Study Fast Ionic Conductors
PS/B-1	M. Armand	Polymer Electrolytes
PS/B-2	P. Vashishta	Use of Computer Simulation Techniques to Study Atomic Migration in Solids
PS/C-1	A. Clearfield	Stoichiometry, Structure and Conductivity of Nasicon
PS/C-2	B. Sapoval	Dynamics of the Creation of Fractal Objects by Intercalation
PS/D-1	B. Dunn	Recent Developments in Beta Aluminas
PS/D-2	I. Raistrick	The Application of Impedance Spectroscopy to Problems in Solid State Ionics
PS/E-1	P. Heitjans	Use of Beta Radiation-Detected NMR to Study Ionic Motion in Solids
PS/E-2	S. Liu	AC Response of Fractal Interfaces
PS/F-1	C.A. Angell	Recent Developments in Fast Ion Transport in Glassy and Amorphous Materials
PS/F-2	P. Dickens	Hydrogen Insertion Compounds of Transition Metal Oxides
PS/G-1	M. Kleitz	Solid Ionic Conductors in Chemical Sensors
PS/G-2	F. Salzano	Application of Solid Oxide Electrolytes to Water Vapor Electrolysis

Insertion Reaction Electrode Materials

D. W. Murphy

AT&T Bell Laboratories
600 Mountain Avenue
Murray Hill, New Jersey 07974

The variety of materials that undergo reversible redox intercalation reactions will be reviewed with a concentration on structural aspects. Comparisons between different polytypes of the same overall composition such as layered, cubic, and amorphous TiS_2 and rutile, anatase, (B), and spinel TiO_2 , will be discussed to illustrate the importance of structural features on lithium insertion. The effect of structural changes on the reversibility of insertion reactions will be illustrated using ReO_3 related shear structures as examples.

P 1

APPLICATION OF DIFFRACTION METHODS TO STUDY FAST IONIC CONDUCTORS

Heinz Schulz, Institut für Kristallographie und Mineralogie, Universität München

Diffraction experiments with X-rays or neutrons allow to measure the positions, the form and the intensities of Bragg reflections and to measure intensities in the reciprocal space between the Bragg reflections (Zwischenreflex-Streuung). The intensities of the Bragg reflections can be used to investigate the average structure of a crystalline ionic conductor. The average structure shows: Positions of the framework- and mobile ions, occupation probabilities of the positions, directions and magnitudes of thermal vibrations, diffusion paths of the mobile ions. The form of the Bragg reflections is influenced by local distortions, arrangements of grain boundaries and so on, which may be important for the ionic transport mechanism. The "Zwischenreflex-Streuung" may show strong features. In this case short range order effects, e.g. domain formations, may be present. Examples for these kinds of investigations will be presented for the fast ionic conductors based on the NASICON and fluorite structure.

München, 5. July 1985

Polymer Electrolytes

M. Armand

Laboratoire d'Energétique Electrochimique CNRS LA 265
B.75 -38402 SAINT MARTIN D'HERES - FRANCE

**

Examples of polymer-salt complexes formation are rapidly growing, as an international effort is aimed at the understanding and improvement of solvent-free electrolytes for battery applications.

On one hand, PEO remains the archetype of the solvating-backbone polymers, and its complexing power was found to extend well beyond the alkali-metal salts. For instance, all the alkaline-earth salts with I^- and ClO_4^- dissolve in PEO, (1) showing that the free energy for solvation of the cation is always favorably negative, and the complex formation is solely governed by the charge dispersion of the counter-anion. However, the "hard" donor properties of the ether oxygens cannot compete in the case of "soft" ions interactions; neither AgI or PbI_2 form complexes, while the corresponding ClO_4^- salts do. This high complexing ability is also found in other polymers which grafted short-chain PEO synthons, like in the poly(phosphazenes) (2).

On the other hand, only scarce examples of complexes including multi-charged anions are known, as the restriction on charge density becomes increasingly difficult to meet.

It is now well established that the ionic conduction only takes place when segmental chain motion is present (3). As a consequence of this quasi-liquid behavior, there is no selectivity in ionic motion, both anions and cations being mobile. Elucidation of the conduction mechanism and the choice of techniques for the measurement of the transport properties must be done very cautiously as the Nernst-Einstein equation is not always valid in these low-dielectric constant compounds.

It is relatively easy to block the cationic conductivity to obtain $t^+ = 1$ electrolytes, as in $PEO-Mg(ClO_4)_2$ (4), but attempts to prepare a $t^+ = 1$ complex important for most electrochemical applications has been so far moderately successful; binding the anions to another polymer results, up to now, in poorly conducting compounds (5). Results with Nafion-PEO alloys shall be presented. Also, the attachment of an anionic complex to the PEO backbone through a donor-acceptor bond does not warrant an electrochemical stability window large enough for lithium metal utilization.

So far, the simple $LiClO_4$ or $LiCF_3SO_3$ complexes, despite their low cationic transference number, have been successfully used in batteries, provided that the back-diffusion of the salt concentration gradient is fast enough at the temperature of operation.

- (1) J.M. CHABAGNO Thèse University of Grenoble (1980).
- (2) P.M. BLONSKY, D.F. SHRIVER ECS Spring Meeting, Abstract # 77, Toronto, Canada, May 12-17, (1985).
- (3) C. BERTHIER, W. GORECKI, M. MINIER, M.ARMAND, P. RIGAUD, J.M. CHABAGNO Solid State Ionics 11-1, 91 (1983).
- (4) A. GANDINI, J.F. LE NEST, M. LEVEQUE, H. CHERADAME Proceedings of the Rolduc Polymer Meeting The Netherlands, April (1985).
- (5) D.J. BANNISTER, G.R. DAVIES, I.M. WARD, J.E. McINTYRE Polymer 25 1291 (1984).

USE OF COMPUTER SIMULATION TECHNIQUES
TO STUDY ATOMIC MIGRATION IN SOLIDS

by

Priya Vashishta

Solid State Science Division
Argonne National Laboratory
9700 South Cass Avenue
Argonne, IL 60439

No Abstract Available

STOICHIOMETRY, STRUCTURE AND CONDUCTIVITY OF NASICON

A. Clearfield, M. A. Subramanian, P. R. Rudolf and A. Moini
 Department of Chemistry
 Texas A&M University
 College Station, Texas 77843

NASICON was originally formulated¹ as a member of the solid solution series $\text{Na}_{1+x}\text{Zr}_2\text{Si}_x\text{P}_{3-x}\text{O}_{12}$, with $x = 2$. Difficulty has been experienced in preparing this composition from high temperature solid state reactions and some ZrO_2 consistently remains unreacted. We have found that this is not the case if some Sc^{3+} is substituted for Zr^{4+} and have prepared solids of composition $\text{Na}_x\text{ScZrSiP}_2\text{O}_{12}$ (rhombohedral) and $\text{Na}_x\text{Sc}_{0.5}\text{Zr}_{1.5}\text{Si}_{1.5}\text{P}_{1.5}\text{O}_{12}$ (monoclinic). The structure of these phases was determined from X-ray powder data and refinement of occupancy factors confirmed the stoichiometry. NASICON prepared by a hydrothermal route, followed by calcination, yielded a single phase of composition $\text{Na}_{1.5}\text{Zr}_{1.5}\text{Si}_{1.5}\text{P}_{1.5}\text{O}_{11.5}$. A similar structure determination by both X-ray and neutron diffraction methods on this non-stoichiometric material revealed that about 0.33Na^+ was located in the Zr^{4+} sites reducing the Zr^{4+} occupancy to 1.67.

Sol-gel preparations of stoichiometric NASICON with $x = 2$ were found to precipitate ZrO_2 at 1150°C whereas similar sol-gel preparations of the non-stoichiometric phase were stable to at least 1200°C . Neutron diffraction on the stoichiometric phase, before and after precipitation of ZrO_2 , was carried out and will be described. It is suggested that the stoichiometry of NASICON is dependent upon the method of preparation and both stoichiometric and non-stoichiometric varieties are possible.^{2,3}

1. H. Y-P. Hong, Mat. Res. Bull 11, 173 (1976).
2. A. Clearfield, Solid State Ionics 9/10, 832 (1983).
3. A. Clearfield, M. A. Subramanian, W. Wang and P. Jerus, Solid State Ionics 9/10, 895 (1983).

DYNAMICS OF THE CREATION OF
 FRACTAL OBJECTS BY INTERCALATION

B. SAPOVAL, M. ROSSO, J.F. GOUYET and J.F. COLONNA
 Ecole Polytechnique, 91128 Palaiseau Cedex (France)

We present a video picture which shows the dynamics of diffusion or intercalation on a 2D square lattice. The images of that film are obtained from a simulation of diffusion in a simple lattice gas model. The static images show the fractal geometry of the diffusion or intercalation front. Different magnifications of the diffusion front exhibits the self similarity which is characteristic of the fractal geometry.

The visual observation of the dynamics of diffusion exhibit a new effect : the dynamic changes of the topography of the objects are erratic : strong changes in the geometry happens at random times. These dynamics changes are produced on a semi-macroscopic scale.

RECENT DEVELOPMENTS IN β'' ALUMINAS

B. Dunn
 Department of Materials Science and Engineering
 University of California
 Los Angeles, CA 90024

The phenomenon of high cationic conductivity in solids has been largely confined to materials which transport monovalent cations such as Na^+ , Li^+ , K^+ , Ag^+ and Cu^+ . In recent years, however, studies of divalent and trivalent β'' aluminas have demonstrated that fast-ion transport in solids can occur with many different cations. These multivalent β'' aluminas appear to be the first family of crystalline solids to support the rapid diffusion of divalent or trivalent cations at moderate temperatures. Furthermore, these compounds exhibit a number of interesting optical properties.

Transport properties have been investigated using a variety of approaches including ionic conductivity, tracer diffusion and spectroscopic mapping techniques. The conductivity for most divalent β'' aluminas is at least $10^{-3} \text{ ohm}^{-1} \text{ cm}^{-1}$ at 300°C and greatly exceeds the values reported for any other divalent solid electrolyte in this temperature range. The trivalent β'' aluminas are more resistive ($\sim 10^{-4} \text{ ohm}^{-1} \text{ cm}^{-1}$ at 400°C) but are, nonetheless, the first solid electrolytes for trivalent cations. Structural studies complement the transport measurements and an understanding of ion/vacancy relationships is beginning to emerge. The unique ion arrangements observed for Pb^{2+} in β'' alumina are believed to be important in establishing why the conductivity of Pb^{2+} β'' alumina is comparable to that of Na^+ β'' alumina at 25°C . There is considerable evidence of short-range correlation effects for most of the other divalent isomorphs. Less information is available for the trivalent compounds, although indications are that lanthanide ions serve as very sensitive optical probes of the conduction plane.

The ability to readily incorporate trivalent cations has led to the investigation of the optical properties of lanthanide β'' aluminas. Nd^{3+} β'' alumina is particularly interesting. It exhibits several significant effects including an anomalously strong optical absorption, a long fluorescence lifetime and lasing action in both pulsed and c.w. modes. The other lanthanide compositions have not been investigated in detail, but generally display rather strong fluorescence. The ion exchange techniques used to introduce the lanthanide ions are very attractive for optical materials because of the ability to control the concentration and the valence state of the optically active ions. Thus, in addition to the unique fast-ion transport properties of multivalent β'' aluminas, there is substantial interest in these compounds as novel phosphors and solid state laser hosts.

THE APPLICATION OF IMPEDANCE SPECTROSCOPY TO PROBLEMS
IN SOLID STATE IONICS

Ian D. Raistrick
 Electronics Division, MS D429
 Los Alamos National Laboratory
 Los Alamos, NM 87545

The applications of complex impedance measurements to solid-state electrochemical systems are reviewed. The electrical response of simple bulk processes such as dielectric relaxation, conductivity, and diffusion is well understood, but the extension of the theory to disordered systems, such as glasses, polycrystalline, and composite media is less well developed. Interpretations of empirical models for impedance spectra in terms of distributions of relaxation times or transport in random environments are discussed.

Impedance spectroscopy is also a useful method for examining electrochemical interfaces, both in the presence and absence of a Faradaic current. Detailed information about the kinetics and thermodynamics of elementary processes, such as charge transfer and adsorption, may be deduced. Again, results in real systems, as found, for example, at rough or porous electrode/electrolyte interfaces, are significantly more complex than expected from simple models. The role of frequency dependent current distributions in impedance methods is discussed.

USE OF BETA RADIATION-DETECTED NMR TO STUDY IONIC MOTION IN SOLIDS

Paul Heitjans

Fachbereich Physik, Universität Marburg, D-3550 Marburg, FRG

The method of beta radiation-detected nuclear magnetic resonance (β -NMR) is introduced and its features and capabilities as a new tool for studying ionic motions on a microscopic scale are discussed, partly in comparison with conventional NMR. Information on ion dynamics is obtained from spin-lattice relaxation rates and resonance spectra of isolated β -active nuclei embedded in the sample. The polarised probe nuclei are produced by a nuclear reaction. Their polarisation is monitored via the anisotropy of the β -radiation distribution.

Recent applications to the field of solid state ionics are reviewed. As examples of β -NMR on solids with a layer structure measurements on the intercalation compound LiC_6 and the ionic conductor Li_3N are discussed. Emphasis is on the questions of anisotropic and low-dimensional diffusion. We further discuss lithium borate and silicate glasses as representatives of strongly disordered solids. Different modes of ionic motion were found by spin-relaxation measurements over wide temperature and magnetic field ranges. We mainly deal with the low-temperature data which reflect the influence of defect centres typical of glasses.

AC RESPONSE OF FRACTAL INTERFACES

S.H. Liu and T. Kaplan
Solid State Division, Oak Ridge National Laboratory
Oak Ridge, TN 37831

and

L.J. Gray
Engineering Physics and Mathematics Division
Oak Ridge National Laboratory, Oak Ridge, TN 37831

ABSTRACT

When a small ac signal passes through the interface between a metal electrode and an aqueous or solid electrolyte, the current is expected to encounter ohmic resistances in both substances and a capacitance across the interface. In reality, however, such an RC circuit often does not give an adequate description of the ac response of the interface. It is sometimes necessary to include a so-called constant-phase-angle element whose impedance has the form $Z = (j\omega)^{-n}$, where ω is the angular frequency, $j = \sqrt{-1}$, and $0 < n < 1$. In recent years it has been demonstrated by many authors that the parameter n is intimately related to surface roughness, with n approaching unity when the surface is made increasingly smooth. We propose to model the rough interface by a fractal called Cantor bar. The equivalent circuit of the model has the property of the constant-phase-angle element with an exponent $n = 3 - d_s$, where d_s is the Hausdorff dimension of the model interface, $2 < d_s < 3$. For a smooth surface $d_s = 2$ and thus $n = 1$ is seen experimentally. The model can be made more realistic if the branching and the scaling are random variables. The frequency exponent of the impedance n and the fractal dimension of the surface d_s are found to satisfy the same relation, i.e. $n = 3 - d_s$. Thus, we speculate that this relation may be correct for all rough interfaces which have the fractal geometry.

*Research sponsored by the Division of Materials Sciences, U.S. Department of Energy under contract DE-AC05-84OR21400 with Martin Marietta Energy Systems, Inc.

RECENT DEVELOPMENTS IN FAST ION TRANSPORT
IN GLASSY AND AMORPHOUS MATERIALSC.A. Angell
Department of Chemistry
Purdue University
West Lafayette, IN 47907

We review new developments in the expanding phenomenology of amorphous solid electrolytes. We consider separately a) the vitreous materials in which the charge carriers are highly decoupled from the supporting matrix, and b) the electrolyte polysolutions in which the charge carriers are coupled to, and move cooperatively with, a locally fluid (though globally elastic) matrix.

In the vitreous cases, new methods of preparation, including vapor deposition and sol-gel processes, are allowing exploration of compositions in previously inaccessible regions, and of new vitreous "states" within known composition regions. Also, use of new heavy element oxide and chalcogenide matrixes with lower glass transition temperatures has yielded improved ambient temperature conductivities with conventionally prepared glasses. The highest conductivities are still obtained with Ag⁺- and Cu⁺- containing glasses. New Ag⁺ glasses containing only halide anions yield $\sigma(25^\circ\text{C}) = 0.047 \text{ ohm}^{-1}\text{cm}^{-1}$, even higher than for the AgI + oxyanion-containing materials. Fast anion-conducting (F⁻, Cl⁻), and possibly fast-divalent cation-conducting (Pb²⁺) glasses have been developed. We emphasize the importance of studying the fast ion motions by mechanical response in addition to electrical response measurements. Data on several systems are now available from low frequency tensile, ultrasonic, and hypersonic (Brillouin light scattering) techniques covering ten decades of frequency. These show that the mechanical response has the same average time constant as the electrical, and the same activation energy but quite different spectral widths (relaxation time distributions). The attempt frequency for each corresponds to the quasi-lattice vibration frequency observed in the far IR absorption spectrum. Of special importance is the observation that the change

in mechanical modulus due to relaxation of the fast ions, decreases with increasing temperature. This seems incompatible with weak electrolyte models which require the number of displaceable ions to increase with increasing temperatures.

In the electrolyte polysolution field, new polymeric solvents with more flexible backbones, hence lower "local" viscosities at ambient temperatures, have been developed. The "solid" electrolytes based on these show behavior which is fully predictable from models developed for ordinary concentrated electrolyte solutions. To elucidate the ion-solvent coupling we examine the correlation of conductivity relaxation times with the "local" structural (viscoelastic) relaxation times probed by dynamic mechanical and light scattering techniques.

HYDROGEN INSERTION COMPOUNDS OF TRANSITION METAL OXIDES

P. G. Dickens and S. Crouch-Baker

Abstract

Many transition metal oxides (and oxide hydrates) $MO_n \cdot mH_2O$ ($m = 0, 1, 2$) react at ambient temperature with dissociated hydrogen to form non-stoichiometric hydrogen insertion compounds $H_xMO_n \cdot mH_2O$ which exhibit unusual electronic and structural features. In this paper the structure, bonding and proton mobility in compounds of this type are examined.

SOLID IONIC CONDUCTORS IN CHEMICAL SENSORS

M. KLEITZ, P. FABRY, J.F. MILLION-BRODAZ, E. SIEBERT-MANTEL

Interest in sensors is rapidly growing because of increasing demand for more efficient industrial production, for environment monitoring and for analysis. Robots and partially automated consumer goods such as automobiles and appliances need sensors. Another driving force is the decreasing cost of small computers which can be associated with imperfect sensors to form practical "intelligent" measuring systems.

Pure ionic and mixed conductors can be implemented in various types of chemical sensors. At present, in most cases, pure ionic conductors (solid electrolytes) are used as sensitive membranes in potentiometric cells. Basic technologies differ depending on whether the analyzed species is ionic or neutral (and whether the "solvent" of the neutral species is electrically insulating or conducting). The small additional electronic conductivity of the solid electrolytes, which is a constant concern in neutral species sensors, is, in principle, not detrimental in ion sensors. Even mixed conductors can be used. Here the risk is possible interference with redox couples probing. Among the various solid electrolytes, crystallized materials are less attractive in terms of technological implementation. On the other hand, they are likely to offer improved selectivity.

Of course, solid state conductors are preferably used in all-solid-state devices. They have several advantages over liquid-containing sensors. For medical and food industry applications they can be thermally sterilized. Another promising advantage is their ability to be miniaturized and therefore integrated with appropriate electronics. Various ChemFETS, ISFETS, GasFETS, have already been tested.

Other cells and other operation modes have been envisaged and implemented. Some devices are operated under constant voltage in a polarographic-like mode. The resulting current is a measurement of the diffusion-limited supply of the analyzed species. Various materials can be used in thin layers as conductivity-sensitive sensors. Intercalation compounds are certainly good candidates for this application. Others can form "ionic bridges" for improved internal references.

Of course, sensors can be associated with various pretreatments of the analyzed media (thermal, enzymatic...) and with ancillary devices (in the oxygen pump-gauge for instance) which extend their field of application.

Solid State Ionics can also contribute new ideas, and explanations, to the sensor field!! An example is the ionically-linked catalytic electrode.

APPLICATION OF SOLID OXIDE ELECTROLYTES TO WATER VAPOR ELECTROLYSIS*

F. J. Salzano
Department of Applied Science
Brookhaven National Laboratory
Upton, NY 11973

ABSTRACT

A substantial amount of energy is required to electrolyze liquid water for the production of hydrogen and oxygen. The energy required in this process decomposes water as well as converting the liquid to vapor. Thus, gains can be made by electrolysis of vapor and further gains made by carrying out the process at higher temperatures, where the free energy of formation of water is decreased. The thermodynamics of high temperature water vapor electrolysis are discussed. Various process considerations are examined in terms of the materials and engineering requirements in which one may make tradeoffs between thermal efficiency, cost and equipment utilization. Gains in efficiency over conventional liquid electrolysis processes can be greater than 40%. Process tradeoffs are discussed in terms of overall thermal efficiencies, voltage/thermal requirements, steam conversions and heat recovery. These analyses show some of the possible tradeoffs between plant complexity, voltage efficiency and show the insentive for continued research to identify improved alternative electrolytes and electrode materials for this application.

*This research was performed under the auspices of the U.S. Department of Energy under Contract No. DE-AC02-76CH00016.

EQUIVALENT CIRCUITS FOR REACTION/DIFFUSION
SEQUENCES AT THREE-PHASE ELECTRODES

Donald R. Franceschetti
Department of Physics
Memphis State University
Memphis, Tennessee 38152

In electrochemical gas sensors, pumps, and fuel cells, the electrode process generally involves the exchange of atoms between three phases: the electrolyte, a nominally inert electrode, and the gas phase. The rate of the electrode reaction can be dependent on the partial pressure of the active gas and may be limited by diffusion within any of the three phases or along the interface between any two phases. In the latter case diffusion may occur in parallel with an adsorption/desorption process.

Small-signal ac techniques are often employed to characterize the electrode processes at three-phase electrodes and a large number of equivalent circuits - involving resistive, capacitive, and Warburg or constant-phase-angle elements - have been employed to analyze the data. Although a number of the circuits so employed have been derived from well-defined models of the interface, other circuits have been chosen with only limited justification. In the present work, the formalism of complex, frequency-dependent rate constants, introduced by Lányi and developed by Macdonald and the author, is used to obtain equivalent circuits for a variety of three-phase electrodes in a systematic way. Special consideration is given to situations involving more than one significant diffusional process and to simultaneous diffusion and adsorption. Diffusion is examined in both cylindrical and linear geometries and the possibility of a distribution of electrode/electrolyte contact areas is treated in an approximate way. The circuits thus obtained involve a number of generalizations of the Warburg element, which are compared to both simple Warburg and constant-phase-angle behavior.

PARTICLE CORRELATIONS IN SILVER CHROMIUM
SULFIDE AND SELENIDE LAYERED COMPOUNDS

J. E. Hammerberg
Dept. of Physics
Virginia Commonwealth Univ.
Richmond, Virginia 23284

Recent measurements of diffuse X-ray scattering in AgCrS_2 have shown a 'liquid-like' radial distribution function for silver ions in the fast ion conducting regime¹. An approximate integral equation for these correlations is derived which takes into account the volume exclusion due to the geometry of conduction paths. Solutions for the averaged pair distribution function will be presented and the question of octahedral occupancy will be discussed.

(1) T. Hibma, Phys. Rev B28, 568 (1983)

Dynamic Bond Percolation and Effective-Medium Models for Ionic
Conduction in Polymer Electrolytes

Stephen D. Druger, A. Nitzan, and Mark A. Ratner
Department of Chemistry and Materials Research Center
Northwestern University, Evanston, IL 60201

Polymeric solid electrolytes, such as polyethylene oxide complexed with various salts, are nearly always studied above their glass transition temperatures, which means that while the bulk material is solid, the local motions are liquid-like, and the local geometry of the host material as seen by the conducting ions is changing rapidly.

Processes in which the carrier transport mechanism involves motion of the host medium on a timescale comparable to that of the carrier motion itself require generalization of the usual models based on carrier hopping in a static medium. Under the assumption that this concurrent motion of the host can be modeled by a random reassignment (or "renewal") of hopping probabilities, with a constant probability λ per unit time for renewal to occur, the effects of host motion on the frequency-dependent diffusion coefficient $D(\omega)$ have been considered, and the diffusion coefficient $D(\omega)$ with renewal has been shown to be obtainable from $D(\omega)$ without renewal through the formal substitution $i\omega \rightarrow \lambda + i\omega$. These results have then been employed to obtain expressions for the time-dependent mean-square displacement of carriers when renewal occurs in terms of the mean square displacement without renewal. Further approximation leads to analytic expressions for the frequency-dependent conductivity and dielectric function of the host-plus-carrier system. Comparison with recent experimental data then yields a reasonably good fit of theory to experiment.

These results have been extended by calculating the time-dependent mean-square displacement of carriers (possibly subjected to an intense electric field) using a coherent-medium approximation applied to the static bond percolation model, leading now to approximate expressions in terms of the percolation model parameters, rather than in terms of unspecified fitting parameters. Agreement has thereby been obtained with many of the features found in numerical simulations carried out concurrently with the present work.

The relations between static and dynamic bond percolation results have been employed to study further the effect of pathway renewal on ionic transport in two and three dimensions, leading to new insights into the frequency-dependent transport mechanisms observed experimentally in the polymer electrolytes. Applications to particular experiments, including microwave conductivity experiments on PEO systems and dielectric relaxation work on a number of polymeric electrolytes are discussed.

IONIC TRANSPORT IN ANION DEFICIENT FLUORITE OXIDES

A.N. Cormack and C.R.A. Catlow

Department of Chemistry, University College London, WC1H 0AJ, UK.

Anion deficient oxides with the fluorite (or fluorite related) structure are well known fast ion conductors, finding a wide range of technological uses.

Although the anion deficiency can arise through non-stoichiometry, e.g. CeO_{2-x} , it most commonly arises from doping with a lower valent cation such as Y^{3+} , Gd^{3+} , or Ca^{2+} , Mg^{2+} . Indeed, ZrO_2 is only stable in the fluorite structure with substantial concentrations of dopants.

It is clear that transport dominated processes such as ionic conductivity will be heavily influenced by interactions between dopant cations and their charge compensating anion vacancies.

In this presentation, we will show how one may highlight the relevant importance of these interactions using computer based theoretical methods. Our discussion will be based on a comparison of the behaviour of tetragonal and cubic zirconia, from which it will be seen that the simple idea of pair association may not always be appropriate. We will also show how vacancy transport in the pyrochlore $\text{Gd}_2\text{Zr}_2\text{O}_7$ (which is, structurally, closely related to fluorite) may be understood as a result of theoretical considerations.

The importance of adequate, and consistent, interatomic potential models is emphasised and the relationship of these interatomic potentials to structural properties such as ionic radius and cell parameter is also considered.

MODEL FOR THE COMPOSITION DEPENDENCE OF CONDUCTIVITY
OF AN IONIC CONDUCTOR CONTAINING SUBMICRON INSULATOR PARTICLES¹

J. C. Wang and N. J. Dudney
Solid State Division, Oak Ridge National Laboratory
Oak Ridge, Tennessee 37831

The ionic conductivity of several metal halides such as AgI and LiI can be enhanced by orders of magnitude by the addition of submicron particles of some insulators such as Al₂O₃.^{2,3} Generally, the conductivity $\sigma(c)$ increases with the volume fraction c of the insulator particles, goes through a maximum when c is between 0.1 and 0.5, and drops to the value of the insulator at $c=1$. It is believed that the enhancement is due to the existence of a high conductivity layer around each particle,^{3,4} but the mechanism of this is uncertain.⁵ In this work, we assume the existence of this high conductivity layer, calculate the composition dependence of the conductivity using a very simple model, and extract information about the structure of the high conductivity layer.

We assume that the insulator particles are cubic and are arranged on a simple cubic lattice embedded in the conducting material. The size of the cubes and the position dependent conductivity outside each cube are treated as parameters. The composite system is approximated with a resistor network, and its conductivity is calculated. It is found that the model can explain some of the reported σ vs c data quite well, and values of the parameters can be extracted from the fitting of these data.

Our results suggest that the high conductivity layer outside each insulator particle has the following structure: Very near the surface, the conductivity increases rapidly to a maximum value and then decreases to that of the conducting material far away from the surface. It is possible that this structure is a combined result of the position dependent charge carrier concentration and mobility.

¹Research sponsored by the Division of Materials Sciences, U.S. Department of Energy under contract DE-AC05-84OR21400 with Martin Marietta Energy Systems, Inc.

²C. C. Liang, J. Electrochem. Soc. **120**, 1289 (1973).

³J. B. Wagner, Jr., Mater. Res. Bull. **15**, 1691 (1980).

⁴A. M. Stoneham, E. Wade, and J. A. Kilner, Mater. Res. Bull. **14**, 661 (1979).

⁵N. J. Dudney, "Enhanced Ionic Conductivity in Composite Electrolytes," this conference.

NMR T_1 AND LINE NARROWING IN SUPERIONICS-
A CONSISTENT INTERPRETATION⁰

J.L. Bjorkstam, J. Listerud and M. Villa⁺
Department of Electrical Engineering
University of Washington, Seattle, WA 98195.

⁺Instituto di Fisica e Gruppo Nazionale di Struttura della
Materia del CNR, 27100 Pavia, ITALY.

A feature which is particularly common in nuclear magnetic resonance studies of superionics is an asymmetrical $\ln T_1$ vs T^{-1} dependence in which the high temperature slope gives an activation energy E_H consistent with conductivity values, while data on the low temperature side of the spin-lattice relaxation minimum yields an activation energy E_L substantially lower than E_H . Analysis of line narrowing gives an activation energy $E_{LN} = E_L$.

In some cases it has been possible to obtain agreement with the $\ln T_1$ vs T^{-1} dependence, and frequency dependence of T_1 in terms of diffusion models for transport (M. Villa and J. Bjorkstam, *Phys. Rev.* **B22**(1980) 5033-42) and/or ad hoc models which relate the "half-narrowing" point of the low temperature line-width to T_1 (J. Bjorkstam, M. Villa, and J. Frye, in "Nuclear and Electron Resonance Spectroscopies Applied to Materials Science," E. Kaufman and J. Shenoy, eds. - North Holland (Amsterdam 1981) p. 295). However, C.A. Scholl has suggested that diffusion models should lead to a low temperature (high frequency) limit in which $E_L \rightarrow E_H$ (*J. Phys. C*, **14** (1981) 447-464). We demonstrate with diffusion models for which there is an exact solution that Scholl's suggestion can be valid, but that this asymptotic limit may be unreachable in actual experiments. We also call attention to the fact that both low temperature T_1 and line narrowing experiments sample the high frequency spectral density so may be expected to give comparable values of activation energy, as we demonstrate experimentally. Comparison is made with several examples of experimental data in which the transport motional contribution to the relaxation processes can be separated from that due to other mechanisms. We are able to give a rather general consistent interpretation of the temperature and frequency dependence of T_1 and line narrowing.

⁰Supported by U.S. Department of Energy Grant DE-FG06-84ER 45065.

APPLICATION OF THE LOGARITHMIC LAW OF MIXING FOR THE
ESTIMATION OF COMPLEX PERMITTIVITY AND ELECTRICAL
CONDUCTIVITY OF FAST ION CONDUCTORS AT MICROWAVE FREQUENCIES

B.V.R. Chowdari, P.S. Neelakantaswamy and S.K. Akhter
Department of Physics
National University of Singapore
Singapore 0511

In practice, electrical conductivity and dielectric constant studies of a fast ion conductor needs extremely accurate measurements owing to its low resistance which may be comparable in magnitude with electrode-electrolyte contact resistance. The complexity of the instrumentation becomes significant if the measurements are to be made at microwave frequencies. Conventional transmission-line techniques in general become less appropriate for the study of high-lossy materials like fast ion conductors at microwave frequencies.

It is well established from the conductivity measurements carried out on materials which contain a mixture of two or more phases with differing conductivities, the measured conductivity is of some form of average of the various constituent conductivities. Such a practical situation makes the test sample made of a mixture of fast ion conductor and an insulator less-lossy and hence enable us to use conventional "Von-Hippel technique" for studies at microwave frequencies.

Variety of formulas have been suggested in the past for the calculation of permittivity of statistical mixtures and among them logarithmic law of mixing has been widely accepted. The general form of the logarithmic law of mixing for a mixture of m components is

$$\log \epsilon^* = \sum_{i=1}^{i=m} y_i \log \epsilon_i$$

where y_i represents the volume fraction of the constituent whose permittivity is ϵ_i . This paper considers the application of the theory of logarithmic law of mixing for the estimation of permittivity and hence the electrical conductivity of a fast ion conductor. As a model material AgI, for which actual measurements over a wide temperature and frequency range are available, has been chosen.

Theoretical analysis of the logarithmic law of mixing showed the existence of some sort of linear relation between the measured value of the permittivity and the volume fraction of packing. The measured data on the mixtures of β -AgI and alumina for various compositions or various volume fractions at various temperatures using microwave slotted line technique in frequency range 8 - 12 GHz is fitted to the theoretically obtained linear relation and finally the value of the dielectric constant ϵ' has been estimated for an 100% AgI sample. Similarly loss tangent and hence ϵ'' , the imaginary part of ϵ^* , has also been estimated. Knowing both ϵ'' and ϵ' , electrical conductivity σ is calculated using the relation $\sigma = \omega \epsilon_0 \epsilon''$ where ϵ_0 is the permittivity of the free space and ω the angular frequency. Estimated values of both permittivity and conductivity for both α - and β -AgI agree fairly well with those reported earlier (1).

1. K.F. Gebhardt, P.D. Soper, J. Merski, T.J. Balle and W.H. Flygare
J. Chem. Phys. 72, 272 (1980).

CONDUCTIVITY, DR, DSC, and NMR STUDIES OF POLY(VINYL ACETATE) COMPLEXED
WITH ALKALI METAL SALTS*

M. C. Wintersgill, J. J. Fontanella, J. P. Calame, M. K. Smith
Physics Department
U.S. Naval Academy
Annapolis, Md 21402, USA

S. G. Greenbaum
Physics Department,
Hunter College, CUNY
New York, NY

C. G. Andeen
Physics Department,
Case Western Reserve University
Cleveland, Oh 44106, USA.

Electrical conductivity, dielectric relaxation (DR), differential scanning calorimetry (DSC) and nuclear magnetic resonance (NMR) studies have been carried out on poly(vinyl acetate) (PVAc) complexed with a variety of lithium and sodium salts including perchlorates, triflates and iodides. The electrical conductivity and dielectric relaxation measurements were carried out using a fully automated complex impedance bridge operating at seventeen frequencies over the range 10^3 Hz. The conductivity varies with the concentration of the salt. For example, at 102°C the conductivity for 8:1 PVAc-lithium perchlorate is about 10^{-7} (ohm-cm) $^{-1}$ while that for 4:1 material is about 5 times greater. The variation of the conductivity with temperature is also described. The electrical relaxation spectrum for pure PVAc consists of four peaks. Significant differences are seen in the complexed material. For example, for 8:1 PVAc-lithium perchlorate most peaks are similar to those observed in pure PVAc while for 8:1 PVAc-sodium perchlorate, the spectrum is strongly affected. The spectra for PVAc-lithium iodide and PVAc-lithium triflate are extremely simple. The DSC studies were carried out using a DuPont 990 DSC and show three thermal features which are dependent upon the salt and the thermal history of the samples. Finally, new NMR studies are presented. The results are considered in the light of previous work on PVAc complexed with lithium perchlorate (1) and a model similar to that for an ionic elastomer.

1. M. C. Wintersgill, J. J. Fontanella, J. P. Calame, S. G. Greenbaum, and C. G. Andeen, J. Electrochem. Soc., 131, 2208 (1984).

*This work was supported in part by the Office of Naval Research.

Linear Polyphosphazene and Polyelectrolyte Solid Electrolytes

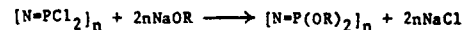
D. F. Shriver, P. M. Blonsky, L. C. Hardy
Department of Chemistry and Materials Research Center,
Northwestern University, Evanston, IL 60201
and

H. R. Allcock, P. Austin and J. Sisko
Department of Chemistry, Pennsylvania State University,
University Park, PA 16802

Previous work on polyethyleneoxide (PEO) and polypropyleneoxide (PPO) based complexes with alkali metal salts, has indicated that polymers with low glass transition temperatures (T_g) and a high concentration of polar groups, are good candidates as hosts for salts in the preparation of polymer electrolytes.

Polyphosphazenes are attractive for electrolyte synthesis on three counts: 1) The linear chlorophosphazene $[N=PCl_2]_n$, can be modified chemically to yield a wide range of substituted polymers. 2) The high molecular weight ($>10^6$) polymers produced are stable and not crosslinked. 3) Fully substituted phosphazene polymers frequently have very low values of T_g .

A series of polyphosphazenes, $[N=P((OC_2H_4)_xOCH_3)_2]_n$ ($x = 1, 2, 4, 7, 11, 42$; $n > 15,000$), were prepared by the interaction of sodium polyether alkoxides with the linear chlorophosphazene:



For $x = 2$ the polyphosphazene is referred to as MEEP, and this polymer was used to form polymer-salt complexes. These complexes were prepared with a variety of mono and divalent triflate salts (Na, Li, K, Rb, Sr, Mg, Ag, Cu, Zn; triflate = $SO_3CF_3^-$). In addition, trivalent salts were also complexed ($Gd_2(SO_4)_3$, $Nd_2(SO_4)_3$, $Na_3Co(NO_2)_6$) by the polymers. Characterization of the pure polymers and polymer-salt complexes were performed by IR, (^{31}P , ^{13}C) NMR, X-ray diffraction, differential scanning calorimetry (DSC), optical microscopy, gel chromatography, ac complex impedance (5-500,000 Hz), and dc polarization methods. Between room temperature and $100^\circ C$, the conductivity of $(LiSO_3CF_3)_{0.25}$ MEEP is 1-3 orders of magnitude larger than that of similar poly(ethylene oxide) systems. Polarization cell experiments, on triflate salt complexes, indicate that the transport number for Ag^+ is 0.03 or less at $50^\circ C$, and for Li^+ it is 0.32 under the same conditions.

In an attempt to prepare polymer electrolytes with unity transport number for the mobile ion, we have explored the properties of solid polyelectrolytes. Ionic conductivity has been induced in the quaternary ammonium polymer poly-(diallyldimethylammonium) with chloride or trifluoromethylsulfonate counter ions by the introduction of a plasticizer, poly(ethylene glycol), PEG. Similarly, sodium poly(styrene-sulfonate) becomes a sodium ion conductor when plasticized with PEG. Ion transport properties in these materials are similar to those of the well known class of solid electrolytes poly(ethylene oxide)-alkali metal salt complexes, except that the ac and dc electrical properties can be attributed to known charge carriers. Conductivity of $10^{-5} \Omega^{-1}cm^{-1}$ at $25^\circ C$ has been achieved for the highly plasticized chloride ion conductor.

ION TRANSPORT AND THERMAL PROPERTIES OF
POLYETHYLENE OXIDE - LITHIUM PERCHLORATE COMPLEXES

Paolo Ferloni, Aldo Magistris and Manlio Sanesi
Centro di Studio per la Termodinamica ed Electrochimica dei Sistemi
Sellini Fusi e Solidi del C. N. R., c/o Dipartimento di Chimica Fisica
Viale Taramelli 16 - 27100 Pavia, Italy

This paper discusses the thermal properties and ion transport characteristics of the complexes formed by polyethylene oxide (PEO) and lithium perchlorate. This polymeric electrolyte has been prepared by dissolving PEO (M.W. = $4 \cdot 10^5$) and lithium perchlorate in acetonitrile and evaporating the solvent at room temperature. We have examined nine different compositions over a $LiClO_4$ concentration range of 0 - 20 mole%.

The thermal stability of the complexes was investigated by thermogravimetric analysis, and the phase transitions were examined by differential scanning calorimetry in the range 200 - 500 K. Complex ac-impedance analysis has been carried out from room temperature to 500 K with blocking electrodes to determine the conductivity and activation energies of the complexes. To characterize the ion transport mechanism, the conductivity has also been measured with the four probe DC method and with the complex impedance method using reversible Li electrodes.

The conductivity of these complexes reaches a maximum for a PEO/Li ratio of about 8:1. The ionic transport numbers have been measured as a function of temperature for this composition.

P11/P-4

TEMPERATURE-DEPENDENT SPECTROSCOPIC STUDIES OF POLY(PROPYLENE OXIDE) AND POLY-(PROPYLENE OXIDE)-INORGANIC SALT COMPLEXES

Dale Teeters
Department of Chemistry
University of Tulsa
Tulsa, Oklahoma 74104

Roger Frech
Department of Chemistry
University of Oklahoma
Norman, Oklahoma 73019

Raman spectroscopic studies have been performed on low molecular weight poly-(propylene oxide) polymers and complexes of these polymers with various inorganic salts. A low frequency vibrational mode at approximately 239 cm^{-1} , tentatively assigned to a bending or torsional motion of the polymer backbone, is the most sensitive to the addition of the inorganic salts. Temperature-dependent Raman scattering spectra have been measured from ambient up to temperatures at which sample degradation occurs. Dramatic spectral changes have been observed over the temperature interval $140\text{--}180^\circ\text{C}$ in polymers complexed with inorganic salts. These data are discussed in terms of models which invoke temperature-dependent bandwidths originating in disordering mechanisms.

P12/P-5

STRUCTURE AND IONIC CONDUCTIVITY IN EVAPORATED THIN FILMS OF POLY(ETHYLENE OXIDE) COMPLEXED WITH LiCF_3SO_3

Yukio ITO, Kiyooki SHAKUSHIRO, Katsuki MIYAUCHI
and Tetsuichi KUDO
Central Research Laboratory, Hitachi Ltd.,
P.O. Box 2, Kokubunji, Tokyo 185, Japan

The complexes formed between poly(ethylene oxide) (PEO) and alkali metal salts have been attracting a great deal of attention because of their potential application as electrolytes in batteries and other electrochemical devices. The polymer salt complex films have usually been obtained by solution casting onto plates and heating under vacuum. Evaporated thin films of PEO complexed with LiCF_3SO_3 are produced. This paper reports on the first preparation and characterization of evaporated polymer complex films, along with information on their structure and electrical properties.

Thin films are formed by evaporating a suitable mixture of powdered PEO and LiCF_3SO_3 charged in a tungsten boat onto silica glass substrates at room temperature. The starting compositions are $(\text{PEO})_x(\text{LiCF}_3\text{SO}_3)_y$ with $4 \leq x \leq 18$. The deposition rate is $\sim 0.5\text{ nm/s}$ in a $5 \times 10^{-4}\text{ Pa}$ vacuum.

The structural information of thin films is obtained by employing infrared absorption spectroscopy. The IR spectra in the region $400\text{--}4600\text{ cm}^{-1}$ for evaporated thin films show a close similarity to the spectra for $(\text{PEO})_x(\text{LiCF}_3\text{SO}_3)_y$ films prepared by solution casting. This result suggests that the fundamental structure of the evaporated films is very similar to that of $(\text{PEO})_x(\text{LiCF}_3\text{SO}_3)_y$ complexes.

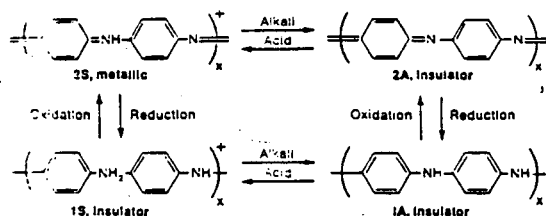
The molecular weights of evaporated films are determined using gel permeation chromatography. Poly(ethylene oxide), used as the starting material, has an average molecular weight of about 600000. The molecular weight of $(\text{PEO})_x(\text{LiCF}_3\text{SO}_3)_y$ complexes formed by casting shows almost the same value as that of the PEO used. When a mixture of PEO and LiCF_3SO_3 is evaporated, the molecular weight of the film obtained decreases to a value of 1000 - 10000.

Conductivities parallel to the evaporated film surfaces are measured on specimens with interdigital Au blocking electrodes fabricated on their surfaces. The conductivity plots of $\log \sigma$ against $1/T$ is approximately linear in the measuring temperature region up to 150°C . Total ionic conductivities extrapolated to room temperature for the evaporated films with $4 \leq x \leq 18$ are $\sim 10^{-5}\text{ }\Omega^{-1}\text{ cm}^{-1}$. This value is about ten times larger than for $(\text{PEO})_x(\text{LiCF}_3\text{SO}_3)_y$ complexes formed by casting. The activation energies for the ionic conduction are about 25 kJ/mol. This ionic conducting behavior for the evaporated thin films is clarified in terms of their structure and molecular weights.

by

N.L.D.Somasiri, and A.G.MacDiarmid, Department of Chemistry and
A.R.McGhie, Laboratory for Research on the Structure of Matter, University
of Pennsylvania, Philadelphia PA 19104

'Polyaniline' has been known for about 100 years as an ill-defined black solid which has never been completely characterized. In this work, we have taken a closer look at this unique material which can be synthesized by both chemical and electrochemical oxidation of aniline, $\text{C}_6\text{H}_5\text{NH}_2$. Several forms of the polymer exist, including one which exhibits metallic conductivity obtained by p-doping via a simple acid/base reaction in aqueous solution which involves no formal oxidation of the polymer. The four idealized forms of the polymer are shown below.



Preliminary⁶ experiments have indicated that polyaniline may function as a lightweight, inexpensive electroactive electrode for use in a rechargeable dry cell battery or fuel cell.

In this work we have investigated the thermal stability of polyaniline in the 2A and 2S forms using both differential scanning calorimetry and thermogravimetric analysis, as a function of oxygen partial pressure. These techniques, in conjunction with elemental chemical analysis, IR, mass spectroscopy, electrochemical studies and conductivity measurements, have been used to characterize polyaniline synthesized by both chemical and electrochemical methods. We have obtained polyaniline in both 2A and 2S form which is thermally stable to temperatures in excess of 100°C and which still retain high conductivity in the 2S state. Samples of 2A show no weight loss up to 300°C although a unique exothermic chemical reaction occurs in the polymer in the temperature range 150-300°C. Details of this process will be presented.

REFERENCES

- 1) R. de Surville, M. Jozefowicz, L. T. Yu, J. Perichon & R. Buvet, *Electrochimica Acta*, **13** 1451 (1968)
- 2) M. Doriomedoff, F. Hautiere-Cristofini, R. de Surville, M. Jozefowicz, L. T. Yu & R. Buvet, *J. Chim. Phys.*, **68**, 1055 (1971)
- 3) A. G. MacDiarmid, J. C. Chiang, M. Halpern, W. Shuang, S. L. Mu, N. L. D. Somasiri, W. Wu and S. I. Yaniger, *Mol. Cryst. Liquid Cryst.*, in press (1985)
- 4) E. M. Genies, A. A. Syed and C. Tsintavis, *Mol. Cryst. Liquid Cryst.*, in press (1985)
- 5) A. Kitani, J. Izumi, J. Yano, Y. Hiromoto and K. Sasaki *Bull. Chem. Soc. Japan*, **57** 2254 (1984); T. Kobayashi, H. Yoneyama and H. Tamura, *J. Electroanal. Chem.* **177**, 281 (1984)
- 6) A. G. MacDiarmid, S. L. Mu, N. L. D. Somasiri and W. Wu, *Mol. Cryst. Liquid Cryst.*, in press.

POLY(ETHYLENE OXIDE)-LiCF₃SO₃-POLYSTYRENE ELECTROLYTE SYSTEMS

Fiona M. Gray, James R. MacCallum and Colin A. Vincent
Department of Chemistry, University of St. Andrews,
St. Andrews, Fife KY16 9ST, Scotland.

Poly(ethylene oxide) doped with lithium salts is, to date, one of the most promising materials for practical use as a polymeric electrolyte. The material is, however, susceptible to creep at elevated temperatures. By introducing a second "structural" polymer of much higher T_g , this effect was considerably reduced but at some expense of ionic conductivity.

Polystyrene ($T_g = 100^\circ\text{C}$) was incorporated into the PEO-LiCF₃SO₃ complex to act as a support polymer and thus improve the physical properties of PEO. A range of polymer systems, (polystyrene)_x(PEO)₁₀LiCF₃SO₃ were prepared by thermal polymerisation of styrene in the presence of the polyether and salt, in the absence of solvent. X represents the volume % polystyrene and $0 \leq X \leq 80$. Spectroscopic data indicated the presence of graft copolymer along with a mixture of pure polymer components. The relative physical strength of these polymer systems was measured by penetrometry, both at room temperature and above the PEO melting point and was shown to increase correspondingly with concentration of polystyrene.

Thin films were formed by a hot-pressing technique and a.c. conductivities measured over a temperature range 20-150°C. Three conductivity regions may be identified: below 60°C, 60-100°C and above 100°C. In general, the conductivities were found to decrease with an increase in polystyrene concentration, but a rapid decrease was not evident, until a percolation limit had been exceeded. The fall in conductivity with respect to concentration was found to be greater in the low temperature region. An interpretation of the conductivity data within the three regions will be given.

Conductivities were compared for films of PEO-LiCF₃SO₃ complexes prepared by various methods. Conductivities of annealed, pressed films were found to be higher by an order of half a decade compared to those of solvent-cast films. Specific conductivity values for systems containing up to 40 volume % polystyrene were greater than published values for a PEO₁₀LiCF₃SO₃ system. The much improved mechanical stability, with a relatively small loss of conductivity above 60°C in 20-60 volume % systems may make these viable materials for electrolytes for cells used in the higher temperature range.

ELECTRICAL PROPERTIES OF LITHIUM CONDUCTIVE SULFUR GLASSES PREPARED BY TWIN ROLLER QUENCHING

Annie PRADEL and Michel RIBES

Laboratoire de Physico-Chimie des Matériaux - UA 407
 USTL - Place Eugène Bataillon
 34060 MONTPELLIER Cedex
 FRANCE

A twin roller apparatus has been designed to be used in a controlled environment, so that even hygroscopic and oxidable glasses may be prepared by fast quenching. The quenched flakes of about 50 μ m thickness and few mm² area have been used to perform electrical measurements.

. Vitreous domain in the system Li₂S-GeS₂ has been extended and a glass with as high as 63 % Li₂S has been prepared which corresponds at 13 % more in modifier than previously. Its conductivity reaches 10⁻⁴ (Ω cm)⁻¹ at 25° C.

. For the first time, glasses have been obtained in the system Li₂S-SiS₂, electrical characteristics of these glasses have been measured.

. Studies on glass formation and electrical conductivity have been carried out in the Li₂S-XS₂-LiI systems with the ratio Li₂S/XS₂ = 3/2 when X = Ge and 2/3 when X = Si.

The electrical characteristics of a fast quenched glass, and of the corresponding glass prepared in the classical way, have been compared in order to evaluate the influence of the cooling rate.

PSEUDOSPIN ECHOES IN A FAMILY OF IONIC CONDUCTING LITHIUM BORATE GLASSES .

M. DEVAUD, J.-Y. PRIEUR and W. D. WALLACE *

Laboratoire d'Ultrasons[†], Université Pierre et Marie Curie,
 Tour 13, 4 place Jussieu, 75230 Paris Cedex 05, France.

We have performed a low temperature study of a family of glasses with the general composition : B₂O₃ - x Li₂O - y LiCl. These glasses are fast ionic conductors. We present here the results of a series of echo experiments. We could produce and observe the echoes from 0.075 K up to 0.600 K, with a sequence of two (or three) acoustic pulses, of frequency about 500 MHz.

At such low temperatures, the ionic conductivity is completely "frozen" : the mobile ions are trapped. But, anyway, if there is no chance for Arrhenius activated hopping, these ions may undergo some quantum tunneling between two neighbouring equilibrium positions ; therefore the addition of mobile ions to B₂O₃, could result, at low temperatures, in a contribution to the so-called "Two Level Systems" (TLS). (Such an argument has already, and successfully, been invoked in the interpretation of acoustic low temperature properties of β alumina). For such TLS, a longitudinal (T₁) and a transverse (T₂) relaxation times are defined.

We have measured T₂ with two-pulse sequences and T₁ with three-pulse sequences, for different temperatures. T₂ and T₁ are of the order of 10 μ s at T = 250 mK, and show a T⁻¹ behaviour. Furthermore, we have measured the power of the echo as a function of the input acoustic power ; through that measurement we can infer that the TLS responsible for the echoes are weakly coupled to the phonons (interaction energy not greater than 10⁻³ eV).

*Permanent address : Department of Physics, Oakland University, Rochester, Michigan 48063, U.S.A.

[†]Associated with the Centre National de la Recherche Scientifique.

P17/G-3

IONIC CONDUCTIVITY AND GLASS TRANSITION OF BOROPHOSPHATE GLASSES

Geetano Chiodelli and Aldo Magistris
 Centro di Studio per la Termodinamica ed Elettrochimica dei Sistemi
 Solidi Fusi e Solidi del C. N. R. c/o Dipartimento di Chimica Fisica
 Viale Taramelli 16 - 27100 Pavia, Italy

Marco Villa
 Dipartimento di Fisica "A. Volta" e Gruppo Nazionale di Struttura della
 Materia del C. N. R. Via Bassi 6, 27100 Pavia, Italy

Oxide glasses obtained from a glass former (such as boron oxide), a metal oxide (M_2O) and a halide salt (MX) can be good cationic (M^+) conductors. Many systematic investigations have been reported which show that conductivity always improves by adding a "dopant" salt (MX), by choosing large and polarizable X-anions and by substituting oxygen with sulfur. This paper focusses upon a less known method of optimizing cation conductivity in oxide glasses based upon partial substitution of one glass former with another. It examines what we will call "mixed anion effects", i.e. the highly non linear behavior of some property as a function of the percentage of the replacement of one glass former by another.

We have explored glass formation regions, conductivity and glass transition phenomena in the systems $MX \cdot M_2O \cdot B_2O_3 \cdot P_2O_5$ ($M=Li, Ag; X=Cl, I$). The activation energies for conductivity in the absence of MX usually reach a minimum in substances with two glass formers. On the other hand, the T_g 's attain the highest values for [B]/[P] ratios that are close to those which optimize conductivity.

The addition of a halide salt always improves the conductivity but does not always affect T_g . At the highest levels of doping, some of the mixed glasses have conductivities close to those observed in the corresponding pure borate glasses. The addition of silver iodide to silver borophosphate glasses with optimized conductivity dramatically reduces T_g . In contrast, the addition of LiCl to lithium borophosphate glasses with optimized conductivity does not significantly change their glass transition temperatures.

CONDUCTIVITY RELAXATION AND SPIN LATTICE RELAXATION IN LITHIUM AND MIXED ALKALI BORATE GLASSES: ACTIVATION ENTHALPIES, ANOMALOUS ISOTOPE-MASS EFFECT AND MIXED ALKALI EFFECT

K. L. Ngai
 Naval Research Laboratory
 Washington, D.C. 20375-5000

and

H. Jain
 Brookhaven National Laboratory
 Upton, New York 11973

Measurements of the frequency and temperature dependences of the spin-lattice¹ and conductivity relaxations² in a series of mixed isotope (⁷Li, ⁶Li) and one mixed alkali (Li, Na) triborate glasses are discussed and described by a unified model of relaxation.³ The frequency dependence of the conductivity relaxation data is found to be well described by the model. This success is no longer a surprise because the same model has been found to also describe well the conductivity relaxation in other ionic conductors such as Na β -alumina, alkali silicate glasses, etc. In the mixed isotope (⁷Li, ⁶Li) triborate glasses, an anomalous isotope-mass effect in the electrical conductivity has been observed. The model predicts a correlation between the shape of the electric modulus frequency dependence curve and the magnitude of the isotope-mass effect. The predicted correlation is found to hold quantitatively at all temperatures of measurement with use of a vibrational frequency which has been obtained by infrared-spectra measurements. Moreover the model predicts the observed activation enthalpy of electrical conductivity E_a is only an apparent one and is related to a more fundamental activation enthalpy E_a^0 by the relation $E_a = E_a^0(1-n)$ where n is the shape parameter of the electric modulus frequency dependence curve. Spin-lattice relaxation times (T_1) measurements of localized alkali motion in the same mixed isotope (⁷Li, ⁶Li) triborate glasses on the low temperature side of the T_g minimum have indeed given the value of activation enthalpy E_{T_1} in good agreement with the predicted E_a^0 . This gives additional support for the relevance of the relaxation model in glasses.

The model has more to say about the difference in magnitudes of the mixed alkali effect observed via E_a^0 and via E_{T_1} .¹ The mixed alkali effect measured for (0.49 Li, 0.51 Na)₂O: 2.75 B₂O₃ via E_a^0 is again an apparent one, related to a more fundamental mixed alkali effect exemplified by E_{T_1} .

1. H. Jain, G. Balzer-Jöllanbeck and O. Kanert, J. Am. Ceramic Soc. **68**, XXX (1985).
2. H.L. Downing, N.L. Peterson, and H. Jain, J. Non-Cryst. Solids **50**, 203 (1982).
3. K.L. Ngai, R.W. Rendell, and H. Jain, Phys. Rev. B **30**, 2133 (1984).

PREPARATION AND CONDUCTIVITY MEASUREMENTS OF $\text{SiS}_2\text{-Li}_2\text{S}$ GLASSES DOPED WITH LiBr AND LiCl

JOHN H. KENNEDY, SAIED SAKANI, STEVEN W. SHEA, AND Z. ZHANG, Department of Chemistry, University of California, Santa Barbara, CA 93106.

A number of conductive sulfide-based lithium glasses, which can be used as electrolytes in lithium solid state devices and batteries have been studied in recent years. The most well known are $\text{P}_2\text{S}_5\text{-Li}_2\text{S}$ glasses and their lithium iodide doped analogs, which show conductivity as high as $10^{-3} \text{ S-cm}^{-1}$ at 25°C . It was recently reported that since $\text{P}_2\text{S}_5\text{-Li}_2\text{S}$ and ($\text{B}_2\text{S}_3\text{-Li}_2\text{S}$) glasses required synthesis in sealed pressure quartz tubes, the $\text{SiS}_2\text{-Li}_2\text{S}$ glasses, which may be prepared under atmospheric pressure offer a viable commercial production alternative. We report here the preparation and conductivity measurements for $\text{SiS}_2\text{-Li}_2\text{S}$ glasses doped with LiBr and LiCl . Extent of glass formation was investigated by varying the molar concentration of LiBr while holding the mole ratio of SiS_2 to Li_2S constant at 1:1.

The $\text{SiS}_2\text{-Li}_2\text{S}$ glasses were prepared by first mixing SiS_2 and Li_2S in a 1:1 mole ratio in a dry box. The mixture was then placed in a vitreous carbon crucible, which in turn was positioned in a Vycor tube. The mixture was heated for about one hour at 950°C under argon. The molten mixture was quickly quenched into a water bath at room temperature to form the vitreous solid. This base glass was doped with various amounts of LiBr or LiCl , and the heating procedure repeated. The final glass samples were ground and pressed into pellets using isostatic pressing.

Complex impedance plots of the glasses with TiS_2 electrodes consisted of a straight line intersecting the real axis at approximately a 45° angle. The bulk resistance of the glass sample was obtained from the extrapolation of the straight line portion of the complex impedance plot to the real axis.

Conductivity of the base glass was $1.6 \times 10^{-4} \text{ S-cm}^{-1}$ and doping with LiBr and LiCl increased this value significantly, reaching above $6 \times 10^{-4} \text{ S-cm}^{-1}$ at room temperature. Doping levels of 30 mole percent LiBr and LiCl were possible with the quench rates available.

^7Li NMR measurements for these glasses have also been made and will be reported as they shed light of the mobility of Li^+ in these conductive glasses.

QUASIELASTIC NEUTRON SCATTERING FROM $\text{AgPO}_3\text{-AgI}$ GLASS

R. MERCIER, M. TACHEZ, J.P. MALUGANI
Laboratoire d'Electrochimie des Solides ERA 810
Faculté des Sciences - Université de Franche-Comté
25030 BESANCON Cédex - FRANCE

A.J. DIANOUX
Institut Laue-Langevin, 156 X, 38042 GRENOBLE Cédex - FRANCE

A quasielastic neutron scattering experiment was performed on the fast ionic conductor $\text{AgPO}_3\text{-AgI}$, which is a vitreous electrolyte.

This experiment was conducted using the time-of-flight spectrometer IN 6 of the Institut Laue Langevin in Grenoble, with the following parameters : $\lambda = 5.1 \text{ \AA}$; $1.25 \text{ \AA}^{-1} \leq Q \leq 2.04 \text{ \AA}^{-1}$; instrumental resolution (FWHM) = 0.070 meV ; transmission factor of the sample : 0.66 ; $299 \text{ K} < T < 368 \text{ K}$.

The spectra generally consist of a quasielastic broadening of the elastic peak and of a long tail up to 10 meV which is due to an inelastic distribution.

In order to obtain the quasielastic contribution, the profile of the central peak was fitted within $\pm 0.6 \text{ meV}$ for the nine channels and for five temperatures. The EISF was constant at 85% . The profile of the quasielastic contribution was found to be Lorentzian.

When plotting the function energy width ΔE corrected by $S(Q)$ [$\Delta E S(Q)$] versus Q^2 : a straight line is obtained for all temperatures, which means that the mechanism of the conductivity is certainly a translational jump diffusion with a coefficient of self diffusion of the silver ions $D = 1.32 \times 10^{-5} \exp - \frac{2080}{RT}$ (activation energy being in calories).

The value of the activation energy is very close to that of $\alpha\text{-AgI}$ measured by electric conductivity. The value of EISF : 0.85 indicates that the observed quasielastic scattering is due to half of the silver ions. These two results seem to confirm our hypothesis on the structure of this glass : small "clusters" of an "amorphous" like $\alpha\text{-AgI}$ are dispersed in the AgPO_3 host glass.

EFFECT OF ADDITION OF LiNbO_3 ON THE ELECTRICAL CONDUCTIVITY OF $\text{Li}_2\text{O}-\text{B}_2\text{O}_3$ SYSTEM

S. Rokade, K. Singh and V. K. Deshpande
Department of Physics, Nagpur University, Nagpur-440010, India

Lithium borate glasses exhibit high ionic conductivity due to migration of lithium ions. Several cathode materials are known which might be employed in lithium transporting systems because of their relatively high lithium diffusion coefficients. In addition, lithium is more electropositive and thus provides the possibility of greater cell voltages.

In order to improve the ionic conductivity of $\text{Li}_2\text{O}-\text{B}_2\text{O}_3$ system, LiNbO_3 has been added in different concentrations in $\text{Li}_2\text{O}-\text{B}_2\text{O}_3$ (40:60 m/o). The electrical conductivity has been measured in the temperature range 400K to 714K. It has been found that LiNbO_3 can be accommodated in the amorphous matrix up to 10 m/o. The samples with more than 10 m/o LiNbO_3 crystallised. The conductivity is found to increase with increasing LiNbO_3 concentration. The enhancement in the conductivity is due to increase in 1) Li ion concentration and 2) mobility of Li ions due to large number of vacant sites provided by the pentavalent Nb ions. The results are comparable with the earlier reportings on parallel systems.

SULFATE ION CONFIGURATION IN MONOCLINIC

AND CUBIC LITHIUM SULFATE

Roger Frech Department of Chemistry
University of Oklahoma
Norman, OK. 73019 U.S.A.

Enzo Cazzanelli Dipartimento di Fisica
Università di Trento
38050 - Povo (Trento) Italy

One of the more widely studied fast ion conductors is lithium sulfate, Li_2SO_4 , which undergoes a first order phase transition from a monoclinic phase to a fast-ion-conducting, face-centered-cubic phase at 573°C (1,2). The high temperature cubic phase is also a plastic phase, and it has been suggested that the ionic mobility in this phase is dynamically enhanced through the reorientational motion of the sulfate ions (3). For this reason it is desirable to study the nature of the sulfate ion motion in both phases, particularly in the vicinity of the transition temperature.

An analysis of the ν_3 molecular vibrational mode of the sulfate ion in the pre-transitional region (450°C - 573°C) suggests critical behavior in the monoclinic phase. The critical exponent ($\beta=1/6$) indicates a weak planar anisotropic environment for the sulfate ion. A detailed study of the ν_3 molecular mode in the cubic phase shows a lifting of the three-fold degeneracy. The depolarization ratio measured across the band contour establishes an A component and an E component, again consistent with a planar anisotropic environment of the sulfate ion.

The barrier heights for the configurational jumps are calculated from the sulfate librational mode frequency data and are found to be in excellent agreement with the barrier height calculations from bandwidth data measured in the pre-transitional region.

1. T. Førland and J. Krogh-Moe, Acta Chem. Scand. 11, 565 (1958).
2. A. Kvist and A. Lundén. Z. Naturforsch. 20 A, 235 (1965).
3. L. Nilsson, J. O. Thomas and B. C. Tofield, J. Phys. C: Solid St. Phys. 13, 6441 (1980).

SIZE EFFECT OF THE ALKALI IONS
ON THE DIFFUSION RATES IN SILVER HALIDES

A.L. Laskar
Department of Physics and Astronomy, Clemson University,
Clemson, SC 29631

P.A. CARDEGNA
Department of Physics, Rochester Institute of Technology,
Rochester, NY 14623

Recent experimental studies of the diffusion of alkali ions in AgBr and AgCl have led to an interesting correlation between the ionic size of the solute and its diffusion rate.^{1,2} As the mismatch between the ionic radii of the solute and the solvent ion increases the diffusivity increases and the activation energy for diffusion decreases. Alkali ions are believed to probe accurately the role of ionic size effect because being homovalent with the host ion, they are not expected to have any association with a vacancy through coulombic forces. Further, the crystal field effects and the affect of d-shell electrons of the solutes on the motional energy of the diffusing solutes will not perturb the vacancy diffusion of these ions.

The present results of the study of Cs⁺ (1.67Å) greatly oversized with respect to the host Ag⁺ (1.16Å) add further support to the earlier observations on the size effect of the solutes on the diffusion rate. Our results for the diffusion of Cs⁺ in AgCl are in excellent agreement with the very fast diffusion observed in an earlier study³. The linear Arrhenius behavior for the diffusivity results from the fact that the expected curvature in the Arrhenius diffusion plot due to the nonlinear temperature dependence of the Gibb's free energy for the formation of vacancies is washed out due to the stress-induced binding of oversized Cs⁺ ion with a vacancy. Surprisingly the diffusion coefficient of Cs⁺ in AgBr is less than that in AgCl. This is indeed an exceptional case. The diffusion coefficients in AgBr is always much larger than that in AgBr for the vast number of solutes (monovalent and divalent) studied so far. Further, the Arrhenius plot exhibits slight amount of curvature in the high temperature region. It is suggested the size-effect is less in AgBr since the lattice constant is larger in AgBr compared to that in AgCl. The solubility of Cs⁺ in AgCl is much less than that in AgBr supporting the general fact that solutes with lower solubility exhibit higher diffusivity.

1. Laskar, A.L., pp 59-74 in "Diffusion in Solids" ed. A.L. Laskar et al. (Trans Tech Publications, Switzerland, 1984).
2. Laskar, A.L. and Cardegna, P.A., Radiation Effects 75, 27 (1983).
3. Batra, A.P. and Slifkin, L.M., J. Phys. Chem. Solids 37, 967 (1976).

POLYMORPHISM AND CATION TRANSPORT PROPERTIES IN 3D SKELETON

ARSENATES Na₃M₂(AsO₄)₃ (M = Al, Ga, Cr, Fe).

F. d'YVOIRE, M. PINTARD-SCREPEL and E. BRETEY.
Laboratoire de Chimie Appliquée, Université Paris-Sud,
91405 ORSAY Cédex, France.

In the search for new solid electrolytes, an increasing attention has been given to the 3D skeleton phosphates A₃M₂(PO₄)₃ (A = Li, Na, Ag, K ; M = Sc, Cr, Fe) particularly to the sodium members which have a Nasicon type structure¹. These solids are poor conductors at room temperature but become superionic conductors at high temperature ($\sigma_{300} \sim 10^{-2} \Omega^{-1} \text{cm}^{-1}$) through a series of phase transitions associated with changes in Na⁺-Na⁺ correlations.

The corresponding arsenates Na₃M₂(AsO₄)₃ don't have the same structure. For M = Cr and Fe, a low-temperature garnet-type form (I) and a high-temperature form (II) have been characterized². For M = Al and Ga, II is the single form observed. The sodium-ion transport properties of the two forms are very different.

Form I. Like Nasicon, the garnet structure contains a 3D framework [M₂(XO₄)₃]_n made up of XO₄ tetrahedra sharing corners with MO₆ octahedra but the arrangement of the polyhedra is different and the structure is more compact [V/Z = 228 Å³ in Na₃Fe₂(AsO₄)₃, 237 Å³ in Na₃Fe₂(PO₄)₃]. The conductivity is low ($\sim 10^{-6} \Omega^{-1} \text{cm}^{-1}$ at 300°C) and cation exchange reactions in molten salts are very slow (Li⁺) or unobservable (Ag⁺, K⁺).

The form II is rhombohedral, R3c or R3c, less compact than I : for M = Fe, a_h = 13.719 Å, c_h = 18.594 Å, V/Z = 253 Å³. The sodium ions are easily exchanged by Li⁺, Ag⁺ or K⁺ in molten nitrates. The conductivity of Na₃Fe₂(AsO₄)₃-II is about 10 times that of Na₃Fe₂(PO₄)₃ at 20°C but is lower at 300°C ($\sim 10^{-3} \Omega^{-1} \text{cm}^{-1}$). It raises with temperature according the Arrhenius law with an activation energy of 0.46 eV. No transition appears until the transformation in form I occurs.

Single crystals of Na₃Fe₂(AsO₄)₃-II have been synthesized by a flux method. By varying the flux composition, crystals exhibiting a non stoichiometry according to Na_{3-3x}Fe_{2-x}(AsO₄)₃ (x ≤ 0.25) have also been obtained. The structural determination of these solids is in progress.

1. M. de la Rochère, F. d'Yvoire, G. Collin, R. Comès and J.P. Boilot, Sol. State Ionics, 9-10, 825 (1983).
2. H. Schwarz and L. Schmidt, Z. anorg. allg. Chem., 387, 31 (1972).

IONIC CONDUCTION IN (K,Rb)-Al-PRIDERITES WITH HOLLANDITE STRUCTURE

S. Yoshikado, T. Ohachi, I. Taniguchi

Department of Electronics, Doshisha University, Kyoto 602, Japan

Y. Onoda, M. Watanabe and Y. Fujiki

National Institute for Researches in Inorganic Materials, Ibaraki 305, Japan

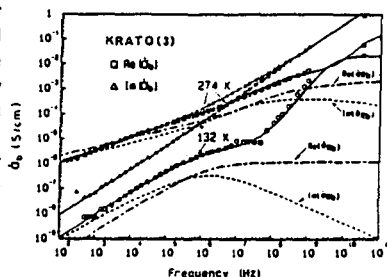
The dynamics of mobile ions in one-dimensional ionic conductors priderites with two kinds of mobile ions is different from that in priderites with a kind of mobile ions in point of the interactions between mobile ions. The interaction between two kinds of mobile ions is characterized by the difference between those ionic radii. The purpose of the present work is to analyze the data of the complex conductivity for various (K,Rb)-Al-priderites $(K_{1-y}Rb_y)_xAl_xTi_{8-x}O_{16}$ using the moving box model proposed by Beyeler et al. [1], and to clarify the interaction between mobile ions.

Six kinds of single crystals of (K,Rb)-Al-priderite with $x \approx 1.5$ and y between 0 and 1 were grown by a flux method [2]. Measurements of the complex conductivity between 100 Hz to 500 MHz were made with an impedance analyzer, and those at 9.54 and 32.55 GHz were made by the standing wave method.

The complex conductivity function for the system with K^+ and Rb^+ ions is described in terms of the moving box model as follows:

$$\hat{\sigma}_b = i\omega\epsilon_{fw}\epsilon_0 + \frac{i\omega\epsilon_K\epsilon_0(\hat{\sigma}_K + \hat{\sigma}_{Rb}) + \hat{\sigma}_K\hat{\sigma}_{Rb}(1 + m^2)}{i\omega\epsilon_K\epsilon_0 + \hat{\sigma}_K + m^2\hat{\sigma}_{Rb}} \quad (1)$$

where ϵ_{fw} is the dielectric constant of the framework, ϵ_0 is the permittivity of free space, ϵ_K is the dielectric constant due to the polarization of K^+ ions within the region enclosed by two successive Rb^+ ions, $\hat{\sigma}_K$ and $\hat{\sigma}_{Rb}$ are the complex conductivity functions for K^+ and Rb^+ ions, respectively, and $m = (1-y)/y$. The Eq.(1) suggests that the contribution of the complex conductivity for each mobile ions to $\hat{\sigma}_b$ is determined by a factor m . The experimental results of the complex conductivity $\hat{\sigma}_b$ for $K_{0.83}Rb_{0.68}Al_{1.73}Ti_{6.27}O_{15.89}$ (KRATO(3)) at 274 and 132 K are shown in Fig.1. The solids lines correspond to Eq.(1) and the dashed lines correspond to $m^2\hat{\sigma}_{Rb}$. Result shows that Eq.(1) derived in terms of the moving box model is Fig.1 Frequency-dependence of $\hat{\sigma}_b$ for adequate even for the system with $m \approx 1$. $K_{0.83}Rb_{0.68}Al_{1.73}Ti_{6.27}O_{15.89}$



[1] Beyeler, H. U. and Strässler, S., Phys. Rev. B 24 (1981) 2121.

[2] Fujiki, Y., Sasaki, T., and Kobayashi, M., J. Jpn. Assoc. Min. Pet. Econ. Geol. 78 (1983) 109.

E. Pusep, C.K.A. Gillow, A.V. Chadwick, and G. McIntyre

(1) Department of Chemistry, U.C.L. London, U.K.

(2) Department of Chemistry, University of Kent, Canterbury, U.K.

(3) Institut Laue-Langevin, Grenoble, France

The perovskite ABX_3 compounds have been extensively studied by NMR and neutron diffraction techniques in order to relate the phase transitions in these systems to the rotations of the BX_3 octahedra. The NMR studies, using ^{19}F relaxation techniques, give information on the dynamics of the fluorine sub-lattice. Relaxation time NMR measurements in KCAF, (1) could not be interpreted in terms of short range rotational motions but only in terms of long range diffusional modes for the fluorine ions, coupled with a large amount of disorder on the anion sub-lattice. This interpretation is underpinned by results obtained during electrical conductivity measurements (1).

The above data suggest that there is extensive thermal generation of defects at temperatures above $300^\circ C$ in this material. We have therefore performed a high resolution single crystal neutron diffraction study on this material at temperatures of $450^\circ C$ and $700^\circ C$ in order to obtain direct information on its defect structure. The experiments were performed on the four circle instrument D9 at the I.L.L. using a neutron wavelength of 0.72 \AA . The value of this type of diffraction study on high temperature superionic systems has been unequivocally demonstrated by the work of Schulz and co-workers (2).

Data have been analysed by both Fourier synthesis and least squares refinement. Differentiation of the point defect formations from the large dynamic effects encountered in superionic materials was aided by the utilisation of high order terms in the temperature factor expression. The results find complex distributions of the scattering density about the calcium and fluorine sites. In this presentation we intend to discuss the possible defect models for this material suggested by the various experimental techniques and relate them to the existence of high fluorine mobilities in the perovskite structure.

(1) A.V. Chadwick, J.H. Strange, G.A. Ranieri and M. Terenzi, Solid State Ionics 9/ 10 555 (1983)

(2) H. Schulz and U.H. Zsüscher, ibid 41 (1983)

ELECTRICAL CONDUCTIVITY, SELF-DIFFUSION AND PHASE DIAGRAM OF LITHIUM SULFATE - LITHIUM CHLORIDE.

Arnold Lundén and Håkan Ljungmark.
Department of Physics, Chalmers University of Technology.
S-412 96 Gothenburg, Sweden.

The phase diagram of Li_2SO_4 -LiCl has been determined by means of differential thermal analysis, DTA. The electrical conductivity has been measured for 2.5 to 33.3 mole % Li_2Cl_2 for temperatures above 480°C . Self diffusion of Li^+ and Cl^- ions has also been studied in the same concentration range. The system is a simple eutectic with the eutectic point at 484°C and 44 mole % Li_2Cl_2 . The solubility of LiCl in Li_2SO_4 is very small but for both cubic and monoclinic Li_2SO_4 a plastic paste is formed in the two phase region. This makes mixtures with a low content of LiCl of interest both for electrolytes in power sources and for the storage of latent heat in the vicinity of the solid-solid phase transition at 575°C .

Electrical conductivity measurements for some Li_2SO_4 -LiBr mixtures indicate that this system is very similar to Li_2SO_4 -LiCl. A previous study of anion diffusion in Li_2SO_4 is reinterpreted.

EFFECT OF PHASE SEPARATION AND CRYSTALLIZATION ON THE CONDUCTIVITY OF a-FIC

Wen-Hai Yu and Yuan Yang
Department of Physics
University of Science and Technology of China
Heifei, Anhui
The People's Republic of China

By continuous measurement of conductance, it has been discovered that the amorphous fast ionic conductor (a-FIC) B_2O_3 -0.7 Li_2O -0.7 LiCl -0.1 Al_2O_3 exhibits anomalous conductivity behavior during the period of isothermal annealing below the glass transition temperature of T_g .

Detailed differential scanning calorimeter (DSC) and X-ray diffraction analysis (XRDA) have demonstrated that the anomaly is due to the amorphous phase separation and crystallization; the former leads to the maximum of the conductivity of specimen. The results of DSC and XRDA have also indicated that the composition of the separating amorphous phases is the lithium borate glasses containing and absenting chlorine, and that of the forming crystalline phases is $\text{Li}_4\text{B}_7\text{O}_{12}\text{Cl}$ and LiBO_2 .

The different crystallization rates of the two phases have been compared. And by the method of phase transition dynamics, the values of the activation energy of crystallization from the amorphous phases have been determined: 86.9 and 94.7 kcal/mol for $\text{Li}_4\text{B}_7\text{O}_{12}\text{Cl}$ and LiBO_2 , respectively.

Considering that the conductivity values of the above-mentioned phases are lower than those of the amorphous matrix, we propose that the interfaces between amorphous and amorphous phases and amorphous and crystalline phases, especially the former, cause the increase of the conductivity of the specimen, and discuss the effect of phase separation and crystallization on the conductivity of a-FIC.

NEUTRON DIFFRACTION OF 'B' AND B"-ALUMINA PHASES OF THE SAME COMPOSITION
 K. G. Frase, R. S. Roth and A. Santoro
 National Bureau of Standards, Gaithersburg MD 20899

The details of the phase-equilibria in the Na-Mg-Al oxide system of the beta/beta"-alumina family of solid electrolytes has long been uncertain. Anomalies appear in the compositional and thermal boundaries to particular phase fields, and anomalous phases such as "ion-rich beta-alumina" appear in some high temperature crystal growths. In addition, the question of short- or long-range ordering, particularly in beta"-alumina, has been discussed without consensus for years. By using low temperature alkoxide synthetic routes to produce ceramic powders in the Na-Mg-Al oxide system, we have demonstrated that for a nominal beta"-alumina composition ($\text{Na}_{1.67}\text{Mg}_{0.67}\text{Al}_{10.33}\text{O}_{17}$), two crystal structures form as a function of synthetic method. A comparison of neutron diffraction (powder profile) structural results for these two structures (the beta"-alumina and the new 'solid solution beta' structures) from a single composition is presented, and related to the critical issue of Mg-ordering in the spinel block.

EXAFS STUDIES OF ND IN β "-ALUMINA SINGLE CRYSTAL¹

R. Wong and W.L. Roth, Department of Physics, S.U.N.Y. Albany, Albany, NY 12222 and E. Dunn, Department of Materials Science, U.C.L.A., Los Angeles, CA 09924

Extended X-ray Absorption Fine Structure (EXAFS) data have been collected on a single crystal of Na β "-alumina in which 35% of the Na⁺ ions have been ion-exchanged with Nd³⁺. The work is being undertaken to resolve an apparent contradiction between x-ray diffraction studies² which indicate that the Nd atoms are primarily in the mid-oxygen site and optical studies³ which suggest that the Nd atoms are in a non-centrosymmetric environment. In order to investigate the local structure about Nd, fluorescent spectra above the Nd L₃-edge have been taken at room temperature. The EXAFS spectra were collected at the Cornell High Energy Synchrotron Source (CHESS) on a small crystal plate (about 1 mm² in area and 0.3 mm thick). The Nd, Na and column oxygen (O(3)) atoms form a 2-dimensional structure in the conduction plane, and therefore spectra were collected with the x-ray polarization vector parallel and at 45° to the cleavage face in order to probe the anisotropy of the Nd environment. The fourier transformed data show marked differences for the two orientations, indicating that it may be possible to determine differences in bond lengths in the conduction plane. However, the interpretation of EXAFS fluorescence spectra collected from the single crystal is complicated by the existence of many strong Bragg peaks which must be eliminated or corrected for in the analysis. We have succeeded in obtaining EXAFS spectra that are nearly free of x-ray contamination by Bragg scattering by adjusting the orientation of the crystal to minimize the number of Bragg reflections incident on the detector and masking strong reflections with Pb absorbers. The EXAFS analysis is being refined by non-linear least square fitting to remove the contributions of the remaining Bragg reflections. In this paper, radial distribution functions and fits of the spectra to single-distance and two-distance models will be presented and discussed with relation to the structures found by x-ray diffraction and spectroscopy.

(1) This work was supported in part by the Office of Naval Research.

(2) Private communication from J.L. Thomas.

(3) H. Jansen et al., Optics Letters 10, 119 (1984).

STUDY OF Na⁺ MOTIONS IN β Al₂O₃ BY QUASI ELASTIC
NEUTRON SCATTERING MEASUREMENTS

G. LUCAZEAU, J.R. GAVARRI, A.J. DIANOUX[†]

Laboratoire Chimie-Physique du Solide, et U.A. au CNRS N° 453,
Université Paris-Nord, 93430 Villetaneuse, France.

[†]Institut Laue Langevin, Grenoble.

Polycrystalline sample of Na⁺ β Al₂O₃ (Al₁₁ O₁₇ + x/2 Na_{1+x} with x = 0.25) has been investigated on a time of flight spectrometer (IN6) at 77, 317, 473, 573, 673 K, using incident wavelengths of 4.1 and 5.1 Å giving an average resolution of 0.180 and 0.130 meV respectively. It is the continuation of previous experiments on Na and Ag β Aluminas (GAVARRI). Long recording times (~12 h) and the high efficiency of IN6 have allowed to overcome the problem of the low scattering length of Na. The quasi elastic signal (QES) has been studied as function of the scattering angle and of the temperature. For Q=1Å⁻¹ at 200°C; the full width of the QES is twice larger than for Ag⁺ β Al₂O₃. Among the various models used for deriving a scattering function able to fit the experimental QES, two models have been selected: (i) for local motions, forth and back single particle jumps between BR and three surrounding mO sites, (ii) for delocalized motions (involved in conductivity process): jumps between Br-mO-aBR-mO-BR-sites including single particle jumps and pair jumps, the last process being likely the most probable.

At 200°C, the QES is dominated by local motions, characterized by a mean correlation time equal to $\tau = 3 \times 10^{-10}$ s and an activation energy of 0.04 eV.

At 300°C and 400°C a second type of motion is observed likely associated with delocalized motions. A mean correlation time of 3×10^{-10} s at 300°C and an activation energy of about 0.1 eV are derived. These results are compared with NMR studies (BAILEY, JEROME). The occupation probability of the BR site and the ratio of fixed Na⁺ to mobile Na⁺ which are parameters fitted in our models compare well with literature data (ROTH, BOILLOT). Our results are also discussed in terms of the conductivity models (WOLF) and theoretical papers giving S(Q,W) for neutron scattering of superionic conductors (DIETERICH, GEISEL).

Conductivity and Structural Analysis of Co²⁺ Stabilized β' -Alumina

S.Chen, D.R.White, M.Sankaraman, H.Sato, J.B.Lewis* and W.R.Robinson*
School of Materials Engineering, Purdue University, West Lafayette, IN 47907

The substitution of divalent metal ions for aluminum ions at the tetrahedral Al(2) sites of the spinel blocks tend to stabilize the β' -alumina structure over the β -alumina structure. Thus far, the β' -alumina lattice has been known to be stabilized by Mg²⁺, Fe²⁺, Ni²⁺, Zn²⁺ and Co²⁺. Due to charge compensation, this substitution process is believed to remove extra oxygen ions from the conduction plane, thereby indirectly affecting the ionic conductivity. In order to understand the general relation of the effect of divalent metal ions on the β -alumina structures and its effect on the conductivity, we have investigated the consequence of adding Co²⁺ ion into both the β' - and the β -alumina lattice.

Single crystalline Co²⁺ stabilized β' -alumina has been synthesized by a flux growth technique using Bi₂O₃ as the flux. Its structure was determined by X-ray crystallographic means. The substituted Co²⁺ ions was found only at the Al(2) site. Spectroscopic studies of the electronic transition of Co²⁺ ions also support the concept that the dopant ions are in distorted tetrahedral environment. Co²⁺ doped β -alumina crystals were made by a skull technique. Chemical analysis of these two materials indicated that the Co²⁺ ion concentration may be important in the formation of one phase over the other. The temperature dependent ionic conductivity of Co²⁺ stabilized β' -alumina, Co²⁺ doped β -alumina and undoped β -alumina has been measured and compared between 25°C and 450°C. A detailed conductivity analysis was made by a phase synchronous detection system in the frequency range 100 Hz to 10 MHz. The conductivity is highest in the stabilized β' -alumina and the lowest in the undoped β -alumina. For Co²⁺ doped β -alumina, a slight bend in the conductivity at around 250°C is seen. The analysis of the conductivity, and in particular, the effect of the dopant Co²⁺ ions on the resulting conductivity will be discussed.

*Chemistry Department, Purdue University

A COMBINED HRXD AND HREM STUDY OF DEGRADATION COLLAPSE IN
 $\text{NH}_4^+/\text{H}_3\text{O}^+$ β "-ALUMINA

John O. Thomas,¹ Anders Eriksson,¹ Jørgen Kjems² and
 Amanda Petford³

¹Institute of Chemistry, University of Uppsala, Box 531,
 S-751 21 Uppsala, Sweden

²Risø National Laboratory, P.O. Box 49, DK-4000 Roskilde,
 Denmark

³Department of Metallurgy and Science of Materials, University
 of Oxford, Parks Road, Oxford OX1 3PH, England

One of the most promising proton conductors discovered to date,
 as seen from a technological standpoint, is the mixed-ion sys-
 tem $\text{NH}_4^+/\text{H}_3\text{O}^+$ β "-alumina (see Ref. 1 and references given there-
 in). It has been found, however, that a loss of NH_3 occurs
 above 200°C (Ref. 2), accompanied by a significant drop in
 conductivity. It is thus important to ascertain the response
 in the crystal microstructure to this deammoniation process.
 In the work reported here, high-resolution X-ray diffraction
 and electron microscopy (HRXD and HREM) are combined to this
 end.

The HRXD shows the emergence of extra reflections which cannot
 be indexed on the basis of the β "-alumina cell, but rather in
 terms of a structure sub-unit comprising a pair of spinel-
 -blocks with the interleaving conduction plane missing.

This can, in turn, be related to HREM observations of the
 development of extended regions in which alternate conduc-
 tion planes are missing, giving double spinel-block regions
 ~ 20.7 Å thick. Moreover, under higher electron-beam current,
 clear correlation could be observed in the propagation of the
 collapse-planes across the crystal. Regions could also be
 distinguished where the conduction planes appear to swell in-
 to disc-shaped pockets (presumably containing evolved NH_3 gas),
 prior to collapse of the planes.

References

1. G.C. Farrington, K.G. Frase & J.O. Thomas. In *Advances in Materials Science*, 1984.
2. J.O. Thomas, K.G. Frase, G.J. McIntyre & G.C. Farrington. (1983) *Solid State Ionics*, 9/10) 1029.

RAMAN SPECTRA OF CADMIUM CONTAINING BETA-ALUMINA CRYSTALS.

G. Mariotto

Dipartimento di Fisica, Università di Trento, 38050 POVO (Italy), and
 Centro C.N.R. di Trento, 38050 POVO (Italy).

Room temperature Raman spectra in the region between 7 cm^{-1} and 1000 cm^{-1} have been performed on mixed Na-Cd beta-alumina single crystals, for different amounts of Na^+ ions exchanged with Cd^{2+} ions.

Our data agree with the Hattori et al. ones (1): the most important variations in the spectra, for all the polarizations, occur in the low frequency region, mainly between 20 cm^{-1} and 40 cm^{-1} , due to the appearance of two Raman peaks associated with the Cd^{2+} ions vibrational motion. These two features show a remarkable increase for both the intensity and the peak frequency, when the percentage of the exchanged sodium passes through the value of about 40%. Such effects seem to be non linear versus the cadmium concentration, showing a switch between two different vibrational dynamics regimes below and above the fraction of Na^+ exchanged with Cd^{2+} for which the distribution of cations over the different sites of the conduction plane approaches the stoichiometry (i.e.: one cation for each elementary cell). The change between the two different vibrational situations is also reflected by the behaviour of the Na^+ ion Raman band, centered at ~60 cm^{-1} : when the Cd^{2+} content reaches the value giving the stoichiometric-like condition, a decrease in the bandwidth is observed, suggesting a more ordered distribution of Na^+ ions among the mirror plane sites. This "ordering" effect is even more clearly revealed by the behaviour of some spinel block modes: in fact, they show a bandwidth minimum when the $\text{Na}^+/\text{Cd}^{2+}$ ratio matches the abovesaid value. On the other side, the broadening of these spinel block modes at more high percentages of Cd^{2+} ions is probably due to the increasing number of Na^+ vacancies in the conduction plane.

All these phenomena are consistent with the observed switch in the ionic conductivity from the interstitialcy mechanism to the vacancy one, when the Na^+ replacement passes through about 40% (2).

- 1) T. Hattori et al., *Solid State Ionics* 9410, 215 (1983)
- 2) P. H. Sutter et al., *Solid State Ionics* 9410, 295 (1983).

INVESTIGATIONS OF CATION ORDER IN Nd-, Gd- AND
Eu BETA" ALUMINA USING HIGH RESOLUTION TEM

Peter K. Davies, Amanda Petford* and Michael O'Keefe*

Department of Materials Science, University of Pennsylvania, Philadelphia,
PA 19104

*Department of Chemistry, Arizona State University, Tempe, Arizona 85287

The recent observations of trivalent ion-exchange in beta" alumina systems have led to the discovery of a new family of lanthanide solid electrolytes (1). Farrington *et al.* have also shown these materials are of considerable interest as a result of their optical properties (2).

In this paper results of a High Resolution TEM study of Nd, Gd and Eu beta" alumina will be presented. Using Phillips 400, 430 and JEOL 200 CX microscopes we have conducted microdiffraction and high resolution investigations of the respective fully exchanged materials. The samples were found to be stable under the electron beam for extended periods of time.

Our results indicate each compound shows both inter-planar long-range cation order and strong intra-planar correlations. A superstructure in which all the original hexagonal unit cell axes are tripled has been characterized. A model for the cationic positions in the ordered structure will be presented.

In addition to the ordered regions considerable micro-structural inhomogeneity was observed in each case, with many intergrowths of a 'disordered' phase being present. Results of experiments on the affect of Na substitution upon the long-range order in Nd-beta" alumina will also be given.

- (1) B. Dunn and G. C. Farrington, *Solid State Ionics*, 9/10, 223 (1983).
- (2) M. Jansen, A. Alfrey, O. Stafudd, B. Dunn, D. Yang and G. C. Farrington, *Optics Letters*, 9, 119 (1984).

This work is supported by the NSF under grant DMR 8316999 (P.K.D.) and by grant DMR 8119061 (A.P. and M.O'K.).

NONSTANDARD BEHAVIOR OF POLYCRYSTALLINE
 β/β'' -ALUMINA MEMBRANES IN SODIUM ENVIRONMENT

G. Staikov, P. D. Yankulov and E. Budevski
Central Laboratory of Electrochemical Power Sources
Bulgarian Academy of Sciences
1040 - Sofia
Bulgaria

It is known that in the sodium-sulfur system, the solid electrolyte/sodium interface is mainly responsible for the degradation of the polycrystalline β/β'' -alumina. This process consists of the propagation under the action of electric current of sodium-filled cracks (mode I degradation) and/or internal sodium electrolysis with associated microcracking (mode II degradation). De Jonghe showed that degradation mode II is preceded and favoured by the partial reduction of β/β'' -alumina in molten sodium, which manifests itself in the darkening of the ceramic (chemical coloration).

The present work deals with the behavior in a sodium environment of polycrystalline β/β'' -alumina membranes fabricated in our laboratory. Specially designed sodium/sodium cells were used which enabled: (i) the use of high purity sodium, purified in the cell by electrolysis through an additional β/β'' -alumina membrane; (ii) the estimate of the faradaic efficiency during current flow, which is a measure of the degree of degradation (appearance of electronic conductivity); (iii) the simultaneous study of degradation modes I and II, and of the chemical coloration process of the solid electrolyte in contact with both molten sodium and sodium vapour. The experiments were performed at 350°C with a current density of 1 A-cm⁻². Two kinds of samples were studied: with the symmetric and asymmetric behavior of the polarization at the β/β'' -alumina/molten sodium interface.

The results showed that in the case of symmetric membranes, failure (i.e., appearance of a considerable electronic conductivity) as a result of mode I degradation is observed only after passing more than 1500 A-cm⁻², while the asymmetric membranes fail considerably earlier. Mode II degradation and the chemical coloration processes proceed also at higher rates in the asymmetric samples.

In accord with De Jonghe's results, we also observed a parabolic relationship between the thickness of the colored layer and time. It was found that the rate of the chemical coloration process of polycrystalline β/β'' -alumina is one and the same in molten sodium and in sodium vapour. A clearly expressed influence of the electric field on the rate of the chemical coloration process in molten sodium was observed. All other conditions being equal, the thickness of the colored layer on the cathodic side is considerably larger and on the anodic one considerably smaller than that observed in the absence of an electric field.

CONDUCTIVITY OF MgO-DOPED ZrO₂

Tinglian Wen, Xiafei Li, Zhoukun Kuo and W. Weppner*
 Shanghai Institute of Ceramics, Academia Sinica
 865 Chang-ning Rd.
 Shanghai
 China

*Max-Planck-Institut für Festkörperforschung
 D - 7000 Stuttgart 80
 Federal Republic of Germany

Stabilized ZrO₂ is one of the most important oxide solid electrolytes at high temperatures. The conductivity characteristics on systems of ZrO₂-CaO and ZrO₂-Y₂O₃ have frequently been reported in the literature. The purpose of the present work is to investigate the conductivity of ZrO₂ doped with MgO. The sintered specimens with MgO dopants, ranging from 4.7 mol.% to 12.7 mol.%, were obtained by sintering at 1600°C the ZrO₂-MgO powders prepared by thermal decomposition of the mixtures of zirconium and magnesium hydroxides, which had been made by coprecipitation of ZrOCl₂ and MgCl₂ under addition of NH₄OH.

The specimens were used as the electrolytes in such symmetric cells as: air, Pt|(ZrO₂)_{1-x}(MgO)_x|Pt, air for the conductivity measurement, which was carried out using the complex impedance bridge during heating and cooling runs at temperatures of 450-1450°C. It was observed that the conductivities increased with MgO dopant from 4.7 mol.% to around 8.2 mol.%, and decreased with the further increase in MgO content. A maximum of conductivity was achieved at ~8.2 mol.% MgO, amounting to 2.43 10⁻² ohm⁻¹·cm⁻¹ at 1000°C.

The dependence of conductivity upon temperature exhibited thermal hysteresis. A jump in conductivity occurred at 1100-1150°C during heating in case of MgO dopant lower than about 8.0 mol.%, whereas a sudden drop in conductivity was observed on the same specimens at around 900°C during cooling. The jump and drop in conductivity diminished with increase in MgO content. As to the specimens containing MgO dopants higher than 8.0 mol.%, the thermal hysteresis did not appear.

X-ray diffraction analysis at high temperatures showed that the thermal hysteresis in conductivity may be attributed to the transition between monoclinic and tetragonal phase. The change in conductivity with MgO content was discussed in terms of the phase transition of ZrO₂, depending on X-ray patterns and the association of oxygen vacancies with dopant cations. The results may indicate that the tetragonal solid solution of ZrO₂ probably is the other good oxygen ion conductor, better than the phase with fluorite structure.

The emf was measured on an oxygen concentration cell such as: air, Pt|(ZrO₂(MgO))Pt, O₂+N₂, using a tube specimen as the electrolyte in order to estimate the average transference number of the specimen. The results suggested that oxygen vacancies are the predominant mobile species as in the other cation-doped ZrO₂ electrolytes.

OXYGEN DISORDER IN THE FLUORITE-TYPE CONDUCTORS
(Bi₂O₃)_{1-x}(Gd₂O₃)_x BY X-RAY AND EXAFS ANALYSES

Kichiro KOTO, Haruki MORI and Yoshiaki ITO

Institute of Scientific and Industrial Research,
 Osaka Univ., Mihoga-oka, Ibaraki, 567 Japan

Of oxygen conductors, δ-Bi₂O₃ is the best known conductor, with a conductivity more than ten times that of conventional oxide conductors such as stabilized zirconia. δ-Bi₂O₃ can be stabilized by adding metal oxides at low temperatures but generally has lower conductivity than pure Bi₂O₃ (Takahashi et al., 1975).

To elucidate the conduction mechanism and the reason of the lowering of ionic conductivity due to additions of metal oxides to Bi₂O₃, the relations between oxygen disorder and conductivity have been investigated by X-ray structure analysis and EXAFS spectroscopy.

Powder samples were first synthesized from mixture of both oxides in appropriate compositions at high temperature in platinum crucible. The fluorite-type single crystals of the (Bi₂O₃)_{1-x}(Gd₂O₃)_x system compounds (x=0.10, 0.15, 0.20, 0.25 and 0.30) were obtained by heating the corresponding powders above melting point, annealing at about 1000°C below melting point and then quenched into cold water. The single crystals thus obtained were ground to spherical shape with diameter ~100μm for X-ray study. The lattice constants versus compositions were in good agreement with those of powder (Takahashi et al., 1975). The compositions of the samples were confirmed by site occupancy refinements during the structure study. The structure analyses were focussed on the relations between oxygen disorder and compositions.

The oxygen ions distribute statistically in the tetrahedral voids of the fluorite-type structure. The displacements of oxygen ions from the normal tetrahedral site (xxx;x=0.25) were observed. The magnitude of displacement parameter δ (x=0.25+δ) has close relation with content of Gd₂O₃. The value of δ=0.044 for 10 m/o Gd₂O₃ crystal is two-thirds that of δ=0.066 for the pure Bi₂O₃ at 774°C (Harwig, 1978). For 25 m/o Gd₂O₃ crystal, the displacements could be little observed. The results indicate that extent of oxygen disorder has close relations with content of Gd₂O₃ and ionic conductivity.

X-ray absorption measurements near the Bi-L III edge (13.426 KeV) were made in transmission with Synchrotron Radiation at National Lab. for High Energy Physics, Tsukuba, Japan. The measurements were carried out for the powder samples with compositions of 10 and 30 m/o Gd₂O₃ at room temperature. The powder was prepared by heating the mixture of Bi₂O₃ and Gd₂O₃ in powder form at about 900°C. The fluorite-type structure was confirmed by X-ray diffraction method before EXAFS measurements.

In obtaining the EXAFS function χ(k), the background level was subtracted from the observed absorption coefficient by using a Victoreen fit and the absorption coefficient for the isolated atom was obtained by the cubic spline technique (Maeda et al., 1982).

The conduction mechanism is discussed based on the results of X-ray structure analysis and EXAFS.

SPECIFIC HEAT OF NON-STOICHIOMETRIC CeO₂

I. Riess, Physics Department, Technion, Haifa 32000, Israel; M. Ricken and J. Noelting, Department of Physical Chemistry and SFB 126 of Goettingen-Clausthal, Goettingen University, 6 Tammannstr., D3400, Goettingen, Federal Republic of Germany.

Cerium dioxide, CeO₂, is reduced at elevated temperatures, T, and low oxygen pressures to form so-called nonstoichiometric phases, CeO_y. For T > 921K, 2 > y > 1.88 a single α phase exists for which y may obtain a continuum of values. At lower temperature reduced ceria exists of discrete compositions^{1,2}. Similar phases were observed in the oxides PrO_y and TbO_y.³

The oxygen vacancies in ceria are quite mobile. Therefore doped Ceria was considered for use in high temperature fuel cells.^{4,5} Reduced ceria is a mixed conductor with a dominant electronic conductivity.

The structure of reduced ceria phases was investigated by X-ray diffraction,^{6,7} neutron diffraction,⁷ and electron microscopy.⁸ Thermogravimetric,¹ electrical conductivity⁹, seebeck⁹, emf¹⁰, and heat of oxygen solution¹¹ measurements reveal some of the thermodynamic properties of reduced ceria.

A measurement of specific heat, c_p, was however not done so far. We report here on c_p measurements on reduced CeO₂ in the composition range CeO₂-CeO_{1.7} and temperature range 320-1200K. The oxide was reduced in situ allowing the variation of the composition in small steps. The temperature was scanned continuously. This yielded detailed information over the y,T plane enabling the construction of a new phase diagram for CeO_y. It differs from that assumed so far and given by Bevan and Kordis.¹ Phases outside the homologous series Ce_nO_{2n-2} as well as new transformation temperatures, were observed. The c_p data for two coexisting phases and their first order transformation is presented and analyzed. Values for the standard enthalpy of the phases are evaluated. Non-equilibrium effects are discussed. They are inherent to the two phase transformations and are due to increased local pressure on incapsulated crystallites.

1. D.J.M. Bevan and J. Kordis, J. Inorg. Nucl. Chem. 26, 1509 (1964).
2. M. Ricken, J. Noelting and I. Riess, J. Solid State Chem. 54, 89 (1984).
3. L. Eyring in "Solid State Chemistry of Energy Conversion and Storage", ed. J.B. Goodenough and M.S. Whittingham, p. 240, Adv. Chem. Series 163, Amer. Chem. Soc. Washington, D.C. (1977).
4. P.N. Ross, Jr., and T.G. Benjamin, J. Power Sources 1, 311 (1977).
5. I. Riess, D. Braunshtein and D.S. Tannhauser, J. Am. Ceram. Soc. 64, 479 (1981).
6. G. Brauer and K. Ginerich in "Rare Earth Research", ed. E.V. Kleber, Lake Arrowhead, CA 1960, p. 96, The MacMillan Comp. (Pub. 1961).
7. S.P. Ray, A.S. Nowick and D.E. Cox, J. Solid State Chem. 15, 344 (1975).
8. P. Knappe and L. Eyring, to be published.
9. H.L. Tuller and A.S. Nowick, J. Phys. Chem. Solids 38, 859 (1977).
10. F.A. Kuznetsov, V.J. Belyi and T.N. Resukhina, Dokl. Akad. Nauk. SSSR 139, 1405 (1961).
11. J. Compserveux and P. Gerdanian, J. Solid State Chem. 23, 73 (1978).

INCOMMENSURATE STRUCTURES IN THE f.c.c. PHASE OF STABILIZED Bi₂O₃

S. Suzuki, H. Iwahara* and M. Tanaka

Department of Physics, Faculty of Science, Tohoku University, Sendai 980, Japan

*Department of Environment Chemistry and Technology, Faculty of Engineering, Tottori University, Tottori 680, Japan

Among the stabilized Bi₂O₃, (Bi₂O₃)_{0.85}(Nb₂O₅)_{0.15} and (Bi₂O₃)_{0.73}(Y₂O₃)_{0.27} have very high ionic conductivities, whose values are about ten times as high as the value of the stabilized ZrO₂. In order to reveal the mechanism of the ionic conduction of these materials, the spacial arrangements of the cations and anions have been studied by the selected-area electron diffraction and high-resolution electron microscopy. One of the authors (H.I.) made the polycrystals of (Bi₂O₃)_{0.85}(Nb₂O₅)_{0.15} and (Bi₂O₃)_{0.73}(Y₂O₃)_{0.27} by sintering at 900°C and 1000°C, respectively. Thin single-crystal fragments were selected out from the polycrystals for the specimens of electron diffraction and electron microscopy.

(Bi₂O₃)_{0.85}(Nb₂O₅)_{0.15} Incommensurate satellite reflections have been observed at the positions of 0.366·d₁₁₁ from all the fundamental reflections. The crystal structure images by the incommensurate reflections show that two commensurately modulated structures which are modulated by the periods of two- and three-times the (111) spacing of the f.c.c. Bi₂O₃ are mixed randomly with the average volume ratio 0.27 x 2 : 0.73 x 3, respectively. The incommensurate value 0.366·d₁₁₁ is obtained from the average volume ratio by the calculation (0.27 x 2 + 0.73 x 3)⁻¹.

If the bismuth ions occupy all the cation sites in every two- and three-(111) planes, the bismuth-ion concentration is expected to be 0.838 by the formula 4α-6α²+4α³-α⁴, where α=0.366 and the value agrees well with that expected from the chemical formula, 0.85. When the (111) bismuth layers are formed, to maintain the local charge neutrality, the (111) vacancy layers in the anion sublattice may be likely to be formed adjacent to the bismuth layers, although the vacancy layers are partially occupied by oxygen ions because the vacancy concentration is lower than the bismuth concentration. The close inspection of the crystal structure images give a confidence about the validity of these speculations. That is, the dark lines run along the [111] direction and are accompanied by white dotted lines. The dark lines would correspond to the (111) bismuth layers and white dotted lines to the vacancy layers.

Localized diffuse scattering appears at the positions of 0.159·d₂₀₀ from the fundamental reflections and has a completely different intensity profile from the incommensurate satellites. Its origin is under investigation.

(Bi₂O₃)_{0.73}(Y₂O₃)_{0.27} Sharp streaks appear along the [111] direction and connect fundamental reflections. This indicates that there exists the modulated structures similar to the (Bi₂O₃)_{0.85}(Nb₂O₅)_{0.15} case. However, the structures in this case have almost continuous modulation spacings along the [111] direction.

The high ionic conductivities of these systems can be explained, because the oxygen ions in the vacancy layers would move much easier than in stabilized ZrO₂.

A STRUCTURAL STUDY OF THE MIXED OXIDE CONDUCTOR M_2O_3 -DOPED Bi_2O_3

P.D. Battle,¹ C.R.A. Catlow² and L.M. Moroney²

¹Department of Inorganic and Structural Chemistry,
Leeds University, Leeds LS2 9JT.

²Department of Chemistry, University College London,
20 Gordon Street, London WC1H 0AJ.

The fluorite-structured δ phase of Bi_2O_3 , stable only above 730°C, exhibits a very high oxygen ion conductivity of approximately $1 \Omega^{-1}cm^{-1}$ [1]. The addition of certain trivalent metal oxides such as Y_2O_3 , and the rare earth oxides to Bi_2O_3 , enables the superionic fluorite-structured phase to be stabilised at room temperature [2]. The mixed-metal systems, however, have a higher Arrhenius energy for oxygen ion migration and thus, a lower ionic conductivity.

In this paper, we report the results of a structural study of the fluorite phase of Y_2O_3 -doped Bi_2O_3 , by a concerted use of Bragg and diffuse scattering techniques and EXAFS with a view to determining the means by which the dopant ion stabilises the fluorite phase and its effect on vacancy ordering within the material at room temperature and at elevated temperatures.

Neutron scattering data have been obtained for two members of the $(Bi_2O_3)_{1-x}(Y_2O_3)_x$ system with $x = 0.27$ and 0.40 at room temperature and 750°C. These reveal an increase in the number of $\langle 111 \rangle$ -displaced anions as the Y_2O_3 concentration decreases, i.e. as the oxygen ion conductivity increases. There is also an increase in the number of $\langle 111 \rangle$ -displaced anions when the sample is heated to 750°C, although the occupation of these off-lattice sites is considerably lower than was observed for the δ phase of Bi_2O_3 , [3]. The diffuse neutron scattering reveals a large amount of short-to-medium range ordering which increases with the Y_2O_3 content of the material. This is attributed to incipient superlattice formation induced by the presence of the dopant. Heating to 750°C reduces the amount of ordering on the oxygen sublattice. The EXAFS data show there is a considerable degree of static displacement within the Y and Bi nearest-neighbour oxygen co-ordination shell and no evidence for cation-cation ordering could be detected. These results will be compared with structural data obtained for the fluorite-related phase of M_2O_3 , doped Bi_2O_3 , where M = Er and Yb. $(Bi_2O_3)_{0.8}(Er_2O_3)_{0.2}$ has been shown to exhibit the largest oxygen ion conductivity of the $(Bi_2O_3)_{1-x}(M_2O_3)_x$ series studied to date [4].

- [1] T. Takahashi and H. Iwahara, Mater Res. Bull. **13**, (1978), 1447.
 [2] T. Takahashi, H. Iwanara and T. Esaka, J. Electrochem. Soc., **124**, (1977), 1563.
 [3] P.D. Battle, C.R.A. Catlow, J. Drennan and A.D. Murray, J. Phys.C., **16**, (1983) 561-566.
 [4] M.J. Vervek, K. Keizer and A.J. Burggraaf, J. Appl. Electrochem. **10**, (1980), 81.

PHASES STABILITY AND CONDUCTION PROPERTIES IN
THE Bi_2O_3 -PbO-PbF₂ SYSTEM

C. HOUTTEMANE, J.C. BOIVIN and D. THOMAS
Laboratoire de Cristallographie et Physicochimie du Solide (UA 452)
Ecole Nationale Supérieure de Chimie de Lille
B.P. 108 59652 Villeneuve d'Ascq Cédex, FRANCE

and
A. TAIRI, J.C. CHAMPARNAUD-MESJARD, D. MERCURIO and B. FRIT
Laboratoire de Chimie Minérale Structurale (L.A.CNRS n°320)
UER des Sciences 123 Avenue A. THOMAS
87060 LIMOGES CEDEX, FRANCE

Fluorides have been extensively investigated for use as separators in electrochemical devices. Oxyfluorides could offer an attractive alternative. They often exhibit higher thermal stabilities and can be easily manufactured as compact membranes. Bismuth-lead mixed oxides and mixed fluorides respectively show high O²⁻ and F⁻ conductivities (1-2). This behaviour can be related to the high polarisability of the the cation framework. Investigations in the PbF_2 - $BiOF$ system performed by MATAR and coworkers (3) show the existence of a fluorite type solid solution with conductivities of the order of magnitude of that of bismuth-lead mixed fluorides.

We present the results of investigations in the ternary system : Bi_2O_3 -PbO-PbF₂. Several solid solutions, belonging to different structural types, have been evidenced. Synthesis conditions and thermal stability range have been investigated by means of X-Ray diffraction technics.

Conductivity measurements performed by a.c. methods show that some compositions exhibit high conduction properties. The σ values will be presented and discussed in relation with the oxygen and fluorine contents.

- 1- HONNART, F., BOIVIN, J.C., THOMAS, D. and DE VRIES, K.J., Solid State Ionics, **10** (1983) 921.
 2- REAU, J.M. and PORTIER, J., Solid Electrolytes, Fluorine Ion Conductors, Academic Press, (1978) 313.
 3- MATAR, S., REAU, J.M. and HAGENMULLER, P., J. of Fluorine Chem., **20** (1982) 529.

CHEMICAL SYNTHESIS AND CONDUCTIVITY STUDY OF DOPED
MULLITE SOLID SOLUTIONS

Guang-yao Meng, Wun-qing Cao and Ding-kun Peng
Department of Applied Chemistry
University of Science and Technology of China
Hefei, Anhui
People's Republic of China

The paper reports that mullite and doped mullite solid solutions were synthesized by a wet chemical method, and the conductivities of samples were measured. The results showed that the conductivities were dependent on the nature and amount of dopant and sintering temperature of samples. The highest value was obtained on a sample of Y_2O_3 -doped material, which was $1.2 \times 10^{-4} (\Omega\text{-cm})^{-1}$ at 800°C and $0.8 \times 10^{-3} (\Omega\text{-cm})^{-1}$ at 1200°C , higher than the best value in the literature by almost one order of magnitude.

La_2O_3 - and ZrO_2 -doped materials exhibited distinctly two-stage conductivity curves, which implied a different defect structure and conduction behaviour at different temperature regions. Ethylorthosilicate ($Si(C_2H_5O)_4$), an inexpensive chemical, was used in addition as a precursor chemical of active SiO_2 to prepare mullite samples by a conventional dry process. The samples obtained showed a better conductivity even than that by a wet method. That is of great significance to practical application and development of the mullite materials.

GRAIN GROWTH IN LIME-STABILIZED ZIRCONIA
IN THE PRESENCE OF A LIQUID PHASE

S. Dou
Department of Chemistry
Northeast University of Technology
Shenyang, China

P. D. Pacey
Department of Chemistry
Dalhousie University
Halifax, NS B3H 4J3

C. R. Masson and B. Marple
National Research Council of Canada
Halifax, NS B3H 3Z1

Abstract

Calcium-doped zirconia, CSZ (7.5 wt % CaO), with impurities of Al_2O_3 , SiO_2 , MgO, Fe_2O_3 and TiO_2 , was sintered in air at 1783 K for times, t , from one hour to 230 hours. The microstructure was studied by electron microscopy and by X-ray analysis and was found to consist of grains of CSZ and small amounts of pores and of a $CaO-Al_2O_3-SiO_2$ eutectic. The grain diameters grew in proportion to $t^{1/3}$. The results were consistent with a mechanism in which grain growth was limited by diffusion of Zr ions through the liquid eutectic. There was a slow decline in the SiO_2 content of the ceramic.

STRUCTURE OF THE MIXED CONDUCTOR $Ni_{2.0}O_{3.4}H$

BY POWDER NEUTRON DIFFRACTION

C. Greaves, A.M. Speed and H.A. Thomas

Department of Chemistry,
University of Birmingham,
Birmingham B15 2TT,
England.

The cathode reaction in most secondary alkaline cells comprises the interconversion of $Ni(OH)_2$ and $NiOOH$, and involves solid state proton transport. However, the small crystallite size of oxidised phases has prevented detailed structural characterisation, and the mechanism of proton migration remains unclear.

Using hydrothermal techniques, a single phase material has been synthesised with an average Ni oxidation state of 2.67. Although the crystallites are still not large - typically platelets of thickness 370(50) Å and diameter 1100(400) Å - the crystallographic and magnetic structures have been determined using an automatic indexing program followed by Rietveld refinement of powder neutron diffraction data obtained at 4.5 K. The unit cell (orthorhombic, Pnmm, $a = 5.084(1)$ Å, $b = 2.9103(6)$ Å, $c = 13.954(3)$ Å) implies a nominal composition Ni_2O_3H with $Z = 4$, but chemical analysis and refined parameters suggested an actual stoichiometry $Ni_{1.95}O_{3.81}H$. The H atoms were located using Difference Fourier techniques and weak O-H...O bonds exist. An interesting feature of the structure is that at the temperature of the determination, Ni^{2+} and Ni^{4+} species are present rather than the expected Ni^{2+} and Ni^{3+} .

The relevance of this phase to battery materials has still to be established, but certain features suggest a relationship to the hitherto uncharacterised β - $NiOOH$. The material is a semiconductor, and proton conductivity has therefore been examined using electron-blocking electrodes. Initial results imply the relatively high conductivity $\sigma_{H^+} \sim 5 \times 10^{-3} \text{ ohm}^{-1} \text{ cm}^{-1}$ at 298 K, very similar to values obtained for β - $NiOOH$.

Electrochemical Insertion of Lithium and Sodium into the two
Crystallographic Forms of a New Molybdenum chalcogenide Phase
 $Mo_{15}Se_{19}$

J. M. Tarascon

Bell Communications Research
Murray Hill, New Jersey 07974

Topotactic redox reactions have been intensively studied for the Chevrel phases Mo_xX_6 ($x = S, Se$), whose structure (build-up of Mo_6X_8 clusters) contains large open channels. New ternary molybdenum chalcogenides ($In_3Mo_7Se_{19}$, $In_2Mo_7Se_{19}$), resulting from a linear condensation of the Mo_6 octahedron have been recently reported. Both materials are composed of Mo_6Se_8 and Mo_7Se_{11} clusters packed three-dimensionally in a different way. Here we will show that indium can be pulled out from these compounds at low temperature (420°C) by oxidation under an HCl flow, yielding a new phase $Mo_{15}Se_{19}$. X-ray studies reveal that during the oxidation the arrangement of Mo_6Se_8 and Mo_7Se_{11} clusters is maintained leading to two crystallographic forms for $Mo_{15}Se_{19}$, denoted A and B when $In_3Mo_7Se_{19}$ and $In_2Mo_7Se_{19}$ are used as starting materials respectively. The crystallographic lattice parameters are $a_0 = 9.793$ Å, $c_0 = 19.775$ Å and $a_1 = 9.587$ Å, $c_1 = 58.151$ Å for A and B respectively. The chemical and electrochemical insertion of lithium and sodium into the two crystallographic forms (A,B) of $Mo_{15}Se_{19}$ will also be presented. For lithium, cycling data down to 1.3 volts, shows that the voltage-composition curves are similar for A and B phases, and furthermore indicates that $Mo_{15}Se_{19}$ can take-up reversibly up to 8 lithiums ($Li_8Mo_{15}Se_{19}$). This value agrees perfectly with the one expected from the limiting ionic formula $[Mo_6Se_8]^{4+}[Mo_7Se_{11}]^{4-}$. In contrast, cycling data reveals a quite different behavior of A and B phases with respect to sodium intercalation, namely an higher discharge voltage as well as a better reversibility for the cell using $Mo_{15}Se_{19}$ (B) as cathode. The different stacking of Mo_6Se_8 and Mo_7Se_{11} clusters in A and B phases leading to different three-dimensional network of channels in which the ternary element can be inserted will be used to explain the observed electrochemical data, namely the anomalies in the voltage/composition curves, and differences between sodium and lithium intercalation.

LITHIUM INSERTION/EXTRACTION REACTIONS WITH LiVO_2 AND LiV_2O_4 L A de Picciotto and M M ThackerayNational Institute for Materials Research, CSIR,
P O Box 395, Pretoria 0001, South Africa

ABSTRACT

Lithium insertion into LiV_2O_4 and extraction from LiVO_2 and LiV_2O_4 have been investigated both chemically and electrochemically. Structural characteristics of the lithiated and delithiated products have been determined.

Lithium extraction from the layered LiVO_2 structure results in a rearrangement of the vanadium ions in the cubic-close-packed oxide lattice; in $\text{Li}_{0.22}\text{VO}_2$ approximately one third of the vanadium ions reside in the octahedral sites of the lithium-deficient layer. The removal of lithium from the structure reduces the c/a ratio of the trigonal lattice constants to almost cubic symmetry. Heat-treatment of $\text{Li}_{0.5}\text{VO}_2$, obtained by chemical delithiation of LiVO_2 , to $\sim 300^\circ\text{C}$ results in a transformation to the spinel LiV_2O_4 . Similar heat-treatment of $\text{Li}_{0.45}\text{VO}_2$ results in the cation-deficient spinel $\text{Li}_{0.9}\text{V}_{0.1}[\square_{0.1}\text{V}_{1.9}]\text{O}_4$ with vacancies on the octahedral B-sites of the spinel structure.

Extensive delithiation of LiV_2O_4 ("a" = 8.24 Å) is possible. The powder X-ray diffraction profile of $\text{Li}_{0.3}\text{V}_2\text{O}_4$ is two-phase: it shows a cubic phase with a contracted "a" lattice parameter (8.21 Å) in which the $[\text{V}_2]\text{O}_4$ spinel sublattice remains intact, and the trigonal phase that characterizes an extensively delithiated Li_xVO_2 product ($x \approx 0.1$). Lithium insertion into LiV_2O_4 generates metastable $\text{Li}_2\text{V}_2\text{O}_4$ in which the $[\text{V}_2]\text{O}_4$ spinel framework is retained; the volume of the cubic unit cell increases by 2.2%.

LITHIUM INSERTION REACTIONS IN URANIUM OXIDE PHASES

M.T.Weller and P.C.Dickens
Inorganic Chemistry Laboratory,
South Parks Road,
Oxford.

Lithium insertion compounds of transition metal oxides have been studied extensively, and in particular with respect to their thermodynamic and kinetic properties. Well known examples include Li_xWO_3 (1), $\text{Li}_x\text{V}_2\text{O}_5$ (2) and Li_xCoO_2 . We have recently investigated the lithium insertion compounds of uranium oxides, with emphasis on U_3O_8 and various polymorphs of UO_3 , and now report on their preparation and characterisation.

The electrochemical insertion of lithium into these materials has been studied by monitoring the voltage of the combination $\text{Li(s)}/\text{LiClO}_4/\text{Li}_x\text{UO}_n$, where UO_n is U_3O_8 , αUO_3 or γUO_3 , as a function of x . The form of the discharge curve in each case was used to determine the ranges of composition for several new phases formed during the reduction. Thermodynamic functions $G^\circ x$ and $G(x)$ were determined for the insertion reaction from open circuit measurements and have been compared with those derived for other lithium insertion compounds. Estimates for the rates of diffusion of lithium in these materials were also derived electrochemically using pulse relaxation methods.

Lithium has also been inserted into U_3O_8 , α and γUO_3 chemically, using LiI or n -butyllithium in an inert solvent as the lithiating agent. Analysis of the products using powder X-ray diffraction shows that the basic oxide framework is unchanged in all cases following lithium insertion. Products formed by the reaction with LiI were those expected on thermodynamic grounds from the electrochemical data.

Further studies are in progress in order to elucidate the structures of these insertion compounds using powder neutron diffraction.

- (1) K.H.Cheng and M.S.Whittingham. *Solid State Ionics*, 1, 151 (1980)
- (2) P.G.Dickens and G.J.Reynolds. *Solid State Ionics*, 5, 331 (1981)

DISCHARGE OF SOLID STATE $\text{Li}_3\text{N}+\text{TiS}_2$ COMPOSITE ELECTRODES

Boye Knutz and Steen Skaarup
 Physics Laboratory III
 Technical University of Denmark
 DK-2800 Lyngby, Denmark

Solid state batteries based on the cell configuration $\text{Li}/\text{Li}_3\text{N}/\text{TiS}_2$, have been shown to be able to withstand current densities up to $2 \text{ mA}/\text{cm}^2$ at 170°C with reasonable cycling efficiency. The slow rate of Li^+ transport in the compact cathodes of pressed TiS_2 limits the thickness of the cathode to about 50 microns if discharge times of the order of a few hours are to be possible, and also necessitates the high temperature.

In order to achieve faster ionic transport experiments have been made using composite solid state cathodes of Li_3N and TiS_2 , each 50% by volume. In an ideal composite electrode, the magnitude and temperature variation of the ionic diffusion is that of the electrolyte compound (here Li_3N) modified by a factor depending on the volume fraction. The experiments verified the improvement in Li^+ transport making possible a lowering of the temperature to 140°C and an increase of electrode thickness.

A 0.1 mm thick cathode was cycled with $2 \text{ mA}/\text{cm}^2$ (stoichiometric discharge time: 1.2 h) about 700 cycles. The cycle efficiency of the first 400 cycles was 99.8%. The decrease in capacity was due mainly to kinetic factors, and not to irreversible loss of capacity, since most of the original capacity was available when temporarily discharging with $.15 \text{ mA}/\text{cm}^2$. The apparent chemical diffusion coefficient for Li^+ was $4 \cdot 10^{-8} \text{ cm}^2/\text{s}$ during the first cycles and $3 \cdot 10^{-9} \text{ cm}^2/\text{s}$ after 700 cycles. The charge factor was 1.1 at $2 \text{ mA}/\text{cm}^2$ due to unidentified processes but very close to unity at $0.15 \text{ mA}/\text{cm}^2$.

A similar cell was cycled at $4.3 \text{ mA}/\text{cm}^2$ in order to test the limits of current density. The charge factor in this case stayed at 1.0 during the 30 cycles before dendrite formation. The separator was .2 mm sintered Li_3N .

The apparent Li^+ diffusion coefficient was $1.6 \cdot 10^{-7} \text{ cm}^2/\text{s}$ - this is far higher than for pure TiS_2 powder showing that the composite electrode works. Theoretical maximum values range from $1-7 \cdot 10^{-7} \text{ cm}^2/\text{s}$ depending on the expression used. The activation energy was .4 eV - rather far from the Li_3N value of .26 eV.

LITHIUM TRANSPORT KINETICS IN
TERNARY LITHIUM-COPPER-OXYGEN CATHODE MATERIALS

Ned A. Godshall

Sandia National Laboratories
 Exploratory Batteries Division 2523
 Albuquerque, NM 87185

INTRODUCTION

The interdependence of thermodynamic parameters, phase equilibria, and electrochemical measurements was used in the investigation of the Li-Cu-O ternary phase system, in order to better understand the cathodic reactions which occur within Lithium/Copper Oxide cells. Li-M-O phase relationships were previously determined in the Mn , Fe , and Co ternary systems at both ambient and elevated temperatures¹. An understanding of the Li-Cu-O ternary phase diagram was undertaken in order to predict battery performance. Both open-circuit voltages and plateau capacities were predicted from such information. Each triangle in a ternary phase diagram represents a three-phase equilibria of the phases lying at the corners of each tie triangle. The constant activity of Li in a tie triangle may be calculated from the free energy of reaction between Li and the three phases in equilibrium.

Effect of Intermediate Ternary Oxides

The free energies of formation of the intermediate ternary oxides were not previously known. They were measured electrochemically at 25°C in cells of the type:

$\text{Li} / \text{PC}, 1.0\text{M LiClO}_4 / \text{Li}_x\text{CuO}_y$
 and were found to be -86.3 kcal/mole for LiCuO and approximately -167 kcal/mole for Li_2CuO_2 . Two equilibrium discharge plateaus were observed in Li/CuO cells, with open-circuit values of 2.20 and 2.08 volts vs. Li ; however, the composition corresponding to the beginning of the lower plateau was somewhat masked by morphological considerations and relatively slow kinetics. X-ray diffraction analyses confirmed the equilibrium cathode reactions.

The system was found to polarize strongly at current densities in excess of $1-2 \text{ mA}/\text{cm}^2$, with correspondingly long equilibration times. The slow kinetics of this system are also apparently manifested in lower observed open-circuit voltages (after partial discharge) than those predicted thermodynamically, $1.6-1.8 \text{ V}$ versus $2.2-2.4 \text{ V}$, respectively. A theoretical discussion of the possible rate-limiting steps in the solid Li_xCuO_y multi-phase cathodes is given. These include 1) transport of Li ions through CuO , 2) formation of marginally-unstable non-equilibrium phases during high cell polarization, and 3) transport of electrons through electronically-insulating Li_2O or LiCuO ternary phases.

REFERENCES

1. N. A. Godshall, I. D. Raistrick, and R. A. Huggins, J. Electrochem. Soc. 131, 543 (1984).

LITHIUM ION INSERTION INTO $\text{Li}_{1-x}\text{CoO}_2$

P.G. Bruce
 Department of Chemistry, Heriot-Watt
 University, Riccarton, Edinburgh,
 EH14 4AS, U.K.

and
 M.G.S.R. Thomas and J.B. Goodenough,
 Inorganic Chemistry Laboratory,
 University of Oxford, South Parks Road,
 Oxford OX1 3QR, U.K.

A.c. impedance measurements have been employed to characterise the processes associated with reversible insertion of lithium ions from the non-aqueous electrolyte, LiBF_4 in propylene carbonate, into the layered intercalation electrode $\text{Li}_{1-x}\text{CoO}_2$. Studies were carried out principally on the composition $x = 0.34$. The frequency dependent a.c. response of this porous insertion electrode can be divided into high and low frequency regions.

The high frequency region is associated with Li^+ -ion exchange at the electrolyte/electrode interface, two semicircles are observed in the complex impedance plane. Models involving a significant charge transfer process coupled with either adsorption or surface layer formation fit the observed response equally well. Time dependent experiments eliminated the adsorption model. Constant voltage experiments and the preparation of electrodes with greater electrolyte/electrode interface area, coupled with electron microscopy, provided evidence for the surface layer model. We propose that propylene carbonate is polymerised on the electrode surface producing a thick ($\sim 30\text{\AA}$) polymeric coating somewhat permeable to lithium ions.

Only by including a constant phase angle expression in the equivalent circuit representing these models could an adequate fit to the observed data be obtained. This arises from the porous nature of the electrode.

The low frequency a.c. response is associated with the diffusion of lithium ions in the electrode. Warburg behaviour is observed which, at the lowest frequencies, turns upwards to form a vertical spike in the complex impedance plane, indicating a transition from semi-infinite to finite length diffusion. We determined the Li^+ -ion diffusion coefficient for $\text{Li}_{0.65}\text{CoO}_2$ by three separate methods.

- (1) Extraction of the Warburg prefactor from the a.c. results.
- (2) Determination of the transition frequency from semi-infinite to finite length diffusion.
- (3) A modified Tubandt technique which couples the traditional Tubandt cell with an a.c. measurement to eliminate interfacial resistances, permitting a direct measurement of the lithium ion conductivity in this mixed conductor.

The three techniques are in close agreement yielding lithium diffusion coefficients in the range $4.7\text{--}5.2 \times 10^{-12}\text{m}^2\text{s}^{-1}$. Over the composition range $0.45 < (1-x) < 0.80$, D_{Li} increases slightly from 5 to $7 \times 10^{-12}\text{m}^2\text{s}^{-1}$, this is amongst the highest lithium diffusion coefficients reported for such systems.

Structural Aspects of Alkali Metal Insertion
Compounds with the Pyrochlore Structure

D. W. Murphy*, R. J. Cava*, K. Rhyne†, R. S. Roth†,
 S. M. Zahurak*, and J. L. Dye†

*AT&T Bell Laboratories
 Murray Hill, New Jersey 07974
 U.S.A.

†National Bureau of Standards
 Washington, D.C. 20234

‡Chemistry Department
 Michigan State University
 E. Lansing, MI 48824

ABSTRACT

Compounds with the pyrochlore structure are of interest both as solid electrolytes and as ion insertion hosts. The cubic framework structure with space group $\text{Fd}\bar{3}\text{m}$ is able to accommodate the alkali metal ions from Na through Cs as well as pseudoalkalies such as H_3O^+ , NH_4^+ and Tl^+ . We recently showed that pyrochlores of stoichiometry A_2NbWO_6 (A=Na, K, Rb) readily undergo insertion reactions with alkali metals to give A_xNbWO_6 . This study presents further data on these compounds including structures determined from neutron powder diffraction data for KNbWO_6 , K_2NbWO_6 , $\text{KNbWO}_6 \cdot \text{H}_2\text{O}$ and hopefully by August some Rb and Na compounds as well.

The structural feature of importance to ionic mobility is the presence of two major sets of sites for the alkali ions. There is one large site (8b) per formula unit which has six nearest oxygen ions and eight more slightly further away, and there are two somewhat smaller six coordinate sites (16d). There also exists the possibility of occupation of a more general site (32e) located along a line between the two special sites. For KNbWO_6 , K is located on 32e approximately 25% of the way from 8b to 16d. Hydration and insertion of K leads to exclusive occupation of the 16d sites by K. The water in $\text{KNbWO}_6 \cdot \text{H}_2\text{O}$ occupies 32e sites. Hydration of KNbWO_6 is rapid and reversible near 100°C , but $\text{NaNbWO}_6 \cdot \text{H}_2\text{O}$ dehydrates only above 300°C . We expect an important difference in the role of water in $\text{NaNbWO}_6 \cdot \text{H}_2\text{O}$.

ELECTROCHEMICAL CHARACTERIZATION AND PREPARATION
OF SEMICONDUCTING MATERIALS

Werner Weppner

Max Planck Institute for Solid State Research
D-7000 Stuttgart-80, Germany

Solid state electrochemical techniques were employed to prepare semiconducting materials and also to investigate their phase equilibria, thermodynamic properties and kinetic behavior. The electronic properties of the semiconductors were sensitively controlled by coulometric titration processes using auxiliary electrolytes for several ternary systems and some classical doped element semiconductors. Local variations of the electronic properties were formed by the application of dc voltages using ionically blocking electrodes.

The electronic species of semiconducting compounds may produce high internal electrical fields which often result in extremely high liquid like ionic (atomic) diffusion coefficients in the solid state. The knowledge of these relationships allows to produce fast semiconducting electrodes for batteries, electrochromic displays and other devices. Semiconducting electrodes will generally show much lower polarizations and faster response times than metallic conductors which were previously favored as electrode materials.

The application of small dc voltages to semiconductors produces inhomogeneities of the composition in a formal analogy to Nernst's law. This produces local variations of the semiconducting properties. p-n junctions were formed and reversibly removed by switching small voltages on and off. Oxygen has been desorbed to the gas phase and reversibly absorbed in the case of oxide semiconductors.

In addition, electrochemical reduction and oxidation processes often produce interesting semiconductor structures by kinetic reasons. These may be very different from thermodynamically expected patterns. Compositions may be formed which would not be expected from a point of view of phase equilibria. These semiconductor structures may be formed at higher temperatures and then quenched to room temperature.

NMR STUDY OF ONE-DIMENSIONAL IONIC CONDUCTOR WITH HOLLANDITE-TYPE STRUCTURE
IV. Rb-PRIDERITE

Y.ONODA, Y.FUJIKI,
National Institute for Research in Inorganic Materials
1-1, Namiki, Sakura-mura, Nihari-gun, Ibaraki 305, Japan

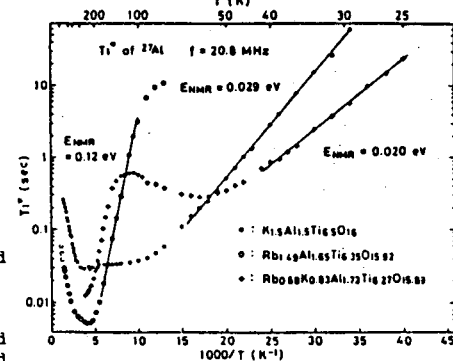
S.YOSHIKADO, T.OHACHI and I.TANIGUCHI
Department of Electronics, Doshisha University, Kyoto 602, Japan

Size effect on the conduction properties of priderites was investigated by NMR using ^{27}Al in the framework as the probe. Temperature dependences of spin-lattice relaxation time T_1 were measured on two samples, $\text{Rb}_{1.49}\text{Al}_{1.55}\text{Ti}_{1.35}\text{O}_{15.92}$ (RATO) and $\text{K}_{0.89}\text{Rb}_{0.68}\text{Al}_{1.73}\text{Ti}_{1.23}\text{O}_{15.89}$ (RKATO) and the results are given in Figure 1.

$\log(T_1)$ of RATO shows linear dependence on $1/T_1$ in the temperature range from 105 K to 167 K and the slope gives a value, $E_{\text{NMR}} = 0.12$ eV. Frequency dependence of T_1 measured at 125 K and in the frequency range from 11.1 MHz to 20.8 MHz is $T_1 \propto \omega^{-1.53 \pm 0.15}$ and is nearly the same with the dependence of K-priderite (KATO), $T_1 \propto \omega^{-1.49 \pm 0.05}$, measured in the frequency range from 10 MHz to 55 MHz. [1] This result indicates that the relaxation of RATO is also described by the continuum model. Therefore, the intrinsic activation energy E of Rb^+ ion is determined to be $E = 0.24$ eV using the relation $E = 2 \times E_{\text{NMR}}$. T_1 reaches the minimum value at 240 K and then it increases with a small shoulder at about 400 K, which is thought to be the effect of the impurity barriers in conduction channels. The slope above 450 K is $E_{\text{NMR}} \sim 0.16$ eV and the ratio of E_{NMR} of RATO and KATO ($E_{\text{NMR}} \sim 0.12$ eV) in the high temperature region is not so large as the ratio (~ 4.0) in the low temperature region.

The spin-lattice relaxation of RKATO below 100 K is dominated by the ionic motion of K^+ ion. Temperature dependence of T_1 shows a symmetrical curve at temperatures around 60 K where T_1 takes a minimum value. E_{NMR} in this region is 0.020 eV and is much smaller than the value of KATO. The value of E_{NMR} is very sensitive to a slight change in the lattice constant of the a-axis [2] and the decrease in E_{NMR} of RKATO is attributed to a slight increase ($\sim 0.26\%$) in the lattice constant. The motion of Rb^+ ion is observed above 110 K. The slope E_{NMR} in the temperature region from 150 K to 200 K is a little larger than that of RATO and it will be also explained by a slight decrease in the lattice constant from the value of RATO.

[1] Y.Onoda et al, to be published
[2] Y.Onoda et al, to be published



A. Fontana+, G. Mariotto+, E. Cazzanelli+, F. Rocca-,
V. Mazzacurati-, G. Ruocco-, G. Signorelli-

+: Dipartimento di Fisica, Università di Trento;
38050-Povo (Trento), ITALY

-: Centro di Fisica degli Stati Aggregati e Impianto Ionico
del CNR di Trento; 38050-Povo (Trento), ITALY

~: Dipartimento di Fisica, Università "La Sapienza";
00185-Roma, ITALY

In a previous paper (1) we have reported temperature dependent Raman spectra in the phase of silver iodide, showing the appearance, between liquid helium and liquid nitrogen temperature, of some broad features not accounted for by the usual normal modes analysis.

We have now carefully repeated the Raman measurements in different polarization settings and with different crystal orientations. The analysis of the the depolarization ratios helps to separate these broad features from the narrow polarized peaks due to the $K \approx 0$ phonon scattering.

The normal modes shift slightly toward lower frequencies and broaden at increasing temperatures, in such a way to be considered almost harmonic.

Therefore, taking away from the spectra the total contribution of the $K \approx 0$ modes and dividing this spectral intensity by the factor $[(n(\omega)+1)/\omega]$, we get a spectral density which can be closely related with the vibrational density of states of the crystal. Above 100°K up to room temperature the main shape of this spectral density does not change; below the liquid nitrogen temperature we can see these "extra-modes" arising below the normal modes, until they get the shape conserved at higher temperatures.

Assuming the induced polarizability mechanism already adopted for the phase (2, 3) and supposing that the increasing disorder produces a lower range of correlation in the local polarizability term, we have been able to extract the overall density of states. Starting from this result we can measure the degree of disorder between 4 and 100°K, represented by the correlation length of the induced polarizability, which explain the shape of the Raman spectral density at any temperature.

The polarizability mechanism adopted in this work is consistent with the experimentally observed depolarization ratios of the "extra-modes" contributions, which are frequency independent and slightly decreasing at higher temperatures. Works are in progress to give a quantitative analysis of the changes in the Raman spectra between liquid helium and room temperatures.

- 1) A. Fontana et alii, Solid State Comm. 28, 35 (1978)
- 2) V. Mazzacurati et alii, Phys. Review B 26, 2216 (1982)
- 3) E. Cazzanelli et alii, Phys. Review B 28, 7269 (1983)

EQUIVALENT CIRCUIT ANALYSIS OF HIGH TEMPERATURE SOLID ELECTROLYTE

NOBORU MATSUI

TOYOTA CENTRAL R&D LABS., INC.
41-1, Aza Yokomichi, Oaza Nagakute, Nagakute-cho,
Aichi-gun, Aichi-ken, 480-11, Japan

Some metal oxides were added to YSZ in order to improve the electrical properties, and the impedance dispersion of these materials was measured. The frequency dispersion of the solid electrolyte/electrode system was analysed in terms of the equivalent circuit representation.

Usually, the complex impedance plane for YSZ systems consists of two semicircles or arcs in high and low frequency ranges. The former corresponds to the dispersion for the grain-boundaries of YSZ and the latter to that for the electrode reaction. The simple R-C network circuit, originally proposed by Bauerle, has been extensively applied to analysis of such impedance dispersion data, but sometimes the simple circuit does not coincide with the data. Therefore, we proposed a different simple equivalent circuit for Pt/YSZ with additives/Pt system(1)(2). This circuit involves a frequency dependent element for the electrode reaction part. Recently, we proposed a new symbol as shown in Fig.1(a) to represent the frequency dependent element (3). The symbol is expressed by

$$\hat{Z}_1 = \frac{A}{\omega^n} (1-j) \quad (1)$$

where A and n are variables, ω is the angular frequency, and j is equal to $\sqrt{-1}$. In the case of $n=1/2$, \hat{Z}_1 has Warburg-like frequency dependency. The symbol does not contain any electrochemical meaning, but merely shows the electrical frequency dependence of the impedance.

For Fe₂O₃-doped YSZ, the impedance locus corresponding to grain-boundary part draws a Cole-Cole type arc, a remarkably depressed semicircle. But R-C circuits are inappropriate to express the shape of this arc, even with various R-C couples of parallel and series combination. The arc can be satisfactorily expressed by a simple equivalent circuit shown in Fig.2, which contains a new symbol shown in Fig.1(b). The new symbol is an extended expression of Fig.1(a). This impedance element is given by

$$\hat{Z}_2 = A \left(\frac{1}{\omega^{n_1}} - j \frac{m}{\omega^{n_2}} \right) \quad (2)$$

where m is a very important factor, indicating the circle depression degree. The smaller m is, the more depressed the circle is.

- (1) N. Matsui, Surface Science, 86 (1979) 353.
- (2) N. Matsui, Solid State Ionics, 3/4 (1981) 525.
- (3) N. Matsui, to be published.

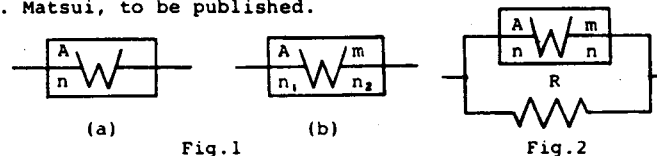


Fig.1

Fig.2

CHARACTERISATION OF THE SOLID COMPOSITE ELECTRODE

MnO₂-γ, acetylen black ; HUP/HUP by impedance spectroscopy

by H. KAHIL, E. J.L. SCHOULER, M. FORESTIER, J. GUITTON

Ecole Nationale Supérieure d'Electrochimie et d'Electrometallurgie de Grenoble, Laboratoire d'Energétique Electrochimique associé au Centre National de la Recherche Scientifique n° 265, B.P. 75, 38402 Saint Martin d'Hères (FRANCE).

This work deals with the characterization of the positive electrode of a "all solid" battery based on a protonic electrolyte (HUP) operating at room temperature.

Different types of electrodes, made either of platinum or of the composite material : MnO₂-γ-acetylen black - HUP have been compared.

The transfer reaction of the proton at the interface has been characterized by impedance spectroscopy at different stages of the discharge.

The relevant diagrams are usually composed of several capacitive loops. In particular conditions of the electrode preparation, additional inductive loops and Warburg lines are observed.

We have shown that the nature of the proton transfer mechanism at the interface is directly related to the composition and preparation technique of the composite electrode.

This result is discussed in terms of the hydratation state of the system.

SOME SUPERIONICS STUDIED BY POSITRONS

S. Linderoth, H.E. Hansen, A. Shishkin*, S. Skaarup**, N.H. Andersen***, M.D. Bentzon and K. Petersen

Laboratory of Applied Physics II, Technical University of Denmark, DK-2800 Lyngby, Denmark

*Visitor from: The Department of Experimental Physics, Moscow Physics Engineering Institute, Moscow, USSR

**Physics Laboratory III, Technical University of Denmark, DK-2800 Lyngby, Denmark

***Physics Department, Rise National Laboratory, DK-4000 Roskilde, Denmark

Abstract

The positron annihilation technique is well established for investigation of defect structures and for measurements of vacancy formation enthalpies in metals [1]. We have employed positrons to study the superionics: Li₃N, BaF₂ and PbF₂, which have been investigated by the means of positron lifetime and angular correlation (ACPAR) measurements.

Li₃N with different content of hydrogen was studied in the temperature range 7-360 K. In Li₃N the average positron lifetime, $\bar{\tau}$, decreases around 80 K by an amount depending on the H-concentration. In the purest Li₃N sample $\bar{\tau}$ decreases again around 200 K. This behaviour of $\bar{\tau}$ seems to be associated with thermal vacancy generation and to support the idea that hydrogen enhances the vacancy concentration in Li₃N [2].

Pure and UF₄-doped BaF₂ has been studied in the temperature range 77-600 K. In the heavily doped samples a lifetime of 238 ps dominates. This component is also present in the pure sample where the intensity increases around 350 K. This component may be associated with interstitial F⁻ ions. Positron lifetime and ACPAR measurements on pure PbF₂ are in progress to throw more light on the positron states in these superionics.

[1] *Positron Solid-State Physics*, ed W. Brandt and A. Dupasquier (North-Holland, Amsterdam, 1983).

[2] T. Labb, S. Skaarup and A. Hooper: *Solid State Ionics* II, 97 (1983).

NMR STUDIES OF THE MIXED CONDUCTOR $\text{Li}_x\text{V}_2\text{O}_5$

Monisha Bose & Anjali Basu
Saha Institute of Nuclear Physics, Calcutta - 9

The mixed conductor $\text{Li}_x\text{V}_2\text{O}_5$ displays different phases depending on the value of x , as also on the method of preparation. Room temperature (rt) lithiation leads to metastable phases α ($0 < x < 0.1$), ϵ ($0.35 < x < 0.5$) and δ ($0.9 < x < 1.1$), where in Li is intercalated between V_2O_5 layers leaving the basic V_2O_5 matrix unaltered. High temperature (ht) technique results in stable phases, wherein α ($0 < x < 0.13$) is a layered orthorhombic, β ($0.22 < x < 0.49$), a monoclinic three dimensional network and γ ($0.88 < x < 1$) a different orthorhombic layered structure. Comparative NMR studies presented here are correlated with structure in an effort to understand the mechanism of conduction. ^{51}V NMR - Intercalated Li exists as Li^+ and creates paramagnetic V^{4+} , which influences the observed V^{5+} spectra. In the slightly perturbed α -phase, the spectra resemble the V_2O_5 (powder) spectrum with satellites and an asymmetric central line with structure in high field side. With increasing x , the paramagnetic effect increases. Thus the satellites becomes weaker and at $x = 0.4$, only the first pair of satellites could be observed. For higher x values, no satellites could be observed for either system. At $x = 0.3$ in rt, where the V_2O_5 layered structure persists, the central line shows only paramagnetic shift and broadening effects. But in the ht β -phase, this line shows a drastic change. For rt, this change occurs above $x = 0.4$. In this region, the broad central line is similar in both comprising a narrow unshifted and a superposed paramagnetically broadened high field shifted line, corresponding to V^{5+} and the mixed valence state arising from $\text{V}^{5+} - \text{V}^{4+}$ exchange. This correlates well with the three different sites in β -phase, where one site does not participate in electron exchange, but exchange occurs between the other two sites. At $x = 1$ for δ and γ phases, the central lines are not very different, as both are layered structures. In ht, the pure γ exhibits two lines from the two different sites, one broad another comparatively narrow. The overall width is less than in rt, where the low field line is very broad.

^{7}Li NMR - In rt, very interestingly a single NMR line almost unchanged in width occurs throughout the composition range, in direct contrast to that in ht. As more Li is introduced in rt, the cell expands (interlayer separation along C increases from 4.4 to 5.0 Å) permitting the creation of new interstitial sites resulting in unchanged Li mobility. In contrast, in the β -phase with an irregular tunnel, the highest Li mobility occurs (line narrows) but in the new layered γ , since Lithium occupies all the available sites at $x = 1$, a highly immobilised Li lattice leads to a broad line.

^{51}V spectra is highly complex and temperature variation studies are contemplated to elucidate the finer details. However, even the present room temperature studies of ^{7}Li and ^{51}V NMR bring out the fact that in rt, possibly the Li is intercalated in 'Stages' and the different phases correspond to the different degrees of 'Staging'. Further the drastic change in ^{51}V spectra at $x = 0.3$ (β) which corresponds to $x = 0.4$ (ϵ) in rt is in consonance with the conductivity values which is maximum at $x = 0.3-0.4$ for ht but at $x = 0.6$ for rt.

ELECTROCHEMICAL DETERMINATION OF THE THERMODYNAMIC PROPERTY OF INTERMEDIATE COMPOUND IN MO-O SYSTEM

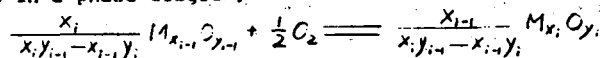
Kuo-chih Chou, Shuang-lin Chen

(Beijing University of Iron and Steel Technology)
(Beijing, People's Republic of China)

ABSTRACT

The thermodynamic properties of intermediate compound M_4O_{11} in MO-O system have been determined by a high-temperature electromotive force (emf) method using stabilized zirconia as the electrolyte over the temperature range from 600 to 800°C.

In order to verify the reliability of our experimental data, a thermodynamic principle, named "the progressive decrease principle of electromotive force in the system containing a series of intermediate oxides", has been developed, that is, for a cell reaction involving two adjacent intermediate compounds in a phase diagram,



where M represents an element and x_i, y_i are stoichiometric coefficients, the corresponding cell electromotive force \mathcal{E} will decrease with increasing the ratio of y_i/x_i and the Gibbs free energy of formation of M_4O_{11} is expressed as

$$\Delta G_{\text{M}_4\text{O}_{11}} = 2X_K \sum_{i=1}^K \frac{x_{i-1} y_i - x_i y_{i-1}}{x_i x_{i-1}} E_i F$$

where F represents the Faraday constant.

The application of this principle to the MO-O system showed that, our results obtained in this investigation are reliable.

There are still plenty of intermediate compounds which thermodynamic properties are not available. The solid electrolytes as an electrochemical cell materials will play an important role in the measuring those properties. It is expected that, the principle introduced here will offer an effective method to verify those experimental data of a series of intermediate compounds in a binary system.

Effective Potentials from Langevin Dynamic Simulations of

Framework Solid Electrolytes

R. O. Rosenberg, A. Nitzan, M. A. Ratner
Department of Chemistry and Materials Research Center
Northwestern University, Evanston, IL 60201

Ionic motion in framework solid electrolytes constitutes a special sort of classical many-body problem. In such electrolytes, the conductivity is due to the motion of interacting mobile ions modulated by the presence of an essentially immobile framework sublattice. Here, a one-dimensional model of interacting particles, governed by Langevin's equations of motion in a sinusoidal potential, is used to calculate particle distribution functions and effective potentials.

The total static potential for ionic motion in a system with N mobile ions contains both one and two body terms:

$$V_N(\{X\}) = \sum_{i=1}^N V_1(x_i) + \sum_{i < j} V_2(x_i - x_j) \quad (1)$$

$V_1(x)$ is the sinusoidal potential,

$$V_1(x) = \frac{A}{2} \cos(2\pi x/a) \quad (2)$$

where A is the barrier height and a is the distance between wells. $V_2(x_i - x_j)$ is assumed to be the sum of pair interactions such as the coulomb potential,

$$V_2(x_i - x_j) = q^2 / |x_i - x_j| \quad (3)$$

where q is an effective charge. The effective potential $V_{\text{eff}}(x)$, is then defined through the density distribution, $\rho(x)$,

$$\rho(x) = z e^{-\beta V_{\text{eff}}(x)} \quad (4)$$

where $\beta = 1/kT$; k is Boltzmann's constant, z a normalization constant, and T the temperature. The Langevin dynamics simulation is used to calculate $\rho(x)$, which in turn gives $V_{\text{eff}}(x)$. In the high friction limit, the dc conductivity of the system can be expressed in terms of the effective potential, [1]

$$\sigma = \rho_0 D_0 \beta \left[\frac{1}{a} \int_0^a dx e^{\beta V_{\text{eff}}(x)} \frac{1}{a} \int_0^a dx e^{-\beta V_{\text{eff}}(x)} \right]^{-1} \quad (6?)$$

where ρ_0 is the average density and D_0 is the bare diffusion coefficient. Thus given the density distribution, $\rho(x)$, one can obtain (in the Smoluchowski limit) the dc conductivity σ .

The dc conductivity and the other distribution functions can be used to investigate commensurability effects, pinning effects, and screening effects. Comparisons can then be made between correct numerical many-body results and various analytical approximations [2],[3].

1. A. R. Bishop, W. Dietrich, and I. Peschel, Z. Phys. **B33**, 187 (1977).
2. A. Bunde, Z. Phys. **B44**, 225 (1981).
3. S. Jacobson, M. A. Ratner, Solid State Ionics **5**, 129 (1981).

A PACKAGE FOR IMPEDANCE/ADMITTANCE DATA ANALYSIS

Bernard A. Boukamp
Twente University of Technology, Department of Chemical Technology,
Laboratory for Inorganic Chemistry and Materials Science, P.O.Box
217, 7500 AE Enschede, The Netherlands.

The analysis of the frequency dispersion of many electrochemical systems is rather complicated because the time constants, associated with the various subcircuits of the equivalent circuit model, are too close together. Thus almost all parameters of the equivalent circuit have to be adjusted simultaneously. This can be accomplished through the use of a nonlinear least squares fit (NLLSF) procedure as, for example, has been described by Macdonald (1).

This still leaves one with the problem of guessing the proper shape of the equivalent circuit and obtaining a set of reasonable starting values for the parameters in order to proceed with the NLLS-fit. A simple procedure is described with which the frequency dispersion data may be analyzed and which will yield a set of useable starting values. This program (written in Basic) is especially suited for use on a personal computer. The principle and operating procedure will be explained and illustrated with some real measurements.

- (1) J.R. Macdonald, J. Schoonman and A.P. Leenen, J. Electroanal. Chem., **131** (1982) 77.

SEQUENTIAL HYPERSONIC DAMPINGS DUE TO FAST ION DIFFUSION AND
 VISCOUS RELAXATION IN AgI-RICH IONIC LIQUIDS

L. Borjesson,⁺ S. W. Martin,^{*} L. Torell⁺ and C. A. Angell^{*}

⁺Department of Physics
 Chalmers University of Technology
 S-412 96 Gothenburg, Sweden

^{*}Department of Chemistry
 Purdue University
 West Lafayette, Indiana 47907, U.S.A.

ABSTRACT

We report the novel observation that in certain ionic liquids two independent relaxation processes can be distinguished by Brillouin scattering. The phenomenon is observed in the liquid states of the so-called "superionic glasses" in which the fast ion conducting modes are highly decoupled from the relaxation modes of the amorphous matrix. Brillouin scattering data for the $(\text{AgI})_x(\text{AgPO}_3)_{1-x}$ systems reveal two independent hypersonic phonon damping mechanisms which are attributed to structural relaxation and to Ag^+ diffusion, respectively. For low AgI-concentrations ($x \leq 0.3$) only one absorption peak is seen, indicating a coupled system where the conductivity relaxation time is about the same as the structural relaxation time, i.e. $\tau_\sigma \approx \tau_\eta$. For higher AgI-concentrations ($x \geq 0.4$), where a greater decoupling ($\tau_\sigma < \tau_\eta$) of Ag^+ diffusion is expected, a second absorption region is observed. For $x = 0.4$, and $x = 0.5$ an absorption peak is found at a temperature predicted by extrapolations into the liquid state of conductivity relaxation time data of the glass though for $x = 0.5$, the second absorption region is very broad. The results imply that we have observed, for the first time, the liquid state equivalent of the mobile cation internal friction peak well known from lower frequency mechanical studies of ionic-conducting glasses.

MONTE CARLO STUDIES OF IONIC CONDUCTORS CONTAINING AN INSULATING SECOND PHASE

A. Bunde^{**,} W. Dieterich⁺, and E. Roman⁺

⁺Fakultät für Physik, Universität Konstanz, Konstanz, W.-Germany

^{**}Center for Polymer Studies and Department of Physics, Boston University, Boston, USA.

The ionic conductivity of LiI and other materials can be considerably enhanced by adding small particles of an insulating second phase. This observation is attributed to an increased density of conducting ions along the internal interfaces in the two phase mixture¹. In this work we formulate a model which displays the characteristic features of such systems. We consider a two-dimensional lattice with randomly distributed blocked regions and map the transport properties of the mixture to a random resistor network which consists of resistors of conductance σ_1 , $\sigma_2 \gg \sigma_1$, and $\sigma_3 = 0$, corresponding to the normal conductivity along the internal interfaces and to the zero-conductivity inside the insulating regions. To solve for the resulting conductivity we map our random resistor network to a random walk model, following a mapping procedure which has been recently introduced by Bunde et al.² in the context of mixed conductors. In our random walk model, the jump rate along the highly conducting interface is strongly enhanced and the sites along the interface are lower in energy so that the interface becomes attractive. We study this model by Monte Carlo simulations and find that the conductivity is strongly increased at low concentrations of the insulating particles, while it drops down at their percolation threshold p_c . We discuss the concentration dependence of the conductivity, in particular the position of the maximum and its behaviour at small concentrations and near p_c , and relate it to experiments.

1 J.B. Wagner, Jr., Mat Res. Bull. 15, 1691 (1980)

2 A. Bunde, A. Coniglio, D. Hong, and H.E. Stanley, J. Phys. A, in press.

Molecular Dynamics Simulation Studies of Li^+ Ion Conductors

by C R A Catlow and M L Wolf, Department of Chemistry,
University College London, 20 Gordon Street, London WC1H 0AJ, UK

We present results of detailed M.D. simulation studies of two Li^+ conducting materials - the layer structured superionic Li_3N and the spinel structured Li_2MgCl_4 . The aim of the simulations, which employ rigid ion, pair potential models, is to elucidate the details of Li^+ migration mechanism. In both cases the simulations reproduce the superionic properties of the materials, and in the case of Li_3N , the observed anisotropy of the conductivity is well reproduced, although the magnitudes of the calculated conductivities are greater than the experimentally measured values - a feature which we attribute to the use of rigid ion potentials. Trajectory analysis of the results for both systems reveal a considerable variety of complex migration mechanisms which in several cases involve complex, concerted processes.

COMPUTER SIMULATION OF Na IN HEXAGONAL WO₃J.H. Newton-Howes¹ and A.H. Cormack²

¹Wolfson Unit for Solid State Ionics, Imperial College, London SW7 2BP, UK.
(Present Address: Department of Physics, Monash University,
Clayton, Victoria, Australia, 3168)

²Department of Chemistry, University College London WC1H 0AJ, UK.

Although most investigations into fast cation conductors have centred on Li as the conducting species, given a suitable host structure, sodium may prove to be an acceptable alternative. Some attention has been focussed on the hexagonal form of WO₃, as a possible electrode material because of the large size of the tunnels in its structure, in addition to its role in electrochromic devices.

In this presentation we report a study of the behaviour of Na in hexagonal WO₃, using well established computer simulation techniques which have previously been used in the investigation of some other fast ion conductors.

We describe how our model, using previously derived interatomic potentials for ReO₃ structured materials, reproduces the structure of hexagonal WO₃. From calculations on two sodium tungsten bronzes, Na_{0.125}WO₃ and Na_{0.25}WO₃, as well as calculations on the behaviour of isolated Na⁺ cations in the hexagonal lattice, we show that our model predicts incommensurate ordering behaviour (which has been seen in the potassium counterpart KxWO₃) and a compositionally dependent diffusion coefficient for sodium transport.

Discrepancies between the experimental data and model predictions will be considered in the light of theoretical limitations and experimental constraints.

Particle Motion Through a Dynamically Disordered Medium: The Effects of Correlation and Application to Polymer Solid Electrolytes

Caroline S. Harris, A. Nitzan, Mark A. Ratner, and D. F. Shriver

Department of Chemistry and Materials Research Center
Northwestern University, Evanston, IL 60201

To study the diffusion of small particles through a dynamically disordered medium, a dynamic bond percolation model has been developed. This dynamic bond percolation model differs from the standard percolation theory, in that the lattice is no longer static but undergoes rearrangements which reassign the open and closed bonds. Physically, these rearrangements correspond to orientational motions of the (polymer) host lattice.

An interesting feature of this model is that, even below the percolation threshold, diffusive behavior can occur, as long as the renewal time τ_{ren} , the time characteristic of the rearrangement of bonds, is short compared to the observation time.

Ionic conductivity in polymeric electrolytes is one of the systems for which this model is useful. In these materials, alkali metal ions diffuse through a medium (the polymer) which is undergoing dynamic motion caused by configurational motions of the polymer. Since polymer chain motions will affect several ion binding sites simultaneously or serially, the model is further elaborated to account for correlations in the segmental motions of the polymer host. The renewal of the bonds is changed from occurring randomly to include simple correlation effects.

Of principal concern in this study is the effect that correlated renewals have on the transport behavior of the model. Simulations were done on a 1-D lattice and a diffusion coefficient calculated. The values of the diffusion coefficients from the two systems (with and without correlated renewal) are studied and their behavior as a function of the fraction of available bonds, f , and the renewal time is compared.

For both correlated and uncorrelated renewals, the systems were diffusive. The diffusion coefficients, in both cases, increased with increasing f and decreasing τ_{ren} , corresponding to an increase in the free volume, the configurational entropy, and the temperature of the polymer systems. The diffusion coefficients from the correlated systems were always smaller than those from the uncorrelated systems, except for the limit $f = 100\%$.

The ratio of the diffusion coefficients for the correlated and uncorrelated systems, respectively, was studied as a function of τ_{ren} and f . This ratio falls off to a constant value as τ_{ren} is increased and reaches a minimum value at $f = 50\%$. This behavior of the ratio as a function of f can be explained by considering the diffusion of the bonds in the lattice for the correlated case.

ELECTRICAL AND THERMODYNAMIC PROPERTIES OF
 $\text{Li}_2\text{SO}_4\text{-Ag}_2\text{SO}_4$ SOLID ELECTROLYTES

Q. G. LIU and W. L. Worrell
 Department of Materials Science and Engineering K1
 University of Pennsylvania, Philadelphia, PA 19104

New solid-state electrochemical sensors using $\text{Li}_2\text{SO}_4\text{-Ag}_2\text{SO}_4$ electrolytes have been developed^(1,2) recently for measuring SO_2 and/or SO_3 in gas mixtures. The electrical conductivities and thermodynamic properties of these solid electrolytes are reported in this paper.

An A. C. impedance technique has been used to measure the electrical conductivities of several $\text{Li}_2\text{SO}_4\text{-Ag}_2\text{SO}_4$ solid electrolytes. Results indicate that the electrical conductivities of the $\text{Li}_2\text{SO}_4\text{-Ag}_2\text{SO}_4$ solid electrolytes are much higher than those for other sulfate electrolytes, i.e. $1.1 \text{ (ohm cm)}^{-1}$ at 530°C for $\text{Li}_2\text{SO}_4\text{-(23 mol\%Ag}_2\text{SO}_4)$ electrolyte. The change in conductivity with the gas composition has also been measured. The independence of the electrical conductivity with the SO_2/SO_3 concentration and galvanic cell measurements indicate that the conduction is ionic.

The thermodynamic properties of $\text{Li}_2\text{SO}_4\text{-Ag}_2\text{SO}_4$ system have been measured using galvanic cells. The activity of Ag_2SO_4 in the $\text{Li}_2\text{SO}_4\text{-Ag}_2\text{SO}_4$ binary system has been measured at temperatures between of 450 and 560°C . Using the Gibbs-Duhem equation the activity of Li_2SO_4 and the Gibbs free energy of mixing for the $\text{Li}_2\text{SO}_4\text{-Ag}_2\text{SO}_4$ binary system have been calculated. Using our galvanic results, the $\text{Li}_2\text{SO}_4\text{-Ag}_2\text{SO}_4$ phase diagram has been revised slightly in the Ag_2SO_4 rich region.

Reference

- (1) W. L. Worrell and Q. G. Liu, J. Electroanal. Chem., 168 (1984) pp. 355-362
- (2) Q. G. Liu and W. L. Worrell, Proc. Int. Meeting Chem. Sensors, Vol 17, Anal. Chem. Symp. Series, Elsevier, New York, 1983, pp 332-337.

NEW FAST SOLID LITHIUM ION CONDUCTORS
AT LOW AND INTERMEDIATE TEMPERATURES

B. Schoch, E. Hartmann, and W. Weppner
 Max Planck Institute for Solid State Research
 D-7000 Stuttgart-80, Germany

The search for fast solid lithium ion conductors requires other strategies compared to the search for classical silver or copper ion conductors. This is mainly due to the generally high binding energy of lithium and the relatively high thermodynamic stability of most lithium compounds. This stability is of course, on the other hand side, a basic requirement for the construction of storage batteries with high energy densities. Three different approaches have recently disclosed a variety of useful solid multinary lithium ion conductors.

Since the presence of other cations than lithium results in an instability against reaction with elemental lithium in the majority of cases, we have looked at multinary lithium systems with several anionic species and lithium as the only cation. Results will be presented for materials based on the ionic conductor Li_2S and lithium halides or oxide as additional constituent.

A few compounds have also been studied which belong to the small group of materials for which, in contrast, the lithium compound is less stable than the salt of the other type of cations. These materials were mainly based on Li_3N . Phase equilibria and electrical conductivity data will be presented.

A third class of materials consists of solid addition compounds of lithium halides and various organic materials such as methanol. These materials show very high ionic conductivity at ambient temperature. In addition, the compounds have many advantages with regard to their preparation, handling and application in solid state galvanic cells.

INTERCHANNEL CORRELATION OF MOBILE IONS IN HOLLANDITES

S. Suzuki, M. Tanaka, M. Ishigame*, T. Suemoto*, Y. Shibata*, Y. Onoda** and Y. Fujiki**

Department of Physics, Faculty of Science, Tohoku University, Sendai 980, Japan

*Research Institute of Scientific Measurements, Tohoku University, Sendai 980, Japan

**National Institute for Research in Inorganic Materials, Ibaragi 305, Japan

Beyler et al. studied the conduction-ion arrangements in the Hollandites, $A_2xMg_xTi_8-xO_{16}$ ($A=K$; $x=0.77$ and $A=Cs$; $x=0.67$) by the rotating crystal method of X-ray diffraction and obtained the following results: 1) There exists no interaction between the conduction ions which are present in different conduction channels. 2) In the K-Hollandite, there are four kinds of superlattices which have three-, four-, five- and six-times cell dimensions in the c-direction of the fundamental cell. The occupation probabilities of these superlattices are 0.15, 0.37, 0.37 and 0.11, respectively. The displacement value of the potassium ions neighbouring to the vacancies is $0.245 C_0$, where C_0 is the lattice parameter in the c-direction. 3) In the Cs-Hollandite, the displacement value of the cesium ions neighbouring to the vacancies is $0.12 C_0$.

We have reinvestigated the conduction-ion arrangements in the K-Hollandite of $x=0.82$ and in the Cs-Hollandite of $x=0.59$ grown by Ishigame, Suemoto and Shibata by the electron diffraction and high-resolution electron microscopy. The obtained results are as follows. 1) For both Hollandites, the conduction ions in a channel are correlated with those in the neighbouring channel. That is, two vacancies in the adjacent two channels occupy the second nearest positions or/and the third nearest positions. The occupation probabilities of the former and the latter positions are 0.7 and 0.3 in the K-Hollandite and 0.81 and 0.19 in the Cs-Hollandite. This interchannel correlation becomes stronger as the specimen temperature is decreased. However, both Hollandites did not transform into the superlattice structures at the liquid nitrogen temperature but stay in a kind of glassy state. 2) The superlattice cell dimension formed by the conduction ion arrangements is essentially of one kind. The dimensions are four- and three-times the fundamental cell for K and Cs-Hollandites, respectively. The vacancy arrangements were directly observed by high-resolution electron microscopy. 3) The displacement value of the conduction ions neighbouring to the vacancies were evaluated from the diffusely scattered intensities of electron diffraction by taking account of the interchannel correlation. In the K-Hollandite, four kinds of K-ions neighbouring to the vacancies can displace differently. The displacement values were determined as $0.25 C_0$, $0.20 C_0$, $0.18 C_0$ and $0.10 C_0$ at room temperature. In the Cs-Hollandite, three kinds of Cs ions are displaced by the amounts of $0.17 C_0$, $0.05 C_0$ and $0.04 C_0$. 4) In the specimens which were grown from specially pure raw materials by Onoda and Fujiki, we could observe the effect of ion arrangements in electron diffraction patterns, but could not observe the vacancy arrangements in the high-resolution electron microscopic images. This fact means that the conduction ions in pure specimens keep the correlation described above and move to the next equivalent position beyond the potential barrier in the exposure time of photographs and that the ions in impure specimens may be pinned and stopped by impurities.

ALKALI ION DIFFUSION IN $M'(AlSiO_4)$ COMPOUNDS WITH FRAMEWORKS OF THE TRIDYMITTE TOPOLOGY AND ITS VARIANTS.

M. Gregorkiewitz, Instituto de Físico-Química Mineral, CSIC, Serrano 115 bis, 28006 Madrid, Spain.

Homoionic, crystalline tectosilicates with the general composition $M'(AlSiO_4)$ were prepared either by direct synthesis or by ion exchange in fused nitrates, leading to a total of 8 samples representing 4 closely related framework topologies (tridymite-nepheline, kaliophilite 01, hexagonal kaliophilite, Icmm; all of them belonging to the family described by J.V. Smith, Amer. Min. 62 (1977) 703) and with Na, K or Cs in the framework cavities or channels.

Electrical conductivities in the temperature range from 260° to $1025^\circ C$ were obtained from impedance measurements, using pressed pellets of the powdered materials in an AC-bridge at frequencies of $50-10^6$ Hz. Additional information was obtained from kinetics of the ion exchange reactions at 270° to $390^\circ C$, some of which were carried out for different grain sizes of the same material in order to ascertain volume diffusion. All samples were investigated by powder and/or single crystal X-ray diffraction techniques for the control of structural changes during conductivity and diffusion experiments.

The conduction is almost entirely ionic and is attributed to a volume diffusion of alkali ions through the framework. Ionic conductivities σ range from $5 \cdot 10^{-7}$ S/cm for Cs-Icmm at $800^\circ C$ up to $7 \cdot 10^{-6}$ and $1.5 \cdot 10^{-2}$ S/cm for Na-nepheline at 300° and $800^\circ C$ respectively, corresponding to diffusion coefficients D between $2 \cdot 10^{-10}$ and $5 \cdot 10^{-6}$ cm^2/s . The activation enthalpies of D and σT lie in the order of 77-122 kJ/mole.

The experimental results are interpreted in terms of structural parameters and lead to interesting new conclusions about the relationship between the alkali ion transport and crystallochemical factors such as void fraction, topology and conformation of the framework.

DYNAMICS OF THE LISICON SYSTEM FROM ^7Li NMR

M. Bose and A. Basu
Saha Institute of Nuclear Physics, Calcutta 700009, INDIA
D. Torgenson
Department of Physics, Iowa State University, Iowa, USA

T_1 measurements have been performed at 40 Mc for polycrystalline Lisicon $\text{Li}_{14}\text{Zn}(\text{GeO}_4)_4$ and its Zn rich analogue (ZRA) in the range 200-666K. T_1 values vary from secs to msec. Assuming a BPP type relaxation mechanism, the data was evaluated by fitting the T_1 's to a single diffusion minimum over the temperature interval wherein motional effect occurs. For Lisicon and its ZRA, the activation energies (ΔE) of 0.375eV/atom and 0.371eV/atom and diffusion attempt frequencies of ν_0 equal to 0.213 and 0.118 sec respectively were obtained. The ΔE 's obtained from our line width studies are still lower viz., 0.19 eV and 0.17eV respectively. From single crystal studies, Chen Li Quan² et al reported several ΔE 's corresponding to different phases for certain temperature ranges viz. 298-353K ($\Delta E=0.58$), 353-413K ($\Delta E=0.92$), 353-573K ($\Delta E=0.62$), 573K($\Delta E=0.36$). The low values obtained from NMR either from the line width or T_1 measurements are not unexpected, as NMR responds to local motion also, whereas conductivity is affected by long range diffusion only.

Fourier transform spectra of both samples at 500K revealed the presence of an asymmetric central line with satellites. The derivative of the central line showed low field structure and this in all possibility arises from the inequivalent Li lattice sites present. Chemical shift anisotropy may be another contributing factor. The interesting point is, for Lisicon the first order quadrupolar splitting ($\Delta Q = 8.5$ KHz at 500K) vanishes at 666K but is clearly present ($\nu_Q = 20.3$ KHz) in the ZRA. Conductivity studies indicate that Lisicon has a higher conductivity at higher temperatures than its ZRA. The reverse is true at lower temperatures, inspite of the larger number of mobile Li ions in Lisicon. The bigger Zn ion increases the bottle-neck size at room temperature and hence the comparatively increased mobility of the ZRA at low temperatures. Interestingly ΔE is not much different in the two compounds. Thus the mobility becomes the factor in determining conductivity. In the ZRA, with the larger bottle-neck size the mobility is not much temperature dependent, whereas in Lisicon it is very much so. Thus at higher temperatures, where the Li becomes more mobile (the ZRA is unaffected), particularly after the phase transition in Lisicon above 573K, the increased mobility averages out the quadrupolar coupling, whereas the ZRA is unaffected. Li/Zi Rong³ also reported that in Lisicon the quadrupolar coupling of 39 Kc/s observed at 329K is strongly temperature dependent. T_1 at 295.5K is of the order of 18.2 μ sec and 18.1 sec for Lisicon and ZRA respectively. Finally the FID data of the two compounds at 666K differ significantly. The ZRA shows many more wiggles than that of Lisicon. This needs further investigation for a proper understanding.

1. D. Mazumdar et al., Material Research 18, 19, 1983
2. Chen Li Quan et al., Acta Physica Sinica 29, 661, 1980
3. LI Zi Rong et al. Acta Physica Sinica 30, T388, 1981

SOME Na_2SO_4 -BASED FAST ION CONDUCTORS

K. SHAHI AND G.P.S. GOPALAN

Department of Materials Science and Physics
Indian Institute of Technology, Kanpur-208016, INDIA

With a view to develop new Li^+ and Na^+ -based fast ion conductors, a number of lithium and sodium salts are being explored. Particular attention is being given to two sulphates, Li_2SO_4 and Na_2SO_4 , as they both exhibit high temperature phases which are fast ion conductors; the normal \rightarrow fast ion phase transition temperatures being $T_c = 575^\circ$ and 240°C respectively. The stabilization of these phases at lower temperatures might thus be expected to result in highly conducting materials.

In this paper we report the results on Na_2SO_4 -based materials, in particular the four systems $\text{Na}_2\text{SO}_4\text{-M}_2(\text{SO}_4)_3$ where $\text{M}=\text{La}, \text{Sm}, \text{Dy}$ and In . These systems have been investigated by means of electrical conductivity (σ) measurements, X-ray diffraction (XRD) and differential thermal analysis (DTA).

The conductivity vs composition curves exhibit maximum around 2-3 mole% $\text{M}_2(\text{SO}_4)_3$. The maximum enhancement in conductivity is obtained when $\text{M}=\text{La}$, the enhancement being more than 1000 times at lower temperatures ($\sim 180^\circ\text{C}$). For example, $\text{Na}_2\text{SO}_4 + 2\% \text{La}_2(\text{SO}_4)_3$ exhibits a $\sigma = 7.6 \times 10^{-3} \text{ ohm}^{-1} \text{ cm}^{-1}$ at 180°C and an activation energy (E_a) of 0.58eV. This may be compared with pure premelted Na_2SO_4 : $\sigma(180^\circ\text{C}) = 6.9 \times 10^{-8} \text{ ohm}^{-1} \text{ cm}^{-1}$, and $E_a = 1.6\text{eV}$ (below T_c).

For $\text{Na}_2\text{SO}_4 + 2\% \text{In}_2(\text{SO}_4)_3$: $\sigma(180^\circ\text{C}) = 3.3 \times 10^{-6} \text{ ohm}^{-1} \text{ cm}^{-1}$ and $E_a = 1.17\text{eV}$.

$\text{Na}_2\text{SO}_4 + 2\% \text{Sm}_2(\text{SO}_4)_3$: $\sigma(180^\circ\text{C}) = 5.5 \times 10^{-5} \text{ ohm}^{-1} \text{ cm}^{-1}$ and $E_a = 0.62\text{eV}$.

It is evident that the enhancement is maximum when the dopant is La^{+3} and least for In^{+3} . Also it is noted that the activation energy is lower when the enhancement is larger, which is self consistent.

The $\text{Na}_2\text{SO}_4\text{-In}_2(\text{SO}_4)_3$ system appears rather unstable. However the other three systems indicate that the high temperature phase of Na_2SO_4 (phase I) can be stabilized at room temperature, a result found consistent in the conductivity measurements, and the DTA and XRD analyses.

PHASE RELATIONSHIP AND ELECTRICAL CONDUCTIVITY OF
 $\text{Li}_{1+x}\text{Ti}_{2-x}\text{Ga}_x\text{P}_3\text{O}_{12}$ AND $\text{Li}_{1+2x}\text{Ti}_{2-x}\text{Mg}_x\text{P}_3\text{O}_{12}$ SYSTEMS

Zu-xiang Lin, Hui-jun Yu, Shi-chun Li and Shun-bao Tian
 Shanghai Institute of Ceramics
 Chinese Academy of Sciences
 865 Chang-ning Road
 Shanghai 200050
 China

Phase relationship and electrical conductivity of the systems $\text{Li}_{1+x}\text{Ti}_{2-x}\text{Ga}_x\text{P}_3\text{O}_{12}$ and $\text{Li}_{1+2x}\text{Ti}_{2-x}\text{Mg}_x\text{P}_3\text{O}_{12}$ were studied.

The results obtained by X-ray analysis are as follows: In the system $\text{Li}_{1-x}\text{Ti}_{2-x}\text{Ga}_x\text{P}_3\text{O}_{12}$, a homogenous rhombohedral solid solution extends to $x = 0.6$. The superstructure lines appeared at $x = 0.4-0.6$ can be indexed by a tripled rhombohedral unit cell. Second phase appeared from $x = 0.7$ and, at the same time, the rhombohedral phase changes gradually to monoclinic. In the system $\text{Li}_{1-2x}\text{Ti}_{2-x}\text{Mg}_x\text{P}_3\text{O}_{12}$, the range of the rhombohedral solid solution is rather narrow. The X-ray diffraction lines characteristic of the rhombohedral phase begins to split to lines of monoclinic at a smaller value of x , accompanying with appearance of a few of very weak lines of unknown phase. The cell constants of the rhombohedral solid solutions increase with increasing x in both the systems.

Bulk conductivities of these systems measured by complex impedance method are presented. Maximum conductivity occurs in both systems. They are 8.4×10^{-3} and 5.3×10^{-3} S/cm at around 300°C and at $x = 0.6$ and $x = 0.3$ respectively.

The results obtained are discussed in view of size and polarizability of the skeleton ions and ionicity of the M-O bonds. Comparisons between the system $\text{Li}_{1-x}\text{Ti}_{2-x}\text{In}_x\text{P}_3\text{O}_{12}$ and each of the two systems investigated here are given.

TIME-OF-FLIGHT NEUTRON POWDER DIFFRACTION STUDY
OF $\text{Na}_2\text{Zr}_2\text{SiP}_2\text{O}_{12}$ AND $\text{Na}_3\text{Zr}_2\text{Si}_2\text{PO}_{12}$

W.H. Baur, Department of Geological Sciences, Box 4348,
University of Illinois, Chicago, Illinois 60680, USA

D.H. Whitmore, Department of Materials Science and Engineering,
Northwestern University, Evanston, Illinois 60201, USA

J. Faber, Materials Science Division,
Argonne National Laboratory, Argonne, Illinois 60439, USA

Abstract

Neutron powder diffraction data were collected by the time-of-flight technique at the Argonne Intense Pulsed Neutron Source. Two dense, ceramic samples were used, $\text{Na}_2\text{Zr}_2\text{SiP}_2\text{O}_{12}$ and $\text{Na}_3\text{Zr}_2\text{Si}_2\text{PO}_{12}$, and each was measured at room temperature and at 572K. The ionic conductivity was measured using an a.c. method on samples cut from the same sintered pellets as had been used for the neutron diffraction experiment.

The powder diffraction profiles were refined by the Rietveld method. After correction for spurious background (due to technical difficulties), the results were self consistent between refinements of the data collected in back reflection and for $2\theta = 90^\circ$. Low values for the structure factor residuals were obtained both for the rhombohedral (0.066 to 0.078) and the monoclinic (0.048) phases. The maximum change in cell constants upon heating from room temperature to 572K is 0.15Å for $\text{Na}_2\text{Zr}_2\text{SiP}_2\text{O}_{12}$, and 0.08Å for $\text{Na}_3\text{Zr}_2\text{Si}_2\text{PO}_{12}$, when it goes through the phase transition from space group $C2/c$ to $R32/c$. The crystal structure of the monoclinic phase has previously not been published. The distances between anions and cations are reasonable, compared with the values expected from the known effective ionic radii. Refinement of the occupancy factors was constrained to the full theoretical content of the Na sites, based on chemical analysis which confirmed the starting composition. The occupancy factors show only insignificant differences between room and high temperatures for $\text{Na}_2\text{Zr}_2\text{SiP}_2\text{O}_{12}$, the Na(1) position being essentially completely occupied at 572K. The same is true for the high temperature phase of $\text{Na}_3\text{Zr}_2\text{Si}_2\text{PO}_{12}$. In the low temperature monoclinic phase, the Na(3) position, six coordinated by oxygen atoms, seems to carry all the vacancies, while the Na(2) and Na(1) positions appear to be fully occupied.

Relations between the structure and the ionic conductivity of these NASICON compositions will be discussed.

NEUTRON DIFFRACTION STUDY OF THE DISTRIBUTION AND THERMAL MOTION OF SILVER IONS IN ALPHA- AND BETA- Ag_3SI

J. J. Didisheim¹, R. K. McMullan² and B. J. Wuensch¹

¹Department of Materials Science and Engineering, Massachusetts Institute of Technology, Cambridge, Mass. 02139, U.S.A. and ²Chemistry Department, Brookhaven National Laboratory, Upton, Long Island, N.Y. 11973, U.S.A.

Fast-ion conducting Ag_3SI , intermediate to AgI and Ag_2S , is of interest in establishing the role of bonding and mobile ion concentration on the Ag distribution and transport properties of these phases. Previous powder diffraction studies and a single-crystal x-ray analysis had established the existence of three phases: α ($T > 240^\circ\text{C}$), space group $\text{Im}\bar{3}\text{m}$, having a disordered bcc anion array and cations disordered among tetrahedral sites; β ($-116^\circ < T < 240^\circ\text{C}$), space group $\text{Pm}\bar{3}\text{m}$, having an ordered CsCl -type anion array and cations disordered in tetrahedral sites; and γ ($T < -116^\circ\text{C}$), space group $\text{R}\bar{3}$, with cations ordered in a subset of available tetrahedral sites. The present single-crystal neutron-diffraction study was undertaken to characterize the Ag distribution more precisely, capitalizing upon the higher resolution afforded by the lack of decrease of scattering length with angle and the fact that, as opposed to x-ray data, Fourier synthesis provides the probability distribution for the cation nucleus, rather than a convolution of the probability with a distribution of orbital electrons of comparable spatial extent. The structures were also examined as a function of temperature for the first time to permit distinction between time-averaged anharmonic thermal vibration and positional disorder.

The β phase was examined at temperatures of 23, 95, 168 and 232°C using Be-monochromated thermal neutrons of 1.05099 Å wavelength at the High Flux Beam Reactor at Brookhaven National Laboratory. Three to six sets of symmetry-equivalent reflections for $\sin\theta/\lambda < 0.78 \text{ \AA}^{-1}$ were recorded to provide 72 independent intensities of which 61 to 55, depending upon temperature were $> \sigma$; internal agreement in I ranged 3.7% to 1.9% for the individual data sets. Refinement indicated partial positional disorder of S and I. Models examined included anharmonic temperature for Ag ions and/or partial occupancy of the octahedral site. The most successful model employed Ag ions solely in a tetrahedral site coordinated by 2S and 2I and anisotropic harmonic temperature factors. The temperature factors were found to vary linearly with temperature. Final weighted residuals, $R_w(F^2)$, including unobserved reflections, ranged 3.9-5.9%.

The anion-disordered α -phase was investigated at 323, 380, 442 and 475°C and 18 to 20 independent structure factors $> \sigma$ were obtained from averages of symmetry-equivalent intensities ranging 26-37 in number, depending on temperature. Final weighted residuals $R_w(F^2)$, including unobserved reflections, vary between 3.3 and 4.5%. The Ag probability density is highly delocalized compared to that in β , being elongated along [100] in a fashion qualitatively similar to α - Ag_2S . Significant differences relative to the sulfide, however, are evidence for occupancy of a site at $\frac{1}{2}\text{kk}$ and fine structure in the probability density. Rather than representing anharmonic effects, the latter features may be explained to satisfaction in terms of positional disorder of the Ag ions which depends on the local configuration of S and I about the site.

QUASI-ELASTIC AND INELASTIC NEUTRON SCATTERING STUDY OF
 $\text{Na}_3\text{Cr}_2(\text{PO}_4)_3$, $\text{Na}_2\text{Zr}_2(\text{PO}_4)_3$, $\text{Na}_4\text{MgZr}(\text{PO}_4)_3$

G. LUCAZEAU^(a), M. BARJ^(a), C. DELMAS^(b), A.J. DIANOUX^(c)

(a) Laboratoire de Chimie-Physique du Solide,
 Université Paris XIII, 93430 Villetaneuse, France.

(b) Laboratoire de Chimie du Solide, Bordeaux I.

(c) Institut Laue Langevin, Grenoble.

Polycrystalline sample of $\text{Na}_3\text{Cr}_2(\text{PO}_4)_3$ has been investigated on a time of flight spectrometer IN6 at 30, 150, 300 and 400°C. Using incident wave lengths of 5.1 Å and 5.9 Å giving mean resolutions of 0.130 and 0.080 meV respectively. For comparison $\text{Na}_2\text{Zr}_2(\text{PO}_4)_3$ and $\text{Na}_4\text{MgZr}(\text{PO}_4)_3$ were investigated at 300°C with $\lambda=5.1$ Å in a Q range comprised between 0.2 and 2 Å⁻¹.

The broad and strong quasi elastic signal (QES) observed for the chromium compound is attributed to the spin fluctuations of Cr^{3+} ions and to Na motions.

The intensity and the fullwidth of the QES have been studied as function of Q and of the temperature. The QES observed for $Q < 1$ Å⁻¹ is believed to be associated to magnetic scattering while the QES observed for $Q > 1$ Å⁻¹ is likely due to Na jumps. The decrease of the width of the QES when the T° is raised from 150 to 400°C indicates that two jump regimes occur. The interpretation of these results is in progress.

The inelastic spectra of these different compounds compare well with IR and Raman data. A new and strong peak at about 10 cm⁻¹ has been evidenced for the chromium compound it has been assigned to Na₁ local mode; its intensity variations from 30 to 300°C have been related to the population of this site.

Na-K EXCHANGE OF THE NASICON-TYPE STRUCTURAL COMPOUNDS

Masayuki NAGAI and Tadashi NISHINO

Musashi Institute of Technology, Tamazutsumi, Setagaya-ku, Tokyo, JAPAN

Study on ion-exchange characteristics of alkali ions is of importance to understand conduction mechanism in alkali ion conductors. From Na-K exchange equilibrium, the activity coefficients of Na⁺ and K⁺ can be determined. As activity coefficients reflect the interaction between Na⁺ and K⁺, we can discuss the site occupancy and the alkali ion distribution on the basis of Na-K exchange data. Activity coefficients greater than unity are usually associated with repulsive interaction between unlike species, while those less than unity are usually associated with attractive interaction between unlike species.

In this study, ion-exchange characteristics of $\text{Na}_2\text{Zr}_2(\text{PO}_4)_3$ (the end member of a solid solution $\text{Na}_3\text{Zr}_2\text{P}_5\text{O}_{14}$ known as a fast ionic conductor) soaked in (Na,K)NO₃ melts was investigated. Usual solid state reaction and freeze drying technique were employed to prepare a series of solid solutions having the compositions of $\text{Na}_{1-x}\text{K}_x\text{Zr}_2(\text{PO}_4)_3$ (0 ≤ x ≤ 1). About 1g of $\text{Na}_2\text{Zr}_2(\text{PO}_4)_3$ powders were mixed with ca. 20g of the nitrate, heated up to 380°C and kept for 15 hours. Subsequently, they were repeatedly washed with water, filtered and dried. Compositional dependence of lattice parameters was used to estimate the quantity of Na and K. As activation analysis was found to be effective to determine Na and K contents in this series of samples, it was also employed for determination of Na and K contents.

It was possible to index the X-ray diffraction patterns for all the samples having the compositions of $\text{Na}_{1-x}\text{K}_x\text{Zr}_2(\text{PO}_4)_3$ with space group R $\bar{3}c$ and hexagonal lattice. In a series of the solid solutions, the lattice constant along a axis shrinks and that along c axis expands linearly with an increase of K content. The change in lattice parameters was large enough to estimate Na and K contents with an error of ±3%. It was also possible to index the X-ray diffraction patterns for the ion-exchanged samples with space group R $\bar{3}c$ and hexagonal lattice. The diffraction pattern for the powders soaked in KNO₃ melt at 380°C for 15 hours was essentially the same as that treated at 380°C for a few minutes. Consequently, it is likely that the Na-K exchange would proceed rapidly and attains an equilibrium state within a markedly short period of time. Moreover, the K content in the exchanged samples determined by X-ray was confirmed by activation analysis.

With respect to the distribution coefficients of Na⁺ and K⁺ between the solid and melt, the shape of the curve with convexity toward the solid indicates preferable distribution of K⁺ in the solid, suggesting that K⁺ would more tightly bind in the lattice than Na⁺. The equilibrium reaction is given by



where (s) represents solids and (l) represents melts. The equilibrium constant and activity coefficients of Na⁺ and K⁺ in the solids were calculated by graphical integration, using the determined distribution coefficients in the solids and liquids and the activity coefficients in the melts available in the literature. The remarkable decrease in the activity coefficient of Na⁺ in the K rich region of the solids suggests that Na⁺ and K⁺ would strongly interact and preferably occupy their own sites.

THERMODYNAMIC AND ELECTROCHEMICAL INVESTIGATIONS OF THE

NASICON SOLID SOLUTION SYSTEM

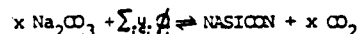
Joachim Maier and Udo Warhus

Max-Planck-Institut für Festkörperforschung
Heisenbergstr. 1, D-7000 Stuttgart 80, W. Germany

The NASICON solid solution system is expected to offer good prospects for a highly conductive and a pretty cheap solid sodium conductor which may be used as an electrolyte for the sodium-sulfur cell. It has been often investigated as far as preparation conditions and conductance properties are concerned. But although it is extremely important to investigate the thermodynamic stability with respect to the end members and with respect to possible reactions with Na and S, reliable thermodynamic data are lacking in the literature.

NASICON compositions in the binary system of Hong (1) as well as in the ternary solid solution system, which has been recently proposed (2) have been prepared as single phase materials (shown by X-ray, microscopic and IR measurements, ICP analysis). Long time sintering tests allow a conservative estimate of the thermal stability of this compositions.

In order to obtain exact data the e.m.f. of formation cells with the overall reaction



has been recorded as a function of temperature. The ϕ_i mean the product phases coexisting with NASICON, if differential amounts of Na_2O are removed. The CO_2 partial pressure has been fixed by both a CaCO_3/CaO buffer system and by gas mixtures. Thus, the enthalpy and the entropy of reaction are obtained.

Independently DSC measurements are used for elucidating C_p , H - and S -values. Different theoretical procedures for estimating the data are included in the calculation process and compared with the experimental results.

The results concerning the solid solution system can be summarized by a thermodynamic mixing model. Referring to the thermodynamic stability against Na and S the Gibbs energies of possible degradation processes can be given and can be compared to kinetic investigations.

References

1. H. Y. - P. Hong, Mat. Res. Bull. 11, 173, (1976)
2. H. Kohler, H. Schulz, O. Melnikov, Mat. Res. Bull. 18, 1143, (1983)

NASICON : Amorphous to crystalline compounds

J.P. BOILOT, Ph. COLOMBAN

Groupe de Chimie du Solide - Laboratoire de Physique de la Matière Condensée
Ecole Polytechnique - 91128 Palaiseau Cedex (FRANCE)

G. COLLIN

Laboratoire de Physique des Solides
Université Paris-Sud, Bât 510 - 91405 Orsay (FRANCE)

NASICON compounds ($\text{Na}_{1+x} \text{Zr}_y \text{Si}_x \text{P}_{3-x} \text{O}_{12} \cdot x/2$, $0 < y < 1$) and analog ones ($\text{Na}_3 \text{M}_2 (\text{PO}_4)_3$, $\text{M} = \text{Sc}, \text{Fe}, \text{Cr}$) belong to the best fast sodium ion conductors. The crystalline framework is constituted by isolated SiO_4/PO_4 tetrahedra with octahedral filled cavities. Sodium ions are distributed on two interstitial type sites generally noted Na(1) and Na(2). According previous studies, there are, at least, three fundamental problems for these compounds : structural transitions, stoichiometry and conduction pathways.

In this paper, we show that these problems are related to the great ability for NASICON compositions to give amorphous compounds.

i) *structural transitions are generally observed above the room temperature. The order of these transitions and associated thermal effects are depending on the fabrication process of NASICON compounds.*

Concerning Zr-compounds, the sol-gel method allows to prepare homogeneous well-densified ceramics and glasses of NASICON type at a temperature selected between 600 and 1250°C. In this temperature range the NASICON structure changes from an amorphous state at 600°C into a monoclinic structure above 1100°C passing by different local ordering with a rhombohedral average symmetry.

Concerning single crystals of NASICON analog ($\text{Na}_3 \text{Sc}_2 (\text{PO}_4)_3$):
- when prepared quickly at high temperature (crystal from melt $T > 1600^\circ\text{C}$) a monoclinic modification is found with a strict order of vacancies and Na ions at least at low temperature (filled Na (1) site). This α -phase presents two sharp phase transition accompanied by changes in the lattice symmetry and parameters (monoclinic \rightarrow rhombohedral), ionic distribution and consequently transport properties. - when prepared by crystallization from the powder (1470°C-2 days) a rhombohedral modification is found. This β -phase corresponds roughly to the intermediate temperature phase of the α type - (partially vacant Na(1) site) and quasi long range ordered 2a-2a-c trigonal superstructure. This superstructure corresponds to the ordering of a filled Na(2) triplet every three planes. This β -phase also presents two phase transitions but shifted towards low temperature with respect to the α phase.
- when prepared from flux (non polluting Na phosphate -1100°C-4 days) another rhombohedral modification is observed. This γ -phase is close to the high temperature modification of the α and β types : large amount of vacancies on Na (1) site and short range order in a 2a-2a-c trigonal superstructure. In this γ -phase one observes a continuous transfer from Na(1) into Na(2) sites.

ii) *Zr deficient compositions only exhibit slight changes of ionic conductivity in comparison with the stoichiometric one.*

NASICON compounds can be prepared as non crystalline solids (gels-glasses), at low temperatures by chemical polymerization from metal or non metal alkoxides hydrolysis. Moreover many compositions besides the NASICON one exhibit, in an amorphous state, a high ionic conductivity, similar to the one of NASICON type crystalline compounds.

iii) *There are two possible conduction pathways in the NASICON type structure jumping between Na(2) positions and jumping from Na(2) to Na(1) to Na(2).* In NASICON compounds, the sodium ion distribution and the activation energy of the conductivity are dependent on the thermal history. This suggests that these two types of mechanism can exist in these compounds.

FREQUENCY-DEPENDENT CONDUCTIVITY OF NASICON SOLID ELECTROLYTES
IN THE MICROWAVE RANGE

J. R. DYKAS
Department of Materials Science and Engineering
and
M. E. Brodwin
Department of Electrical Engineering and Computer Science
Northwestern University
Evanston, Illinois 60201, USA

Abstract

Complex permittivity of dense, ceramic NASICON solid electrolytes ($\text{Na}_{1-x}\text{Ir}_2\text{Si}_x\text{P}_3\text{-xO}_{11}$ with $x=1$ and $x=2$) has been measured at microwave frequencies ranging from 0.3 to 37.0 GHz over the temperature range 20 to 400°C. A new measurement technique, which eliminates systematic errors associated with the loss of contact between the walls of rectangular waveguide and the conductive specimen during thermal cycling, has been developed and used at frequencies between 9.0 and 37.0 GHz. In the frequency range 0.3 to 7.0 GHz measurements were made in coaxial line using the variable termination method, but temperature had to be limited to below 100°C by the contact problems.

Low frequency complex impedance data were analyzed in terms of a generalized equivalent circuit and compared with the microwave frequency results. Frequency dependence of conductivity at different temperatures, and the apparent activation energies at different frequencies were related to the mechanism of ionic transport. In case of the $x=2$ NASICON, effects of the structural phase change on the frequency-dependent conductivity were observed. By contrast, no pronounced effects of temperature on frequency dependence of conductivity was observed for the $x=1$ NASICON, which exhibits only moderate ionic conduction. Comparison of the results from the two compounds with similar framework structure but different ionic conductivities allows one to isolate characteristic features of permittivity which are associated with fast ionic transport.

P_2O_5 BASED VITREOUS ELECTROLYTES
IDENTIFICATION OF THE STRUCTURAL UNITS BY ^{31}P NMR-MAS

Marco Villa
Dipartimento di Fisica "A. Volta" e Gruppo Nazionale di Struttura della
Materia del C. N. R. Via Bassi 6, 27100 Pavia, Italy

Geetano Chiodelli
Centro di Studio per la Termodinamica ed Elettrochimica dei Sistemi
Salini Fusi e Solidi del C. N. R. c/o Dipartimento di Chimica Fisica
Viale Taramelli 16 - 27100 Pavia, Italy

Phosphate salts contain tetrahedral PO_4 units which may differ in their nominal charge or, if one prefers, in the number of oxygens that are shared with other PO_4 units. This work presents the first results of an NMR investigation showing that the ^{31}P resonance, observed with the Magic Angle Spinning (MAS) technique, often provides an unambiguous and straightforward identification of these units in solid samples. The trace of the ^{31}P chemical shift tensor in PO_4 units assumes values which are spread over a ~100 ppm interval. This fact is likely to make the ^{31}P NMR-MAS technique the most powerful tool for investigating the structural chemistry of phosphates.

This paper analyzes the ^{31}P NMR-MAS spectra of glasses of the system $\text{MX} \cdot \text{M}_2\text{O} \cdot \text{B}_2\text{O}_3 \cdot \text{P}_2\text{O}_5$ (MX=AgI or LiCl). The major conclusions of the work are the following:

- the disorder of glasses is partly responsible for spreading the resonance of a unit over a ~10 ppm interval. However, deconvolution of signals from different units is rather straightforward and the fractions of the various units can be accurately determined in most cases
- relatively small changes in composition, such as the substitution of ~10% of P_2O_5 with B_2O_3 , can substantially change the ^{31}P spectra. These modifications are related to the way the negative charge is distributed in the borophosphate glass network
- rather unexpectedly, the addition of silver iodide causes the appearance of new ^{31}P peaks and the disappearance of others. This means that AgI acts as a network modifier in the borophosphate glasses while it apparently causes minor modifications of the local order in the borate glasses
- nucleation of orthophosphate phases is detected by ^{31}P NMR in samples with compositions near the boundary of the glass forming region

IN-SITU DETERMINATION OF THE KINETICS OF REACTION
BETWEEN LITHIUM AND FAST ION CONDUCTING LITHIUM BORATE GLASSES
BY

MICHEL W. BARSOU and HARRY L. TULLER
DEPARTMENT OF MATERIALS SCIENCE AND ENGINEERING
MASSACHUSETTS INSTITUTE OF TECHNOLOGY
CAMBRIDGE, MASS. 02139

ABSTRACT

A novel electrochemical method, based on coulometric titration in the double electrochemical cell Al-LiAl/Glass/Al-LiAl, for the in situ determination of the chemical stability domains of solid electrolytes was developed. This technique was used to determine, for the first time, the stability range and kinetics of reaction of fast Li-ion conducting glasses with Li. The glasses used were Li-borate and Li-chloroborates. The chloroborate glasses were found to react with Li at very low activities and form a crystalline reaction layer of $3\text{Li}_2\text{OB}_2\text{O}_3$. The chemical diffusivity of Li in the reaction layer was found to be about $5 \times 10^{-10} \text{ cm}^2/\text{sec}$ at 380°C with an activation energy of about 0.7 eV. The power of the method in elucidating the nature and diffusivity of the rate limiting species (i.e. ionic or electronic) in the reaction layers will be discussed in detail.

DIVALENT CONDUCTION IN $Pb_{1/2}-PbO-B_2O_3$ GLASSES.F.M. Schleitweller and W.B. JohnsonDepartment of Metallurgical Engineering
The Ohio State University, Columbus, OH 43210

High ionic conductivity glasses are attractive materials for application as solid state electrolytes in electrochemical cells. The ability to easily handle the amorphous materials, a lowered sensitivity to compositional fluctuations, and lack of preferred direction of conduction provides advantages over conventional solid electrolyte materials.

The ionic conductivities of divalent ions in superionic glasses has not been extensively investigated. In this study the Pb^{2+} conduction in a series of $Pb_{1/2}-PbO-B_2O_3$ glasses is evaluated. Conventional melting techniques are employed. Samples are prepared by slicing wafers of the glass formed after quenching from the melt and subsequently sputtering gold electrodes. The complex impedance has been measured with an a.c. 4-terminal pair technique at frequencies of 5Hz to 13MHz over a temperature range of 25-500 C. An IBM personal computer was used for data acquisition. Activation energies for the lead divalent species will be reported.

Present studies are oriented toward further enhancing the conductivity as well as understanding the mechanisms and relative importance of divalent lead ion transport in these amorphous materials.

THERMOELECTRIC POWER MEASUREMENTS OF SILVER-CONTAINING GLASSES

P. Bean and M. Tomozawa
Materials Engineering Department
Rensselaer Polytechnic Institute
Troy, NY 12180 USA

Thermoelectric power measurements were made on silver borate glass ($30 Ag_2O-70B_2O_3$), "mixed-alkali" silver-sodium borate glass ($24Ag_2O-6Na_2O-70B_2O_3$) and silver borate glass containing silver iodide ($40AgI-30Ag_2O-30B_2O_3$). The last glass is known to be a superionic conducting glass. These measurements were made using steady-state thermal gradients across the glass specimens with silver electrodes at temperatures between 75 and 225°C in air. The heat of transport of the conducting species (Ag^+ for these glasses) was determined from the thermoelectric power data.

It was found for glasses without silver iodide that thermoelectric power was independent of temperature and that the heat of transport was approximately zero. On the other hand, for the glass with silver iodide thermoelectric power increased with increasing temperature and the heat of transport was 3.5 kcal/mole. This value is nearly equal to the activation energy of d.c. conduction.

It has been suggested that the heat of transport is equal to the energy of migration minus the energy of vacancy formation. It is concluded from the present measurement that the conduction mode of silver ions in both silver-borate glass and silver-sodium-borate glass is similar to the vacancy mechanism and no difference in conduction mechanisms exists between the single and the "mixed-alkali" glasses. On the other hand, the conduction mode of the silver iodide-containing glass is similar to the interstitial mechanism.

Ionic Conductivity in Glasses: A Monte Carlo Study of
Ordered and Disordered One-Dimensional Models

A. Pechenik,* D. H. Whitmore, M. A. Ratner, S. Susman**
Departments of Materials Science and Engineering
and Chemistry and Materials Research Center,
Northwestern University, Evanston, IL 60201

β -eucryptite ($\text{Li}_2\text{OAl}_2\text{O}_3 \cdot 2\text{SiO}_2$) is an interesting fast ionic conductor exhibiting highly anisotropic ionic conductivity. The material crystallizes in space group $P6_322$. The conductivity along the c axis is 10^3 higher than along the a axis. This effect arises because Li ions are located in framework channels running parallel to the c axis. The channels are defined by alternating SiO_4 and AlO_4 tetrahedra. Thus the motion of Li ions can be modeled as hopping of interacting particles on a one-dimensional lattice with two types of alternating inequivalent sites: (1) a deep potential well near the Al and (2) a shallow well near Si.

This material can also be prepared as a glass. In a companion paper at this Conference we report on an investigation of ionic conductivity and structure of LiAlSiO_4 glass using complex impedance, IR and Raman spectroscopy. We found that the IR and Raman spectra of the glass can be easily understood on the basis of the Continuous Random Network (CRN) of AlO_4 and SiO_4 tetrahedra connected by their vertices, but otherwise distributed in a random fashion. According to the charge neutrality requirement, Li ions are situated in the neighborhood of AlO_4 tetrahedra and can hop from one such site to another via a site near SiO_4 .

The proposed mechanism of ionic conductivity in glassy β -eucryptite has been tested using a MC simulation technique. In this study only the effect of the Si-Al disorder has been considered. Two one-dimensional lattices have been investigated: (a) an ordered array of deep and shallow potential wells and (b) a disordered array of the same two types of potential wells. Ionic conductivity is simulated using a Monte-Carlo procedure in the usual way [1]. We calculate $\ln \sigma T$ vs. $1/T$ and σT vs. ρ (ρ = the ion occupational number on the lattice) plots. We observe an interesting influence of Si-Al disorder on activation energy measured from $\ln \sigma T$ vs $1/T$ plot. The activation energy for the disordered arrangement of Si-Al ions is lower than for the ordered one. This result is in agreement with the experimentally-observed increase in activation energy in going from glassy to crystalline β -eucryptite.

We also discuss effects of ion-ion correlations in one-dimensional systems and give a simple physical interpretation of the charge correlation factor, f_c .

[1] G. E. Murch and R. J. Thorn, *Phil. Mag.* 35 (1977) 493.

*Dow Chemical Corp., Midland, MI 48640

**Argonne National Labs., Argonne, IL 60439

"Ionic Conduction in Glasses:
a New Look at the Weak Electrolyte Theory"

James A. Bruce, Malcolm D. Ingram, Margaret A. MacKenzie
Department of Chemistry, University of Aberdeen, Aberdeen, Scotland.

According to the weak electrolyte theory, ⁽¹⁾ the strong compositional dependence of ionic conductivity in $\text{Na}_2\text{O}-\text{SiO}_2$ glasses, $\sigma \propto (\text{Na}_2\text{O})^{1/2}$, is related to changes in the concentration of mobile ions rather than to changes in ionic mobility. We have examined a highly conducting sodium borosilicate glass ($4\text{Na}_2\text{O} \cdot \text{B}_2\text{O}_3 \cdot 5\text{SiO}_2$), ⁽²⁾ using the *isovalent doping* technique of Moynihan and Lesikar. ⁽³⁾ The concentration of mobile ions (defects) at 150°C is actually *less* than that of an aluminosilicate glass of much lower conductivity.

The weak electrolyte theory therefore will have to be modified to take account of changes both in ionic mobilities and in the ionic dissociation equilibria.

- (1) D. Ravaine and J.L. Souquet, *Phys. Chem. Glasses*, **18** (1977) 27.
- (2) C.C. Hunter and M.D. Ingram, *Solid State Ionics*, **14** (1984) 31.
- (3) C.T. Moynihan and A.V. Lesikar, *J. Am. Ceram. Soc.*, **64** (1981) 40.

STUDIES ON $\text{AgI-Ag}_4\text{P}_2\text{O}_7$ SUPERIONIC CONDUCTING
GLASS SYSTEM.

K.A.Murugesamoorthi and S.Radhakrishna
Department of Physics
Indian Institute of Technology
Madras 600 036. INDIA.

$(\text{AgI})_x(\text{Ag}_4\text{P}_2\text{O}_7)_{1-x}$ (where x ranging from zero and five) solid electrolyte systems were prepared in the form of glass, by quenching the molten mixtures of the compounds of the appropriate composition in liquid Nitrogen. Earlier the compounds were taken in thin waled evacuated glass ampoules. The final glassy compounds were well ground into fine powder and stored in dark. The glassy nature of the samples were confirmed by the X-ray diffraction. The conductivity studies of the glasses were carried out at 1 KHz on pellets having the electrodes of the mixtures of electrolyte and silver powder, 2:1 by weight, in the temperature range 300 K to 365 K. The contact resistances were evaluated by measuring the resistances at 1KHz for the pellets of different thicknesses. The glass with the composition $4\text{AgI-Ag}_4\text{P}_2\text{O}_7$ is found to have the maximum conductivity among all the glasses of the system and it is about one order higher than that of the polycrystalline sample of the same composition. It is also seen from the conductivity values of all the glasses, and reported polycrystalline conductivity values, the conductivity of any glass is higher than that of the polycrystalline sample of the same composition at room temperature. The activation energies of all the above glasses were evaluated from the $(\log \sigma T \text{ vs } 1000/T)$ curve. The activation energy for the glass of the composition $4\text{AgI-Ag}_4\text{P}_2\text{O}_7$ was found to be minimum of all the other glasses of the system, but higher than the corresponding polycrystalline sample.

When the samples were annealed at 90°C , the conductivity was found to decrease gradually with time and reaching a constant values after some time. The final value of the conductivity is less than that of the polycrystalline sample of the same composition. The electronic conductivity of the samples were measured by Wagner's technique. The glass of the composition $4\text{AgI-Ag}_4\text{P}_2\text{O}_7$ was found to have minimum electronic conductivity and it increased with the deviation in the composition.

A solid state cell of the structure (Ag+electrolyte)/Electrolyte/(C, I₂, Electrolyte) have been constructed and the discharge characteristics investigated.

THEORETICAL STUDY OF THE INFLUENCE OF ION-ION INTERACTION ON INTERCALATION KINETICS

by : F. DALARD, D. DEROO, D. PEDONE

Laboratoire d'Energétique Electrochimique LA 265 - Domaine Universitaire
BP 75 - 38402 - Saint Martin d'Hères - France

The influence of ion-ion interaction has been studied by numerical simulation with a constant current command and a linear sweep voltage. This study is based on Armand's Model with repulsive interaction (by)

$$\mu_M^+ = \mu_M^{\circ+} + RT \ln \left(\frac{y}{1-y} \right) + b y$$

The following results has been obtained :

1 - Galvanostatic study

- The depth of discharge increase when the intercalation constant b increase. A decrease of voltage appears simultaneously. The intercalation is easier.
- The diffusion coefficient obtained with Atlung's curves is greater than without interactions. This results explain the difference between RMN and Electrochemical determination.

2 - Voltammetric study

- An increase of b provoke a decrease of the peak potential and the difference between cathodic and anodic peak increase too like in literature data for Li_xTiS_2 .
- The same phenomenon has been observed with a decrease of kinetics constants.
- The study of the reversibility of interfacial process has shown a great dependance of the curves with surface and deep interactions. We have successively examined the intercalation material :
 - without interactions
 - with null interactions at the interface material/electrolyte
 - with same interactions at the interface and in the depth of the material
 - with different interactions at the interface and in the depth of the material

If the interfacial interactions increase the peak current decrease but the difference between anodic and cathodic peak potential decrease.

All these results has been discussed in terms of energy share at the interface.

ON DIFFUSION HINDERED BY STICKS, SITE PERCOLATION, AND THE MIXED ALKALI EFFECT

A. Bunde^{**}, H. Harder⁺, and W. Dieterich⁺⁺Fakultät für Physik, Universität Konstanz, Konstanz, W.-Germany^{**}Center for Polymer Studies and Department of Physics, Boston University, Boston, USA

By varying the Na/K concentration in $\text{Na}_x\text{K}_{1-x}$ - β -alumina the ionic conductivity shows a strong minimum, which becomes more pronounced when the temperature is lowered¹. This effect is called Mixed-Alkali-Effect (MAE) and appears also in related Alkali- β -alumina mixtures¹ and in glasses with low dimensional conducting paths. Recently attention has been called to the possibility that there exists an effective attractive interaction between different Alkali ions which may cause the ions to form clusters thus leading to a pronounced minimum in the ionic conductivity². In this work we consider the extreme case of a strong effective attractive interaction, which causes the mobile ions of a different type to form immobile sticks. The current is only carried by the excess ions of one type. Using Monte Carlo simulations we investigate how the conductivity σ is influenced by the presence of the sticks. To this end, we consider a square lattice with different concentrations of sticks, perform a cluster analysis, and determine numerically the threshold concentration $p_c^{(s)}$, where the sticks start forming an infinite cluster and the threshold concentration $p_c^{(f)}$, where the free lattice sites stop forming an infinite network. We determine σ for small stick concentrations and around $p_c^{(f)}$ where it drops down and compare the results with the experimental situation:

1. G.M. Chandrasekhar, L.M. Foster, Solid State Commun. 27 (1978) 269-273
J.A. Bruce, M.D. Ingram, Solid State Ionics 9 & 10 (1983) 717-724
2. A. Suzuki, H. Sato, and R. Kikuchi, Phys. Rev. B 29, (1984) 3550-3566

Strong Correlation Effects on Ionic Motion In Framework Solid Electrolytes:
Computer Simulation of Interacting Particles in Periodic Potentials

Y. Boughaleb and M. A. Ratner

Department of Chemistry and Materials Research Center
Northwestern University, Evanston, IL 60201

The diffusion of Brownian particles in a periodic medium is a situation that can be found in several physical problems. If no interparticle interactions are included, the model is well understood in all ranges of the values of the characteristic parameters of the problem such as the friction γ . In real systems, at finite particle density, the single particle model must be extended to include interactions between particles.

In the last few years many kinds of interaction potential have been studied. However, the explicit results have been found only for certain limiting cases such as low potential barriers and high friction. Our purpose is to extend the study of the interacting particles to the low friction limit by using Langevin dynamic simulation. We find that for long range interaction, the general behavior of the dynamic properties is essentially the same, independent of the coupling of the mobile particles to the rigid lattice.

In this paper, we restrict ourselves to hard-core interaction

$$V(x) = V\left(\frac{b}{x}\right)^n \quad n > 2$$

and soft-core interaction ($n=2$) similar to those used in references [1] and [2].

We have calculated the conductivity $\sigma(\omega)$ and the pair correlation function for different particle concentration and values of the interaction diameter, b .

For heavily damped particles, we found good agreement with the analytical results of references [2],[3]. In the low friction limit and for small values of the interaction diameter compared to the lattice spacing, the change of the shape of the conductivity terms indicate that the forward scattering between mobile particles dominates the bounce back effect. In this limit, then, the "caterpillar" mechanism occurs freely, and the low-frequency slope of the microwave conductivity, which must be positive for any hopping model, may become negative in certain cases.

- [1] A. R. Bishop, W. Dieterich, and I. Peschel, Z. Physik B33, 187 (1979).
- [2] A. Bunde and W. Dieterich, Solid State Communication, 37, 229 (1982)
- [3] H. D. Vollmer, Z. Physik B33, 103 (1979).

FRACTAL DIMENSIONS OF IONIC TRAILS AND ISOSETS IN SUPERIONIC CONDUCTORS*

I Ebbesild, The Studsvik Science Research Laboratory, S-611 82 Nyköping, Sweden

P Vashishta and RK Kalia, Argonne National Laboratory, Argonne, IL 60439

SW de Leeuw, Department of Physics and Astronomy, Michigan State University,
East Lansing, MI 48824

Although the ions of superionic conductors obey well defined equations of motion the rapidly changing environment of each diffusing ion results in its following a trajectory that, to the microscopic observer, appears as a random walk in space - the phenomenon of Brownian motion. In the world of fractals, the Brownian motion in fluids finds widespread applications ranging from studies of coastlines to the occurrence of errors in communication systems. Surprisingly enough, the fractal nature of Brownian motion is one of the least understood aspects of fluids as well as superionic conductors: theoretical and computer simulation studies have stuck to the conventional approach of characterizing the single particle motion by the constant of self-diffusion. However, it has been emphasized recently that the fractal dimensionality of Brownian motion is also a useful characterization of single-particle motion. The fractal behavior of Brownian motion has two aspects, one which is associated with the ionic trajectories and the other with Brownian zerosets¹. In an ionic conductor the length of an ionic trajectory, $L(t)$, measured in units of step distance, g , scales as $L(t) \propto t^{1-D}$ where D is the fractal dimension of an ionic trajectory. The other fractal aspect of Brownian motion deals with isosets of coordinates of ions, $x(t), y(t)$ or $z(t)$, called Brown functions. The isosets consists of instants of time $t=s$ at which a Brown function becomes a constant. The so-called Brownian isosets are self-similar in that the parts and the whole reduced by similarity have identical distributions. Associated with the gaps between successive values of s is a probability distribution, $Pr(G>g)$, for finding a gap of duration, G , greater than a certain value g , which scales as g^{-D} where D is the fractal dimension of the Brownian isoset.

Fractal behavior is observed in the molecular dynamics simulation of ionic motion in superionic and molten Ag_2S . We obtain $D=2$ and $\bar{D}=1/2$ in agreement with Mandelbrot's predictions. The self similarity in the ionic trajectory and Brownian isosets as a function of the length of the ionic trajectories and temperature of the system will also be discussed.

¹Mandelbrot JB, The Fractal Geometry of Nature (Freeman, San Francisco, 1982)

*This work supported by the U.S. Department of Energy

NETWORK ANALOGUE FOR ONE-DIMENSIONAL SOLID IONIC CONDUCTORS.

By G. Roth and H. Böhm, Institut für Mineralogie der Universität Münster, D-4400 Münster, Corrensstr. 24.

Impedance plots from single crystals of solid state ionic conductors often exhibit features which cannot be interpreted by standard concepts.

The common method of representing the electrical properties of a sample by an equivalent circuit which comprises a voltage generator, an ohmic resistor and two capacitors, is obviously not adequate for the majority of solid state ionic conductors.

In many cases boundary effects are responsible for the deviation from the expected behaviour.

The objective of the present investigation is to outline the bulk effects of a single crystal which can be responsible for the observed anomalies in the impedance plots.

Based on a classical "hopping-model" the jumps of overdamped charged particles between discrete positions are described by a system of coupled linear differential equations of first order (master equation).

The analogue of this system of differential equations is an isomorphic system of equations describing the currents in an electrical network of voltage generators, ohmic resistors and capacitors.

The topology of this network is correlated to that one of the jump diffusion process in the crystal space.

One-dimensional single particle models can be represented as simple "ladder networks", whereas one-dimensional multi-particle models lead to branched networks.

The values of the network components can be determined from the static properties of the model (e.g. site occupancies in field-free equilibrium, potential barrier heights etc.).

There is an unambiguous correlation between network components and microphysical processes in the crystal:

The potential barriers correspond to the resistors, the potential minima to the capacitors and the voltage generators account for the potential change induced by the external electric field.

The proposed concept is applied to single- as well as multi-particle problems.

The results of the theoretical investigations of such networks are described and they are compared to experimental data.

In addition, the dependence of the impedance on various parameters of the model (e.g. concentration of mobile ions, interaction energy, potential distribution along the diffusion path etc.) is discussed.

Percolation Efficiency and Mixed Alkali Effect

H. Sato, K. Wada*, and A. Suzuki
 School of Materials Engineering, Purdue University,
 West Lafayette, IN 47907

Earlier, we presented a theoretical model for the mixed alkali effect in glasses and β -aluminas in terms of the percolation efficiency based on the Path Probability method (PPM) of irreversible statistical mechanics^{1,2}. We present an improved treatment of the percolation efficiency which gives far better agreements with experimental observations. We have shown that the decrease in f_1 (the physical correlation factor or the percolation efficiency), but not in the number or the mobility of the conduction ions, upon the addition of second species is the major cause of the mixed alkali effect.^{1,2} Because f_1 represents the efficiency of motion of conduction ions for long distances, it is also shown that f_1 eventually approaches unity and mixed alkali effect practically disappears in the high frequency limit. This agrees with experimental observations. However, the results of calculation by the original formalism of the PPM have some undesirable features. The decrease in f_1 is caused by the correlation of two species of conduction ions through their mutual interactions. In the original treatment, the decrease in f_1 only occurs by the development of the long range order in the distribution of two kinds of ions and the decrease is limited to a narrow composition range. These undesirable features have been found to be due to an inadequate averaging method utilized in the original PPM. In dealing with transport phenomena, the introduction of the instantaneous distribution conversion process and the time conversion process to the original PPM has been found to be necessary. The result of the introduction of these two conversion processes shows that even a minor amount of fluctuation in the distribution is enough to suppress f_1 and hence in systems with low connective diffusion paths such as in glasses and β -aluminas, the decrease in f_1 occurs in a wide composition range. The result of calculation also agrees well with the Monte Carlo simulation method.

1. H. Sato, A. Suzuki and R. Kikuchi, Solid State Ionics **9-10** 725 (1983).
2. A. Suzuki, H. Sato and R. Kikuchi, Phys. Rev. B **29** 3550 (1984).

*Present address: Physics Department, Faculty of Science, Hokkaido University, Sapporo, Japan.

DEBYE-HÜCKEL-TYPE RELAXATION PROCESSES IN SOLID IONIC CONDUCTORS: THE MODEL

K. FUNKE and I. RIESS *

Institut für Physikalische Chemie und Elektrochemie der Universität
 Hannover, Callinstr. 3 - 3A, D-3000 Hannover, Federal Republic of Germany

* On sabbatical leave from the Technion, Haifa

We discuss the possibility of adapting the basic idea of the Debye-Hückel-Onsager-Falkenhagen theory to solid electrolytes. In our mathematical treatment we abandon the Debye-Hückel continuum-ansatz in favor of a description of the diffusion dynamics in terms of hopping processes along discrete lattice sites. Generally, we consider the effect of the Coulomb interaction among the charge carriers on the transport properties. In the model, each charged defect experiences the periodic lattice potential plus the Coulomb potential due to the distribution of the other defects. After an "initial" hop of a charged defect, the defect either hops back again into its absolute potential minimum, or the surrounding "defect cloud" moves forward, shifting the Coulomb minimum towards the new position of the defect.

Our calculation yields the following results. At high frequencies the motion of the single charge carrier is decoupled from that of the surrounding "defect cloud", resulting in a relatively high conductivity in this limit. At low frequencies, on the other hand, the slower motion of the "defect cloud" yields a conductivity which is generally lower than the conductivity in the high frequency limit. At sufficiently low temperature we find

$$[\sigma(\omega) - \sigma(0)] \propto \omega^p \quad \text{with } 0 < p < 1$$

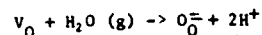
in a wide range of intermediate frequencies, i.e., we recover the characteristics of the "universal dielectric response" put forward by Jonscher in 1977.

On the basis of our model, we can explain a great number of experimental results, including not only $\sigma(\omega)$ data but also quasielastic neutron-scattering spectra of solid electrolytes, and the dependence of formal activation energies for hopping processes in solids on the concentration of the mobile charged defects.

PROTONIC CONDUCTION IN ACCEPTOR-DOPED KTaO₃ CRYSTALS*

Wing-Kit Lee and A.S. Nowick, Columbia University, New York, N.Y. 10027
and L.A. Boatner, Oak Ridge National Laboratory, Oak Ridge, TN 37830

Potassium tantalate crystals, which have the cubic perovskite structure, may be doped with transition metal ions (e.g. Cu²⁺, Fe³⁺ or Ni³⁺). These dopants substitute for the Ta⁵⁺ ions and therefore require charge compensation, most probably by oxygen vacancies, V_O. When such crystals are heated in water vapor at elevated temperatures (~900°C), protons are introduced which manifest themselves in the form of a sharp IR absorption peak at 3485 cm⁻¹ when measured at 77K.¹ This band provides a monitor of the H⁺ content of the crystal after various treatments. The OH⁻ band can be removed by vacuum annealing. Undoped crystals, on the other hand, do not appear to be susceptible to the introduction of H⁺. A simple model for the introduction of H⁺ is the defect reaction:



Conductivity measurements (by means of complex impedance measurements) were made on several Cu-, Fe- and Ni-doped crystals containing H⁺. The conductivity shows a unique activation energy of 1.10 ± 0.05 eV. Additional experiments involve the substitution of deuterium (D⁺) for H⁺. A strong isotope effect in the conductivity (σ_{D+}/σ_{H+} ~ 2.5) is observed with a small difference in activation enthalpy ~ 0.04 eV. This shows that: a) protons are responsible for the conductivity, and b) that non-classical behavior is involved in proton migration.

The conductivity behavior seems to be similar to that of acceptor doped SrCeO₃ which has been studied extensively by Iwahara et al.² The latter is a polycrystalline ceramic, however, and so does not permit observation of an OH⁻ band.

Additional information about the defects present in KTaO₃, both before and after the introduction of H⁺ is obtained by means of EPR studies of the transition metal ions and by dielectric relaxation studies at low temperatures.

1. H. Engstrom, J.B. Bates and L.A. Boatner, J. Chem. Phys. 73 (1980) 1073.
2. H. Iwahara et al., Solid State Ionics 3/4 (1981) 359; 11 (1983) 117.

* Research sponsored by the Division of Materials Sciences, U.S. Department of Energy under grant DE-FG 02-85 ER 45187 with Columbia University and contract DE-AC 05-84OR21400 with Martin Marietta Energy Systems Inc.

HIGH TEMPERATURE PROTON CONDUCTORS
NOTE I: BORON AND ALUMINUM PHOSPHATES*

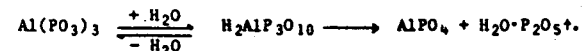
E. Montoneri
Dipartimento di Chimica
Industriale e Ingegneria
Chimica del Politecnico
Pz. L. da Vinci 32
20133 Milano, Italy

and

E. Findl, F. Kulesa and F. J. Salzano
Department of Applied Science
Brookhaven National Laboratory
Upton, New York 11973-5000

ABSTRACT

The chemical stability and conductivity of boron and aluminum phosphates with P/B and P/Al atomic ratios >1 are reported as functions of temperature (100-280°C) and steam pressure (up to 5 atm). Aluminum phosphates are much more stable than the boron analogues. Al(PO₃)₃ and H₂AlP₃O₁₀ undergo the reactions



At 280°C and P_{H2O} = 5 atm the product is a mixture of AlPO₄ and H₂AlP₃O₁₀ and the conductivity is in the 10⁻² ohm⁻¹ cm⁻¹ range. With boron phosphates high material loss and poor conductivity are caused by the instability of the BPO₄ phase, due to the reaction



The results show that because of the occurrence of dehydration or hydrolytic reactions, increasing the water vapour pressure does not always lead to higher conductivity and that neutral phosphates may have a key role in relation to the stability and conductivity of the solid acid electrolytes.

*Work performed under the auspices of the U.S. Department of Energy.

HIGH TEMPERATURE TYPE PROTONIC CONDUCTOR BASED ON SrCeO AND ITS APPLICATION TO THE EXTRACTION OF HYDROGEN GAS

H. IWAHARA, T. ESAKA, H. UCHIDA, T. YAMAUCHI and K. OGAKI
 Department of Environmental Chemistry and Technology,
 Faculty of Engineering, Tottori University,
 Koyamacho Tottori 680, JAPAN

Recently, we found that some sintered oxides based on strontium cerium trioxide exhibit appreciable proton conduction in hydrogen-containing atmosphere at high temperatures.¹⁾ SrCe_{0.95}Yb_{0.05}O_{3-α}, SrCe_{0.95}Yb_{0.05}O_{3-α} and SrCe_{0.95}Sc_{0.05}O_{3-α} belong to this class of conductors. Attempts to apply these oxides as electrolytes for fuel cell, galvanic cell type²⁻⁵⁾ hydrogen sensor, steam sensor etc. were made by us and reported elsewhere. In principle, such a proton conducting solid electrolyte can be used to extract hydrogen gas from hydrogen-containing gases or hydrogen compounds.

In the present study, electrical properties of SrCe_{0.95}Yb_{0.05}O_{3-α} ceramic under various atmosphere were investigated, and, using this ceramic as a solid electrolyte diaphragm, the extraction of hydrogen from various gases were examined.

Well sintered ceramic of SrCe_{0.95}Yb_{0.05}O_{3-α} was stable when one side of the ceramic disc was exposed to hydrogen gas and the other to oxygen at high temperatures up to 1000°C. In this condition, the conduction was mainly protonic and, partially but slightly, electronic. The electronic conduction was clarified to be p-type by investigating the dependence of electronic conductivity on oxygen partial pressure. This ceramic was also a stable protonic conductor even when both sides of the ceramic disc was exposed to hydrogen gas at 800°C. However, appreciable n-type electronic conduction was observed at 900°C, although reduction of the oxide was not so remarkable in the case of wet hydrogen.

Using a thin disc of SrCe_{0.95}Yb_{0.05}O_{3-α} ceramic as a solid electrolyte diaphragm and porous platinum as an electrode material, electrochemical hydrogen extractor was constructed by way of experiment. On introducing CO+H₂O mixed gas into anode compartment and on sending a direct current to the ceramic disc, hydrogen could be obtained at the cathode compartment of the extractor at 800-900°C. Hydrogen extraction rate was close to the theoretical value calculated from the amount of electricity. We could also extract hydrogen from thermal cracking gases of ethane, alcohol and hydrogen sulfide.

As previously reported, we could electrolyze water vapor using this type of solid electrolyte.⁵⁾ In the present experiment, a bench-scale steam electrolyzer was fabricated and pure hydrogen gas could be extracted in a rate of a few l/hr. The purity of hydrogen gas thus obtained was higher than 99% and the partial pressure of water vapor in the gas was less than 0.3 Torr.

[Reference]

- 1) H. Iwahara, T. Esaka, H. Uchida and N. Maeda, Solid State Ionics, **3/4**, 359 (1981)
- 2) H. Iwahara, H. Uchida and S. Tanaka, Solid State Ionics, **9**, 1091 (1983)
- 3) H. Iwahara and H. Uchida, Proc. Intern. Meet. Chemical Sensors, 1983 Fukuoka p227
- 4) H. Iwahara, H. Uchida and J. Kondo, J. Appl. Electrochem., **13**, 365 (1983)
- 5) H. Iwahara, H. Uchida and N. Maeda, J. Power Sources, **2**, 293 (1982)

PROTON TRANSPORT IN AMMONIUM PARATUNGSTATE (NH₄)₁₀W₁₂O₄₁.5H₂O

S.K. Tolpadi, S. Chandra and S.A. Hashmi
 Physics Department, Banaras Hindu University, Varanasi-221005, India

The possibility of Ammonium paratungstate (NH₄)₁₀W₁₂O₄₁.5H₂O as an efficient proton conductor has been explored. Coulometry, Infra Red Spectra, temperature and frequency dependence of the electrical conductivity of the above materials have been studied. The results of the above investigations are summarised below.

- (i) Direct D.C. electrolysis or coulometry was performed in a specially designed coulometer in which the volume of gases evolved at the electrodes could be measured by the movement of mercury column in a micropipette. This experiment suggests that about 70% of the charge is transported by H⁺ ions or the proton transference number is about 0.7.
- (ii) On electrolysis it has been found that the sample surface near the anode was blackened suggesting an electrode charge transfer reaction. There was a little blackening at the cathode also.
- (iii) The I.R. spectrum of the sample near the cathode and the anode ends were recorded after electrolysis along with the original sample. It has been found that due to the proton transport there is (a) a decrease in the relative intensity of NH₄⁺ and H₂O at the anode side (b) an increase in the relative intensity of NH₄⁺ and H₂O bands on the cathode side and (c) the appearance of a broad band around 1060 cm⁻¹ on the cathode side which is possibly due to enhanced librational motion of W-O of tungstate group.
- (iv) Temperature variation of the electrical conductivity has been studied in the frequency range (100 Hz - 100 KHz). The result has been interpreted in terms of thermally activated motion accompanied possibly by structural phase transition.

A detailed analysis of the above results suggests that for charge transport, protons are contributed both by NH₄⁺ and H₂O structural groups in the sample.

ELECTRICAL CONDUCTIVITY OF $\text{HTaWO}_6 \cdot \text{H}_2\text{O}$ AND HTaWO_6 .

C.M. Mari, F. Bonino, M. Catti, R. Pasinetti, S. Pizzini

Dipartimento di Chimica Fisica ed Elettrochimica, Università degli Studi, Via C. Golgi 19, 20133 MILANO - ITALY

The NMR technique has been used to investigate the motion of hydrogen ions in $\text{HTaWO}_6 \cdot \text{H}_2\text{O}$ and HTaWO_6 [1,2]. The results suggest that these compounds are fair hydrogen-ion conductors in which individual protons are the only specie responsible for the conduction process. Aim of the paper is to present the electrical conductivity measurements carried out on such materials and to compare the activation energies for the conduction processes as well as the diffusion coefficient with those obtained by NMR technique.

References

- [1] M.A. Butler, R.M. Biefeld, Phys. Rev. B 11, 5455 (1979).
 [2] R.M. Biefeld, M.A. Butler, L.J. Azevedo, Solid State Comm. 38, 1125 (1981).

SPECTROSCOPIC STUDIES OF THE FAST PROTON

CONDUCTOR LITHIUM HYDRAZINIUM SULFATE

Scott H. Brown and Roger Frech
 Department of Chemistry
 University of Oklahoma
 Norman, OK. 73019

Lithium hydrazinium sulfate, $\text{LiN}_2\text{H}_5\text{SO}_4$, crystallizes in the orthorhombic space group $\text{Pna}2_1$ (C_{2v}^9) (1) and has been shown to be a proton conductor (2). At room temperature, the dc conductivity was found to be very anisotropic with the direction of highest conductivity along the c-axis.

In an effort to better understand the mechanism of proton transport in solid $\text{LiN}_2\text{H}_5\text{SO}_4$, a series of spectroscopic studies have been initiated. First in this series was an analysis of the polarized Raman spectra of $\text{LiN}_2\text{H}_5\text{SO}_4$ single crystals at room temperature. The Raman spectra of the deuterated analog were also obtained and used in making normal mode assignments. Although the N-H stretching modes are expected to be broad due to the extensive hydrogen bonding in this crystal, there is a very sharp and intense N-H stretching mode at 3331 cm^{-1} .

In addition, a preliminary temperature-dependent Raman study indicates interesting band shape and bandwidth changes as a function of temperature. Anomalous intensity behavior has been noted in a low frequency mode (52 cm^{-1}) in the temperature range 300K-20K in which the intensity of the mode dramatically increases with increasing temperature. The implications of all these spectroscopic observations are discussed in terms of current theories of proton transport in solids.

1. M. R. Anderson and I. D. Brown, Acta. Cryst. B30, 831 (1974).
2. J. Vanderkooy, J. D. Cuthbert and H. E. Patch, Can. J. Phys. 42, 1871 (1964).

MECHANISM OF PROTON TRANSPORT IN HUP (H₂UO₂PO₄·4H₂O)

B. K. Sen and S. Sen
Department of Chemistry
University College of Science
700 009 Calcutta
India

HUP (and HUAs) has recently attracted the attention of both physicists and chemists as an intrinsic proton conductor. The mechanism of proton transport in this is a process which is very little understood. The position of uranyl and phosphate ions and the orientation of the water-squares in a layered structure of HUP is known from its crystal structure studies. Neutron diffraction data do not precisely locate the position of the protons in the structure, although they adequately indicate the dynamics of the protons in the crystal. These findings severely restrict the applicability of the idea of movement of a "vehicle" like H₃O⁺. Certain other mechanisms involving "proton jumps" and water reorientation have been proposed for proton transfer in HUP. However, in all these interpretations, the role of phosphate (or arsenate) ions in aiding the proton transport has been overlooked, and all investigators have so far concentrated solely on the motion of protons through the water network. The phosphate groups are joined to the water network and each square contains on an average one vacant orbital containing a lone pair of electrons on an oxygen atom. This vacant orbital can accommodate a proton from an adjacent in-square member according to the mechanism proposed by us earlier. The transfer of a proton from one water square to another might take place through the participation of the π -electron cloud of the phosphate group. (The same mechanism can explain the transfer of a proton in a KDP crystal.) The mechanism of the intra-square and inter-square "proton jumps" has been explained by the application of the idea of π -proton bonds. The drastic reduction in the value of proton conductivity in NH₄UO₂PO₄·3H₂O is easily explained by the fact that no free lone pair of electrons on the oxygen or nitrogen atoms forming the square are available. There is thus no vacancy which can accept a proton and allow for the transport process to occur.

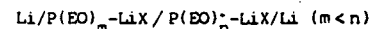
53

POTENTIOMETRIC MEASUREMENTS OF IONIC MOBILITIES IN PEO-LiX COMPLEXES

A. BOURIDAH, F. DALARD, D. DEROO, M. ARMAND

Laboratoire d'Energétique Electrochimique - LA 265
BP 75 - 38402 - SAINT MARTIN D'HERES - FRANCE

We report on electrochemical method to determine the cationic transport number and the salt diffusion coefficient in PEO-LiX complexes. This method is based on the E.M.F. measurements of galvanic cells of the following type :



The two half cells are initially separated. After contact is made at t=0, the E.M.F. is recorded.

The recorded E.M.F. at t=0 is equal to the junction potential between the two merging electrolytes and is expressed by :

$$E = -2 \frac{RT}{F} \int_n^m t_{X^-} d \ln a_{\pm}$$

The anionic transference number assumed independent from activity, can be calculated, provided that the respective salt mean activities are known. At t > 0, as LiX diffuses until equilibrium the potential decreases. D_{LiX} is then determined by fitting the experimental potential versus time dependence with simulated curves for various D_{LiX} values.

We have investigated complexes with X⁻ = I⁻, ClO₄⁻, CF₃SO₃⁻ at 90°C.

It is known that these materials exhibit several phases. Based on the published phases diagram (1,2) we have selected a concentration range in which the electrolytes are fully amorphous at 90° : the ratio O/Li are respectively 8 to 120 for LiI and LiClO₄ and 30 to 120 for LiCF₃SO₃.

The mean activity was estimated from cell E.M.F. with the following anion specific electrodes : Ag-AgI/LiI and a redox polymer electrode/LiClO₄ and/LiCF₃SO₃.

From our results it appears that :

- t_{Li⁺} is close to 0.5 in each complexes.
- LiCF₃SO₃ diffuses much more rapidly than either LiI or LiClO₄.

- (1) - C. BERTHIER, W. GORECKI, M. MINIER, M.B. ARMAND, J.M. CHABAGNO and P. RIGAUD, Solid State Ionics 11, (1983), 91
- (2) - C. ROBITAILLE, D. FAUTEUX, to be published in J. Electrochem. Soc., (1985)

PREPARATION AND PROPERTIES OF PEO COMPLEXES
OF DIVALENT CATION SALTS

L. L. Yang, R. Hug, G. C. Farrington

Department of materials Science
University of Pennsylvania
3231 Walnut Street, Philadelphia, PA 19104

We have prepared several polyethylene oxide (PEO) compositions with $MgCl_2$, $PbCl_2$, and several other salts of divalent cations. $MgCl_2$ compositions were prepared over a range, $MgCl_2(PEO)_4$ to $MgCl_2(PEO)_{24}$. Similar compositions were prepared with $PbCl_2$.

DSC and X-ray diffraction studies of the $MgCl_2$ -PEO films show no evidence of free $MgCl_2$ and suggest that PEO and $MgCl_2$ do indeed form well-defined complexes and not simply mixtures of salt and polymer.

Conductivity measurements were made using complex ac impedance analysis. Samples of the divalent halide films were compared with a sample of a standard film of $LiCF_3SO_3(PEO)_9$ and with a film of pure PEO. Of the family of $MgCl_2$ compositions, the best conductor was $MgCl_2(PEO)_{16}$ which had a conductivity of about $10^{-10}(\text{ohm-cm})^{-1}$ at 30°C , about an order of magnitude less than the $LiCF_3SO_3$ complex. However, the conductivity of the $MgCl_2$ complex at 100°C was comparable to that of the $LiCF_3SO_3$ complex.

This paper discusses the preparation, physical characteristics, and conductivity of these interesting divalent cation salt complexes of polyethylene oxide.

NMR, DSC, and Conductivity study of a poly(ethylene oxide) complex electrolyte: $PEO(LiClO_4)_x$

W. Gorecki, R. Andr ani, C. Berthier
Laboratoire de Spectrom trie Physique, U.S.M.Grenoble, BP 87
38402 Saint-Martin d'H res, France

M. Armand,
LEE-ENSEEGrenoble, B.P. 75 38402 Saint-Martin d'H res, France

M. Mali, J. Roos, and D. Brinkmann
Physics Institute, University of Zurich, 8001 Zurich,
Switzerland

It is now well known that the alkali metal salts polyethylene oxide adducts are among the best potentialities as future solid electrolytes for advanced batteries(1,2). Recently, we have discussed the ionic conductivity mechanism in those systems which present phase diagramm analogous to $PEO(LiCF_3SO_3)_x$, which are inhomogeneous systems over a wide range of temperature.(3)

In this paper, we concentrate on the $PEO(LiClO_4)_x$ system, which exhibits several peculiar features:

-First, the existence of two crystalline phases of distinct stoichiometry $x^{-1}=3$ and 6, with respective melting temperature of 420 K and about 345 K can be inferred from our DSC and NMR measurements and has been confirmed by structural measurements from Robitaille et al (4).

-Second, the very slow kinetics of crystallization of the stoichiometric complexes allows their study in a wide temperature range where the system stays as a fully homogeneous melt.

Determination of the self-diffusion coefficient by the pulsed field gradient technique(5) has been performed in samples of concentration $x^{-1}=6, 8, 20$. Conductivity and DSC measurements are currently in progress in samples issued from the same membranes, as well as spin-lattice relaxation of lithium, chlorine, and proton.

Preliminary comparison with conductivity measurements available in the literature (2,4) leads to cationic transport number of 0.3-0.5. This contrasts strongly with the behaviour of $PEO(LiCF_3SO_3)_x$. For this compound, when comparing the diffusion coefficient determined from NMR (6) and the conductivity data (3), one observes that about a quarter of the ions are really participating to the conductivity and that ions pairs are also mobile.

REFERENCES

- ¹ M.B. ARMAND, J.M. CHABAGNO, M.J. DUCLOT, "Fast Ion Transport in Solids", eds. P. Vashishta, J.N. Mundy, G.K. Shenoy (North Holland), 1979, p. 13)
- ² J.M. CHABAGNO, Thesis, Grenoble (1980)
- ³ M. MINIER, C. BERTHIER, and W. GORECKI, J. Physique **45** (1984), 739
- ⁴ C. ROBITAILLE, D. FAUTEUX, to appear in J. Electrochem. Soc. (1985)
- ⁵ E.O. STEJSKAL and J.E. TANNER, J. Chem. Phys. **42**, (1965), 288
- ⁶ M. MALI, J. ROOS, and D. BRINKMANN, Proceedings of the XXIInd Congress Ampere, eds K.A. HULLER, R. KIND, and J. ROOS, Zurich, Sept. 1984

POLYMERIC ELECTROLYTES BASED ON POLY(ETHYLENE IMINE) AND LITHIUM SALTS*

C. K. Chiang, G. T. Davis and C. A. Harding
 Polymers Division
 National Bureau of Standards
 Gaithersburg, MD 20899

T. Takahashi
 Ube Industries
 Tokyo, Japan

Linear poly(ethylene imine) has been shown to dissolve sodium iodide with a loss of crystallinity up to a molar ratio of salt to polymer of 0.15. Between 0.15 and 0.3 mole ratio, a high-melting crystal phase involving the polymer and the salt removes NaI from solution. The behavior of lithium salts (LiF, LiCl, LiBr, LiI, LiSCN, LiC₂O₄, LiBF₄, and LiCF₃SO₃) in linear PEI has been examined because of their importance in battery applications. All of these salts dissolved in the polymer as evidenced by a decrease in the heat of fusion (DSC) and an increase in the glass transition of the polymer. The triflate (CF₃SO₃⁻) salt caused the greatest reduction in crystallinity following evaporation of the common solvent used in preparing the mixtures. However, once melted and then cooled, many of the mixtures remained in the amorphous state. No evidence for a crystalline complex between the linear PEI and these lithium salts was observed. The dc conductivity of mixtures containing 0.1 moles of LiBF₄ or LiC₂O₄ per mole of polymer was on the order of 1×10^{-8} S/cm at room temperature but increased to 1×10^{-3} S/cm at 150°C. The polymer prepared so far is of rather low molecular weight (~2000) and exhibits poor mechanical properties at elevated temperatures.

*Work supported in part by Office of Naval Research

A Pulsed Field Gradient NMR Study of Cation and Anion Diffusion in the Amorphous Phase of the Polymer Electrolyte (PEO)₈LiCF₃SO₃

Sankar Bhattacharja, S. W. Smoot and D. H. Whitmore
 Department of Materials Science and Engineering
 Northwestern University
 Evanston, Illinois 60201
 USA

Abstract

Pulsed field gradient (PFG) NMR measurements of the cation and anion diffusion coefficients, D_{Li} and D_{PF} , are reported for the amorphous phase of the poly(ethylene) oxide-lithium triflate [(PEO)₈ - LiCF₃SO₃] complex in the temperature range 428-448K. These diffusion data, which allow unambiguous determination of the cation (t_+) and anion (t_-) transference numbers for this amorphous electrolyte, show that both kinds of ions are mobile in the amorphous complex, with t_+ ranging from 0.34 at 428K to 0.41 at 448K. We also report some a.c. conductivity results on the same amorphous complex, along with some self-diffusion coefficients for PEO obtained by monitoring its proton diffusion behavior by the PFG method. These latter observations are discussed in the light of predictions about polymer self-diffusion behavior based on the well-known de Gennes reptation model of a polymer chain.

THIN FILM SOLID STATE POLYMER ELECTROLYTES CONTAINING SILVER AND COPPER IONS AS CHARGE CARRIERS

Teresa Abrantes, Luis Alcacer and Cesar Sequeira

Departamento de Quimica, Instituto Superior Tecnico,
Av. Rovisco Pais, 1096 Lisboa Codex, Portugal

ABSTRACT

The domains of redox stability and the ionic conductivities were determined for solid state thin films based on polymer complex salts containing silver and copper ions as charge carriers.

Polyethylene oxide (PEO) and similar polymers were complexed in various proportions with simple silver and copper salts and solid state thin films were prepared using solution casting techniques. The electrochemical behaviour, including the domains of redox stability, was determined by cyclic voltammetry in cell systems of the type Pt/PEO:M⁺X⁻/Pt. The ionic conductivities were measured by standard methods.

These polymer electrolytes were also combined with several electrodes such as conducting polymers (polypyrrole and polyaniline), insertion compounds such as V₆O₁₃, composite materials such as MnO mixed with carbon black in a polymer matrix, and appropriate metals in systems of the type M/PEO:M⁺X⁻/M' where M' is one of the above mentioned electrode materials. Some preliminary results on these systems with view to their performance applications in solid state electrochemical devices will be presented.

CHEMICAL MODIFICATION OF POLY(ETHYLENE IMINE) FOR POLYMERIC ELECTROLYTE

Toru Takahashi
Ube Industries
Tokyo, Japan

G. T. Davis, C. K. Chiang and C. A. Harding
Polymers Division
National Bureau of Standards
Gaithersburg, MD 20899 USA

Sodium iodide can be dissolved in linear poly(ethylene-imine), PEI, up to mole ratios of salt to polymer of about 0.15. DC conductivities as large as 3×10^{-4} S/cm at 100°C have been measured. At higher concentrations of salt, a high melting complex crystal phase involving PEI and NaI is formed and dc conductivity is greatly reduced. The linear PEI has been chemically modified in an attempt to prevent formation of the crystalline complex without altering its ability to dissolve salts and conduct ions. Three main systems were investigated: (a) poly(N-acetyl-ethyleneimine), (b) partially quaternized PEI with ethyl or butyl groups, and (c) PEI lightly cross-linked with diepoxycetane. Dissolution of salt was followed by x-ray diffraction on the mixtures and changes in T_g as determined by DSC. In all cases, the crystallinity was destroyed but conductivity of salt-containing polymer was not improved.

* Work supported in part by Office of Naval Research

Interface between Cosintered $(U,M)O_{2+x}$
Electrodes and Yttria Zirconia Electrolyte

S.P.S. Badwal and F.T. Ciacchi
CSIRO, Division of Materials Science
Advanced Materials Laboratory
P.O. Box 4331, Melbourne
Vic., Australia 3001

D.K. Sood
Microelectronics Technology Centre
RMIT, Melbourne
Vic., Australia 3000

Abstract

Solid state electrochemical cells have been prepared by cosintering prereacted electrode and electrolyte materials together. The electrodes under investigation are the nonstoichiometric oxides of the general formula $(U,M)O_{2+x}$ ($M=Sc,Y$). The electrolyte is an oxygen ion conductor. Both the electrode and the electrolyte phases have the fluorite structure. The techniques used for characterisation of the cosintered samples were x-ray diffraction, Rutherford back scattering, scanning electron microscopy - EDAX and optical microscopy. The electrochemical behaviour was studied by impedance spectroscopy and galvanostatic current interruption method. For $M=Sc$, an intermediate phase which also has the fluorite structure is formed and is responsible for the strong bonding of the electrode layer to the electrolyte. The thickness of the intermediate phase was about 2-3 μm . For $M=Y$, no evidence for the formation of such a phase was found and the adhesion of the electrode to electrolyte was poor. Considerable loss of uranium, which in some cases led to destabilization of the fluorite phase, was observed from the surface of the electrode layers. The thickness of the uranium depletion zone extended to a depth of about 1.5 μm . The charge transport across the unified $(U,Sc)O_{2+x}$ /yttria stabilized zirconia interface is slow and appears to be diffusion controlled. The presence of the intermediate layer in the case of urania-scandia solid solutions is detrimental to the electrochemical behaviour.

OXYGEN SURFACE EXCHANGE AND DIFFUSION
IN FAST IONIC CONDUCTORS

J. A. Kilner, A. E. McHale and B. C. H. Steele
Wolfson Unit for Solid State Ionics
Imperial College, London SW7 2BP U.K.

M. van Hemert and A. J. Burggraaf
Laboratory of Inorganic Chemistry and Materials Science
Twente University of Technology
P. O. Box 217, 7500 AE Enschede, The Netherlands.

A significant and largely unexplored phenomenon in the performance of oxides used in electrochemical devices is the gas/solid exchange mechanism operative at the oxide surface in a variety of operating conditions. The rate of exchange of oxygen between the gas phase and the surface of an electrolyte can be the rate limiting step in the performance of electrodes for various electrochemical devices constructed using solid oxide electrolytes and is also a significant factor in the performance of new electrocatalytic compounds.

In an effort to understand the fundamental phenomena involved in the surface exchange of oxygen, we have studied the rate of exchange of isotopic ^{18}O with the surface of several important oxide electrolytes including $Zr(Y)O_{2-x}$, $(Bi_{1-x}Er_x)_2O_3$, $(Bi_{1-x}Y_x)_2O_3$ and pyrochlores in the system $Nd_2Zr_2O_7 - Nd_2Ce_2O_7$. Measurements on both single crystals and polycrystalline materials were performed when possible.

For the measurements, single crystal and/or polycrystalline specimens were heated in an ^{18}O -enriched atmosphere. The penetration profiles of the tracer ^{18}O were then determined using a high sensitivity dynamic SIMS technique. A typical profile obtained for a sample of $Nd_2Ce_2O_7$ is shown in Fig. (1).

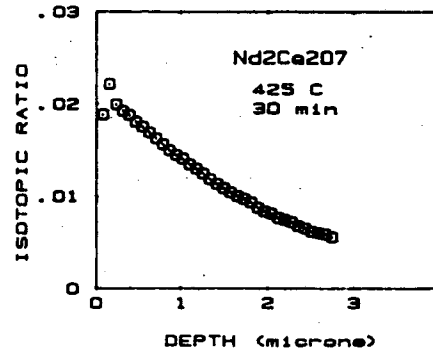


Fig. 1. Experimental SIMS data.

Analysis of the measured penetration profile yield values of D , the self diffusion coefficient, and K , the surface exchange coefficient, for each specimen. In all cases studied, the exchange of oxygen between the gas phase and the solid is limited by the rate of surface exchange and not the diffusion coefficient of oxygen.

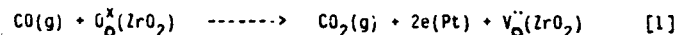
The results of these analysis will be discussed with reference to the known "bulk" defect chemistry of the compounds, contrasting the behavior of the different electrolyte types, and with reference to tendency of these materials to exhibit surface segregation of one component. For example, preliminary results in doped bismuth oxide indicate a high surface exchange rate relative to zirconia, perhaps related to the different surface chemistries of these materials as well as their electronic structure. Results of limited experiments on the effects of applied bias on the rate of oxygen exchange will also be discussed in reference to probable effects on surface defects and segregation.

ELECTROCATALYTIC MECHANISMS IN THE OXIDATION OF
CO ON A SCANDIA STABILIZED ZIRCONIA
ELECTROLYTE SURFACE

Bang C. Nguyen and David M. Mason
Department of Chemical Engineering
Stanford University
Stanford, California 94305

A general survey of the electrocatalytic behavior of the following individual hydrocarbons: H_2 , CO , CH_4 , CH_3OH and C_2H_5OH as well as O_2 in the temperature range 700-850°C has been made. Scandia stabilized zirconia of composition 7-10 mole% Sc_2O_3 in the form a disc was used as the electrolyte. Engelhard Au and Pt pastes were employed as electrodes. The fuel cell was operated in a differential mode. Two very interesting results have emerged from this investigation. First, it is found that the electrocatalytic reactivity of each of the above hydrocarbon compounds and O_2 is very similar whether porous Au or Pt electrodes were used; though the ordinary non-electrochemical catalytic activities and chemisorption characteristics of these metals are widely different. An analysis of the data in the low overpotential region yields activation energies for the anodic oxidation of the above hydrocarbons which is independent of the nature of the metal electrode (ranging from 20 kcal/mole for C_2H_5OH to 30 kcal/mole for CO). It has also been found that the O_2 cathodic reaction has an activation energy of about 31 kcal/mole for both Au and Pt. The second interesting feature of the current overpotential data is the fact that there is a very large enhancement in the electrode reaction rates when the electrolyte is in a blackened state. These results indicate that the major mechanistic steps of the electrode reactions at both the cathode and anode involve sites on the electrolyte surface rather than the metal electrode surface.

A more detailed mechanistic study was performed employing CO/CO_2 mixtures. The overall reaction can be written as:



where $O_x^{\cdot\cdot}$ is an oxygen ion in the electrolyte and $V_O^{\cdot\cdot}$ is an oxygen vacancy. Information regarding the mechanism of the above reaction can be obtained by examining the dependence of the exchange current density I_0 on the ratio of the partial pressures of CO and CO_2 and temperature. A possible reaction sequence involving the electrolyte surface assumes that the electrons found in the immediate vicinity of the gas/electrode/electrolyte three-phase boundary are capable of diffusing to the reaction sites on the electrolyte surface, probably surface oxygen vacancies, to form neutral oxygen vacancies (F centers). Evidence supporting this type of surface electronic conductivity comes from TEM analysis of the blackened electrolyte specimens which reveals the existence of a surface zirconia suboxide which is intrinsically electronically conducting. The induced electronic conductivity is not a bulk effect but is restricted to the electrolyte surface. These neutral vacancies then react with CO to give CO_2 . The above reaction mechanism along with several other alternatives are currently being examined in order to arrive at the best detailed description of the anodic and cathodic electrode reactions.

CYCLIC VOLTAMMETRY AT METAL-ZIRCONIA ELECTROLYTE INTERFACE

by

D. GOZZI, L. PETRUCCI and M. TOMELLINI

Dipartimento di Chimica, Università di Roma "La Sapienza"
P.le Aldo Moro 5, 00185 ROMA-ITALY

In some recent papers (1-3) were shown the results of several experiments concerning the oxidation kinetics of nickel at high temperatures and low oxygen pressures through zirconia electrolyte cells. In those experiments the metal under study was the working electrode of a zirconia electrolyte cell subjected to galvanostatic steps producing oxygen at the metal-electrolyte interface.

A model, based on the C. Wagner theory modified for the presence of an electric field according to Kroger, was proposed for explaining the associated chronopotentiometric curve.

The analysis of such curves allowed to derive all the kinetic parameters of the tarnishing reaction of nickel as described in the above mentioned papers.

In order to obtain a more complete understanding of the phenomena occurring at that interface some cyclic voltammeteries were kept between successive galvanostatic steps.

As elsewhere described (3), the experiments can be carried out in a high vacuum furnace and the pressure recording during the cell operation gives an independent way to study what happens when the current flows through the cell both in galvanostatic and potentiostatic mode.

In fact, as well known, in a zirconia cell, oxygen can be produced at one of the interfaces, accordingly to the polarity, and its flow-rate is proportional to the current density.

Some cyclic voltammeteries coupled with pressure recordings will be shown as a function of temperature in the range between 760 and 1150 C for different specimens of nickel.

Voltammetric curves will be explained through a model based on the oxidation of nickel the kinetics of which affects the capacity of the double layer located at the Metal/Electrolyte interface.

REFERENCES

1. D. Gozzi- High Temperature Kinetics of Metal-Oxygen Reactions by Solid Oxide Electrolyte Cells: an Applications to Nickel- MATERIALS CHEMISTRY AND PHYSICS, 8 (1983) 502-530
2. D. Gozzi-Kinetic of Metal-Oxygen Reaction by Solid Oxide Electrolyte Cells- SOLID STATE IONICS, 14 (1984) 239-245
3. D. Gozzi and G. De Maria -High Temperature Kinetics of Nickel-Oxygen Reaction by Ceramic Electrolyte Cells - HIGH TEMPERATURE SCIENCE, in press

IMPEDANCE OF METAL-SOLID ELECTROLYTE INTERFACES¹

J. B. Bates and J. C. Wang

Solid State Division, Oak Ridge National Laboratory
Oak Ridge, Tennessee 37831

The impedance of metal/solid electrolyte/metal cells can often be represented by $Z(\omega) = R + A(j\omega)^{-n}$ over several decades of frequency within the range from $\sim 10^0$ to $\sim 10^5$ Hz, where R is the bulk resistance of the electrolyte, A is a constant, and $0 < n < 1$. The term $A(j\omega)^{-n}$ has been called a constant phase angle element,² a universal capacitor,³ or, more recently, a d-fractance.⁴ With $D = A \sin(n\pi/2)$, the impedance can be expressed as $Z(\omega) = R + D \cot(n\pi/2) / \omega^n - jD/\omega^n$, where $j = \sqrt{-1}$. The characteristic property of a cell whose contacts behave as a universal capacitor is the frequency-dependent real part of Z which is proportional to ω^{-n} .

Two-point and four-point impedance measurements were made on several kinds of β -alumina, β'' -alumina, and zirconia cells over the frequency range from 0.1 to 10^7 Hz and at temperatures above and below 300 K. The texture of the electrolyte surfaces onto which metal contacts were sputtered varied from "rough" with features as large as $10 \mu\text{m}$ to "smooth" with features smaller than $0.5 \mu\text{m}$. For all of the cells investigated, the two-point and four-point data show that the frequency dependence of $\text{Re}(Z)$ is due to the metal-electrolyte interface and not to a bulk effect of the electrolyte.⁵ The value of the parameter n depends on surface texture and, for β - and β'' -alumina, is a strong function of temperature. At 300 K, n increases as the interface becomes smoother, but always remains less than one. The value of n decreases from ~ 0.9 at 300 K to ~ 0.6 at 670 K but remains nearly constant below 300 K.

The impedance function $A(j\omega)^{-n}$ has recently been derived from a fractal model of a rough interface.⁶ In this model, n is directly related to the fractal dimension of the interface. An alternative model⁷ based on a distribution of pores of different sizes and shapes at the interface can account qualitatively for the temperature dependence of n, and the calculated impedance matches closely the experimental data over a wide frequency range.

1. Research sponsored by the Division of Materials Sciences, U.S. Department of Energy under contract DE-AC05-84OR21400 with Martin Marietta Energy Systems, Inc.
2. P. H. Bottelberghs and G. H. J. Broers, *J. Electroanal. Chem.* **67**, 155 (1976).
3. A. K. Jonscher, *Dielectric Relaxation in Solids*, (Chelsea Dielectrics Press, London, 1983), p. 91.
4. A. L. Le Mehaute and G. Crepy, *Solid State Ionics* **9A10**, 17 (1983).
5. D. P. Almond, A. R. West, and R. J. Grant, *Solid State Commun.* **44**, 1277 (1982).
6. S. H. Liu, "A Fractal Model for Charge Diffusion Across a Rough Interface," *Phys. Rev. Lett.* (in press) 1984.
7. J. C. Wang and J. B. Bates, "Model for the Interfacial Impedance Between a Solid Electrolyte and a Metal Electrode," this conference.

THE LITHIUM-POLYMER ELECTROLYTE INTERFACE

F. Bonino and B. Scrosati

Dipartimento di Chimica, University of Rome 'La Sapienza',
Piazzale A. Moro 5, 00185 Rome, Italy.

The bulk properties of polymer electrolytes based on the combination of poly(ethylene oxide) with lithium salts, have been extensively studied(1) and these electrolytes are currently proposed for the development of high energy, rechargeable batteries(2,3).

However, relatively few studies have been so far reported on the characteristics and properties of the electrochemical processes at the electrode-polymer electrolyte interface.

On the other hand, the evaluation of these processes is of importance for the determination of the effective cyclability of the polymer batteries.

In this paper we report preliminary results of an investigation of the lithium-polymer electrolyte interface, performed by voltammetry, polarization and a.c. impedance measurements.

REFERENCES.

- 1)-M. Armand, *Solid State Ionics*, **9&10**, 745 (1983).
- 2)-A. Hooper and B.C. Tofield, *J. Power Sources*, **11**, 33 (1984).
- 3)-M. Gauthier, D. Fauteux, G. Vassort, A. Belanger, M. Duval, P. Ricoux, J.M. Chabagno, D. Muller, P. Rigaud, M. Armand, D. Deroo, 2nd Intl. Conference on Lithium Batteries, Paris, April 25-27, 1984.

Microstructure of Pt Electrodes and its
Influence on the Oxygen Transfer Kinetics

S.P.S. Badwal and F.T. Ciacchi
CSIRO, Division of Materials Science
Advanced Materials Laboratory
P.O. Box 4331, Melbourne
Australia 3001

Abstract

Electrode morphology plays a key role in establishing O_2/O^{2-} redox equilibrium at the Pt electrode/ O^{2-} conducting solid electrolyte interface and is believed to be the major cause for the reported discrepancies in the mechanism of oxygen transfer reaction. The temperature and the gas composition to which these interfaces are exposed have a strong influence on the electrode microstructure. In this paper a systematic study of the effect of temperature, time of heat treatment, electrode thickness and gas atmosphere on the electrode microstructure and impedance behaviour has been made. The electrodes studied were sputtered Pt of different thicknesses and three commercial pastes.

For kinetic and microstructural studies the electrodes were deposited on one or both sides of polished polycrystalline discs of yttria stabilized zirconia and heat treated for different times at 600, 750 and 900°C in pure oxygen. The influence of other gases (such as O_2/Ar , CO/CO_2 and CO_2/H_2 mixtures), substrates (such as sapphire, ceria, urania and single crystal zirconia) and substrate preparation was also investigated but for only one thickness of sputtered Pt. The electrodes in the as deposited state have very high initial surface area, small crystallite size (50-100 Å) and extensive three phase contact boundary. The crystallite size after heat treatment at 600°C was $< 0.1 \mu m$ but it increased to $> 1.0 \mu m$ after the 900°C heating. The sintering and grain growth of Pt particles led to increases in the time constant and the electrode resistance. The relationship between microstructure and the electrode behaviour was intricate. The electrode arcs in the impedance plane were invariably skewed, dispersed and in some cases two arcs were clearly separated. The optimum electrode thickness is a function of maximum temperature, time and gas composition to which the electrodes are exposed. For paste electrodes it was almost impossible to reproduce microstructure and hence the electrode behaviour.

NOVEL SOLID STATE POLYMERIC BATTERIES

A J Patrick, M D Glasse, R J Latham and R G Linford
School of Chemistry, Leicester Polytechnic, PO Box 143, Leicester LE1 9BH, UK

Subject to the lifting of a British Government secrecy order on a patent application, we propose to present results on some novel room-temperature, low current density solid state batteries. Voltage against time characteristics for loaded and unloaded cells will be discussed. Conductivity data on the novel electrolytes, obtained by complex plane analysis will be presented for a range of temperatures and stoichiometries. A minor modification of conventional X-ray powder diffraction methodology will be described, and the results of application of this technique to the electrolyte films will be reported. Variable temperature optical microscopy studies and differential scanning calorimetric measurements of the electrolyte materials have been carried out and results will be discussed. The results of SEM/EDAX investigations of cell components after discharge will be interpreted in terms of transport of electrochemical active material.

It is anticipated that the secrecy order will be lifted in the near future, at which time a more detailed abstract can be submitted for issue to conference delegates.

RECHARGEABLE SOLID ELECTROLYTE CELLS WITH A COPPER ION CONDUCTOR, $Rb_4Cu_{16}I_2Cl_{12}$

O. YAMAMOTO, Y. TAKEDA, R. KANNO and Y. IKEDA

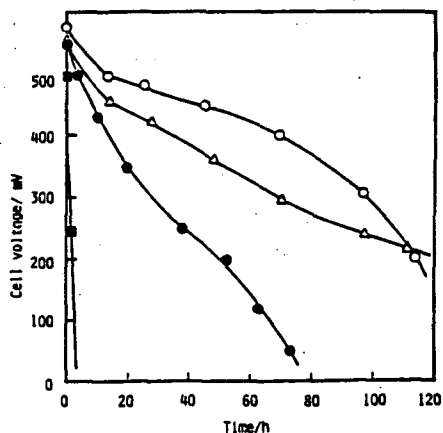
Department of Chemistry, Faculty of Engineering
Mie University, Tsu 514, Japan

Solid electrolyte batteries are a promising system for microwatt rechargeable batteries because of the long shelf-life stability and of no leakage after prolonged storage. In this study, the copper Chevrel phase ($Cu_5Mo_8S_8$) was examined as anode of the cell using solid electrolyte, $Rb_4Cu_{16}I_2Cl_{12}$. Further, various calcogenides with layered structure such as metal disulfides, metal diselenides and metal ditellurides have been examined as cathode materials.

The solid electrolyte, $Rb_4Cu_{16}I_2Cl_{12}$, was prepared by the method described in a previous paper. The copper Chevrel phase and various metal calcogenides were prepared by methods described in literatures. A mixture of copper Chevrel phase and the electrolyte in 2:1 weight ratio was used as the anode. The cathode of the cell was a mixture of the electrolyte and metal dicalcogenides. The cell was pressed at 300MPa to form a pellet in 13mm diameter.

Anode The electrolyte, $Rb_4Cu_{16}I_2Cl_{12}$, was reported to be unstable in contact with copper metal. The cells using the copper anode showed a poor discharge performance after they were stored for a certain period. However, for the cell with the copper Chevrel phase anode, no appreciable deterioration has been observed after a certain period storage. This suggests that the copper Chevrel phase is a good anode material for the cell using the electrolyte, $Rb_4Cu_{16}I_2Cl_{12}$.

Cathode The constant current discharge curves of the cells with the copper Chevrel anode and metal disulfide cathodes are shown in Fig. 1. The cells with NbS_2 and TiS_2 show better discharge performances than those with other cathode materials. For the cell with NbS_2 , 0.3mol of copper is intercalated into NbS_2 to the cut-off voltage of 0.4V.



Constant current(100uA) discharge curves of the cell $Cu_5Mo_8S_8/Rb_4Cu_{16}I_2Cl_{12}/MS_2$
 M: ○ Nb, ● Ta, ■ Mo, △ Ti

THIN FILM ARRAYS OF LITHIUM - PEO CELLS

J R Owen,* R D Rudkin and B C H Steele
 Dept. Met. and Mat. Sci., Imperial College, London SW7
 *Dept. Chem. University of Salford, Manchester M5 4WT

Arrays of cells were formed by thin film techniques. The positive electrodes, V_2O_5 , were evaporated onto a pattern of Al current collector pads supported on insulating substrates. $(PEO)_8LiClO_4$ was dip coated onto the electrodes from solution in CH_3CN , dried, and coated by evaporation with an array of Li negative electrodes. Cr was applied as a current collector which was inert to Li and gave some protection from the atmosphere.

A microcomputer was equipped with up to 16 D/A and 32 A/D interfaces for simultaneous measurements on cells using a variety of discharge/charge programmes. Some cells were selected for complex impedance analysis in order to determine the relative limitations of electrode and electrolyte.

The mass production of cell arrays in thin layer geometries matched to multichannel analysis hardware greatly increases the rate of device testing and, via specially constructed cells, the rate of determination of the thermodynamic and kinetic data which relate to the reaction of lithium with oxidizing materials.

COMPLEX IMPEDANCE BEHAVIOUR OF THE CELL
 $\text{Li} | \text{LiClO}_4(\text{PC}) | \text{V}_6\text{O}_{13}$

H. S. Maiti and N. C. Chakrabish
 Materials Science Centre
 Indian Institute of Technology
 Kharagpur-721 302
 India

V_6O_{13} has been prepared by control decomposition of ammonium metavanadate (NH_4VO_3) in a specially designed glass tube heated in air. This method produced better results than decomposition in flowing argon, in which the product was usually contaminated by a small amount of V_2O_5 . For conductivity measurement and cell fabrication, V_6O_{13} powders were sintered at 500°C in argon using 5 wt.% lead borosilicate glass powder as a sintering aid. Sintered pellets showed room temperature (25°C) conductivity of $4 \times 10^{-1} \text{ ohm}^{-1} \text{ cm}^{-1}$, which is slightly higher than usually reported.

Laboratory-type cells were fabricated with a lithium ribbon electrode (thickness 0.4 mm) and sintered V_6O_{13} pellets (thickness ~2 mm). Open circuit voltage of these cells has been found to be between 3.4-3.5V, which is much higher than previously reported. Complex impedance of the cell has been measured in the 13 MHz to 5 Hz range at different states of discharging and also with different DC bias voltages. Interface resistance (~2 k Ω) is found to be much larger than the electrolyte resistance (~650 Ω). While the latter increases only slightly, the former increases quite significantly with the progress of discharge. Even though both the anodic and cathodic interfaces contribute to the polarization, diffusion at the cathodic interface becomes rate limiting.

IN-SITU FORMATION OF A SOLID/LIQUID COMPOSITE
 ELECTROLYTE IN Li/I_2 BATTERIES

J.B. Phipps, T.G. Hayes, P.M. Skarstad, and D.F. Untereker

Medtronic, 6700 Shingle Creek Parkway, Brooklyn Center, MN 55430

The Li/I_2 battery is considered the prime example of a commercially available, solid electrolyte battery. In 1975 Greatbatch et. al (1) discovered that by coating the lithium anode with polyvinylpyridine (PVP) the resistance of the LiI discharge layer could be reduced by a factor of 10 to 100 as compared to cells with uncoated anodes, thus greatly improving battery performance. While several investigators have linked the improved performance of PVP-coated batteries to microstructural changes in the LiI electrolyte, the exact mechanism responsible for the reduced electrolyte resistance was discovered only recently (2).

This presentation will report on the findings of a detailed microstructural study of the discharge process in Li/I_2 cells, which was undertaken to better understand the mechanism of enhanced performance. To accomplish this goal, a special Li/I_2 battery was constructed so that the discharge product was formed between two glass slides as a thin, translucent layer. This design made it possible to continuously monitor the electrolyte formation process during discharge.

As reported previously (2), this study led to the discovery of a liquid phase which forms a continuous capillary network throughout the LiI discharge product. The liquid phase is formed from an electrochemical reaction between the PVP coating, lithium anode, and iodine. Moreover, this liquid is an electrolyte through which lithium ions can rapidly migrate. The reduced internal resistance of Li/I_2 batteries with PVP-coated anodes can be directly attributed to the presence of this liquid electrolyte.

Isolation of the liquid electrolyte for spectral analysis was accomplished by constructing a "gas cathode" cell. This type of cell was very similar to commercial Li/I_2 batteries except that the iodine in the cell was present as a gas, rather than as the normal I_2/PVP cathode material. This innovation made it possible to separate the liquid electrolyte phase formed during discharge from the other battery components.

It is evident from this study that the $\text{Li}/\text{PVP}/\text{I}_2$ system, which was previously thought to be a classic example of a self-forming solid electrolyte battery system, actually belongs to a new battery class; a class characterized by the presence of a self-forming liquid electrolyte. A discussion of the unique properties of this solid/liquid composite electrolyte system and a time-lapse film of the discharge process in $\text{Li}/\text{PVP}/\text{I}_2$ batteries will highlight this presentation.

- (1) W. Greatbatch, R. Mead and F. Rudolph, U.S. Patent, 3,957,533 (1976).
- (2) J.B. Phipps, T.G. Hayes, P.M. Skarstad, and D.F. Untereker, Extended Abstracts of the 166th Meeting of the Electrochemical Society, New Orleans, Louisiana, Vol. 84-2, p. 258 (1984).

CONDUCTIVITY OF THE BINARY SYSTEM IODINE-PHENAZINE.

J.I. Franco (*); L. Perissinotti (**), and N.E. Walsbe de Reza (***)
 (*) CITEFA; (**) CIC and (***) CITEFA and CONICET,

PRINSO (Program of Research in Solid State Physics of CONICET-
 National Council for Scientific and Technological Research)
 Zufriategui 4380. Villa Martelli, (1603), Buenos Aires, Argentina.

Abstract

The polarization phenomena in cells of the type $Ag/AgCl/I_2.Ar/C$, under discharge conditions, involves not only the known contributions in aqueous electrochemistry, such as ionic migration or charge transfer, but another phenomenon due to the variation of the cathode resistance. The waste of the active component of cathode (I_2) generates a concentration gradient of the halogen in the electrode. Due to the strong dependence of its conductivity with composition, important electric resistances arise in the zones close to the electrolyte. This fact points out the importance of studying the electrical transport properties in charge transfer complexes as well as their dependence with the electrode composition.

The aim of this work is to contribute to the understanding of the conductivity phenomena in the iodine-phenazine system, between 5°C and 60°C and in the composition range $0 < x_1 < 1$. Conductivity measurements were performed by the four-point-probe method. The phase diagram of the binary system shows an intermediate compound I_2 -phenazine (1).

Conditions under which, the Lichtenecker rule is valid for the conductivity of heterogeneous, ideal mixtures are discussed (2). This rule is applied to results of conductivity measurements, for the first time in this kind of systems and in the whole range of compositions and temperatures.

An extrapolated value for the conductivity of the complex I_2 -phenazine of $\kappa(I_2-Phen) = 3.55 \cdot 10^{-9} \text{ S.cm}^{-1}$ at 25°C and an activation energy of 1.37 eV are reported.

- (1) J.I. Franco, L. Perissinotti and N.E. Walsbe de Reza. "Behavior of mixtures of iodine with anthracene, phenazine and thianthrene", to be published in Solid State Ionics.
- (2) K. Lichtenecker, Physikal. Z. 25 (1924) 169.

SOLID STATE BATTERIES

J. R. Akridge and H. Vourlis
 Union Carbide Corporation
 Battery Products Division
 Technology Laboratory
 P.O. Box 45035
 Westlake, Ohio 44145

The discovery^(1,2) of high lithium ion conductivity vitreous solid electrolytes having good thermal stability and good moldability has enabled the construction of high performance solid state lithium batteries. The batteries to be discussed are all of the form: Li/Solid electrolyte/cathode. The level of performance achieved to date for current density, shelf stability, operating temperature range, etc., approaches that obtained for lithium nonaqueous coin cells.

Battery construction will be discussed. Data will be presented detailing discharge performance as a function of current density and temperature. Performance after long term shelf storage at room and elevated temperature will be shown. Microcalorimetry results will be given to support claims of long term battery shelf life.

1. J.P. Malugani and G. Robert, Solid State Ionics, 1, 519 (1980)
2. J.R. Akridge, U.S. Patent 4,465,746 (August 14, 1984)

THERMAL HISTORY AND POLYMER ELECTROLYTE STRUCTURE: IMPLICATIONS FOR SOLID STATE BATTERY DESIGN

R J Neat, M D Glass, R G Linford
School of Chemistry, Leicester Polytechnic, PO Box 143, Leicester LE1 9RH, UK

and A Hooper
Material Development Division, AERE Harwell, Oxon, England

Complexes of alkali metal salts with polymers are favoured as electrolytes in solid state batteries because they possess desirable mechanical properties and adequate conductance. Both these attributes are structure-dependent. Several factors affect structure; and we wish here to draw particular attention to thermal history. We report the results of experiments that identify:-

- i) the crystalline structure of some electrolyte films.
- ii) the influence of thermal history on the crystalline structure.
- iii) the affect of structural changes on conductance and mechanical properties.

We have observed three different partially crystalline regions (spherulites) in our polymeric electrolyte films, no more than two of which occur simultaneously. These melt over different temperature ranges and have different conductivities. We view the amorphous content of the spherulite as providing the conducting pathway and the crystalline content the structural stiffness.

Each spherulite type not only melts separately, but can also be recreated by controlled cooling or annealing. We will discuss:-

- a) Whether the deliberate imposition of a time and temperature profile can be used to control conductance and mechanical properties.
- b) The possible affect of thermal history imposed during preparation and operation of the battery system.

Volume changes occur during both crystallisation and melting, and these may be localised and cause distortion. Such deformation could lead to a rupture of the contact with electrodes under certain circumstances. The formation of a particular spherulite type may produce changes on the overall flexibility of the electrolyte material.

It is believed that an examination of the thermal history of the polymer electrolyte may provide an explanation of some battery performance parameters.

THE PHOTO-INTERCALATION BATTERY:

PROGRESS AND DIFFICULTIES

by

G. Betz and H. Tributsch

Hahn-Meitner-Institut
D-1000 Berlin 39
Federal Republic of Germany

Results obtained with the first solar-powered intercalation battery;

Cu_3PS_4 (hv)/ Cu^+ (acetonitrile)/ Cu_3FeS_4 are discussed.

MICROMECHANISM OF FORMATION OF AMORPHOUS THIN FILMS OF $\text{Li}_2\text{O}-\text{B}_2\text{O}_3$,
 $\text{Li}_2\text{O}-\text{SiO}_2$, and $\text{Li}_2\text{O}-\text{P}_2\text{O}_5$ BY PVD

Li-Wei Zhang, M. Kobayashi and K. S. Goto
 Tokyo Institute of Technology
 Meguro-ku, Ookayama 2-12
 Tokyo, Japan

The thin films of $\text{Li}_2\text{O}-\text{B}_2\text{O}_3$, $\text{Li}_2\text{O}-\text{SiO}_2$, and $\text{Li}_2\text{O}-\text{P}_2\text{O}_5$ systems have been prepared into amorphous state by PVD process.

The intention of the present work is to specify the molecules of vapors and to measure the deposition rates. The micromechanism of the formation of the thin films will be clarified in relation to the composition and temperature of vapor sources and to the substrate temperature.

The composition of the amorphous films has been determined by chemical analysis and ion micro-analyzer. Furthermore, X-ray diffraction was used in determining the amorphous state.

The results are suggesting that large molecules of interoxide compounds are vaporizing out and the some fractions are depositing on the films. The concentration gradient and pore distribution in the thin films will be discussed.

STRUCTURAL AND ELECTRICAL STUDIES ON THE DEFECT PYROCHLORE MATERIALS
 $\text{Pb}_{1-x}\text{M}_x\text{O}_{3-x}$ (M = Ta, Nb)

E. Beetz¹, C.R.A. Catlow¹, A. Santoro², B.C.H. Steele³
 (1) Department of Chemistry, U.C.L. London, U.K.
 (2) Reactor Division, N.B.S. Gaithersburg, Maryland, U.S.A.
 (3) Department of Metallurgy and Materials Science, Imperial College, London, U.K.

Since the work of Van Dijk (1) which demonstrated the existence of high oxygen mobilities in the pyrochlore lattice, materials with this structure have received increasing amounts of attention. In this presentation we report a study of the structural and electrical properties of the defective pyrochlore structured compounds $\text{Pb}_{1-x}\text{M}_x\text{O}_{3-x}$ where M is either tantalum or niobium.

The structural properties were probed using neutron diffraction techniques. Powder diffraction patterns were taken on the high resolution diffractometers at the N.B.S. Washington and I.L.L. Grenoble. Processing the data using the Rietveld refinement technique (2) led to structures displaying large amounts of unordered vacancies on the oxygen sublattice. The electrical conductivity of the materials was investigated via impedance techniques. Even at high temperatures (700°C) the samples are predominantly electronic conductors, with only a small ionic contribution to the total conductivity.

Whereas no evidence for defect ordering could be extracted from the Bragg diffraction data sets, an experiment on the diffuse scattering diffractometer D7, at the I.L.L. revealed the presence of extensive vacancy ordering. The diminution of the ionic conductivity from the values anticipated for a defect pyrochlore can be explained in terms of the ordered defect structure revealed in the diffuse scattering experiment.

A model will be presented to explain both the evolution of the defect structure and its relationship to the observed defect mobilities. The central feature of the model is the existence of a competition between interactions such as those between the lone pair electrons of the lead ions and the vacancies in the lattice which drive the formation of non-stoichiometry and vacancy-vacancy repulsion interactions which oppose defect incorporation in the lattice.

(1) M.P. van Dijk, K.J. de Vries and A.J. Burggraaf
 Solid State Ionics 9/10 913 (1983)

(2) H.M. Rietveld J. Applied Cryst 2 65 (1969)

ELECTRICAL TRANSPORT IN NiO - CeO₂ MIXTURES

V. B. Tare

Department of Metallurgical Engineering
Institute of Technology
Baranas Hindu University
Varanasi - 221005, INDIA

and

G. M. Mehrotra and J. B. Wagner, Jr.
Center for Solid State Science
and Departments of Chemistry, Physics and
Mechanical and Aerospace Engineering
Arizona State University
Tempe, AZ 85287 USA

In recent years, there has been considerable interest in the study of electrical transport in two-phase mixtures due to their technological importance. Anomalous electrical conduction behavior in NiO containing uniformly dispersed metallicly conducting, second phase particles of Ni₃S₂ or Ni has recently been reported.

The present paper describes the results of our measurements of total electrical conductivity of the two-phase NiO - CeO₂ mixtures as a function of composition and temperature (600° - 1000°C). The variation of specific conductivity and of the activation energy for conduction with composition shows a small deviation from ideal behavior at the CeO₂ rich compositions. The results are explained by postulating the trapping of transporting species at the NiO - CeO₂ interfaces.

THE EFFECT OF THE HUMIDITY ON THE ELECTRICAL-CONDUCTIVITY OF "AS RECEIVED" COMMERCIAL ZrO₂/Y₂O₃ - DOPED SOLID ELECTROLYTE.

F. Croce: ENEA-CRE-Casaccia, DIP/TIB, Divisione Chimica
00060, Via Anguillarese 301, Roma, Italia

The electrical conductivity is one of the most important properties of the practical solid electrolytes.

In these materials there is a close relation between the conductivity and the defect structure:

- the concentration and the mobility of the predominant defects influence directly the conductivity.

This latter experimental quantity is principally affected by:

- temperature, oxygen partial pressure, composition and microstructural features of the material.

Furthermore, in many practical applications as oxygen sensor, the solid electrolyte is in contact with an hydrogen containing atmosphere. As in these conditions a water shift equilibrium is established, it seems to us very interesting to study the electrical conductivity of the polycrystalline sinters exposed to inert gases with different moisture concentrations.

The poster will concern with the electrical properties of sintered ZrO₂/Y₂O₃ used as solid electrolyte in the commercially available Italian oxygen sensor* for liquid steel and furnace gaseous atmosphere. The X-ray spectra and the SEM photographs of the sinters will be preliminary shown.

Then their bulk and grain boundary conductivities, obtained by impedance spectroscopy analysis, will be reported as function of the temperature, oxygen and/or water partial pressure.

Finally the transport number determination results, obtained by EMF measurements, will be illustrated too.

* FER- Ceramica Industriale S.p.A.
20038 Seregno (MI) Via Pacini, 49
Italy

HIGH OXYGEN ION CONDUCTION OF A BISMUTH OXIDE-CADMIUM OXIDE PHASE :
CONDUCTIVITY AND TRANSPORT NUMBER MEASUREMENTS ; STRUCTURAL INVESTIGATIONS

T. GRAIA, P. CONFLANT, J.C. BOIVIN and D. THOMAS
Laboratoire de Cristallochimie et Physicochimie du Solide (UA 452)
ENS de Chimie de Lille
B.P. 108 59652 VILLENEUVE D'ASCQ Cedex (FRANCE)

A NEW PHENOMENON - THE INDUCTIVE IMPEDANCE IN
Bi₂O₃-BASED OXYGEN IONIC CONDUCTORS

Guan-Yao Meng, Ming Zhou and Ding-kun Peng
Department Applied Chemistry
University of Science and Technology of China
Heifei, Anhui
The People's Republic of China

Bismuth oxides and bismuth-based mixed oxides are known to exhibit high oxygen conduction at moderate temperature (1-3). Up to now three different structural types have been investigated :

- The fluorite structural type

It is the structure related to the high temperature form of Bi₂O₃ (6) ; it can be stabilized towards room temperature by addition of a rare-earth dopant to Bi₂O₃ (4)

- The rhombohedral structural type

It results from the addition of an earth alkaline (Ca, Sr, Ba) (5) or rare earth (6) cation to Bi₂O₃

- The bcc structural type

It has been observed when lead oxide is added to bismuth oxide and occurs over a wide range of composition. Conductivity values as high as $1(\Omega \cdot \text{cm})^{-1}$ at 870 K are reached (7).

Unfortunately, the later cannot be stabilized down to room temperature. That difficulty can be overcome when cadmium is used instead of lead. The paper reports the synthesis conditions, stability range, conductivity measurements by complex impedance technic, and transport number measurements by e.m.f. method, of a bismuth cadmium oxide solid solution which exhibits the b.c.c. structure.

Results of single crystal X-ray investigations using a four circle diffractometer will also be described.

- 1- TAKAHASHI, T. and IWAHARA, H., J. Appl. Electrochem., 2 (1972) 97
- 2- HARWIG, H.A. and GERARDS, A.G., J. Solid State Chem., 26 (1978) 265
- 3- VERKERK, M.J., KEIZER, K. and BURGRAAF, A.J., J. Appl. Electrochem., 10 (1980) 81
- 4- CAHEN, H.T., VAN DEN BELT, T.G.M., DE WIT, J.H.W. and BROERS, G.H.J., Solid State Ionics, 1 (1980) 411
- 5- BOIVIN, J.C. and THOMAS, D., Solid State Ionics, 5 (1981) 523
- 6- IWAHARA, H., ESAKA, T., SATO, T. and TAKAHASHI, T., J. Solid State Chem., 39 (1981) 173
- 7- HONNART, F., BOIVIN, J.C., THOMAS, D. and DE VRIES, K.J., Solid State Ionics, 10 (1983) 921

The AC impedance and admittance measurements on the samples of a number of binary and ternary Bi₂O₃-based oxide systems were made in the frequency range of 5 Hz to 1 MHz and the temperature range of 250°C to 800°C. It was found that, in the lower temperature region, all samples showed a standard complex plane plot which could be represented by an equivalent RC parallel circuit and, in the higher temperature region (typically higher than ~550°C), showed an unusual inductive impedance: impedance spectra in the higher frequency region were an almost vertical line below the real axis and the respective admittance spectra were a nearly perfect semicircle below the real axis. This unique phenomenon has not been reported in the current literature on solid electrode-electrolyte systems. The fact that it was independent of the sample preparation method, the nature and amount of the dopants, electrode material and measuring instrument systems indicated that the above phenomenon was a feature of Bi₂O₃-based materials themselves.

An LRC equivalent circuit was proposed and, assuming that L and C are independent of temperature, a good description of the electrical behavior was obtained. The existence of inductive impedance along with bulk resistance implies that the motion path of oxygen ions in Bi₂O₃-based oxygen ionic conductors is screw-like, which is surely related to its crystal structure. Obviously, the new phenomenon discovered in this work is of certain theoretical and practical significance, and is worth further study.

CHEMICAL DIFFUSION IN CALCIA-DOPED
ZIRCONIA CERAMIC

Shixue Dou
Department of Chemistry
Northeast University of Technology
Shenyang, China

C. R. Masson
Atlantic Research Laboratory
NRC of Canada, Halifax, NS

P. D. Pacey
Department of Chemistry
Dalhousie University
Halifax, NS Canada

Abstract

Chemical diffusion of oxygen in Calcia-doped zirconia (CSZ) with impurities of Al_2O_3 , SiO_2 , MgO , Fe_2O_3 and TiO_2 was studied by the non-steady state permeation and the desorption techniques at 960-1450°C. The concentration of excess oxygen in CSZ was found to be proportional to the content of iron oxide within experimental error. The electron holes were largely contributed from converting Fe_{Zr}^{2+} to Fe_{Zr}^{3+} . The chemical diffusion coefficient, D , was found to be inversely proportional to the relative deviation from stoichiometry, and to increase with increasing P_{O_2} . The results were consistent with a trapping mechanism in which the holes are divided into free and trapped ones. D is reduced by the trapping factor. The time constant of equilibration processes with a surrounding atmosphere is increased as the concentration of the trapping centers is increased. The CSZ electrolyte free of Fe_2O_3 gives fast response in EMF.

Topotactic Redox Reactions of One-Dimensional Ternary Molybdenum Chalcogenides Mo_2X_6 (X = Se, Te)

J. M. Tarascon

Bell Communications Research
Murray Hill, New Jersey 07974

Over the last few years low-dimensional compounds such as NbSe₃ or MX₃ (M = transition element; X = Se, Te) have generated a great deal of interest for their potential application as cathode in secondary lithium cells. Recently we reported the synthesis of new one-dimensional ternary molybdenum chalcogenides (Li_xMo₂X₆) which has a structure that can be thought of as composed of (Mo₂Se₆)_n chains separated by two rows of lithium atoms. The close structural relationship between this compound and the ones alluded to above may suggest that Mo₂X₆ can also act as host with respect to lithium. Here we will report the chemical and electrochemical insertion of lithium into Mo₂X₆ (X = Se, Te) using n-BuLi as reagent and swagelok test cells, respectively. The starting materials (Mo₂X₆) were prepared at 480°C by oxidation of In₂Mo₂X₆ under a HCl flow. Cycling data show that Mo₂X₆ can take up reversibly 2.3 lithiums down to 1 volt and furthermore indicate that these cells contain their capacity over several cycles (20 is the maximum that we have tried). The discharge curve exhibits two slopes with a break near x = 1.3. We will show that this behavior is closely related to the band structure of these materials. Reaction with n-BuLi confirms the electrochemical data yielding compounds of formula Li_xMo₂X₆. Furthermore, X-ray diffraction measurements of the lithiated phases indicate that Mo₂X₆ can accommodate reversibly 2.5 lithium without structural change (i.e. the basic chain structure is maintained on lithiation). The electrochemical insertion of sodium into the Mo₂X₆ compounds will also be presented and discussed.

ELECTRIC AND ELECTROCHEMICAL PROPERTIES OF SOME OXYGEN CATALYTICALLY ACTIVE ELECTRODE MATERIALS.

A.J. Burggraaf, M.P. van Dijk, K.J. de Vries.
Laboratory for Inorganic Chemistry, Materials Science and Catalysis,
Twente University of Technology, P.O. Box 217, 7500 AE Enschede,
The Netherlands.

It has been shown (1-5) that both the nature of the surface of the oxidic electrolyte and of the electrode metal plays an important role in gas electrode (redox) reactions. This is especially true at higher temperatures.

A better understanding of electrode reactions is of prime importance for designing good electrodes for application such as fuel cells, electrolysers, sensors and oxygen pumps, and may lead to oxide electrode materials without the use of noble metals. The literature is rather confusing however and there is no general agreement on the rate controlling steps under specific conditions.

Oxygen vacancies, the occurrence of electronic conductivity and the presence of (catalytically) active sites most probably play an important role (1-6). In this paper we shall present some new results concerning the effect of ordering and of mixed (ionic and electronic) conductivity on electric and electrode properties of some zirconia and ceria based oxides with fluorite or pyrochlore structure. Results of a detailed study of the defect chemistry and of the electrode properties within the system Tb_xGd_{1-x}Zr₂O₇ shall be presented and shall be compared with preliminary results of ceria based mixed conducting electrode materials.

Lit. ref.

1. E.J.L. Schouler, *Solid State Ionics* **9/10** (1983) 945.
2. a. M.J. Verkerk, M.W.J. Harmink, A.J. Burggraaf, *J. Electrochem. Soc.* **130** (1983) 70.
b. M.J. Verkerk, A.J. Burggraaf, *ibid.*, 78.
3. A.J.A. Winnubst, A.H.A. Scharenborg, A.J. Burggraaf, *Solid State Ionics* **14** (1984).
4. H. Isaacs, Z.Y. Olmer, *J. Electrochem. Soc.* **129** (1982) 436
5. E.C. Subbarov, *Solid State Ionics* **11** (1984) 317.
6. M.P. van Dijk, A.J. Burggraaf et al., *Mat. Res. Bull.* **19** (1984) 1149, 1271 (part 2).

DOPED CATHODES FOR ZIRCONIA BASED
WATER VAPOR ELECTROLYZERS

E.J.L. Schouler, J. Oumari, A. Hammou
Laboratoire d'Energétique Electrochimique
LA CNRS 265

E.N.S.E.E.G. B.P. 75 - F. 38402 - St Martin d'Hères - France -

SUMMARY

This work dealt with the improvement of the water vapor reduction in stabilized zirconia based cells by doping the cathode interface with the Ce^{4+}/Ce^{3+} redox couple. A preparation technique of such an interface transposable to an industrial scale is proposed. It consists in coating porous zirconia substrates by spraying a dilution of ceria in water prior to high temperature sintering. Automatisation of the spraying phase guarantees the homogeneity and reproducibility of the layer.

The catalytic activity of the doped interface has been studied by impedance spectroscopy in dynamical conditions. Besides the nature of the electrode material, the temperature, the concentration of the vapor, the major parameter of the study was the concentration in cerium. It has been shown that the maximum efficiency of the doped interface was obtained for a concentration in cerium ranging between 4 and 10 weight percent. The results has been analyzed by considering the relative contribution of the ionic and electronic conductivities of the electrolyte surface.

The stability of the doping effect has been studied with respect to time, current density and repeated oxydo-reduction cycling.

TRANSPORT PROPERTIES OF THIN FILM TiS_2

D. A. Zehnder, E. Dunn and E. F. Buschak
Department of Materials Science and Engineering
University of California, Los Angeles, CA 90024

The transport properties and electrochemical behavior of thin film TiS_2 material were investigated. The thin films were produced by evaporating titanium in the presence of an H_2S plasma (activated reactive evaporation or ARE). This process allows thin films (2 microns thick) of dense, nearly stoichiometric TiS_2 to be deposited on a variety of substrates. In the experiments reported here, both sapphire and soda-lime glass substrates were employed. The films exhibited a preferred orientation with the c-axis of TiS_2 aligned parallel to the plane of the substrate. The films displayed a fine-grained microstructure in contrast to the needle-like morphology produced by chemical vapor deposition methods.

The TiS_2 films could be lithiated both chemically, with n-butyllithium, and electrochemically. For the latter case an electrochemical cell using TiS_2 thin films was constructed. Open circuit voltages recorded for the composition limits of this material were: +1.73 V for Li vs $LiTiS_2$ and +2.71 V for Li vs TiS_2 . These values agree well with those reported for thin film TiS_2 prepared by CVD techniques. Preliminary cell cycling experiments show limited lithium reversibility, however, additional measurements are in progress.

The thin film configuration is quite convenient for monitoring the electrical properties of TiS_2 during electrochemical operation. The electrical conductivity values for thin film TiS_2 are in excellent agreement with data published for bulk TiS_2 ($\sim 1 \times 10^3 \text{ Ohm}^{-1} \text{ cm}^{-1}$ at 300 K). In addition we found that the intercalation of lithium did not affect the magnitude of the electrical conductivity. There was no evidence of any appreciable ionic contributions to the conductivity of Li_xTiS_2 as $x \rightarrow 1$. Initial measurements of Li^+ diffusion suggest a substantially lower diffusion coefficient in thin films as compared to bulk materials. The origin of this behavior and the more general issue of how film stoichiometry and morphology influence Li^+ diffusion will be presented.

This work was supported in part by the U.S. Army Research Office.

1. K. Kanohori, K. Matsumoto, K. Miyachi and T. Kudo, Solid State Ionics 2/10, 1443 (1983).

TITANIUM DISULFIDE FILMS FABRICATED BY PLASMA CVD

Keiichi Kanehori, Yukio Ito, Fumiyoshi Kirino
 Katsuki Miyazuchi and Tetsuichi Kudo
 Central Research Laboratory, Hitachi Ltd.
 (P.O. Box 2, Kokubunji, Tokyo 185, Japan)

Thin film secondary lithium batteries are regarded as one of the most desirable types of microbatteries for various kinds of electronic devices due to their high energy density, high reliability and good rechargeability.

Titanium disulfide is well known as a cathode material for secondary lithium batteries. However, when TiS_2 is to be used as a cathode film, it should have the preferred orientation whereby the crystallographic c-axis is parallel to the substrate plane. The authors previously reported that such TiS_2 films can be fabricated by CVD using $TiCl_4$ and H_2S , and the cell, $Li/Li_{3.6}Si_{0.6}P_{0.4}O_4/TiS_2$, has sufficient potential for use as a secondary lithium battery.

The film formation mechanism in the plasma enhanced CVD (PECVD) is different from that of the conventional CVD, since source gases are excited by plasma. From this point of view, it is expected that stoichiometry and electrochemical properties of TiS_2 films may be improved by using PECVD as a fabrication process.

An inductively coupled PECVD apparatus was used for fabrication. The microstructure of the film fabricated by PECVD consists of small, narrow plate-like crystals. It was found that this film was single phase of TiS_2 , and had a strong orientation of the crystallographic c-axis parallel to the substrate plane by X-ray diffraction analysis. The composition of the PECVD-film and CVD-film, which were fabricated under the condition of $(H_2S)/(TiCl_4) = 7.4$, were $Ti_{1.02}S_2$ and $Ti_{1.07}S_2$, respectively. It was found that the composition of the PECVD-film became more stoichiometric. Furthermore, when $(H_2S)/(TiCl_4)$ was changed from 4 to 12, the composition changed slightly, i.e. $Ti_{1.03}S_2$ to $Ti_{1.01}S_2$. It was thought that these effects were due to the high concentration of the active sulfur species produced by plasma.

Thin film cells for measuring electrochemical properties were prepared by depositing $Li_{3.6}Si_{0.6}P_{0.4}O_4$ electrolyte film and Li anode film sequentially through sputtering method and vacuum evaporation. The apparent chemical diffusion coefficient of Li in the PECVD-film was $10^{-14} m^2/s$, which was larger than that of the CVD-film. This improvement should be due to the fact that the PECVD-film contained less excess Li. Discharge capacity (2.5-1.5 V) of the cell using $7 \mu m$ PECVD-film was 90% of the theoretical capacity at 200 mA/m², which was large compared to the capacity of the CVD-film, i.e. 55-160 mA/m². This result coincides with the fact that the PECVD-film has larger chemical diffusion coefficient.

In conclusion, this study revealed that TiS_2 films having preferable crystallographic orientation, nearly stoichiometric composition and desirable electrochemical properties can be fabricated by PECVD.

BINARY AND TERNARY LI-ALLOYS AS ANODE MATERIALS IN RECHARGABLE ORGANIC ELECTROLYTE LI-BATTERIES

J.O. Besenhard, P. Komenda, A. Paxinos
 Inorganic Chemistry Department, Technical University of Munich,
 Lichtenbergstr. 4, D-8046 Garching

M. Josowicz,
 Department of Bioengineering, University of Utah,
 Salt Lake City, Utah 84112, USA

Various intermetallic phases containing lithium are characterized by high Li-mobility; the thermodynamics and transport properties of many of these phases have been investigated carefully because they are candidates for anode materials in rechargeable Li-batteries. In fact there are several binary and ternary Li-alloys which meet reasonable energy density and power density requirements even at room temperature, among them alloys with Al, In, Ga, Sb, Bi or Bi-Sn.

In organic electrolytes, however, the bottleneck preventing a practical application of these anode materials is the poor deep cycling and storage stability; this is related with surface reactions and morphology changes. Surface filming e.g. of β -LiAl in $LiClO_4$ propylene carbonate (PC) electrolytes effectively prevents bulk corrosion - but this filming is an irreversible reaction. During cycling new surfaces are created permanently and electronically insulating substances are accumulated on the electrode. Moreover, cycling of unsupported LiAl causes the material to become spongy and poorly adherent. Finally, the contact area inert substrate/LiAl is very sensitive to deep cycling.

There are ways to improve at least by small steps the three crucial points:
 1) surface filming, 2) morphology changes, 3) contact to inert substrate.

Nonreactive surfactants such as paraffines can support very much the protection of Li-alloy surfaces against attack by the electrolyte. This is a reversible adsorption process which does not use up the surfactant (1). Paraffines even protect Li-In surfaces in $LiClO_4/PC$; without paraffine additives Li-In alloys are quickly and quantitatively oxidized by $LiClO_4/PC$.

Morphology changes e.g. of β -LiAl active material can be significantly reduced by embedding it in a nonreactive or at least much less reactive matrix. When e.g. Si-containing Al is used as base material for β -LiAl, the Si-fraction is practically nonreactive at room temperature. The disadvantage of reduced Li-mobility in Si-contaminated Al is overbalanced by the much less morphology changes during long-term cycling.

The mechanical and electrical contact inert substrate/base metal of Li-alloy is in general destroyed when the supply of base metal is completely consumed. Metallic coupling agents which can create 3-dimensional interfaces improve the contact and allow deep cycling of the electrode. An ideal coupling agent alloys with the inert substrate as well as with the base metal of the Li-alloy. The latter is diluted by the coupling agent and its concentration gradually goes to zero on the substrate side of the 3-dimensional interface. In the simplest case the base metal of the Li-alloy is diluted by alloying with the inert substrate itself; e.g. deep cycling of β -LiAl on a Ti-substrate is much improved by a Ti-Al alloy interface (2).

- (1) H.P. Fritz, J.O. Besenhard, Ger. Offen. 28 34 485
 (2) J.O. Besenhard, E. Wudy, H.P. Fritz, Ger. Offen. 32 30 410

LITHIUM THERMODYNAMICS AND KINETICS OF THE GAMMA
LITHIUM VANADIUM BRONZE STRUCTURE

Boryann Liaw, Ian D. Raistrick and R.A. Huggins

Department of Materials Science and Engineering
Stanford University
Stanford, CA 94305

The reaction of lithium with alkali metal vanadium bronzes has been studied recently by several investigators, as these materials are of interest as possible positive electrode constituents in both solid state and molten salt electrolyte secondary lithium batteries.

There are several different structures in both the pure lithium vanadium bronzes and mixed alkali bronzes, and lithium insertion and delation has been found to occur in them, in some cases at high rates and over appreciable ranges of composition. These materials also typically have low lithium activities, and thus high voltages compared to lithium.

Its layer-like atomic arrangement and high voltages versus lithium make the gamma phase structure an especially attractive electrode reactant for use in lithium systems. Two types of sites between the vanadium-oxygen chains are occupied by the inserted lithium ions. At least one of these can be deleted rather easily.

Electrochemical methods have been employed to determine the equilibrium potential-composition relations, and data will be reported on the equilibrium electrochemical titration curve. In addition, the chemical diffusion coefficient has been measured at several compositions by the galvanostatic transient technique, and also by the use of AC impedance methods. These kinetic parameters are similar to those previously found in materials with the beta structure.

LUMINESCENCE OF Cr^{3+} IN BETA-ALUMINA CRYSTALS.

C. Mariotto, M. Montagna and F. Rossi

Dipartimento di Fisica, Università di Trento, 38050 Povo (Italy), and
Istituto per la Ricerca Scientifica e Tecnologica, 38050 Povo (Italy).

Luminescence spectra of Cr^{3+} doped beta-alumina crystals, containing various conducting monovalent cations, were taken at different temperatures between 4.2 and 300 K. From luminescence excitation spectra we obtain a level scheme similar to that of ruby, where the emission lines are interpreted as due to the ${}^4E \rightarrow {}^4A_2$ transition of Cr^{3+} ion, substitutional for the Al^{3+} ion in the octahedral sites of the spinel block structure. We use time-resolved spectroscopy technique in order to separate the contributions from non equivalent centers, characterized by lifetimes ranging from ~ 1 ns to ~ 60 ns.

The shape of the emission lines, showing characteristics intermediate between those observed in ordered crystals and in glasses, reflects the anomalous nature of the host system: a crystalline matrix with high degree of disorder in the distribution of the monovalent cations over the sites of the conduction plane, separating two adjacent spinel blocks.

Energy peaks and linewidths due to the inhomogeneous broadening of the observed lines depend on Cr^{3+} ion site and on the composition of the host crystal, being sensitive to the different substitutional monovalent ions. Homogeneous linewidths are, also, measured by fluorescence-line-narrowing technique as a function of temperature.

We discuss the observed inhomogeneous and homogeneous broadenings in terms of static disorder and of dynamics of the mobile cations, respectively.

AN ALTERNATIVE FABRICATION ROUTE TO H_3O^+ β "-ALUMINA via
 $\text{NH}_4^+/\text{H}_3\text{O}^+$ β "-ALUMINA

John O. Thomas,¹ Garry J. McIntyre² and John DeNuzzio³

¹Institute of Chemistry, University of Uppsala, Box 531,
 S-751 21 Uppsala, Sweden

²Institut Laue-Langevin, 38042 Grenoble, Cedex, France

³Department of Materials Science and Engineering K1, University
 of Pennsylvania, Philadelphia, PA 19104, U.S.A.

Of the protonic β -/ β "-aluminas so far investigated the mixed-ion system $\text{NH}_4^+/\text{H}_3\text{O}^+$ β "-alumina is the best conductor of protons: $\sigma \sim 7 \times 10^{-4} \Omega^{-1} \text{cm}^{-1}$ at 30°C, rising to $\sim 2 \times 10^{-2} \Omega^{-1} \text{cm}^{-1}$ at 200°C (Ref. 1). An earlier single-crystal neutron diffraction study has exposed the detail of the network of NH_4^+ ions, H_3O^+ ions and H_2O molecules contained in the conduction plane (Ref. 2). Extending this work to higher temperatures has indicated that the decomposition (earlier shown by TGA methods to begin above 200°C) involves the loss of NH_3 from the conduction plane; the remaining proton forming a OH^- group on the spinel block (Ref. 3). Recent σ -measurements made on powders indicate that the conductivity falls as deammoniation proceeds; approaching the value observed for H_3O^+ β "-alumina at higher temperatures (Ref. 4).

In the work reported here, a large single-crystal has been heated in air at 350°C for 21 days, followed by a heat treatment at 250°C for 3 days in one atm. of water vapour. The aim here was to create an H_3O^+ β "-alumina crystal whose structure was then investigated by neutron diffraction at the ILL, Grenoble. This structure will be discussed and compared with the results of a study of a crystal of D_3O^+ β "-alumina made by acid exchange of Na^+ β "-alumina in conc. D_2SO_4 .

References

1. G.C. Farrington, K.G. Frase & J.O. Thomas. In *Advances in Materials Science*, 1984.
2. J.O. Thomas & G.C. Farrington. (1983) *Acta Cryst.* B39, 227.
3. J.O. Thomas, K.G. Frase, G.J. McIntyre & G.C. Farrington. (1983). *Solid State Ionics*, 9/10, 1029.
4. J. DeNuzzio, To be published.

THE $\text{Eu}^{3+} + \text{Eu}^{2+}$ REDUCTION PROCESS IN Eu^{3+} β "-ALUMINA

Wilder Carrillo-Cabrera¹, John O. Thomas¹ and
 Gregory C. Farrington²

¹Institute of Chemistry, University of Uppsala, Box 531,
 S-751 21 Uppsala, Sweden

²Department of Materials Science and Engineering K1, University
 of Pennsylvania, Philadelphia, PA 19104, U.S.A.

Ion exchange of Na^+ β "-alumina crystals in EuCl_2 and EuCl_3 at elevated temperatures has been demonstrated to produce Eu^{2+} β "- and Eu^{3+} β "-alumina. Both materials have furthermore been shown to fluoresce (yellowish green and red, respectively) under UV-light (Ref. 1). Preliminary experiments have also shown that heating Eu^{3+} β "-alumina in vacuum produces a change in the fluorescence from red to yellowish green under UV-light, suggesting a reduction of Eu^{3+} to Eu^{2+} ions.

In this present work, single-crystals of Eu^{2+} β "- and Eu^{3+} β "-alumina have been studied by X-ray diffraction, as well as a crystal of Eu^{3+} β "-alumina after heating in vacuum at 1000°C for 15 h.

In both Eu^{2+} β "- and Eu^{3+} β "-alumina, the majority of Eu ions (83% and 96%, respectively) occupy mid-oxygen (9d) sites. This is by far the largest mid-oxygen occupation yet observed in a divalent β "-alumina. The study of the heat-treated crystal indicates the creation of a significant quantity of both Al and O vacancies, suggesting a high degree of disruption in the crystal. This has been confirmed by recent HREM measurements on the same crystal (Ref. 2).

References

1. B. Ghosal, E.A. Mangle, M.R. Topp, B. Dunn & G.C. Farrington. (1983) *Solid State Ionics*, 9/10, 273.
2. A. Petford. Private communication.

ON INTERACTIONS BETWEEN H₂O MOLECULES AND MOBILE M⁺ IONS
(M⁺ = Li, Na⁺, Ag⁺, K⁺, Rb⁺, Ti⁺) OF BETA ALUMINAS

J. Garbarczyk, W. Jakubowski and M. Wasiucionek
Institute of Physics
Warsaw Technical University
Koszykowa 75, 00-662 Warszawa
Poland

Our previous investigations (conductivity and TGA/DTA measurements) have shown that kind of mobile ions strongly affected rate and extent of water absorption by beta-alumina. This uptake was the most pronounced for Li⁺ beta-alumina, less for Na⁺ beta-alumina and almost negligible for the Ag⁺-isomorph. Other authors have reported that also beta/beta'-alumina with K⁺, Rb⁺, or Ti⁺ mobile ions practically do not absorb water, although the widths of conduction slabs in these isomorphs are larger than in Na⁺ beta alumina. All these results strongly suggest that strength of water bonds to beta/beta'-alumina depends mainly on H₂O-M⁺ interactions and it decreases for larger M⁺ ions.

To explain this, we assumed simple model of two-body interaction between H₂O dipole and M⁺ ion (M⁺ = Li, Na⁺, Ag⁺, K⁺, Rb⁺, Ti⁺). Into the total potential of interaction we included three following terms:

- i) electrostatic attraction between H₂O dipole and M⁺cation
- ii) electrostatic attraction between induced dipoles and
- iii) short-range Born-Mayer's repulsion.

The minima of calculated potential curves gave values of theoretical energy of M⁺-H₂O bonds. For Li⁺-H₂O interactions it is equal to 1.1 eV, being in good agreement with experimental results having been reported for hydrated Li⁺ beta alumina. It is also interesting, that equilibrium distances for Li⁺-H₂O and Na⁺-H₂O pairs are less than 3.2 Å (i.e. 6c-6c distance of beta'-alumina). On the other hand the M⁺-H₂O (M⁺ = Ag⁺, K⁺, Rb⁺, Ti⁺) equilibrium distances are longer than 3.2 Å and binding energies much smaller than in the cases of Li⁺ and Na⁺ ions. This seems to be responsible for negligible water uptake by Ag⁺, K⁺, Rb⁺ and Ti⁺ beta/beta'-aluminas.

The presented model predicts that binding energies of H₂O dipole with M²⁺ or M³⁺ mobile ions depend not only on sizes of the cations but also on their charges and polarizabilities.

The role of weak hydrogen bonds (0.2 eV) between H₂O molecules and oxygen ions from spinel blocks of beta alumina, will be discussed in the paper.

CONDUCTIVITY CHANGE DURING THE REPLACEMENT OF SODIUM BY
SILVER IONS IN POLYCRYSTALLINE BETA-ALUMINA

M.W. Breiter and M. Maly-Schreiber

Institut für Technische Elektrochemie, TU Wien, 9 Getreide-
markt, A-1060 Wien, Austria

B. Dunn

Department of Materials Science and Engineering, UCLA,
Los Angeles, CA 90024, USA

The longitudinal conductivity was determined by a four-probe technique at 1000 Hz as a function of time during the replacement of sodium ions by silver ions from the inside of a closed end tube at about 300°C in molten silver nitrate. The melt was periodically removed by a preheated pipette before the resistance measurement and added again afterwards. This procedure eliminated the contribution of the co-conductance of the melt and assured a fresh melt for each time interval of exchange. Similarly the radial conductivity was measured during the exchange starting from the outside. An exchange of the melt was not necessary here. The conductivity-time curves, resulting from both measurements, display a minimum with a conductivity value below that of silver beta-alumina. Simple considerations show that such a minimum should not be observed. It is suggested that the minimum results from the slow diffusion of sodium ions through regions which are largely exchanged to silver beta-alumina. These regions are partly located close to the surface of crystallites, which possess a mixed, non-equilibrium composition, and partly inside the grain boundaries.

β and β'' alumina - Structure, local order and conductivities.

- G. COLLIN (a), J.P. BOILOT (b), Ph. COLOMBAN (b), R. COMES (a)
 (a) Labo de Physique du Solide, Université Paris Sud, Bât 510, 91405 Orsay France.
 (b) Groupe de Chimie du Solide, Laboratoire Physique Matière Condensée Ecole Polytechnique, 91128 Palaiseau, France.

β and β'' alumina type materials provide host lattices stable and inert enough in order to carry out very fundamental studies or superionic conductivities without interference with the more or less pathological behavior of the matrix. We will present some new results.

1) Concerning the alkaline materials

The simultaneous examination of long and short range orders leads to a model of ion-ion correlation in a 2D type superlattice. The determination of the diffraction functions explains this pure 2-D character, the difference in coherence length due to faulting and the microscopic homogeneity of these materials.

An interpretation of the anharmonic properties is proposed. From these results, it is possible to build up a system of state equation based on the equilibrium conditions of the β alumina type materials. This shows that the model-experimentally found-of cells occupied by 1BR or 3mO Na ions is everywhere energetically more stable than the B-R, a B-R one. In a second step, the state equations for β'' alumina appears to be a perturbation due to a host lattice polarization. Quantitative determination of the polarization amplitude gives the homogeneity ranges of β alumina - 1. - 1,56 Na⁺ per unit formula and β'' alumina 1.56 - 1.67 Na⁺. Starting from the works of Sato and Kikuchi a modified P.P.M. is proposed in order to account for the transport properties. In β'' alumina the antiferroelectric order observed at low temperature is progressively destroyed upon heating and leads to a double contribution to activation energy: a temperature independent hopping energy and a temperature dependent dissociation energy function of the coherence length.

The model is used to account quantitatively for the conductivity curves.

2) Concerning the silver ions materials

In silver β ferrite (β alumina type compound), silver metallic centers are directly formed by reduction of Ag⁺ by Fe²⁺ and consequently the mechanism of metallic precipitation, which is probably at the origin of the electrolyte degradation in batteries, can be studied.

This mechanism can be summarized as follows :

- Reduction of Ag⁺ conducting ions by Fe²⁺
- Clustering of silver atoms in two-dimensional aggregates
- Growth of clusters which remain coherent with the β alumina lattice
- Precipitation of metallic silver and collapse of the β alumina into a spinel-type structure.

3) Concerning the multivalent ion materials

The Na⁺ content of rich β or β'' alumina can be replaced by a variety of divalent (Sr²⁺, Cd²⁺, Pb²⁺...) or trivalent (Gd³⁺...) cations in simple ion exchange reactions and these materials exhibit multivalent conductivities greater than that known for any other multivalent conductor at low temperature. When a 2-D local order is observed at all temperatures in multivalent rich β alumina, β'' ones can exhibit interplanar correlations at low temperature, due to polarization effects (host lattice or conducting ions).

When the temperature increases, order-disorder transitions can be observed in β'' alumina, with a cross-over from a 3-D (short or long range) order to a 2-D local one.

PREPARATION AND PROPERTIES OF Pb β'' ALUMINA

J. Tegenfeldt, J. D. DeNuzzio, and G. C. Farrington

Department of Materials Science, University of Pennsylvania,
 3231 Walnut Street, Philadelphia, PA 19104, USA

Pb β'' alumina differs from other divalent cation substituted β'' aluminas in several respects, including the conductivity, which is remarkably high in the Pb-substituted material. While preparing samples of Pb β'' alumina by ion exchange of Na β'' alumina single crystals we observe, under certain conditions, a weight change greater than that corresponding to 100% exchange, suggesting that an excess of lead ions have entered the crystal during the exchange process. This would require charge compensation, for example by oxygen moving into the crystal, making this material a potential candidate for oxygen ion conduction. We have investigated some of the properties of Pb β'' alumina and their dependence on conditions of preparation and heat treatment, including measurements of spectroscopic properties in the mid- and far-infrared region.

STABILIZERS FOR BETA"-ALUMINA

Maria Zaharescu, Victor Stancovschi, Constanta Parlog,
Nicolae Dragan, Ana Braileanu, Dorel Crisan and Tudor Surdeanu*
ICECHIM-Center of Physical Chemistry
Spl. Independentei 202
Bucharest
Romania

*SINTEROM
3400 Cluj
Romania

The stabilization process of beta"-alumina using additions of ions with different charges has been investigated. The composition ranges where the stabilization effect occurs have been determined.

The stabilizing aptitude of the investigated bi-, tri- and tetravalent ions has been correlated with the charge field of each ion, on the basis of the Dietzel-type approach.

The influence of these additions on the microstructure of sintered beta"-alumina bodies has been investigated, and a comparative evaluation of the advantages and disadvantages of using such stabilizers with respect to the classical use of Li⁺ has been made.

EFFECTS OF SELF-VIBRATIONS FOR HOPPING CONDUCTION

Tadao Ishii

Applied Physics, School of Engineering, Okayama
University, Okayama 700, Japan

Starting with the linearized master equation, we have recently presented a first-principles approach to hopping conduction to discuss an exact conductivity formula [1,2]. The formula provides a systematic foundation for Movaghar-Pohlmann-Schirmacher's Green function method [3], which can result in, for example, Odagaki-Lax's low frequency conductivity for the one-dimensional M-site chain [4,5].

Solid electrolytes are the materials which have shown up a variety of behaviors on the frequency-dependent conductivity $\sigma(\omega)$. One typical feature observed in common exists in the low-frequency region where the conductivity has the crossover from a diffusion process to an oscillatory behavior. This characteristic profile on the conductivity may partly originate from twofold motion of the mobile ions: the mobile ions vibrate around lattice sites, and hop from site to site. This has been discussed by extending the above conductivity formula to include the vibrational motion of particles [1].

The purpose of this paper is to mainly discuss the temperature dependence of the conductivity, whose curves on the $\sigma(\omega)T - 1000/T$ plane display some interesting deviations from an activation type usually found. One of the interesting deviations from the activation type of conductivity has been found by Fontanella, Wintersgill, Welcher, Chadwick and Andeen in some fluorides where they discussed the relation between bound and free ion motion [6].

Commensing with the master equation we have the conductivity expression

$$\sigma_{uv}(\omega) = \beta \frac{(ze)^2}{V} \langle \phi | (WQ_V)^* \frac{-i\omega}{\hat{W}^+ - i\omega} Q_U | \phi \rangle$$

$$= \sigma_R + \sigma_S + \sigma_S^* ; \quad (1)$$

$$Q = R + S, \quad \hat{W} = W - iL_{\Xi}, \quad (2)$$

where iL_{Ξ} is the Liouvillian for the vibrational degree of freedom ($\Xi = S, \dot{S}$). The asymptotes are, for example for a finite system, $\sigma(\omega)T = \exp(-\beta\Delta) \{1 + f(\omega)/\beta + g(\omega)/\beta\}$ for $\omega \neq \omega_S$ when $\beta \rightarrow \infty$, and $\sigma(\omega)T = \exp(\beta\Delta) \times (\omega^2 + h(\omega) + k(\omega)/\beta)$ for $\omega_S \gg \omega$ when $\beta \rightarrow 0$.

- [1] T. Ishii: Solid State Commun. 47 (1983) 717.
- [2] T. Ishii: unpublished (submitted to Progr. Theor. Phys.).
- [3] B. Movaghar, B. Pohlmann and W. Schirmacher: Phil. Mag. B41 (1980) 49.
- [4] T. Odagaki and M. Lax: Phys. Rev. Lett. 45 (1980) 847.
- [5] T. Ishii: unpublished.
- [6] J.J. Fontanella, M.C. Wintersgill, P.J. Welcher, A.V. Chadwick and C.C. Andeen: Proc. Int. Conf. on Fast Ionic Transport in Solids, ed. J.B. Bates and G.C. Farrington (North-Holland, Amsterdam, 1981) p.585. See also U. Strom and K.L. Ngai: *ibid.* p.167.

A NEW HYBRID SCHEME OF COMPUTER SIMULATION BASED ON HADES
AND MONTE CARLO: APPLICATION TO IONIC CONDUCTIVITY IN Y^{3+} DOPED CeO_2

G. E. Murch*

Materials Science and Technology Division
Argonne National Laboratory, Argonne, IL 60439

A. D. Murray and C. R. A. Catlow

Department of Chemistry, University College London,
London WC1H 0AJ, ENGLAND

In the modeling of transport and thermodynamics of complex disordered solids, a realistic computer simulation scheme has long been required that avoids the very heavy demands put on computer time by Molecular Dynamics. Static relaxation codes, notably the HADES/CASCADE programs developed by Catlow and coworkers, have provided reliable estimates of defect formation and migration energies. Such calculations have been made for Y^{3+} doped CeO_2 in which energies were calculated for 30 various atomic environments encountered by the anion vacancy [1]. However, the statistical sampling of these energies to calculate ensemble or time averaged quantities such as chemical potentials, d.c. ionic conductivities, and tracer diffusion coefficients, is a most difficult task. To make the problem analytically tractable, grossly simplifying assumptions need to be made about the distribution of defects and correlation effects.

In order to avoid these assumptions we have recently used the Monte Carlo method to provide the statistical sampling of the energies in a two-stage hybrid calculation of quite general applicability. In the case of Y^{3+} doped CeO_2 , the vacancy migration energies were first calculated using the CASCADE program. Next, a large 50,000 site lattice of CeO_2 containing Y^{3+} ions (immobile) and anion vacancies was generated. A weak d.c. electric field was imposed. Vacancy jumps were directed by standard Monte Carlo procedures [2] in conjunction with a fast pattern recognition algorithm. The results for the d.c. ionic conductivity were in very good agreement with the experimental data. The characteristic maximum in conductivity and the corresponding minimum in activation energy as a function of increasing vacancy content were faithfully reproduced.

1. C. R. A. Catlow and S. C. Parker, in Computer Simulation of Solids edited by C. R. A. Catlow and W. C. Mackrodt (Springer-Verlag, Berlin, 1982).
2. G. E. Murch in Diffusion in Crystalline Solids edited by G. E. Murch and A. S. Nowick (Academic, New York, 1984).

*Work supported by the U.S. Department of Energy.

EFFECTS OF SPACE CHARGE AND NONUNIFORM TEMPERATURE ON A
SOLID STATE GALVANIC CELL

Bruce K. Borey and Frederick H. Horne
Department of Chemistry, Michigan State
University, East Lansing, MI 48824

The complete set of differential equations of nonequilibrium thermodynamics has been solved for a solid state galvanic cell consisting of single electrolyte sandwiched between electrodes. Electro-neutrality is not assumed anywhere, and it is therefore possible to assess the effects of nonzero space charge in the electrolyte near the electrodes. A special transformation of concentration variables into a "neutral" part and a "charge" part facilitates both the analytical and the numerical solution of the mathematical problem. Formulas are obtained for the electric field, the ionic concentration, the space charge, the cell potential, and the efficiency of the cell at steady state. Inclusion of appropriate temperature gradient terms in all equations permits evaluation of the effects of nonuniform temperature on all cell properties including efficiency. For specificity, numerical results are obtained for the particular galvanic cell consisting of cerium oxide doped with calcium oxide as the electrolyte contained between oxygen electrodes. Efficiency is enhanced - more current is produced with less ohmic loss - if the product $Q^*(\Delta T)$ is negative, with Q^* the heat of transport of the electrolyte and ΔT the temperature difference between the cathode and the anode.

COMPUTER SIMULATION STUDY OF δ -BISMUTH OXIDE

P.W.M. Jacobs and D.A. MacDónaill

Department of Chemistry, University of Western Ontario,
London, Ontario, Canada, N6A 5B7

The δ -phase of Bi_2O_3 has an exceptionally high conic conductivity. This is because only 3/4 of the available oxygen sites in the fluorite structure are occupied at any one time. Bi^{3+} - Bi^{3+} , Bi^{3+} - O^{2-} , and O^{2-} - O^{2-} potentials were obtained from electron gas calculations; O^{2-} shell-model parameters conformed to previous work on other oxides; the Bi^{3+} - O^{2-} potential parameters and the Bi^{3+} shell-charge and force constant were adjusted to eliminate lattice strains and to give reasonable values of elastic and dielectric constants. Two models for the perfect crystal were investigated: the Gattow model, in which each O^{2-} site is occupied for 3/4 of the time, and the Sillen model in which 3/4 of the O^{2-} sites are occupied so that there is a $\langle 111 \rangle$ ordered superlattice of vacancies. The Gattow model was simulated by scaling the pre-exponential and Van der Waals' terms in the O^{2-} - O^{2-} potential by $(3/4)^2$. The perfect crystal can be modelled successfully in this way, but acute problems arise when vacancies are introduced. Nevertheless our calculations showed that anion Frenkel defects, with the interstitials at cube-centre sites, are not formed readily ($\mu_f = 4.5$ eV).

In the Sillen model, if sufficiently high polarizabilities are used to give the dielectric constants correctly (assuming $\epsilon_0(\delta) = \epsilon_0(\alpha)$) a displaced O^{2-} ion oscillates in the neighbourhood of its lattice site. While this behaviour may be realistic, it makes it impossible to model the material satisfactorily. Consequently, a rigid-ion model was employed. A perfect $\langle 111 \rangle$ superlattice of vacancies is more stable than either a $\langle 110 \rangle$ or $\langle 100 \rangle$ superlattice. However, local $\langle 110 \rangle$ and $\langle 100 \rangle$ defects are thermodynamically stable by -4.3 eV and -3.8 eV respectively. A $\langle 110 \rangle$ defect requires an activation energy of 0.68 eV; once one of these defects forms it catalyzes the formation of a second $\langle 110 \rangle$ defect which requires only 0.09 eV. Thus our model for δ - Bi_2O_3 is an overall superlattice of $\langle 111 \rangle$ vacancies containing chains of $\langle 110 \rangle$ defects. O^{2-} vacancies can form in the Sillen structure by the lattice O^{2-} ion moving from an occupied lattice site to one of the normally vacant sites. (We term this a "pseudo-Frenkel" defect.) The vacancy is a charged defect and its motion leads to charge transport, in contrast to that of $\langle 110 \rangle$ defects which do not carry a charge. When a vacancy is added to a $\langle 110 \rangle$ defect, the 'charged' and 'uncharged' vacancies became undistinguishable, so charge migration can occur by adding a vacancy to one end of a $\langle 110 \rangle$ string and removing it from the other end. The calculated activation energy for the motion of an isolated vacancy is 0.3 eV, in good agreement with experiment. This energy increases slightly if the O^{2-} and Bi^{3+} are made polarizable, but in general the rigid-ion model seems to be a good guide to the behaviour of Bi_2O_3 .

MODEL OF DIFFUSION LENGTHS

Peter Nwoye O. Mbaeyi
Division of Theoretical Chemistry
University of Tuebingen
d-7400 Tuebingen 1
F.R.G.

In transport processes, the concepts of mobilities, diffusion (according to Ficks/Darcey's laws) and brownian diffusion are often treated as though they are wholly independent of one another. These concepts are interlinked to one another by constructing dynamical models of the diffusion variable (for this purpose use is made of an approximative analytic form obtained by developing mechanical analogues of diffusing using fluidic systems - "Mechanical Models of Diffusion and Relaxations," 5th Inter. Math. Modeling Conf., Berkeley 1985). Then dynamical relationships between diffusion and mobilities on the one hand, and mobilities and brownian diffusion on the other are established. On this basis, the actual diffusion lengths are defined and formulated in the form of (boundary) control models. Applications to fast transport, multiphase flows in membranes are used as guidelines (in the case of membranes, the dependence of diffusion of thickness will feature in " δ -Layer Dynamics (Energetics Models of Boundary Layer Phenomena)" to appear in Proc. Inter. Conf. on Num. Methods in Laminar and Turbulent Flows, Swansea, July 1985).

X-RAY AND NEUTRON SCATTERING FROM IONIC MOTIONS IN SUPERIONIC CONDUCTORS*

P. Vashitsa, Argonne National Laboratory, Argonne, IL 60439

I Ebbsjö and R Dejus, The Studsvik Science Research Laboratory
S-611 82 Nyköping, Sweden

A model of the superionic conductor Ag_2S is proposed and studied by the molecular dynamics technique using effective pair potentials. Interesting results have been obtained by Cava and McWhan who have studied the X-ray diffuse scattering in β - Ag_2S . They observe in the superionic phase anisotropic discs of intensity in the vicinity of the point $Q_0 = (1.6, 1, 0)$. In addition Grier et al. in their inelastic neutron scattering experiments observe anomalous intensities similar to those observed in diffuse X-ray scattering. A low energy (~ 2 meV) excitation is also observed in the non-superionic phase which disappears in the superionic phase. A motivation for this work is to investigate if it is possible to describe structural and dynamical properties of superionic conductors such as Ag_2S using effective pairwise potentials. We have calculated the constant of self-diffusion for silver, the mean square displacement for sulfur, the partial pair distribution functions and the density map of silver ions in the unit cell. In addition the X-ray and neutron diffuse intensities are calculated in the vicinity of Q_0 . We find that the anisotropic discs of intensity around Q_0 are entirely due to the correlated motions of Ag ions reflected in the partial structure factor $S_{AgAg}(Q)$ which in turn determines the diffuse scattering. Our interpretation is that the dynamic interference between Ag ions over the range of the charge neutrality of 5-6 Å, coupled with the fact that there are frequent octahedral to tetrahedral jumps as well as tetrahedral to tetrahedral jumps in Ag_2S leads to the anomalous intensity in the diffuse scattering. The phonon density of states, the frequency dependent ionic conductivity and the temperature dependence of the Haven's ratio are also calculated. The spectrum of density fluctuations, $S(Q, \omega)$, is studied in the entire (Q, ω) space. The intensities, line widths and temperature dependence of the quasielastic peak and the low energy excitation agree with the inelastic scattering experiments.

¹ Cava RJ and McWhan DB Phys Rev Lett 45, 2046(1980)

² Grier BH, Shapiro SM and Cava RJ Phys Rev B29, 3810(1984)

FK-MODEL APPROACH TO A COUPLED CHAIN SYSTEM:
3RD-ORDER COMMENSURATE IONIC CONDUCTORS

K. Takahashi, I. Mannari and T. Ishii*

Department of Physics, Faculty of Science
Okayama University, Okayama 700, Japan.*Applied Physics, School of Engineering
Okayama University, Okayama 700, Japan

The Frenkel-Kontorova [FK] model has been extensively studied to understand the modulated structures with periods [1]. In the study of one-dimensional ionic conductors, Beyeler-Pietronero-Strässler have proposed a configurational model, a version of the FK model with a finite density of defect [2]. Ishii have investigated the static structure factor by solving the transfer integral equation [TIE] for the FK model to find rather a consistent result with the experiment [3].

Recently K-priderites having the K^+ ion density $\rho=0.75$ have been studied experimentally by electron diffraction and X-ray diffraction, and found that there exists an interchain coupling [4,5].

The purpose of this paper is to study the FK-model with 3rd-order commensurability where the natural spacing of chain is $a=4b/3$ with b being the period of substrate potential, and to discuss the equilibrium configurations, excitation spectrum, and thermodynamic properties. The potential energy of the system is given by

$$V = \sum_{a=x,y} \alpha_{a,x,y} v_a + v_{xy}; \quad (1)$$

$$v_a = \sum_n \frac{u}{2} (\alpha_{n+1} - \alpha_n - a)^2 + \sum_n \frac{u}{2} (1 - \cos(2\pi\alpha_n/b)), \quad (2)$$

$$v_{xy} = \sum_n \lambda \frac{z}{2} (|x_n - y_n - \frac{a}{2}|^2 + (|x_{n+1} - y_n - \frac{a}{2}|^2)), \quad (3)$$

where λ is the coupling constant and z is the number of nearest neighbor chains. In obtaining the configurations and excitation spectrum, we solve a set of coupled equations.

i) $\lambda=0$: case of independent chain. There exist two configurations for ground state and saddle state. The difference of their energies can be estimated as, for example, $\Delta E=0.019$ eV/3-particles for $ub^2/2=0.75$ eV and $U=0.15$ eV. As to the excitation spectrum we have three phonon branches with nonzero frequencies at $q=0$. The gap of the lowest excitation at $q=0$ is evaluated as $\Delta\omega=0.0034$ eV for the above parameters.

ii) $\lambda \neq 0$: coupled case. The ground state configuration found from eq.(1) is quite consistent with the experimental observations of [4,5].

Investigation of thermodynamic properties is now in progress by a numerical calculation of the TIE for the 3rd-order commensurate structure.

- [1] P.Bak: Rep. Progr. Phys. 45 (1982) 587.
 [2] H.U.Beyeler, L.Pietronero and S.Strässler: Phys. Rev. B22 (1980) 2988.
 [3] T.Ishii: Solid State Commun. 48 (1983) 543, J. Phys. Soc. Jpn. 52 (1983) 4066, J. Phys. Soc. Jpn. 53 (1984) 2622.
 [4] S.Suzuki, M.Tanaka, M.Ishigame, T.Suemoto and Y.Shibata: unpublished (private communication).
 [5] H.Terauchi, T.Futamura, T.Ishii and Y.Fujiki: J. Phys. Soc. Jpn. 53 (1984) 2311.

STRUCTURAL AND CONDUCTIVITY STUDIES IN

A SODIUM-ZINC-SULFATE SYSTEM

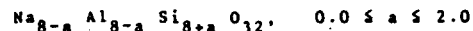
William A. Redman and Roger Frech
 Department of Chemistry
 University of Oklahoma
 Norman, OK. 73019

We have begun a comprehensive study of the structure and transport properties in a sodium-zinc-sulfate system. A new compound, $\text{Na}_a\text{Zn}(\text{SO}_4)_4 \cdot 2\text{H}_2\text{O}$, has been synthesized and the crystal structure determined. This compound crystallizes in the triclinic space group $\text{P}\bar{1}$ (C_1) with one molecular unit in the primitive cell. The differential thermal analysis indicates a loss of water over the temperature interval 185°-210°C. The resulting anhydrous compound then undergoes a complex series of phase transitions at 356, 369 and 381°C. The melting point is approximately 700°C. Conductivity measurements of pressed pellets of the anhydrous compound show a complex transition into a high conductivity phase above 400°C with an activation energy of 0.61 eV. The high temperature deformation of the pressed pellets suggests that the conducting phase is also a plastic phase.

IONIC CONDUCTIVITY OF SODIUM-NEPHELINE SINGLE CRYSTALS.

By H. Böhme and G. Roth, Institut für Mineralogie der Universität Münster, D-4400 Münster, Corrensstr. 24.

The specific ionic conductivity of synthetic single crystals of Na-Nepheline with the composition



has been determined as a function of frequency (0.1Hz to 1MHz) temperature (20°C...700°C) and crystal orientation.

Single crystals of acceptable size and quality have been grown from a NaVO_3 -flux at about 1050°C.

Impedance measurements were carried out using the current/voltage technique; the experimental setup consisted of a micro-computer-controlled frequency response analyzer.

One property which is common to all compositions is the strong anisotropy of the specific ionic conductivity:

The conductivity along the crystallographic c-axis is larger by a factor of 10^4 for $a=0.8$ and by a factor of 10^2 for $a=1.5$, respectively. The difference in the anisotropy is mainly due to a difference in the specific conductivity along c. It reaches values of up to $1.0 \cdot 10^{-3} \Omega^{-1} \cdot \text{cm}^{-1}$ at 700°C for $a=0.8$. Single crystals of $a=0.8$ exhibit an anomaly in the impedance plot when compared to other solid ionic conductors. This anomaly results in a dielectric constant of about $4 \cdot 10^3$ (20°C, 100 kHz) along c, which increases with increasing temperature. This "thermally activated dielectric constant" may be related to a jump process.

AC- and DC-experiments with Na-electrodes indicate that the anomalously high dielectric constant is due to a bulk effect, not a surface effect.

The observed property of single crystals with $a=0.8$ may be related to a flat potential barrier of about 0.2 eV, which favours the local Na-diffusion at high frequencies, whereas the DC-conductivity is determined by a high barrier of about 1.0 eV.

The dielectric properties have been studied as a function of stoichiometry for various compounds in the composition range mentioned above. Both the room temperature dielectric constant and the high temperature conductivity exhibit a discontinuity at about $a=1.0$. This observation indicates that the two compounds considered ($a=0.8$ and $a=1.5$) may be related to two different phases. Structure determinations have been carried out for both compounds. They show that both structures are closely related to the crystal structure of natural Nepheline.

The origin of the strong anisotropy as well as the differences in the dielectric properties are correlated with the results of the structure determinations.

NMR STUDIES IN SINGLE CRYSTAL AND
DISPERSED PHASE LITHIUM IODIDE^o

J.L. Björkstam, D. Brinkmann[†], M. Mali[†],
J. Roos[†], J.B. Phipps[†] and P.M. Skarstad[†]
Department of Electrical Engineering
University of Washington, Seattle, WA 98195.

[†]Physik-Institut, University of Zurich
8001 Zurich, Switzerland.

^{*}Medtronic, Inc.
6700 Shingle Creek Parkway
Brooklyn Ctr., MN 55430

The introduction of a dispersed phase component of Al_2O_3 , SiO_2 , etc. into sintered LiI has been reported to give order of magnitude enhancement of Li^+ conductivity. We have carried out nuclear magnetic resonance (NMR) studies of spin-lattice-relaxation time T_1 , line narrowing and pulsed-magnetic-field-gradient diffusion on a large range of compositions, including single crystal LiI, over the temperature range from 80-700K. It is thus possible to separate the contributions of bulk and interfacial transport to the 7Li spectral and relaxation results. The substantial differences which we observe depend upon composition, mean grain size, sintering methods, etc. We relate these NMR data to conductivity results which have been previously reported (Phipps and Whitmore, Solid State Ionics 9 & 10 (1983) 123-130).

^oSupported in part by U.S. Department of Energy Grant DE-FG06-84ER 45065.

LITHIUM ION AND PROTON CONDUCTORS IN THE SYSTEM $AB(IV)_2(PO_4)_3$ (B-Ti, Zr, Hf)

M. A. Subramanian, R. Subramanian and A. Clearfield
Department of Chemistry
Texas A&M University
College Station, Texas 77843

In order to investigate the effect of framework cation substitution on the Li ion conductivity in the system $AB(IV)_2(PO_4)_3$, we have prepared compounds of the type $Li_{1-x}Ti_{1-x}M_x(PO_4)_3$, (M=Sc, Ga), $Li_{1-x}Hf_{1-x}In_x(PO_4)_3$, $LiZr_{1-x}Ti_x(PO_4)_3$, and $Li_{1-x}Zr_{1-x}Sc_x(PO_4)_3$. In the system $Li_{1-x}Ti_{1-x}M_x(PO_4)_3$, X-ray diffraction analysis shows the formation of rhombohedral solid solutions, the limits of which depend on the size of the M^{3+} cation, the smaller the size the larger the value of x. In the system $LiZr_{1-x}Ti_x(PO_4)_3$, the compounds in the composition range $0.5 < x \leq 1.5$ gave X-ray diffraction patterns with broadened reflections while all the patterns outside this composition except $LiZr_2(PO_4)_3$ were hexagonal. Ionic conductivity measurements were performed on all these solid solutions and the results will be discussed in relation to the number of conductors and framework size.

We have also synthesized compounds of the type $AZr_2(PO_4)_3$, ($A^+=NH_4^+$, H_2O and H) with the aim of obtaining proton conductors in the above system. The compound $NH_4Zr_2(PO_4)_3$ was obtained by hydrothermal treatment of $Zr(NH_4PO_4)_2$. Two forms of $HZr_2(PO_4)_3$ were obtained, a rhombohedral phase stable above 600°C and a more stable low temperature phase with a complex structure. Although $HZr_2(PO_4)_3$ remained anhydrous at ordinary conditions, $(H_2O)Zr_2(PO_4)_3$ was prepared by refluxing in water or under hydrothermal conditions. The compounds were characterized by X-ray, IR and thermal methods. We have also attempted to synthesize NH_4^+ and H_3O^+ substituted nasicons of the type $Na_{1-x}A_xZrScSiP_3O_{11}$. Ionic conductivity data of the above compounds will also be presented.

PLASTIC CRYSTAL FAST Li⁺ ION CONDUCTORS (PLICFICS)
FOR 25-100°C APPLICATIONS

E. I. Cooper and C. A. Angell
Department of Chemistry
Purdue University
West Lafayette, Indiana 47907

ABSTRACT

One of the great advantages of the polymer-salt type solid electrolyte is the fact that the electrolyte can change shape under mechanical stress without failure. A disadvantage is that anion transport numbers are not zero. We think the former advantage can be had without the latter disadvantage by using an appropriate anion rotator phase in which the cation or one of the cations is mobile. Li₂SO₄ is the prototype material of this type but is limited to high temperature applications. We describe a low temperature material--a double salt of LiBF₄ and ethoxy ethyldimethyl ammonium fluoroborate which may conduct in the same manner, which exhibits a strong disordering transition at -90°C, and which at 70°C conducts almost as well as the best polyethylene oxide + Li salt combination reported to date. Some variants on this theme and their properties and performance will also be described.

IONIC CONDUCTIVITY IN COMPOUNDS BASED ON CHEMICAL
SUBSTITUTIONS IN Na₂ZnSiO₄.

J. Grins

Department of Inorganic Chemistry, Arrhenius Laboratory,
University of Stockholm, S-106-91 Stockholm, Sweden.

ABSTRACT

Various compounds based on chemical substitutions in Na₂ZnSiO₄ were prepared by solid state reaction in air ;
(i) Na_{2-2x}ZnSi_{1-x}P_xO₄ with 0 ≤ x ≤ 0.45 ,
(ii) Na_{1.85}Zn_{0.925+x/2}Si_{1.075-3x/2}P_xO₄ with 0 ≤ x ≤ 0.15
and (iii) Na_{2-x}Zn_{1-x}Ga_xSiO₄ with 0 ≤ x ≤ 1. The materials were characterized by their X-ray powder photographs and the ionic conductivities determined by impedance measurements at different temperatures. The best conductors are found to be isotypic with the high-temperature form of Na₂ZnSiO₄. The phosphorous-substituted compounds (i) exhibit a maxima in conductivity at 600 K of 1.3·10⁻³ (Ωcm)⁻¹ for compositions x = 0.05 - 0.15. The compounds (ii) show a linear decrease in conductivity at 600 K from 1.0·10⁻² (Ωcm)⁻¹ for x = 0 to 6.6·10⁻⁴ (Ωcm)⁻¹ for x = 0.15. The gallium compounds (iii) show a maxima in conductivity of 2.1·10⁻³ (Ωcm)⁻¹ at 600 K for x = 0.05. The conductivity data are compared with previously obtained results for the sodium zinc silicates Na_xZn_{x/2}Si_{2-x/2}O₄, 2 ≥ x ≥ 1.25.

P14/AC-21

RAMAN SPECTRA OF SOLID SULPHATE ELECTROLYTES; PADDLE WHEEL MIGRATION DUE TO REORIENTATIONAL MOTION

L. Börjesson and L. M. Torell
 Department of Physics, Chalmers University of Technology,
 S-412 96 Gothenburg, Sweden

In solid sulphate electrolytes the superionic phases are characterized by a high degree of orientational oxygen disorder. This together with a high latent heat compared to the heat of fusion suggest a premelting process with rapid rotational re-ordering of the sulphate groups. In view of the broad variety of possible mobile ionic species in sulphate-based solid electrolytes a migration model has been suggested, the "paddle-wheel" model, where rotations of the sulphate ions have been proposed to enhance the cation diffusion and thus explain the high conductivity. In the present work Raman scattering has been used to investigate the dynamics of the sulphate ions in solid sulphate electrolytes. Raman spectra of fcc-Li₂SO₄, bcc-LiAgSO₄ and bcc-LiNaSO₄ have been recorded across the entire temperature range of stability of each compound. Comparison of polarized and depolarized spectral bandwidths for the symmetric A_g sulphate internal mode permits a component due to the sulphate ion reorientation to be separated, which confirms the plastic behaviour of the superionic phases of the three crystals. In case of Li₂SO₄ the derived reorientation time corresponds well with the value, 2 ps, recently reported on the basis of computer simulation studies. Our measurements are precise enough to yield the temperature dependence of the reorientation time in each type of crystal. These values are sufficiently close to the temperature dependence of the cation diffusion to constitute a support of the "paddle-wheel" migration postulate for this type of plastic crystal.

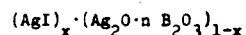
SOUND VELOCITY BEHAVIOUR IN SILVER BORATE GLASSES.

G. Carini, M. Cutroni, M. Federico and G. Tripodo
 Istituto di Fisica Generale and Gruppo Nazionale di Struttura della
 Materia del CNR, Messina, Italy.

The sound velocity behaviour of 5 MHz longitudinal waves was measured in AgI:Ag₂O:B₂O₃ "ternary" glasses in the 77 - 400 K temperature range. The measurements were performed by a pulse-echo overlap technique.

The presence of dispersive effects was revealed, whose contribution increases with the AgI content. These effects were ascribed to the thermally activated relaxations of mobile Ag⁺ ions, that jump between nearly equivalent positions, available in the glassy network.

From a quantitative point of view the whole behaviour was explained by the overlap of two different mechanisms: the relaxational one and the one coming out of the anharmonicity of the system (three-phonon interactions). The latter effect implies, in the quasiharmonic approximation, a linear temperature dependence of the elastic constants in all the explored range.

¹⁰⁹Ag NMR INVESTIGATIONS OF THE SUPERIONIC GLASSES

Steve W. Martin

Department of Chemistry, Purdue University, West Lafayette

and

M. Mali, J. Roos, and D. Brinkmann

Physik-Institut, University of Zurich, 8001 Zurich, Switzerland

Recent interest (1,2) in superionic glasses based upon in large part AgI has produced a wide range of glasses exhibiting an ionic conductivity as high as $(1-5) \times 10^{-2} (\Omega \text{ cm})^{-1}$ at room temperature. Detailed information on the microscopic processes involved in the conduction events, however, is quite lacking. Previous NMR studies (3) of the stationary ¹¹B nuclei performed near and above the glass transition temperature, have dealt with the dynamics of the borate units.

In this paper we report on the first NMR investigation of the mobile silver ions. Measurements of the spin-lattice relaxation, the linewidth, and the intensity of the ¹⁰⁹Ag signal were initiated. Preliminary results for a $n = 2$, $x = 0.65$ sample yield very low apparent activation energies for the processes which are responsible for relaxation (0.04 eV) and linewidth (0.11 eV), respectively. The correlation time of the relaxation process is 1.6×10^{-8} s at room temperature. For comparison, in crystalline RbAg₄I₅ the same correlation time is reached already at 140 K (4). At present, no indication for the existence of two types of silver ions differing strongly in mobility is found. Further studies on samples with various values of x and n together with an NMR determination of the Ag self-diffusion coefficient are in progress.

- (1) G. Chiodelli, G. Campari Viganò, G. Flor, A. Magistris, M. Villa, *Solid State Ionics* 8 (1983) 311.
- (2) G. Robert, J.P. Malugani, A. Saide, *Solid State Ionics* 3/4 (1981) 311.
- (3) G. Chiodelli, A. Magistris, M. Villa, J.L. Bjorkstam, *J. of Non-Crystalline Solids* 51 (1982) 143.
- (4) H. Looser, D. Brinkmann, M. Mali, J. Roos, *Solid State Ionics* 5 (1981) 485.

TRANSPORT AND THERMODYNAMIC PROPERTIES OF AgI - Ag OXSALT(S) GLASSES

Alberto Schiraldi, Elisabetta Pezzati* and Primo Baldini
Dipartimento di Chimica Fisica, Università di Pavia
Viale Taramelli 16, 27100 Pavia, Italy

* Centro di Studio per la Termodinamica ed Elettrochimica
dei sistemi salini fusi e solidi del CNR, Pavia (Italy)

A number of glasses showing a high ionic conductivity at room temperature has been recognized in the systems AgI-Ag₂O-M_nO_m, where M_nO_m is a Lewis acid which.

Studies concerning such glasses are spread over many experimental and theoretical works [1-12], mainly dealing with the composition-structure-transport correlation.

However, only systems showing a wide glass formation region allow a reliable achievement of this aim, inasmuch as they provide a suitable composition range to verify the actual role of the AgI content.

It is indeed possible to state that the silver ion population of these glasses is to be shared into two subtypes, viz., the mobile ions, coming from AgI, and those, coming from the Ag oxysalt, practically resting in fixed positions. These two Ag⁺ species are in thermodynamic equilibrium and their mixture may be described as a regular solution. The latter statement comes from the approach to the thermodynamic properties of these ions via thermoelectric power determinations carried out with silver electrodes thermocells.

It has also been verified (within the errors involved in the extrapolation of the molar heat-temperature trend of the AgI standard modifications) that the ideal composition limit of these glasses, viz., N(AgI) = 1, actually corresponds to the hypothetical glassy AgI which would be obtained by quenching the melt, inasmuch as the latter would have the same glass transition temperature and the same entropy.

1. A.Schiraldi, *Electrochim.Acta*, 23 (1978) 1039
2. J.P.Malugani, A.Waniewski, M.Doreau, G.Robert and A.Al-Rikabi, *Mat.Res.Bull.*, 13 (1978) 427
J.P.Malugani, A.Waniewski, M.Doreau, G.Robert and R.Mercier, *ibidem*, 13 (1978) 1009
3. J.L.Souquet, *Ann.Rev.Mater.Sci.*, 11 (1981) 211
4. M.D.Ingram and C.A.Vincent, *Ann.Rep.A Chem.Soc.London*(1977) 23
5. S.W.Martin and A.Schiraldi, "Formation of high conductivity glasses in the system AgI-AgPO₃-Ag₃AsO₄", to be published
6. T.Minami and M.Tanaka, *Rev.Chim.Min.*, 16 (1979) 283
7. T.Minami, H.Nambu and M.Tanaka, *J.Am.Cer.Soc.*, 60 (1977) 283
8. A.Magistris, G.Chiodelli and A.Schiraldi, *Electrochim.Acta*, 24 (1979) 203
9. G.Chiodelli, A.Magistris, M.Villa and J.L.Bjorkstam, *J.Non Cryst.Sol.*, 51 (1982) 143
10. G.Chiodelli, G.Campari Viganò, G.Flor, A.Magistris and M.Villa, *Sol.Stat.Ionics*, 8 (1983) 311
11. S.W.Martin and A.Schiraldi, *J.Phys.Chem.* (1985) to appear
12. A.Schiraldi, E.Pezzati and P.Baldini, *ibidem*, to appear

BRILLOUIN SCATTERING IN α -AGI AND AgI RICH GLASSES

L. Börjesson and L. M. Torell
 Department Of Physics, Chalmers University of Technology
 S-412 96 Gothenburg, Sweden

Brillouin scattering experiments have been performed in single crystals of superionic α -AgI to get a better understanding of the cation dynamics and how it depends on structure. Spectra were obtained at different crystal orientations and temperatures. The longitudinal and the strongest transverse acoustic modes with phonon frequencies of 9.6-11.3 GHz and 4.1-5.5 GHz respectively, were present in most of the spectra, whereas the second transverse mode (7.8-8.2 GHz) was very weak and only observable in a few spectra. Longitudinal phonons have been observed in Brillouin spectra of α -AgI in other laboratories^{1,2} but so far no observations of any of the two transverse peaks have been reported. From the measured frequency shifts the longitudinal and the transverse hypersonic velocities can be calculated as well as the elastic constants. For the hypersonic velocities the orientation dependent values are $(1.68-1.97) \times 10^3 \text{ ms}^{-1}$ and $(0.72-0.96) \times 10^3 \text{ ms}^{-1}$ for the longitudinal and the strongest transverse phonon respectively. The elastic constants could only be estimated since the crystals so far were unoriented.

Brillouin scattering have also been performed in superionic $(\text{AgI})_x(\text{AgPO}_3)_{1-x}$ glasses for $x=0.0, 0.1, 0.3, 0.4, 0.5$. Both longitudinal and transverse modes were obtained and their frequency shifts as a function of temperature were measured to determine the elastic constants. The velocity data extrapolate linearly to those of α -AgI in support of a microdomain model, which suggests that the introduction of AgI does not effect the glass network chemically but tends to reproduce, on the local level, microdomains of pure α -AgI.

1. Winterling, G; Senn, W; Grimsditch, M; Katiyar, R; Proc. Intern. Conf. on Lattice dynamics, ed. M. Balkanski (Flammarion, Paris, 1977)
2. Sasaki, W; Sasaki, Y; Ushioda, S; Taylor, W; J. Phys. Colloq. 42 (1981) C6-181

HEAT CAPACITY OF GLASSY IONIC CONDUCTORS $(\text{AgI})_x(\text{Ag}_2\text{O} \cdot 2\text{B}_2\text{O}_3)_{1-x}$ BETWEEN 1.5 AND 40 K.

A. Avogadro, S. Aldrovandi and F. Borsa.

Dipartimento di Fisica "A. Volta" e Gruppo Nazionale di Struttura della Materia, Via Bassi 6, 27100 PAVIA (Italy).

The glassy ionic conductors $(\text{AgI})_x(\text{Ag}_2\text{O} \cdot 2\text{B}_2\text{O}_3)_{1-x}$ have attracted a great deal of interest⁽¹⁾ because of the high ionic conductivity at room temperature which can be controlled over a large interval by changing the glass composition x . Measurements of specific heat yield important information about the integrated spectrum of the excitations which in our case may be expected to be anomalous because of both the superionic properties and the glassy state of the matrix. Previous measurements⁽²⁾ at high temperature of specific heat have shown an almost linear increase by increasing temperature in samples with $x = 0$ and $x = 0.5$. Here we present measurements of heat capacity, performed by means of a high resolution adiabatic calorimeter in the temperature range $1.5 \div 40$ K, for samples with $x = 0, .2, .5, .65$. The measurements plotted as C_p/T display a maximum centered at about $6 \div 8$ K whose amplitude and position depend upon the x value of glass composition. The extra contribution to the heat capacity (with respect to the Debye term due to acoustic phonons) can be interpreted formally in terms of low frequency optical or local modes and it appears to be a common feature of amorphous materials and anharmonic crystals. In the present case the microscopic origin of the above mentioned low energy excitations is discussed in relation to the known transport properties. Moreover, we discuss the possibility to interpret the temperature behavior of the heat capacity over the whole temperature range (from 0 °K up to the glass transition temperature) by considering the contribution of the normal elastic phonon modes and the anharmonic or local modes originated by the motion of Ag ions in the BO_3 - BO_4 networks.

- (1) G. Carini, M. Cutroni, A. Fontana, G. Mariotto and F. Rocca, Phys. Rev. B 29, 3567 (1984) and references therein.
- (2) A. Avogadro, A. Dworkin, P. Ferloni, M. Ghelfenstein, A. Magistris, H. Szwarc, S. Toscani, J. of Non-Crystalline Solids 58, 179 (1983).

STUDIES ON MIXED-ANION AgI-Ag₂MoO₄-Ag₂SeO₄
GLASS-FORMING FAST ION CONDUCTORS

Hemlata Senapati
Solid State and Structural Chemistry Unit
Indian Institute of Science
Bangalore - 560012
India

Glass-formation in systems containing AgI and mixtures of divalent tetrahedral oxyanions like MoO₄²⁻, SeO₄²⁻ and WO₄²⁻ has been investigated. The infrared spectra, glass transition temperatures and conductivity (σ) behaviour of glasses in the AgI-Ag₂MoO₄-Ag₂SeO₄ system have been studied. It is found that glass-formation in the xAgI-Ag₂MoO₄-zAg₂SeO₄ system is particularly easy and extensive, ranging from 45 to 85 mole percent AgI, the glasses exhibiting values as high as $5 \times 10^{-3} \text{ ohm}^{-1} \text{ cm}^{-1}$ at ambient temperatures. While keeping the value of x constant, it is possible to vary the oxyanion ratio y/z continuously between the binary limits. This yields a series of glasses where the AgI content is fixed and the total number of Ag⁺ ions is also being held constant. It thus becomes possible to decant out the contribution of the nature (size/polarizability) of the oxyanion-matrix to properties like glass-transition temperatures, conductivity values and energies of activation.

SUPERIONIC CONDUCTING GLASS: GLASS FORMATION AND
CONDUCTIVITY IN THE (AgI)_x-(Ag₃AsO₄)_{5-x} SYSTEM.

K.A.Murugesamoorthi, K.Hariharan and S.Radhakrishna
Department of Physics
Indian Institute of Technology
Madras 600 036 INDIA.

Studies on superionic conducting glass have assumed importance since high conductivities ($10^{-1} \text{ } \Omega^{-1} \text{ cm}^{-1}$) at room temperature have been reported in contrast to ordinary insulating glasses such as silicates, borates and so on. The present work deals with the studies on glass formation, structure and electrical conductivities on (AgI)_x-(Ag₃AsO₄)_{5-x} solid electrolyte system. The samples were prepared by heating the evacuated glass ampoules containing the appropriate quantities of the materials at 450°C for forty eight hours and quenching in liquid Nitrogen. The X-ray diffractograms of the samples confirmed the glassy nature of the materials formed. The electrical conductivity of the pulverized glasses pressed together with electrode mixtures of silver and glass (1:2 by weight) under 3000 Kg/cm² to form pellets of 10 mm diameter, were carried out in the temperature range 300 K to 365 K at 1 KHz. Also conductivity measurements on polycrystalline samples have been carried for the sake of comparison. The ionic conductivity of the glassy sample was higher than that of the polycrystalline sample at any temperature. It is found to have the highest conductivity ($0.016 \text{ } \Omega^{-1} \text{ cm}^{-1}$) which is one order of magnitude higher than that for the corresponding polycrystalline sample ($0.004 \text{ } \Omega^{-1} \text{ cm}^{-1}$). The activation energies ranged from 0.33 eV to 0.4 eV and increased with the decrease in conductivity. It is to be noted that the activation energies of the glassy samples were larger by ~ 0.1 eV than that of the corresponding polycrystalline sample. Conductivity measurements on annealed glassy samples indicate that the conductivity decreases with the time of annealing, reaching a constant value which is less than that of the polycrystalline sample. Electronic conductivities of the samples were obtained by using Wagner's polarization cell technique with the configuration: Ag/Electrolyte/C. Glassy material of the composition 4AgI-Ag₃AsO₄ was found to have low electronic conductivity, the value of which increases with the change in composition.

A typical galvanic cell with glassy sample of the composition 4AgI-Ag₃AsO₄ as electrolyte having the configuration (Ag, Electrolyte/Glassy Electrolyte/ C, I₂, Electrolyte) has been constructed and its discharge characteristics investigated.

SIMULTANEOUS PROTON AND OXYGEN ION TRANSPORT IN SOLID
MOLYBDIC ACID DUE TO POSSIBLE ELECTROLYSIS OF INTERLAYER
WATER OF CRYSTALLISATION

BY

S. Chandra, B. Singh and N. Singh
Physics Department, Banaras Hindu University, Varanasi, India

Molybdc acid is an aquoxide with both coordinated and inter layer hydrated water molecules. Each coordinated water molecule donates its hydrogen atoms to two interlayer water. Each interlayer water donates one hydrogen to an unshared oxygen in the next layer and the other to a weak bifurcated bond of a coordinated water molecule and an oxygen shared between octahedra. While exploring this material as a possible proton conductor, we came across definite evidence showing electrolysis of interlayer water of crystallisation which give rise to interesting ion transport and physical properties. Briefly, these can be stated as follows:

(i) DIRECT CURRENT ELECTROLYSIS OR COULOMETRY : A sample pellet was kept in a specially designed coulometer similar to that used by S. Chandra and N. Singh (J. Phys. C. 16, 3081, 1983) with an additional provision for measuring volumes of gases evolved both at the cathode and anode. It was found that hydrogen and oxygen are evolved respectively at the cathode and anode.

(ii) IR AND LASER RAMAN SPECTRA : After electrolysis, the anode side became yellowish while there was only a slight change in whitish shade of $\text{MoO}_3 \cdot 2\text{H}_2\text{O}$ at the cathode. The IR and laser Raman analysis of the samples near the two electrodes show that the dihydrate $\text{MoO}_3 \cdot 2\text{H}_2\text{O}$ has been changed to yellow monohydrate $\text{MoO}_3 \cdot \text{H}_2\text{O}$ at the anode while at the cathode white monohydrate or $-\text{MoO}_3 \cdot \text{H}_2\text{O}$ is formed. This confirms our hypothesis of likely electrolysis of water of crystallisation.

(iii) ELECTRICAL CONDUCTIVITY : The following significant observations were made : (a) the a.c. electrical conductivity is a function of signal level, (b) this effect was more prominent at low frequencies (100 Hz) than at frequencies greater than 10 KHz, (c) the a.c. conductivity increased with simultaneous application of d.c. bias, (d) the conductivity decreased more rapidly with time in vacuum than in humid atmosphere on constant application of electrical signal. These observations fit a transport mechanism where the role of ions obtained by electrolysis is considered.

(iv) NMR UNDER D.C. BIAS : Variation of NMR line width with temperature and d.c. bias has been studied. On application of d.c. bias, a narrow line shoulder appears superimposed over a broad proton resonance line. This indicates that protons attached to one of the two water molecules of $\text{MoO}_3 \cdot 2\text{H}_2\text{O}$ have only been made mobile. It is suggested that NMR study under d.c. bias could be an interesting tool for the study of solid electrolytes in general.

RAPID ION TRANSPORT IN COMPOSITE ELECTROLYTES

By

A. C. Khandkar and J. B. Wagner, Jr.
Center for Solid State Science
Arizona State University
Tempe, AZ 85287 USA

During the past several years, several investigators have reported on the anomalous enhancement in conduction in electrolytes containing a dispersion of sub-micron sized insulating particles such as Al_2O_3 and SiO_2 . This effect has been commercially exploited with the successful use of $\text{LiI} - \text{Al}_2\text{O}_3$ composite electrolyte batteries. Yet, the mechanism responsible for the enhancement in conductivity has not been completely explained. In this paper, we have systematically investigated the effect of water or the "degree of dryness" of the dispersoid and its role in determining the magnitude of the enhancement in $\text{LiI} - \text{composite electrolytes}$. Conductivity data from 298 K to within 10° of the melting point of the host electrolyte material, at 100 Hz to 10 kHz will be presented. These results will be supplemented with thermogravimetric (TGA) data and differential scanning calorimetry (DSC) data on the composite electrolytes. Recent work on the $\text{LiBr} - \text{H}_2\text{O}$ system indicates the presence of the hemihydrate phase. Our DSC data on the LiI system shows behavior similar to the LiBr case, but the TGA data are inconclusive and more work is in progress to resolve this.

Finally, recently obtained data on LiI composites containing zeolites as the dispersoid will be presented. The conductivity enhancement is about 2 orders of magnitude and the behavior with respect to temperature is unusual in comparison to composites containing Al_2O_3 or SiO_2 . NMR investigations on these electrolyte composites are currently in progress. Our preliminary results lead us to speculate that zeolite composites may be useful in addressing some electrode/electrolyte interface problems prevalent at high drain rates in solid state Li batteries. The 3-D channel network structure of the zeolite is likely to provide rapid conduction paths with relatively longer diffusion lengths thus making zeolite dispersed LiI a better candidate for use in batteries.

ENTROPY EFFECTS IN IONIC CONDUCTIVITY

D.P. Almond,
University of Bath,
School of Materials Science,
Claverton Down, Bath BA2 7AY, U.K.

A.R. West,
University of Aberdeen,
Dept. of Chemistry,
Meston Walk, Aberdeen AB9 2UE, U.K.

Estimates of the entropy of activation for conduction show that it is a principal source of variation in the magnitude of the conductivity preexponential factor for a wide variety of solid electrolytes. Different kinds of entropy effect are proposed. In materials that conduct by a simple activated hopping mechanism and that exhibit a disordering transition in the mobile ion sublattice, the entropy term may be estimated using $S = E/T_d$ where E is the activation energy for conduction at temperatures well below the disordering temperature, T_d . For materials that conduct by an interstitialcy mechanism or some other cooperative process, the magnitude of the entropy is reduced and may be negative.

Entropy data have been analysed for a variety of solid electrolytes. This has permitted a general rationalisation of the entropy term and the establishment of a correlation between entropy, crystal structure and conduction mechanism.

STABILITY OF ALKALI ION-CONDUCTING SOLID AND LIQUID ELECTROLYTES;
THERMODYNAMIC ASPECTS

Gerhard Doublein and Robert A. Huggins

Department of Materials Science and Engineering
Stanford University
Stanford, CA 94305

While most of the attention has been given in recent years to the question of the magnitude of the ionic conductivity of solid electrolytes, their scientific and technological applications are often actually limited by their decomposition or reactions with species in the electrodes.

This problem is especially acute in the case of alkali ion-conducting electrolytes, due to the great relative stability of alternative alkali ion-containing phases that are potential reaction products.

The tendency for decomposition and reactions with the electrodes can be understood in terms of thermodynamic considerations. The principles that are involved in assessing the stability of both binary and ternary electrolytes, as well as experimental techniques that can be used for their determination will be reviewed.

Experimental results as well as predictions of the stability windows of several new solid and liquid electrolytes will be presented. This will include several families of hydroxide and hydride-containing materials.

STRUCTURE OF ADDITIVES IN β -ALUMINA AND ZIRCONIA SUPERIONIC CONDUCTORS¹W.L. Roth^a, R. Wong^a, A.I. Goldman^b, E. Canova^b, Y.H. Kao^b, B. Dunn^c

- a. Department of Physics, S.U.N.Y. Albany, Albany, NY 12222
 b. Department of Physics, S.U.N.Y. Stony Brook, Stony Brook, NY 11794
 c. Department of Materials Science, U.C.L.A., Los Angeles, CA 09924

Additives that are commonly termed stabilizers must be incorporated in many compounds to obtain structures which exhibit superionic conductivity. Here we consider sodium conductors with the rhombohedral β -alumina structure which has been stabilized by Zn^{2+} and Co^{2+} and oxygen conductors with the cubic zirconia structure which has been stabilized with different concentrations of Y^{3+} . Although the average crystal structures of these compounds have been determined by x-ray and neutron diffraction, the local structures in the vicinity of the additives and the host ions are not known, since elastic scattering gives only the average atomic arrangement of ions in solid solution. In YSZ, Y^{3+} replaces Zr^{4+} in the cation sublattice, and charge is compensated by O^{2-} vacancies; in β -alumina, the stabilizers replace Al³⁺ ions in tetrahedrally coordinated Al(2) sites. We have used Extended X-Ray Absorption Fine Structure (EXAFS) to investigate the local structure of Y^{3+} and Zr^{4+} in yttria-stabilized zirconia (YSZ) and of Zn^{2+} and Co^{2+} that are incorporated to stabilize Na β -alumina. The local structure of Mn implanted at high energy in Na β -alumina has also been determined; particle backscattering and channeling studies were previously reported.²

Absorption spectra were taken at room temperature above both the Y and Zr K-edges of YSZ compounds ranging from 9.4 to 24 mole percent Y_2O_3 and above the Zn, Co, and Mn K-edges of the stabilized and implanted β -aluminas. Spectra of ZrO_2 , $SrSrO_3$, $CaZrO_3$, Y_2O_3 , ZnO , CoO , $CoAl_2O_4$, MnO and $MnAl_2O_4$ were collected for use as model compounds. It has been found that there are substantial differences in the local structure of the additive and host ions in solid solution. In YSZ, the Y-O bond lengths are longer than the Zr-O bond lengths, and the oxygen vacancies are preferentially bound to the Y^{3+} ions. In β -alumina, the Zn-O and Co-O bond distances are longer than the average M^{IV} -O bond distances measured by x-ray and neutron diffraction. In Mn-implanted Na β -alumina, the Mn ions are tetrahedrally coordinated and probably occupy the same Al(2) sites as the stabilizers in β -alumina. We will discuss the implications of these results to the anomalous conductivity and conductivity aging of YSZ, stabilization of the β -alumina crystal structure, and material synthesis by ion-implantation.

- (1) This work was supported in part by the Office of Naval Research.
 (2) W.L. Roth, R.E. Benenson, C. Ji, and L. Wielunski, Solid State Ionics **9-10** (1983) 1459-1464.

EFFECTS OF THERMAL HISTORY UPON THE BEHAVIOUR OF CRYSTALLINE FAST IONIC CONDUCTORS

Fernando Garzon, Thomas Feist and Peter K. Davies

Department of Materials Science
 University of Pennsylvania
 Philadelphia, PA 19104

Thermodynamic studies have been made upon crystalline fast ionic conducting systems whose high conductivity is mainly a result of the presence of vacancies introduced by "aliovalent framework" substitutions. In particular we have examined the effects of thermal history upon the behaviour of this class of materials. The two systems so far studied are NASICON materials, $Na_{1+x}Zr_2Si_xP_{3-x}O_{12}$ ($1.9 \leq x \leq 2.4$), and lithium-stabilized Na beta alumina.

The energetics of the second-order transition in NASICON, $x=2$, have been studied previously (1). We first examined the variation of the enthalpy of this transition with x and found the expected decrease as x increases. In an attempt to study any effects of thermal history upon the behaviour of NASICON we re-heat treated samples both by long-term annealing at 650°C and by rapid quenching from a 12 hour treatment in a sealed platinum capsule at 1000°C. For each of the samples studied the enthalpy of the low-temperature, ~ 420 K, phase transition was changed by as much as 15% by the thermal treatment. No structural decomposition was observed by X-ray diffraction. Samples subjected to the low temperature anneal also show evidence of a second, broad transition at a higher temperature.

Commercial (Ceramtec) lithium-stabilised sodium beta alumina ceramic were also annealed at 700°C for extended periods, and rapidly quenched from short-term treatments at 1350°C. No decomposition of the samples was detected by X-rays. Using DSC (Setaram DSC 111) a broad endothermic transition was observed at $\sim 200^\circ\text{C}$ for an untreated sample, the annealed sample showed a broad transition at $\sim 75^\circ\text{C}$. Both peaks were observed even after repeated cycling under argon. No peaks were detected in the quenched sample. Using thermogravimetric analysis the hydration/dehydration behaviour of the three samples revealed substantial differences for each. The annealed material shows a much lower water uptake than either the fast quenched or untreated samples. The untreated ceramic did not show weight loss until 150°C, the annealed and quenched samples lose all water by 50°C. We believe the DSC anomalies reflect, at least in part, the thermal characteristics of the dehydration behaviour. Once again it is clear the thermal history has significantly influenced the low temperature energetic behaviour of these materials.

- (1) U. V. Alpen, M. F. Bell and W. Wichelhaus, Mat. Res. Bull., **14**, 1317 (1979).

This work is supported by the NSF under grants NSF/MRL DMR 8216718 (F. G.) and DMR 8316999 (P. K. D.).

THE MIXED ALKALI EFFECT
IN CRYSTALLINE SOLID ELECTROLYTES

James A. Bruce and Malcolm D. Ingram

Department of Chemistry, University of Aberdeen, Aberdeen, Scotland.

In mixed cation β -alumina a great diversity of behaviour is found, including deep conductance minima (typical of mixed alkali effects in glass) and conductance maxima which are described as "co-ionic" effects. These results were presented in Grenoble^(1,2) in 1983, where we argued that these phenomena reflect differing cation site preferences. We have now tested these ideas by determining partial site occupancies in mixed cation crystals from structural refinements based on X-ray data.

A coherent pattern emerges. We can reconcile the conductivity trends to the site occupancies by means of the *paired interstitial* model. If the foreign cation enters interstitial sites directly, then the conductivity may fall sharply, and the slope of the isotherm may then be interpreted in terms of *weak electrolyte theory*. When the foreign ion avoids these sites, there can still be a "blocking" effect, which depends on the closing off of conduction pathways in the crystal. The co-ionic effect (see also ref. (3)), depends however on the "unlike" cations being able to exchange sites readily, and is found in Na/Ag and Na/Li β -alumina.

These results permit useful comparisons to be made between conduction mechanisms in glasses and crystals, and enable important similarities and differences to be highlighted.

- (1) J.A. Bruce, M.D. Ingram, *Solid State Ionics*, **9 & 10** (1983) 717.
 (2) J.A. Bruce, C.C. Hunter, M.D. Ingram, *ibid.*, **9 & 10** (1983) 739.
 (3) W.L. Roth, C.C. Farrington, *Science*, **196** (1977) 1332.

Water Vapour Electrolysis using Hydronium β alumina.
Ion Exchange and Cell Performance.

M.F. Bell and M. Sayer,
Department of Physics,
Queen's University, Kingston K7L 3N6,
Ontario, Canada.

P.S. Nicholson and M.Z.A. Munshi,
Department of Metallurgy and Materials Science,
McMaster University, Hamilton,
Ontario, Canada.

The production of high quality hydronium beta alumina ceramics requires the preparation of mixed alkali compositions of β, β' alumina as precursors¹. To explain the conductivity behaviour in these precursors, a theory¹ was developed which takes into account not only the proportion of β phase but also the effects of grain misorientation and the presence of two mobile ions. This theory suggests that the presence of two mobile ions produces effects similar to those observed for the "mixed alkali effect" in that the conductivity shows a pronounced minimum at some intermediate composition.

In this paper, we show that the mixed alkali effect also plays a role during ion exchange in that the ceramics exhibit unusual conductivity changes as the sodium ions are replaced by hydronium ions. We believe that as the hydronium ion is univalent and similar in size to the potassium ion, it is behaving like the alkali ion causing a drop in conductivity due to site preference.

Water vapour electrolysis units have been built and preliminary tests show promising performance. The theoretical performance of units using protonically-conducting membranes is reviewed and compared with experimental data for hydronium β alumina cells at a number of temperatures.

REFERENCE

1. M.F. Bell, M. Sayer, D.S. Smith and P.S. Nicholson, *Solid State Ionics*, **9 & 10** (1983) 731-734.

PREPARATION AND PROPERTIES OF TRANSITION METAL BETA' ALUMINAS

J. D. Barrie, B. Dunn, and O. M. Stafsudd
Department of Materials Science and Engineering
University of California, Los Angeles, CA 90024

G. C. Farrington, Materials Science Department
University of Pennsylvania, Philadelphia, PA 19104

The ion exchange properties of beta' alumina have enabled us to synthesize a wide range of divalent and trivalent compositions.^{1,2} However, we have yet to consider circumstances in which ions capable of multiple valences have been introduced into the conduction plane. In this paper we report on a family of compounds based upon the 3d transition metals in which, by means of careful processing, we have been able to prevent the occurrence of mixed valence states. The synthesis, ionic transport behavior, and optical properties of these materials are described.

The materials were prepared from single crystals of sodium beta' alumina by different processes. Complete exchange of Na⁺ with Co²⁺ and Mn²⁺ was achieved by immersing the crystals in appropriate molten salts at 600 to 700 C, while complete Cr³⁺ exchange was obtained via vapor phase transport at 700 C. Substantial ion exchange of Ti³⁺ and Ni²⁺ was also attained by the vapor method. In all cases the use of controlled atmospheres during exchange resulted in no apparent electronic conduction due to mixed valences. For example, Mn²⁺ beta' alumina exhibited only ionic conduction processes as indicated by complex impedance measurements. The conductivity for this material ($\sim 1 \times 10^{-1}$ ohm⁻¹ cm⁻¹ at 300 C) and its activation energy (~ 0.60 eV) are comparable to that of other divalent beta' aluminas. However, initial diffusion measurements with Co²⁺ suggest that this ion is not as mobile as other divalent cations in beta' alumina. Our work also indicates that the valence states of these ions are unaffected by thermal cycling in inert atmospheres.

In addition to transport measurements, we have investigated the optical properties of several transition metal beta' aluminas. The transition metal ions are of interest for solid state tunable lasers because of their broad band fluorescence properties. Both Cr³⁺ and Ti³⁺ exhibit broad emission spectra, the latter ranging from 0.64 μ to 1.1 μ , with peak emission at 0.68 μ . Fluorescence lifetimes were found to be in close agreement with published data for these ions in other oxide hosts.

In summary, the unique ion exchange properties of beta' alumina have enabled us to prepare a family of transition metal solid electrolytes. It is possible to achieve specific valence states and to obtain ionically conductive materials. Furthermore, the optical properties of these beta' aluminas should be of interest for both structure and spectroscopy studies:

1. G. C. Farrington, B. Dunn and J. O. Thomas, *Appl. Phys. A*, **32**, 159 (1983).
2. G. C. Farrington, B. Dunn, *Solid State Ionics* **7**, 267 (1982).

CORROSION OF Na β - AND Na β' -ALUMINA IN CO₂-H₂O¹

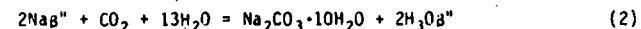
J. B. Bates and R. L. Anderson

Solid State Division, Oak Ridge National Laboratory
Oak Ridge, Tennessee 37831

Sodium β' -alumina reacts² with CO₂ and H₂O at 25°C according to



when exposed to a high pressure of CO₂ ($P_{\text{CO}_2} = 10^5$ Pa) saturated with H₂O or according to



when the electrolyte is exposed to H₂O-saturated air, with $P_{\text{H}_2\text{O}} = 3$ kPa. Under these conditions, the occurrence of reaction (2) requires the standard free energy of H₃O β' -alumina to be lower than that of Na β' -alumina by at least 35 kJoule/mol.

During the course of these reactions, Na⁺ ions removed from the surface of the electrolyte are replaced by H₃O⁺ ions. The reaction proceeds until the layer of bicarbonate or hydrated carbonate formed prevents further contact of the gas phase species with the electrolyte surface. The NaHCO₃ layer formed on the surfaces of a commercial Li-stabilized Na β' -alumina ceramic is estimated to be 20 to 50 μm thick after exposure to H₂O-saturated CO₂ for several days. On heating a specimen exposed to CO₂-H₂O, the H₃O⁺ ions in the conduction layers decompose to form OH⁻ groups. The removal of OH⁻ from the specimen by heating to 600°C is believed to occur² by formation and elimination of H₂O which implies an irreversible loss of oxygen from the conduction layers.

The formation of NaHCO₃ and Na₂CO₃·xH₂O on the surfaces of single crystal and polycrystalline samples of Na β - and Na β' -alumina can be observed using scanning electron microscopy. The formation of NaHCO₃ on freshly polished surfaces is first noticed by the appearance of crystalline, plume-shaped clusters having many small filaments extending from several branches. Evidence of film formation can be seen in some regions of the surface after exposure to H₂O-saturated CO₂ for 1 day. During exposure for several days, large crystalline clusters are evidently formed at the expense of smaller ones, and the presence of an underlying film of bicarbonate is more obvious. Similar features were seen after exposure of Na β -alumina to CO₂ and H₂O, but their rate of growth was slower.

¹Research sponsored by the Division of Materials Sciences, U.S. Department of Energy under contract DE-AC05-84OR21400 with Martin Marietta Energy Systems, Inc.

²J. B. Bates, D. Dohy, and R. L. Anderson, *J. Mater. Sci.* (in press), 1984.

Influence of Stoichiometry and the Nature of the Spinel-Block
Stabilizing Element on Proton Transport Behavior in Solid
Electrolytes with the β' -Alumina Structure

S. W. Smoot, W. P. Halperin and D. B. Whitmore
Departments of Materials Science and Engineering and Physics,
Northwestern University
Evanston, Illinois 60201
U.S.A.

Abstract

As an extension of prior work done in this laboratory on
proton transport in $\text{NH}_4\text{-H}_2\text{O } \beta'$ -alumina, we report here new proton
diffusion coefficient and conductivity measurements on: (a)
magnesia-stabilized $\text{NH}_4\text{-H}_2\text{O } \beta'$ -alumina crystals with a substan-
tially different stoichiometry than in those used earlier; and
(b) $\text{NH}_4\text{-H}_2\text{O } \beta'$ -gallate crystals where stabilization of the as-
grown crystal involves sodium substitution in the spinel block.
Proton diffusion coefficients on both compounds were accomplished
over the temperature range 300-450K with the aid of a pulsed
field gradient NMR technique, whereas a complex admittance method
was employed to obtain the protonic conductivities reported here
for the same temperature interval. In the light of the present
and earlier observations of protonic transport behavior, ideas
are discussed concerning (a) possible mechanisms of proton trans-
port and (b) the role played by stoichiometry and the type of
spinel-block stabilizing element in these β' materials.

THE EFFECT OF QUENCHING ON THE Na^+ ION DISTRIBUTION IN
 $\text{Na}^+\beta$ -ALUMINA

Maggie Aldén,¹ John O. Thomas¹ and Peter Davies²

¹Institute of Chemistry, University of Uppsala, Box 531,
S-751 21 Uppsala, Sweden

²Department of Materials Science and Engineering K1, University
of Pennsylvania, Philadelphia, PA 19104, U.S.A.

Single-crystal neutron diffraction has detected short-range-
ordering in the Mg/Al occupation of the Al(2) site at the
centre of the spinel-block in $\text{Na}^+\beta$ -alumina (Ref. 1) -
a result inaccessible to earlier X-ray studies. Implicit in
this discovery is that this lowering in the local symmetry in
the spinel-block can influence the electrostatic potential and
hence the effective local ionic arrangement in the conduction
plane.

More recently a study has been made of the ionic conductivity
of single-crystals of $\text{Na}^+\beta$ -alumina which had been quenched
rapidly from above 1000°C. In a few cases it was found that the
crystals displayed anomalously high conductivities and low
activation energies at low temperatures (Ref. 2). The notion
suggests itself that this enhanced conductivity is related to
the freezing-in of Mg/Al occupation randomness at the Al(2)
site. Single-crystal neutron diffraction studies of quenched
and unquenched crystals were undertaken to probe this situa-
tion further.

Little difference was, in fact, observed in the Mg/Al ordering,
while differences were found for the Na^+ ions such that a less
ordered Na^+ arrangement was obtained at ambient temperature in
the quenched crystal. This result has important implications
as regards the mode of fabrication of $\text{Na}^+\beta$ -alumina, especial-
ly for battery applications where optimal ionic conductivity
is of major importance.

References

1. K.G. Frase, J.O. Thomas & G.C. Farrington (1983) *Solid State Ionics*, 9/10, 307.
2. P. Davies. Unpublished results.

"FABRICATION, CHARACTERISATION AND STEAM ELECTROLYSIS PROPERTIES OF
POLYCRYSTALLINE H_3O^+ - β/β'' -ALUMINAS"

Authors: Patrick S. Nicholson, Masayuki Nagai, Zafar Munshi, Govind Singh,
Kimihiro Yamashita
Ceramic Engineering Research Group
Department of Metallurgy and Materials Science
McMaster University
Hamilton, Ontario, Canada

and Michael Sayer, Michael Bell
Department of Physics
Queens University
Kingston, Ontario, Canada

Polycrystalline H_3O^+ - β/β'' -Alumina ceramics have been fabricated and used successfully to electrolyse steam at +100°C. The ceramic precursor is a mixed alkali β/β'' -alumina of sufficient mechanical strength to withstand the necessary potassium and hydronium ion exchange procedures required to produce the hydronium β/β'' -alumina polycrystals.

The fabrication and ion exchange procedures are described. The rate of ion exchange in hot concentrated H_2SO_4 was monitored via changes in the alkali solution content. Field assisted ion-exchange in dilute H_2SO_4 was also studied from the current/time characteristics of the process. The ion exchange process kinetics were modelled assuming the diffusion of H_3O^+ to be rate determining of the process.

The interphase relationships and the residence phase of the alkali components have been studied by quantitative scanning-transmission-electron-microscopy and the results are described.

The H_3O^+ - β/β'' - Al_2O_3 ceramics have been used in steam cells and steam electrolysis demonstrated. Cell design is described and the current/voltage/time characteristics discussed. Platinum has been used as a successful electrode material but seal and electrode problems have been encountered at the higher temperatures.

THERMODYNAMICS OF MIXING IN BETA ALUMINAS-RELATION
TO THE MIXED ALKALI EFFECT

Peter K. Davies, Gregory Pfeiffer and S. Canfield

Department of Materials Science
University of Pennsylvania
Philadelphia, PA 19104

Several studies have been made of mixed-cation beta and beta'' aluminas. It is well known that relative to the pure materials the mixed-ion beta aluminas generally show a large decrease in conductivity and an associated increase in activation energy (1,2). This phenomenon is analogous to the behaviour of mixed alkali glass systems and is termed the mixed-alkali effect (3). Many attempts at modelling and interpreting this effect have been made. Recent models for beta alumina systems have relied upon a weak electrolyte model and assumptions concerning the site preferences of the alkali ions (2).

Using equilibrium ion-exchange techniques we have determined the thermodynamic mixing properties of the binary Na-K, -Ag, -Li and -Tl beta alumina systems and the Na-K beta'' alumina system. All the beta alumina binaries, with the notable exception of Na-Tl, show a strong mixed alkali effect. Our activity data indicate each system shows negative deviations from ideal behaviour, indicative of cation order. Na-Tl beta aluminas are anomalous in that small positive deviations occur. The Na-K beta'' alumina binary system shows a transition from negative to positive deviations with increasing K content.

We have modelled behaviour for Na-K beta alumina using modified regular solution models. In this model complete order via Na-K ion pairing is assumed in the 'interstitial' sites, with ideal or small positive deviations on the BR sites. An excellent fit is found between the experimental data and the model. Using re-calculated 'effective activities' of ions in the interstitial sites we predict conductivities in reasonable agreement with experimental data.

We believe our data strongly supports an 'ion-pair' model for the behaviour of the binary beta aluminas. Drawing analogies with behaviour in molten-salt systems we will suggest a possible driving-force for the order observed in these binary systems.

- (1) M. D. Ingram and C. T. Moynihan, *Solid State Ionics*, **6**, 303 (1982).
- (2) J. A. Bruce and M. D. Ingram, *Solid State Ionics*, **9-10**, 717 (1983).
- (3) J. Isard, *J. Non Cryst. Solids*, **1**, 235 (1969).

This work is supported by the NSF under grants NSF/MRL DMR 8216718 (G. P.) and DMR 8316999 (P. K. D.).

Evidence of Mobile Ion Correlation Between Conduction Planes in β -alumina*

S. Chen, N. Otsuka and H. Sato

School of Materials Engineering, Purdue University, West Lafayette, In 47907

Due to the mutual, repulsive interaction between conduction cation, an ordered structure of these ions can form in the conduction plane. This ordered arrangement however, can cause a significant decrease in the ionic conductivity of the material. X-ray diffuse scattering studies have shown that as a result of ordering, an $a\sqrt{3} \times a\sqrt{3}$ superlattice can exist co-planar to the conduction layer. However, any cation ordering in the third dimension i.e. between conduction planes, have not been clearly established.

Using crystalline β -aluminas grown by a melt and a flux growth technique, the correlation between conduction cation have been examined by electron diffraction in ion exchanged Na^+ , K^+ , Rb^+ and Ag^+ β -aluminas. In addition to the correlation of mobile ions within the conduction plane, the correlation between conduction layers have also been detected in Rb^+ β -alumina with periods of 88.4\AA and 22.8\AA or three and one multiples of the c dimension. The correlation in the c direction is not as strong as that in the a - b or conduction plane. A model to account for this ordered structure in the c direction as well as a possible mechanism for such long distance correlation through spinel blocks are discussed.

* Accepted for publication in the January issue of *Solid State Ionics*, 1985.

A COMPARISON BETWEEN 'MIXED PHASE ELECTRODE' AND PERCOLATION MODELS FOR COMPOSITE ELECTRODES IN SOLID STATE CELLS

Kenneth D.M. Harris, Michael D. Rogers and Colin A. Vincent,
Department of Chemistry, University of St. Andrews,
St. Andrews, Fife KY16 9ST, Scotland.

A mixed phase region, situated between the electronic terminal and the ionic conducting phases of an all solid state cell, and consisting of particles of both ionic and electronic conductor, is frequently used to improve the power output of such a cell by increasing the effective contact area between the two bulk phases. A simple computer model (MPE model) of such systems has been described previously in which the operative contact area is estimated in terms of the number of 'links' counted between chains of electronically and ionically conducting particles.

Certain similarities exist between this model and percolation models used to describe electrical conduction in systems consisting of mixtures of conducting and insulating phases. Conduction in typical percolation models requires that the particles of the conducting phase are connected simultaneously to both end faces of the region under investigation. In the MPE model the requirement is rather different, namely that the chains of electronic and ionic conducting particles are connected back only to their own respective bulk phase, i.e. to a single end face.

The computer model for the mixed phase region has been modified to enable a count of the operative links to be made under a variety of percolation conditions. A direct comparison between the original MPE model and models based on standard percolation conditions has been undertaken over a full composition range of each component. When both phases are above a certain critical percolation 'threshold' a close similarity is observed; for either phase below the threshold, marked differences between the models exist, with the most striking divergence occurring at composition values just below the threshold.

In general, the results using the most realistic model confirm that increasing the thickness of a composite electrode increases the operative contact area in a proportional manner, provided that the percentage of each component is above a particular value. Below this limit, there is no sharp cut-off in the effectiveness of the minor component, but its usefulness diminishes rapidly as the thickness of the composite region is increased.

Within the models, different shapes and sizes of lattice and the variation in relative particle size have been examined, and the results of these calculations will be discussed.

Cu DIFFUSION COEFFICIENT IN V_6O_{13} -BASED COMPOSITE ELECTRODES DETERMINED BY
A GALVANOSTATIC PULSE RELAXATION TECHNIQUE.

C.A.C. SEQUEIRA

Laboratório de Electroquímica, Instituto Superior Técnico,
Av. Rovisco Pais, 1096 Lisboa Codex (Tel. 804589 - Telex 63423 IST UTL/F)

The importance of V_6O_{13} -based composites as hosts for the electrointercalation of atomic species has recently been pointed out by various authors. The diffusion coefficient of the relevant species is certainly one of the most important parameters characterizing a mixed conductor; therefore, in view of possible applications its determination seems useful. In this respect non-stationary electrochemical techniques offer considerable advantages.

The main aim of the present study was the determination of the diffusion coefficient of copper in V_6O_{13} -based composite electrodes employing a galvanostatic pulse relaxation technique. The study covered a range of composition and temperature.

In all-solid state cylindrical cell utilizing a disc of $Rb_4Cu_4I_2Cl_{13}$ as electrolyte, a composite working electrode based on V_6O_{13} , a disc of Cu as counter electrode and a $Cu/Rb_4Cu_4I_2Cl_{13}$ annular reference electrode, has been used for the measurements. $Rb_4Cu_4I_2Cl_{13}$ was obtained from Basic Volume Limited, London. Composite electrodes were fabricated by an intimate mixing of pre-ball-milled V_6O_{13} powder together with acetylene black, to provide additional electronic conductivity, in the appropriate solution of polyethylene oxide, isopropyl alcohol and anhydrous acetonitrile. This was followed by casting directly onto a metal foil current collector.

Galvanostatic pulses of short duration ($\sim 1s$) in the range $10-250 \mu A cm^{-2}$ were applied to the cell and the resulting overpotential/time curves were analyzed. Plotting $\eta = f(t)$ straight lines were obtained, from which the diffusion coefficients could be calculated.

The chemical diffusivity of copper in V_6O_{13} -PEO composite structures is temperature & composition dependent, and its average value suggests the potential usefulness of these cathode materials for advanced solid state copper electrochemical cells.

LITHIUM INSERTION INTO IRON SPINELS

C.J. Chen and M. Greenblatt
Department of Chemistry
Rutgers, The State University of New Jersey
New Brunswick, New Jersey 08903

Several iron spinels, $MIIFe_2O_4$ with $MII = Mn, Fe, Co, Ni, Cu, Zn$ or Cd have been lithiated using $n-BuLi$ and electrochemical methods, respectively. The amount of Li ions that may be inserted into the cavities of the spinel framework structure (i.e. x in $Li_xMFe_2O_4$) is dependent on the nature and distribution of cations, and is in the range $0.3 < x < 2.0$ for the various compounds studied. The inverse spinels with reducible Fe^{3+} occupying the tetrahedral sites can accommodate a greater amount of Li ions than the normal spinels. The size of the cations appears to have negligible effect on the extent of lithium insertion. Intensity changes of the reflection peaks of the x-ray powder diffraction patterns of the lithiated spinels compared to the hosts indicate that the cations are redistributed upon lithium insertion. The spinel structure transforms to the rock salt structure for the fully lithiated spinels in each case, in agreement with the reaction mechanism of lithium insertion in spinels proposed by Goodenough.

^{57}Fe Mossbauer results show the presence of mixed valent $Fe(III)$ and $Fe(II)$ and in the temperature range $50K < T < 300K$ a valence averaging (electron hopping) phenomenon. The electrical conductivity of the lithiated spinels is several orders of magnitude larger than that of the host materials confirming charge hopping. The temperature variation of magnetic susceptibility of the lithiated spinels indicates very large magnetic exchange interactions and transition to a spin glass state at low temperatures.

Results of a neutron diffraction powder profile analysis of $Li_2Fe_3O_4$ will be discussed.

The Crystal Structures of Lithium Inserted
Metal Oxides: LiV_2O_5

R. J. Cava^{*}, A. Santoro⁺, D. W. Murphy^{*} and R. S. Roth⁺

^{*} AT&T Bell Laboratories
600 Mountain Avenue
Murray Hill, NJ 07974

⁺ National Bureau of Standards
Washington, D.C. 20234

The insertion of lithium at ambient temperature into V_2O_5 to a stoichiometry LiV_2O_5 has been studied extensively both chemically and electrochemically. The reaction was reported by various groups to be without significant structural change of the host, based on the power X-ray diffraction patterns of the product. The idealized structure of V_2O_5 is a crystallographic shear of the ReO_3 type structure with block size 2 octahedra wide and infinite in the 2 other directions. Neighboring blocks are joined by edge sharing and all other octahedra are joined through corner sharing. With only 1 set of shear planes present, the ideal host structure is flexible about the many shared corners of VO_6 octahedra. In the real structure, however, there is one long V^{O} bond in each VO_6 "Octahedron" which results in an effectively layer-like structure, and thus allows the possibility of further structural distortion on insertion.

We have found that the structure of lithium inserted V_2O_5 is, in fact, significantly distorted during Li insertion: the Li is accommodated through separation, puckering, and shifting of the layers in the host; which occurs through the breaking of the long V-O bonds in the host. The distorted host has sites of perfect geometry for Li accommodation. Because the host is significantly altered during Li insertion, highly unconventional techniques had to be employed to solve the structure based on powder diffraction data, which is the only data available due to breaking of single crystals of host materials during insertion reactions.

DISORDER AND TRANSPORT IN β -LITHIUM/ALUMINUM^{*}

Torben O. Bruun, Sherman Susman, Jens-Erik Jørgensen,
John Faber, Jr. and Kenneth J. Volin

Argonne National Laboratory
Argonne, Illinois, U.S.A.

Neutron diffraction experiments in $\beta\text{-Li}_x\text{Al}_{1-x}$ have now been extended to the upper phase boundary ($x = 0.536$) and to the lower phase boundary ($x = 0.480$) for the purpose of determining the mechanism of Li-ion transport. Temperature-dependent neutron diffraction measurements were performed from 460°C to 625°C and at room temperature. Improved instrumentation and sample-containment techniques have resulted in enhanced quantitative accuracy. Rietveld refinement of the diffraction patterns has been used to test various defect models for $x = 0.536$. The best fit is to a disorder model in which Li_{Al} and Al_{Li} reciprocal, anti-site, defect pairs are generated in increasing concentrations with increasing temperature. By extrapolation of the integrated areas of low Q reflections in a Wilson plot ($\log \text{intensity vs. } \sin^2\theta/\lambda^2$), it is shown that ~ 5% of the lithium lattice is occupied by aluminum at 625°C. Difference Fourier maps give no indication of interstitial Li. We submit that this order-disorder process is present for all $\beta\text{-Li}_x\text{Al}_{1-x}$ compositions in high-temperature, Li-metal sulfide batteries ($T > 415^\circ\text{C}$). For $x < 0.507$, hopping of free vacancies is the dominant mechanism of Li-ion transport. For $x > 0.507$, the order-disorder process is the transport mechanism.

ELECTRICAL AND OPTICAL PROPERTIES
OF LITHIUM INTERCALATED III - VI COMPOUNDS

E. HATZIKRANIOTIS, C. JULIEN and M. BALKANSKI

Laboratoire de Physique des Solides
associé au CNRS

Université Pierre & Marie Curie

4 Place Jussieu

75230 PARIS CEDEX 05, FRANCE

97
III - VI Layered compounds such as InSe and GaSe are intercalated with Lithium by spontaneous reaction in n-butyllithium and electrochemical process. These compounds show to be good hosts for the insertion of lithium at ambient temperature. In this report we present results obtained on lithium insertion reaction of several such compounds. The insertion reaction is characterized by the time resistivity variation of the host material.

The Li intercalation into InSe is studied by galvanostatic electrochemical methods. We have investigated the charge and discharge at different current densities over the range of EMF'S commonly encountered in secondary cells. Electrical transport measurements on Li intercalated InSe and GaSe are studied, the results show a change by 3-orders of magnitude of the conductivity with respect to non intercalated samples.

Optical properties have been investigated by Raman spectroscopy and excitation spectra. The effect of Li intercalation on the phonon spectra of the host lattice has been studied by Raman scattering. We observe a broad band at low frequency for the excitation by 488 nm Laser Line, and see a resonance enhancement in the Raman scattering of Li intercalated samples at 4.2 K. The effect of Li intercalation on the electronic structure of the host material is studied in the E_1^1 exciton region in $Li_x InSe$. The excitation spectrum shows a strong band at 2.535 eV and a complex structure at lower energy. By further investigation of the excitation spectra we hope to be able to demonstrate that this method is a good probe for the diffusion processes into these electrode materials.

ELECTRODE MATERIALS ON THE BASE OF CUPROUS
CHALCOGENIDES

L. D. Yushina and V. I. Terekhov
Institute of Electrochemistry
Ural Science Center, USSR Academy of Science
Sverdlovsk
USSR

Investigating the electrode materials which can convertibly function on the boundary with Cu^+ -conducting solid electrolytes, we have synthesized a great number of composites on the base of univalent cuprous chalcogenides. Cuprous tellurides and selenides were taken as initial salts since they possess properties which suggest mixed conductivity.

Physico-chemical properties of binary and ternary systems of general compositions $(Cu_{2-x}Te)_a(Ag_4P_2O_7)_b$; $(Cu_2S)_a(Cu_{2-x}Te)_b(Ag_4P_2O_7)_c$; $(Cu_{2-x}Te)_a(Na_4P_2O_7)_b$; $(Cu_{2-x}Se)_a(Ag_4P_2O_7)_b$; and $(Cu_{2-x}Se)_a(Na_4P_2O_7)_b$ have been studied.

In an attempt to obtain electrode materials having high electronic conductivity with a marked ion conductivity, we introduced a stabilizing phosphate ion into the lattice of nonstoichiometric cuprous chalcogenide. But since cuprous phosphates decompose long before the initial salts start to melt, we had to use sodium and silver phosphates as a carrier of the phosphate groups.

For the materials being synthesized, the total, electronic and ionic conductivities, was being defined as well as cumulative and electrolytic capacities, structure and other parameters. At the same time, by means of solid-phase coulometric titration, we evaluated the maximum concentration of copper which can electrochemically dissolve in the material.

In making electrochemical measurements, $RbCu_2Cl_3$ and $RbCu_{1.75}Cl_{3.25}$, whose synthesis was effected according to the techniques described in the literature, were used as solid electrolytes.

The research done allowed a number of composites to be chosen as optimal electrode materials. In using such types of electrodes, an electrochemical cell permitted multiple cycling.

OXYGEN DIFFUSIVITY IN Mo-MoO₂ REFERENCE ELECTRODE OF OXYGEN PROBE FROM
ELECTROCHEMICAL MEASUREMENTS²

Wang Nanmeng
Shanghai Metallurgical Instruments
and Measurements Factory
China

The oxygen diffusivity in a Mo-MoO₂ reference mixture of oxygen probe was measured by an electrochemical method, at 1600°C to be: $D_0 = 7.08 (-2.80) \times 10^{-4} \text{ cm}^2/\text{s}$. Comparing the values of D_0^{Mo} obtained here with the values of D_0^{Fe} and the oxygen diffusivity in steel melt reported in the literature, we found that D_0^{Mo} is as 3-5 times as D_0^{Fe} . This indicates that oxygen diffusion in molten steel is the main rate-controlling step in the kinetic processes of oxygen cells.

ESR STUDY OF COLOR CENTERS IN YTTRIA STABILIZED ZIRCONIA

J. Shinar, D.S. Tannhauser, Department of Physics
and

B.L. Silver, Department of Chemistry
Technion, Israel Institute of Technology, Haifa, Israel

Single crystals of yttria stabilized zirconia with a composition $\text{Zr}_{0.84}\text{Y}_{0.16}\text{O}_{1.92}$, grown by skull melting, were colored by reduction to equilibrium at 1100°C in a flowing atmosphere of 15% H₂ in N₂. An ESR signal, which disappeared on reoxydation, was detected in the colored crystals at room temperature. The concentration of spins in the sample ($3 \times 10^{17} \text{ cm}^{-3}$) agrees with other measurements⁽¹⁾ of electron concentration in reduced samples.

The g-tensor was determined with the use of a sample of DPPH as standard, the same sample served to calibrate the strength of the signal in number of spins. The spectrum could be accounted for completely in terms of a single type of paramagnetic center having four possible orientations in the crystal. The g-tensor of the center is axially symmetric and has principal values of 1.86 and 1.95. The unique axis is aligned along the <111> direction in the crystal. The linewidth of the signal varies from ~33 gauss for the magnetic field along the axis associated with the high g-value, to ~65 gauss for the low g-value plane.

The results can be rationalized in terms of an electron trapped at an oxygen vacancy adjacent to an yttrium ion. The nearest neighbors of the vacancy are four tetrahedrally arranged cations, which will therefore include one yttrium and normally three zirconium ions. Such a center will have axial symmetry, as observed. Since the abundance of Zr⁹¹ is only 11%, the dominant contribution to the ESR line will be given by centers not containing any Zr ions with a magnetic nucleus. The ESR lines from these centers will be inhomogeneously broadened by the hyperfine interaction with Y⁸⁹. The anisotropic nature of this interaction should result in a g-dependent linewidth which varies by a factor of two as indeed observed within experimental error. We observed only one type of center, in contrast to at least three types observed in crystals reduced electrolytically.⁽²⁾

References:

1. W. Weppner, Z. Naturforsch. 31a, 1336 (1976).
2. J.S. Thorpe, A. Aypar and J.S. Ross, J. Mat. Science, 7, 729 (1972).

STRUCTURAL STUDIES ON ZrO_2 - Y_2O_3 SYSTEM BY ELECTRON DIFFRACTION AND ELECTRON MICROSCOPY

S. Suzuki, M. Ishigame* and M. Tanaka

Department of Physics, Faculty of Science, Tohoku University, Sendai 980, Japan

*Research Institute for Scientific Measurements, Tohoku University, Sendai 980, Japan

The oxygen-ion arrangements in the f.c.c. phase of 10-50 mol% Y_2O_3 - ZrO_2 have been investigated by electron diffraction and high-resolution electron microscopy. One of the authors (M.I.) made bulk single crystals by melting the mixture of ZrO_2 and Y_2O_3 powder using the solar furnace of Tohoku University.

The diffuse scattering has been observed in the electron diffraction patterns and is sorted into three types, or 10, 20-30 and 40-50 mol% Y_2O_3 types. By analysing the diffuse scattering, we have determined these crystal structures, which are characterized by the specific displacements of oxygen-ions. The structure of 10 mol% Y_2O_3 obtained in this study is completely the same as that obtained by Faber et al.¹⁾. The structure of 20-30 mol% has been found to be the modulated structure which has the wave number of the modulation $\bar{q}=\pi/a_0[111]$ and is accompanied by periodic anti-phase domain boundaries, where a_0 is the lattice constant of the f.c.c. ZrO_2 . The structure of 40-50 mol% has been revealed as a random mixture of two modulated structures whose wave number vectors are $\bar{q}=\pi/a_0[1\bar{1}0]$ and $\bar{q}=2\pi/a_0[110]$. The high-resolution electron microscopic images for the structures of 20-50 mol% have been interpreted consistently by the above results obtained by electron diffraction. The structures of 20-50 mol% did not develop to any ordered states. We can say that each observed state is a kind of glassy state. It is emphasized that these modulated structures have been found in the phase which has been believed to be a single f.c.c. phase until now. The characteristic changes of the oxygen ion displacements from pure ZrO_2 to pure Y_2O_3 can be clarified systematically by describing the displacements in terms of the molecular- and lattice-vibrational modes. The ionic conductivity in this system reaches to the maximum at about 10 mol% Y_2O_3 , although the apparent vacancy concentration increases as the amount of Y_2O_3 increases. This fact is readily expected from the present experiments. That is, the modulated structures are formed and the vacancies available for ionic-conduction are decreased, when the amount of Y_2O_3 is beyond 10 mol%.

1) J. Faber et al.: Phys. Rev. **B17** (1978) 4884. β -NMR STUDIES OF IONIC MOTIONS IN LAYERED AND GLASSY COMPOUNDS

Paul Heitjans

Fachbereich Physik, Universität Marburg, Renthof 5, 3550 Marburg, W.-Germany

The method of β -radiation detected nuclear magnetic resonance (β -NMR) is introduced and its features and capabilities as a new tool for the study of ionic motions on a microscopic scale are discussed, partly in comparison with conventional NMR. Information on atom dynamics is obtained from spin-lattice relaxation rates and resonance spectra of isolated β -active nuclei embedded in the sample. The polarized probe nuclei are produced in situ by irradiating the sample with polarized thermal neutrons. The nuclear polarization is monitored via the anisotropy of the β -radiation. Recent applications to the field of solid state ionics are reviewed. As examples of β -NMR on solids with a layer structure measurements on the intercalation compound LiC_6 and the ionic conductor Li_3N are discussed. Emphasis is on the questions of anisotropic and low-dimensional diffusion. As representatives of strongly disordered solids we deal with lithium borate and silicate glasses. By spin-relaxation measurements over wide temperature and magnetic field ranges different modes of ionic motion were found. We discuss in particular the low-temperature data which can be explained by inhomogeneous relaxation of the isolated nuclear spins via defect centres typical of glasses. Comparison with results from conventional NMR yields additional information on the defect centres.

NEUTRON DIFFRACTION AND TSDC ON $Ba_{1-x}U_xF_{2+2x}$ SOLID ELECTROLYTES

M.Ouwerkerk, N.H.Andersen*, F.F.Veldkamp, J.Schoonman[†]
 Solid State Department *Risø National Laboratory
 Utrecht University P.O.Box 49
 P.O.Box 80.000 DK-4000 Roskilde
 3508 TA Utrecht Denmark
 The Netherlands

[†]present address: Laboratory of Inorganic and Physical
 Chemistry
 Delft University of Technology
 P.O.Box 5045
 2600 GA Delft, The Netherlands

ABSTRACT

The defect structure of $Ba_{1-x}U_xF_{2+2x}$ solid solutions ($x < 0.17$) which exhibit fast fluoride ion conductivity has been investigated by neutron diffraction, Thermally Stimulated Depolarization Current (TSDC) measurements, and a novel technique comprising neutron diffraction on a polarized solid solution.

The diffraction pattern was scanned in the X00/OYY plane, and fitted to computed diffraction patterns of defect clusters. It appeared that the major fraction of the UF_4 content is present in (212) clusters comprising one dopant ion, four fluoride interstitials, and two fluoride ion vacancies. They do not form larger aggregates at high solute levels like the reported cluster aggregation in $Ba_{1-x}La_xF_{2+x}(1)$.

The TSDC spectra of $Ba_{1-x}U_xF_{2+2x}$ ($x < 0.05$) reveal six relaxation peaks with concentration invariant positions, but concentration dependent magnitudes. A space charge peak related to ionic conductivity decreased over 200 degrees with increasing solute content. Migration enthalpies derived from the space charge peaks compare very well with conductivity activation enthalpies.

The six dipolar relaxations can be related with the possible reorientations of a polarized (212) cluster. A direct indication of its freedom of orientation is obtained from neutron diffraction experiments at liquid helium temperature on a polarized $Ba_{0.95}U_{0.05}F_{2.10}$ crystal. This novel approach in the study of defect clusters revealed a significant change in the diffraction pattern due to a polarized state of the (212) cluster.

The results of the present study will be related to the composition dependence of the ionic conductivity of the $Ba_{1-x}U_xF_{2+2x}$ solid electrolytes.

1. J.K.Kjems, N.H.Andersen, J.Schoonman, K.Clausen: Physica 120B, 357 (1983)

NEUTRON POWDER DIFFRACTION STUDY OF THE STRUCTURE OF THE COMPOUND



E. LUKACEVIC, A. SANTORO, and R. S. ROTH
 National Bureau of Standards, Gaithersburg, MD 20899

The structure of the title compound has been analyzed by neutron powder diffraction techniques and by the Rietveld method. The material crystallizes with the symmetry of space group $I4_1/a$. The lattice parameters are $a = 5.335$, $c = 11.579$ Å. The framework structure is of sheelite type. The La^{3+} ions are statistically distributed on the sites 4b. The Mo^{6+} ions fully occupy sites 4a and the O^{2-} ions sites 16f with $x = .1413$, $y = .0116$, $z = .2074$. The R-factors at this stage of refinement are $R_N = 6.52$, $R_p = 6.27$, $R_w = 8.01$ and the expected value is $R_E = 4.46$. There are several possible locations for the Li^+ ions. A likely position would be site 8e with $z \approx 3/8$. In this configuration the Li^+ ions would be placed halfway, along the b-axis, between the Mo^{6+} and the La^{3+} cations. So far, however, attempts to locate these ions have been unsuccessful and refinements of the structure seem to be peculiarly insensitive to the Li^+ positions.

STRUCTURAL STUDY OF $\text{AgI:Ag}_2\text{O:B}_2\text{O}_3$ GLASSES
BY EXAFS SPECTROSCOPY

G. DALBA[†], A. FONTANA[†], P. FORNASINI[†], F. ROCCA[‡]

[†] Dipartimento di Fisica, Università di Trento, 38050 POVO TN, ITALY
[‡] Centro di Fisica degli stati aggregati ed impianto ionico del CNR,
38050 POVO TN, ITALY

EXAFS spectroscopy is a powerful tool for the investigation of the short range order in amorphous materials. In particular for multicomponent systems EXAFS, due to its selectivity, can give direct information on the coordination of single atomic species.

The structural study of the fast ion conducting glasses $\text{AgI:Ag}_2\text{O:B}_2\text{O}_3$ by EXAFS is in progress since two years.

Our attention was firstly dedicated to the binary matrix $\text{Ag}_2\text{O:B}_2\text{O}_3$ at different relative concentrations of the components. The coordination of silver ions has been determined . (1,2)

In this work we present structural results concerning the ternary glasses $\text{AgI:Ag}_2\text{O:B}_2\text{O}_3$. EXAFS measurements have been performed at the L_3 and K edge of silver and at the L_3 edge of iodine for various relative concentrations of the components.

The EXAFS at the L_3 edge of iodine shows a first coordination shell strikingly similar to that of $\beta\text{-AgI}$ for all the glasses considered. This means that each iodine ion is surrounded by four silver ions at a distance of about 2.8 Å. This similarity lacks beyond the first shell, the glasses being characterized by a more disordered situation. A more accurate analysis is in progress to study the slight variations of interatomic distances and Debye-Waller factors for the first shell as a function of concentration, and to verify the possible existence of a second shell due to iodine-iodine distances.

The EXAFS study is completed by the analysis of the edges of silver. This analysis discriminates the two possible first shell coordinations of silver: Ag-O and Ag-I , and will allow to determine interatomic distances and coordination numbers for the Ag-I bonds.

Final aim of the EXAFS analysis is to give a precise picture of the bonds of the silver ions on the one hand with the borate network, on the other with the iodine ions. This should contribute to understand whether all silver ions contribute to the ionic conduction in the same way or the silver ions bonded to iodine play a predominant role.

(1) E. Bernieri et al., Sol. St. Comm. 48, 421 (1983)

(2) G. Dalba et al., to be published

INVESTIGATION ON ION TRANSPORT IN SOLIDS USING ELECTRON MICROPROBE

Chu-Kun Kuo and Xian Ting Li
Shanghai Institute of Ceramics
Chinese Academy of Sciences
865 Chang-ning Road
Shanghai 200050
China

Electron microprobe X-ray analysis (EPMA) studies have been conducted of ion conductive solids of various electrical conductivities. Electron bombardment during EPMA can create a negative potential which induces ions to migrate and excite X-ray photons for in situ analysis of the concentration of both mobile and immobile ion components.

1. Ionic crystals of negligible conductivity

In this group of solid charge transfer generally comes from thermally activated point defects. Very low content carrier at low-moderate temperatures makes the mobile ions or vacancies concentrating and deconcentrating appreciably. Stable EPMA curves were obtained for the normal chloride and oxide single or polycrystals.

2. Solids of low ion conductivity

The instability of EPMA counts was observed on alkali-containing glasses and minerals some years ago. Decrease in Na X-ray counts against bombarding time has been reproduced here for the silicate glass and crystalline materials. The fall of EPMA curve is dependent upon the probe beam diameter as well as the beam current.

3. Fast ion solids

The Na and Ag X-ray counts of the sodium and silver ion conductors of high conductivity increase with the EPMA time. In most cases the curves are characteristic of more or less steep rise in counting rate and a followed plateau. Decrease in the concentration of immobile components also occurs accompanying with the accumulation of mobile ions.

4. Ion transport mechanism

The composition changes induced by EPMA can be fitted by using the ion transport equation with a source of diminished carrier concentration. Good agreement has been reached among the observed and calculated X-ray counts for both the sodium and silver ion conductors. The decreasing EPMA counting rate of some poorly conductive solids may be tentatively accounted for by ion transportation followed by charge neutralization and metal vaporization processes.

ANION DISORDER AND ITS RESULTING IONIC CONDUCTIVITY OF $\beta\text{-Pb}_{1-x}\text{Bi}_x\text{F}_{2+x}$ ($x \leq 0.30$) and $\beta\text{-Pb}_{1-x}\text{Y}_x\text{F}_{2+x}$ ($x \leq 0.20$) SINGLE CRYSTALS

Yoshiaki Ito and Kichiro Koto
Institute of Scientific and Industrial Research, Osaka University,
Mihogaoka 8-1, Ibaraki, Osaka, 567 Japan

Shinzo Yoshikado and Tadashi Ohachi
Department of Electronics, Doshisha University, Kyoto, 602 Japan

It has been found by many workers that the ionic conductivity of $\beta\text{-PbF}_2$ can be increased by both monovalent (Liang and Joshi, 1976, Bonne and Schoonman, 1977) and trivalent (Lucat et al., 1976 and 1980, Reau et al., 1983) cation dopants in the extrinsic region. Reau et al. (1983) investigated the influence of polarizability of the trivalent cations on ionic conduction. Their results did not give any suggestion on the ionic conduction of anion excess $\beta\text{-PbF}_2$. All the above works and structure studies (Lucat et al., 1980) were carried out using powder samples. In this work using single crystals, we studied the crystal structures of $\beta\text{-PbF}_2\text{-BiF}_3$ and $\beta\text{-PbF}_2\text{-YF}_3$ solid solutions and the effect of the high concentrations of trivalent cations (Bi and Y) in $\beta\text{-PbF}_2$ on the ionic conductivity.

$\alpha\text{-PbF}_2$ (99.9%, Merck), BiF_3 (low temperature form, ultrapure, Alfa) and YF_3 (99.9%, Alfa) in powder form were used without further purification. The solid solutions were prepared by melting well-blended mixtures of appropriate amount of PbF_2 and MF_3 (M = Bi and Y) in the nitrogen atmosphere. An amount of 1000 mg for each sample was sealed in an Au capsule under nitrogen gas. The sealed sample in the capsule was heated at temperature above the melting point of $\beta\text{-PbF}_2$ for 30 min in an electric furnace. The sample was then quenched from high temperatures to room temperature.

The intensity data collection of the Bragg reflections was made using a four circle diffractometer at room temperature. $\text{Mo K}\alpha$ (60 kV, 200 mA) was monochromatized by pyrolytic graphite. Symmetry-independent about $80(|\text{Fo}| > 3\sigma(|\text{Fo}|))$ reflections within $2\theta < 100^\circ$ were obtained by averaging the equivalent reflections in an octant in reciprocal space. The structure refinements were carried out by the least-squares and Fourier synthesis methods. The scale factor and independent temperature factors of Pb(M) and F ions were refined and then the difference Fourier syntheses were calculated with the structure factor of only Pb(M) ions. The electron density distribution around F ions thus obtained shows anharmonicity and the existence of the interstitial positions. However, the aspects of the distribution of the interstitial sites are apparently different for $\beta\text{-PbF}_2\text{-BiF}_3$ and $\beta\text{-PbF}_2\text{-YF}_3$ solid solutions.

The measurements of the ionic conductivity on single crystals were carried out in the temperature range from 240 to 370 K. The measurements of the complex conductivity were made from 10 Hz to 10 MHz with a HP 4192A LF impedance analyzer in an atmosphere of dry nitrogen gas. The frequency-independent part of real part of the complex conductivity has been considered as an ionic conductivity concerned with fluorine ions. The value of ionic conductivity at any temperature for $\beta\text{-PbF}_2\text{-BiF}_3$ solid solution has the maximum value at 20 m/o BiF_3 and the activation energy has the minimum one at the same value which contrast with the results which were reported to be at 25 m/o BiF_3 by Lucat et al. (1976). However, that for $\beta\text{-PbF}_2\text{-YF}_3$ solid solution has neither the maximum value for the ionic conductivity nor the minimum one for the activation energy which are similar to the results using powder samples (Reau et al., 1983).

AN EXAFS STUDY OF ABF_2 FLUORITE-RELATED ANION CONDUCTORS

C.R.A. Catlow,¹ A.V. Chadwick,² G.N. Greaves¹ and L.M. Moroney¹

¹Department of Chemistry, University College London,
20 Gordon Street, London WC1H 0AJ.

²Department of Chemistry, University of Kent at Canterbury,
Canterbury, Kent CT2 7NH.

³Science and Engineering Research Council, Daresbury Laboratory,
Daresbury, Warrington WA4 4AD.

Analysis of the extended X-ray absorption fine structure (EXAFS) observed on the high-energy side of the X-ray absorption edges yields information about the local structural environment of the absorber atom type. It is possible with this technique to study short range structural ordering about different specific atom types within one sample. We have applied the technique to the fluorite phase of the anion conductor RbBiF_4 , which has an exceptionally high fluoride ion conductivity ($5 \times 10^{-2} \text{ ohm}^{-1}\text{cm}^{-1}$ at 100°C [1]). Our work reveals marked differences in the Rb and Bi environments over a range of temperatures. This effect could not be detected using diffraction techniques which yield the average cation environment only. In the case of the Bi L(III) EXAFS, there was a negligible change in amplitude and frequency of the EXAFS over the temperature range 80 K to 473 K. The Rb K edge EXAFS showed a marked decrease in frequency and amplitude over the same temperature range. This effect was attributed to a preferential stabilisation of F vacancies at sites rich in Rb nearest neighbours. The stabilisation is thought to involve significant relaxations of ions around the vacancy resulting in an increase in the asymmetry of Rb-F distances which would lead to the observed changes in amplitude and frequency of the EXAFS. This suggests that the electrostatic advantages conferred by vacancy formation adjacent to the monovalent cation outweigh the potential vacancy stabilisation offered by delocalisation of the Bi³⁺ lone electron pair. To explore the role of polarisability and charge of the two cations in these compounds further, we have measured the EXAFS over a range of temperatures for the related compound, PbSnF_6 . In addition to these data, we have obtained EXAFS information for RbReF_6 compounds where Re is a trivalent rare earth ion. The results of computer simulation predictions of relaxations of ions in response to the formation of vacancies at anion sites with differing ratios of the two cation types in the nearest-neighbour shells will also be presented.

[1] S.F. Matar, J.M. Reau, C. Lucat, J. Grannec and P. Hagenmuller, Mater. Res. Bull., **15**, (1980), 1295-1301.

CONDUCTIVITY OF Gd-DOPED NaYF_4

K. Narasimha Reddy
Physics Department
Osmania University
Hyderabad 500 007
India

Solids of different types have been used as solid electrolytes. NaYF_4 is such a solid now investigated from various points of view to yield valuable information about its transport properties. NaYF_4 -type of solids have structure isomorphous with CaF_2 in which Ca ions are replaced randomly by Na and Y ions. In such a system, no studies have been done so far to understand the dynamic behaviour of mobile fluoride ions and yttrium ions at high temperatures. The conductivity of NaYF_4 pellets doped with different compositions of gadolinium, $x = 0.01, 0.03, 0.05, 0.10$ and 0.15 , was measured at several temperatures over the range of 25 to 500°C . It is found from these measurements that with increasing x , the conductivity increases and passes through a maximum at $x = 0.05$ at 300°C . The solid material is thermodynamically stable and can be prepared easily. These results are explained on the basis of thermal ionization of impurity and imperfections.

103

Revised Subsolidus Phase Diagram of the System SrF_2 - LaF_3

Masahiro YOSHIMURA, Kwang Jin KIM, Shigeoyuki SŌMIYA

The solubility in the system SrF_2 - LaF_3 were studied by solid state reaction ($1400, 1300, 1000$ and 750°C) using Pt capsule and hydrothermal reaction ($750, 650$ and 500°C) using the 10wt% LiCl or other solutions. Starting samples were (1) mixed and (2) fired samples of SrF_2 and LaF_3 powders (99.9%). At any temperatures, a linear relation between the compositions and the lattice parameters of the solid solutions of each phase (SrF_2 s.s. or LaF_3 s.s.) could be obtained corresponding to the Vegard's law. The solubility limits in SrF_2 ss were 48, 48, 47, 47 and 46 mol% LaF_3 , and those in LaF_3 ss were 15, 10, 6, 4 and 2 mol% SrF_2 (all deviation ; ± 1 mol%) at $1400, 1000, 750, 650$ and 500°C respectively by X-ray measurements.

Res. Lab. Eng. Mater., and Dept. Mater. Sci., Tokyo Inst. Technology
4259, Nagatsuta, Midori, Yokohama, 227 Japan.

The Electrochemical Insertion of Lithium Into Bleached Potassium Hexatungstate Thin Films: A New Electrochromic Material

S-K Joo, I.D. Raistrick and R.A. Huggins

Dept. of Materials Science and Engineering
Stanford University
Stanford, CA 94305

The potential use of $K_{0.3}WO_{3.15}$ thin films as a lithium-based electrochromic display materials has been studied. The chemical diffusion coefficient of lithium in thin films of this material prepared by thermal vacuum evaporation and bleached by oxidation has been measured as a function of lithium concentration using the galvanostatic transient technique. Chemical diffusion coefficients as high as 10^{-10} cm²/sec at room temperature were obtained in preferentially oriented thin films. No degradation was observed after over 1000 deep cycles using constant voltage pulses.

104

SOLID ELECTROCHROMIC SYSTEM BASED ON
TUNGSTEN OXIDE AND NICKEL HYDROXIDE

A.R.LUSIS, E.V.PENTYUSH, V.V.BETS, J.A.BENDERS, G.E.BAJARS
Institute of Solid State Physics, Latvian State University,
8 Kengaraga Street, Riga, 226063, USSR.

The most deeply and widely studied solid electrochromic system today is the Deb's thin films system ($SnO_2/WO_3/SiO_2/Au$). Protons and electrons for coloration-bleaching process in the WO_3 are supplied by electrolysis of water adsorbed from atmosphere at the Au/SiO_x interface [1]. The water adsorption and evolution of gases on the top electrode Au leads to extra energy losses, increase of response time and decrease of stability of the system. A system with cathodic and anodic electrochromic materials has to be without these shortcomings [2].

We have investigated the system ITO/ $WO_3/SiO_2/Ni(OH)_2/Me$, where Me stands for different metals. The electrochromic behaviour of $Ni(OH)_2$ has been simulated in other systems with solid or liquid electrolytes. The electrophysical properties of the system have been determined and interpreted on the basis of data of voltammetric, coulometric and optical measurements. It has been shown that the values of differential electrochromic efficiency depends on the applied voltage and charge. At small voltages it is determined by the recharge of electrode capacities, but at high voltages ($\pm 2V$) by the evolution of O_2 and H_2 . The electrode Me does not take part in the electrochemical reactions involving protons for coloration process as it is in the Deb's system. The rate of the coloration-bleaching process is determined mainly by the velocity of the proton transport through the SiO_2 layer from one electrochromic layer to the other.

1. A.R.Lusis, J.J.Kleperis, A.A.Brishka, E.V.Pentyush, Solid State Ionics, 13, 219 (1984).
2. J.L.Lagzdons, G.E.Bajars, A.R.Lusis, Phys.stat.sol.(a), 84, K 197 (1984).

MODEL FOR THE INTERFACIAL IMPEDANCE
BETWEEN A SOLID ELECTROLYTE AND A METAL ELECTRODE¹

J. C. Wang and J. B. Bates
Solid State Division, Oak Ridge National Laboratory
Oak Ridge, Tennessee 37831

The interfacial impedance between a solid electrolyte and a metal blocking electrode can often be described by the form

$$Z(\omega) = A(j\omega)^{-n} \quad (1)$$

over several orders of frequencies,² where A is independent of frequency ω and $j = \sqrt{-1}$. The value of n usually lies between that for a pure capacitor ($n=1$) and that for a Warburg impedance ($n=1/2$). In this paper we present a model to relate the impedance shown in Eq. (1) to the roughness of the interface.

The roughness of the interface is modeled by pores on the electrode, and the impedance of a pore is approximated with a transmission line with distributed resistance and capacitance per unit length, $r(x)$ and $c(x)$. When both r and c are constant, the impedance of the transmission line becomes that of a Warburg ($n=1/2$). This corresponds to a pore in form of a long channel which has been used by De Levie to model a porous electrode.³ We have generalized the Warburg impedance to values of n other than $1/2$ by deriving several pairs of $r(x)$ and $c(x)$ that give the impedance in the form of Eq. (1). For example, if $r(x) = \exp(ax)$ and $c(x) = \exp(bx)$, then $n = a/(a+b)$. If $r(x) = (c+x)^a$ and $c(x) = (c+x)^b$ with c being a small constant, then $n = (a+1)/(a-b+2)$. This means that if pores with these $r(x)$ and $c(x)$ exist, they will behave according to Eq. (1).

Pairs of $r(x)$ and $c(x)$ for pores of various shapes and sizes have been calculated. It is assumed that the material inside the pores has the same conductivity as that of the electrolyte and that $c(x)$ is mainly determined by the double layer capacitance at the metal surface inside the pores. The results demonstrate that some of the pores have an impedance close to the form of Eq. (1) over wide frequency ranges and that pores with diameters of several microns are relevant to impedance measurements over frequencies of interest.

In general, an interface may contain many pores with various values of n . When they are put in parallel, it can be demonstrated that the resultant impedance can be described roughly by Eq. (1) with some effective value of n , \bar{n} . The value of \bar{n} is controlled by pores with large n at low temperatures. This can quantitatively explain the experimental result that \bar{n} decreases with increasing temperatures.²

¹Research sponsored by the Division of Materials Science, U.S. Department of Energy under contract DE-AC05-84OR21400 with Martin Marietta Energy Systems, Inc.

²J. B. Bates and J. C. Wang, "Impedance of Metal-Solid Electrolyte Interfaces," this conference.

³R. De Levie, *Electrochim. Acta* **8**, 751 (1963).

TRACER DIFFUSION IN A ONE-DIMENSIONAL LATTICE GAS IN THE
PRESENCE OF A DRIFT FORCE

R. Kutner: Institute of Experimental Physics, University of
Warsaw, Hoża 69, 00-681 Warszawa, Poland

H. van Beijeren: Institut für Theoretische Physik A, Rheinisch-
Westfälische Technische Hochschule, D-5100 Aachen,
West Germany

The influence of an external constant drift force on tracer particle diffusion in a one-dimensional lattice gas is investigated analytically as well as numerically by Monte-Carlo simulations, very good agreement being obtained between both independent approaches. The lattice gas model consists of particles of arbitrary concentration which interact only like repelling hard point cores. The particles can jump stochastically to unoccupied neighboring sites with different jump rates in and against the direction of the drift force, respectively.

A theory for the dispersion / i.e. mean-square displacement of a tracer particle with respect to its average drift / as a function of time [1] is developed by a direct extension of the method given in Ref. 2. The dispersion is shown to behave diffusively for large times, in contrast to the case where no external force is present.

References

1. R. Kutner and H. van Beijeren, *J. Stat. Phys.*, to appear.
2. H. van Beijeren, K.W. Kehr and R. Kutner, *Phys. Rev.* **B28**, 5711/ 1983/.

SIMULATION OF FRACTALS OBJECTS OBTAINED
BY INTERCALATION IN LAYERED COMPOUNDS

B. SAPOVAL, M. ROSSO and J.F. GOUYET
Laboratoire de Physique de la Matière Condensée
Ecole Polytechnique
91128 PALAISEAU CEDEX FRANCE

A computer simulation of the diffusion of ions on a 2D lattice is presented. It is obtained in the case of hardcore interaction with first nearest neighbor. After a given time the line separating the diffusion source from isolated intercalated clusters is a fractal object with fractal dimension $D = 1.76 \pm 0.02$. (see Fig. 1). Discussion of this problem in connection with percolation theory predicts $D = 7/4$.

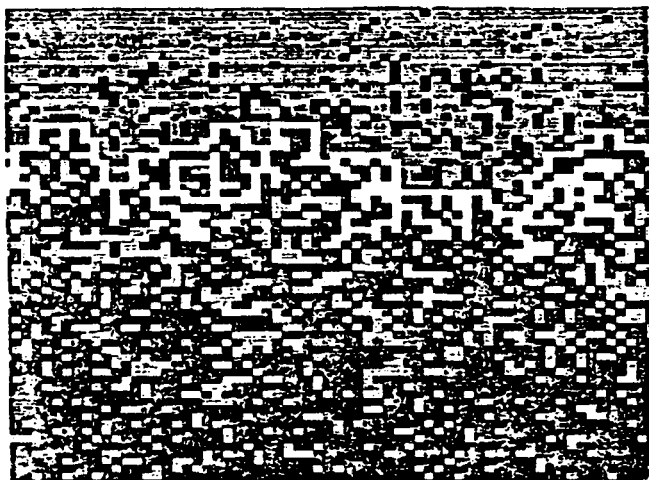


Figure 1. Fractal diffusion front: ions are represented by a square here grey or white. They are diffusing from the top of the figure on a 2D square lattice. The concentration at the diffusion source is kept constant, equal to one. The empty sites are black. The diffusion front is made of those ions which are connected to the diffusion source via first neighbors and which are near an empty site connected to the empty lattice. It is shown as the white line. This is a fractal object.

UNDERDAMPED SYSTEMS AND LATTICE GAS MODELS

T. GOBRON and J.F. GOUYET

Laboratoire de Physique de la Matière Condensée,
Ecole Polytechnique, 91128 Palaiseau, France

The generalization of lattice gas models to Kramers regimes⁽¹⁾ has been considered on one hand in the case of dilute systems for which a Boltzmann equation has been derived which put on clear physical basis the model proposed in 1972 by Rice and Roth⁽²⁾ for ionic transport in superionic conductors. On the other hand for systems with a large density of mobile particles a model of elastic collisions is considered, for which some interesting results can be obtained.

(1) Y. Boughaleb and J.F. Gouyet, *Solid State Ionics* 2 & 10, 1401 (1983).

(2) M.J. Rice and W.L. Roth, *J. Solid State Chem.* 4, 294 (1972).

SIMULATION OF THE INTERGRANULAR IMPEDANCE
OF SODIUM ION CONDUCTIVE CERAMICS

Kuo CHU-KUN and YAN YI-MIN

Shanghai Institute of Ceramics, Chinese Academy of Sciences,
865 Chang-ning Road, Shanghai 200050, China

Observations on Na⁺ fast ion polycrystals usually give complex impedance diagrams showing non-ideality, where the intergranular component impedance degrades to an arc with its center below the real axis. The non-ideal intergranular impedance can be interpreted by a model of distribution of ion conductivity relaxation times. The equivalent circuit involved here is composed of a series of parallel RC pairs. The composite intercrystalline impedance therefrom is expressed as follows:

$$Z^* = \text{Re}(Z) + i\text{Im}(Z) = \sum_k \frac{R_k}{1 + i\omega C_k R_k}$$

where R_k and C_k represent the resistance and capacitance of k th component. When neglecting the variation of the capacitance and inserting an one dimensional probability function into the impedance formalism, we obtain

$$Z^* = \text{Re}(Z) + i\text{Im}(Z) = \sum_x \frac{x f(x)}{1 + i\omega C x}$$

where x is resistance variable and $f(x)$ is a specified probability function. Simulation and fitting computations have been performed on given probability functions.

Examples presented concern the Nasicon and Beta alumina ceramics. The distributive pattern of the intergranular impedance is assumed to be associated with the varying of the concentration of the mobile ions.

INTERFACE RESISTANCE IN A HOPPING MODEL

R. Blender and W. Dieterich

Fakultät für Physik, University of Konstanz, 7750 Konstanz, F.R.G.

Diffusion across the interface between two solid ionic conductors is a problem of great practical importance. The properties of hopping models in the presence of an interface, however, have not been studied sufficiently in the past, despite of their success in describing transport properties of bulk ionic conductors. Here we consider the simplest case of a many-particle hopping model with exclusion of multiply occupied sites. Our aim is to relate the interface resistance to the parameters of two specific barrier models. In the first case the hopping rates in a plane boundary are modified as compared to the bulk. The frequency-dependent conductivity is obtained exactly. Secondly, we assume that the boundary leads to modified site energies. The main difference to the previous case are the nontrivial correlations which appear in the current-carrying steady state. This point as well as the current-voltage characteristics are examined by Monte Carlo studies.

**LOCALIZATION VERSUS DELOCALIZATION OF ORBITALS IN THE
QUASI-ONE-DIMENSIONAL CONDUCTOR $\text{Na}_{0.33}\text{V}_2\text{O}_5$**

by

Irina M. Curelaru

Department of Materials Science and Engineering

University of Utah, Salt Lake City, Utah 84112

and

Eero Suoninen

Department of Physical Sciences

University of Turku, 20500 Turku, Finland

The beta phase of the sodium vanadium oxide bronze $\text{Na}_{0.33}\text{V}_2\text{O}_5$ extends from $x=0.2$ to $x=0.4$. Well inside the stability range, at $x=0.33$, the electrical conductivity undergoes an abrupt change and the material becomes a quasi-one-dimensional conductor. We present a study of the electronic structure of $\text{Na}_{0.33}\text{V}_2\text{O}_5$ by x-ray photoelectron spectroscopy (XPS) and appearance potential spectroscopy (APS). While the difference between the Fermi level of the sample material (as determined by XPS) and the edge of the vanadium APS spectrum indicates strong final state many-body effects due to the localized character of the excited orbitals, the presence of a negative undershoot in the APS spectrum suggests a rather efficient screening (therefore an extended charge mobility) at the site of the excited atom. These apparently conflicting data support the idea of domain formation in the sodium vanadium oxide bronze $\text{Na}_{0.33}\text{V}_2\text{O}_5$.

FAST HALIDE ION CONDUCTING LEAD METAPHOSPHATE GLASSES -
A FAILED DIVALENT CATION CONDUCTOR

H. G. K. Sundar and C. A. Angell
Department of Chemistry
Purdue University
West Lafayette, Indiana 47907

ABSTRACT

Following the observation that Pb^{2+} cations may be highly mobile in $\beta-Al_2O_3$, we have explored the possibility that Pb^{2+} cations may also have a high mobility in appropriately chosen oxide glasses. Acting on the evidence that monovalent cation halides dispersed in metaphosphate glasses behave as if under isotropic tension, we conducted initial studies on $Pb(PO_3)_2-PbX_2$ glasses. These have wide glass-forming ranges--up to 80 mol% halide in the case of $PbBr_2$, except in the case of PbI_2 which could not be incorporated. Conductivities use exponentially with mole fraction of halide and reach $10^{-5} \Omega^{-1} cm^{-1}$ at $25^\circ C$ for $PbCl_2$ at $X_{PbCl_2} = 0.60$, the highest ambient temperature anionic conductivity on record. The conductivity is attributed to anions as the $PbCl_2$ glasses have higher conductivity at equal mole fraction than for $PbBr_2$ glasses. The pre-exponent is also larger for the $PbCl_2$ -containing glasses consistent with expectations for a simple "rattle-and drift" mechanism.

Ionic Conductivity, Raman and IR Spectra of $LiAlSiO_4$ Glass

A. Pechenik,* D. H. Whitmore, M. A. Ratner, S. Susman**

Departments of Materials Science and Engineering and Chemistry and
Materials Research Center, Northwestern University, Evanston, IL 60201

β -eucryptite and its glassy counterpart, $LiAlSiO_4$ glass, are good Li conductors at elevated temperatures ($>500^\circ C$). Studies of $LiAlSiO_4$ glass are reported here. The glass has been prepared by a high-temperature melting technique and characterized by density measurements, differential thermal analysis, and X-ray diffraction. It has been determined that the prepared glass contained less than 0.01 weight per cent of the crystalline phase, exhibited heterogeneous nucleation, and was of the same stoichiometry as that of its crystalline counterpart, β -eucryptite. The glassy material exhibits high values of ionic conductivity at elevated temperatures ($\sigma \sim 10^{-3} (\Omega cm)^{-1}$ at $500^\circ C$).

The structure of $LiAlSiO_4$ glass has been investigated using Raman and IR spectroscopy and the assignment of vibrational modes to observed bands in the Raman and IR spectra has been performed. We discuss Raman and IR spectra of $LiAlSiO_4$ glass in terms of the normal vibrational modes of SiO_4 and AlO_4 tetrahedra, strongly coupled through an intertetrahedral angle.

Based on the results of the experimental work, the following model for ionic transport in this material is proposed: The glassy network of SiO_4 and AlO_4 tetrahedra constitutes a disordered lattice of available sites for Li ion migration. There are two types of Li^+ sites on the lattice: sites which are close to SiO_4 tetrahedra and sites which are close to AlO_4 tetrahedra. The two sites are not energetically equivalent since it is expected that Li^+ sites which are close to AlO_4 tetrahedra should have stronger bonding energies than Li^+ sites which are close to SiO_4 tetrahedra. The two types of sites are randomly distributed in the matrix. We show that the Lowenstein rule is not satisfied for $LiAlSiO_4$ glass. Lithium ions occupy only one-half of the available sites and can migrate from one site to some nearest-neighbor unoccupied site by a hopping mechanism. The jumping frequency of Li^+ ions is found to be close to $\sim 6 \times 10^{12} sec^{-1}$ ($\sim 200 cm^{-1}$).

*Dow Chemical Corp., Midland, MI 48640

**Argonne National Labs., Argonne, IL 60439

ALL-HALIDE SUPERIONIC GLASSES

Changle Liu and C. A. Angell
 Department of Chemistry
 Purdue University
 West Lafayette, Indiana 47907

ABSTRACT

To date all the highest conducting Ag^+ and alkali cation glasses have involved admixture of a halide, usually the iodide, with some oxyanion salt of the same cation. In this paper we report cases where the oxyanion can be omitted. Instead a second cation is introduced to provide, together with a mixture of anions, the immobile quasi-lattice through which the mobile cations Ag^+ or Cu^+ can migrate. In these new systems conductivities at 25°C can reach record values. Glass transition temperatures are lower than for oxyanion-containing glasses of the same conductivity. Since they contain only heavy monovalent ions the far IR transparency of the new glasses is unprecedented. Near 20 mole% CsCl crystallization of the quenched glass to a transparent polycrystal, with an even higher 25°C conductivity, of 0.14 occurs. This phase shows C_p and E_A anomalies at -80°C like those in RbAg_4I_5 . It is metastable, however, and with further heating recrystallizes to a low-conducting form which is probably multiphase. This implies that the high conductivity of the glass is due to a local structural organization similar to that in the RbAg_4I_5 crystal.

ANELASTIC RELAXATIONS IN AgI-DOPED BOROPHOSPHATE GLASSES

G. Carini, M. Cutroni, M. Federico and G. Tripodo
 Istituto di Fisica Generale and Gruppo Nazionale di Struttura della
 Materia del C.N.R. - Mesina, Italy.

An ultrasonic study ($5 + 45$ Mhz) of the loss characteristics in glasses of the "quaternary" system $\text{AgI}:\text{Ag}_2\text{O}:\text{B}_2\text{O}_3:\text{P}_2\text{O}_5$ was carried out in the $77 + 400\text{K}$ temperature range.

The loss behaviour is characterized by a broad peak that shifts at higher temperatures with the frequency and by an f^n dependence in the high ($n \approx 2$) and low ($n \approx 0.7$) temperature tails of the peak. The height and the temperature location of the peak are respectively increasing and decreasing functions of the AgI content.

Thermally activated relaxations of Ag^+ ions, weakly bonded and mobile in the glassy network, are assumed to be the origin of the observed dissipative processes.

The experimental data were fitted by a Gaussian-like distribution of relaxation times and such an analysis permits us to obtain some parameters, connected with the microscopic arrangement of the mobile ions: the most probable activation energy E_m , the width of the distribution E_0 and the deformation potential B , expressing the coupling between the ultrasonic stress and the system. The behaviour of these parameters with the AgI content suggests interesting conclusions about the possible influence of the glass structure on the ionic dynamics.

THERMODYNAMIC APPROACH TO IONIC CONDUCTIVITY
ENHANCEMENT BY DISSOLVING HALIDE SALTS IN
INORGANIC GLASSES

A. KONE^{*} and J.L. SOUQUET

Laboratoire d'Energétique Electrochimie

ENSEEG Domaine Universitaire

BP 75, 38402 St Martin d'Hères - France

^{*}Laboratoire de Chimie Physique - Faculté des Sciences

04 BP 322, ABIDJAN 04 - Côte d'Ivoire

Numerous recent investigations have shown that halides may be dissolved in oxide or sulfide based glasses to increase ionic conductivity, of by several orders of magnitude. Interpretation of this behaviour on the basis of weak electrolyte theory leads to the assumption of large variations of the halide thermodynamic activity depending on its content in the glass. The authors show that it is possible to explain these variations by assuming that the halide salt-glass solutions behave as regular solution. The mixing enthalpies which may then be deduced from conductivity data are in the order of some kilocalories per mole, comparable to the usual mixing enthalpies for molten salts.

ELECTROCHEMICAL MEASUREMENT OF THE DIFFUSION COEFFICIENT
OF SILVER IN THIN FILMS OF $V_2O_5 - P_2O_5$ GLASS

L. JOURDAINE, M. BONNAT, J.L. SOUQUET

Laboratoire d'Energétique Electrochimie

ENSEEG Domaine Universitaire

BP 75, 38402 St Martin d'Hères - France

Thin films of $V_2O_5 - P_2O_5$ glasses were made by vacuum evaporation. These layers have a molar composition 45 $V_2O_5 - 55 P_2O_5$; their electronic conductivity at room temperature is about $10^{-7} \Omega^{-1} \text{cm}^{-1}$ ($E_0 = 0.43 \text{ eV}$).

An electrochemical cell with glassy solid electrolyte :

Ag/Ag conductive glass/thin film $V_2O_5 - P_2O_5$

was used to measure the diffusion coefficient of silver, D_{Ag} in these layers. The techniques used were potentiostatic intermittent titration and impedance spectroscopy at low frequency. Measurements at different temperatures lead to a value $D_{Ag} = D_0 \exp(-E_D/RT)$ where $D_0 = 0.55 \text{ cm}^2 \text{ s}^{-1}$ and $E_D = 0.88 \text{ eV}$. At room temperature, D_{Ag} is small and has an approximate value of $10^{-10} \text{ cm}^2 \text{ s}^{-1}$.

IONIC CONDUCTIVITY OSCILLATIONS IN SILVER - ARSENIC -
- SELENIUM - TELLURIUM CHALCOGENIDE GLASSES

Yu. G. Vlasov, E. A. Bychkov and B. L. Seleznev

Department of Chemistry, Leningrad
University, Leningrad 199164, USSR

Silver-containing chalcogenide glasses are convenient materials for investigation of the transport processes in amorphous solids. We have found earlier (1), that doping of silver ion conducting Ag-As-Se vitreous alloys by copper results in a sharp decrease of ionic conductivity and increase of hole conductivity. Glasses containing more than 5 at.% Cu are non-crystalline semiconductors. Solid electrolyte - semiconductor transition can be supposed in the case of Ag-As-Se-Te glassy alloys as well, because silver-arsenic-tellurium ternary glasses are p-type semiconductors (2). The investigation of transport properties of $Ag_{15}As_{42.5}Se_{42.5-x}Te_x$ glasses revealed, that vitreous alloys containing up to 20 at.% Te are mainly ionic conductors, their hole conductivity σ_p being from 1 to 50 % of the total conductivity, depending on tellurium concentration.

First tellurium additions (2-8.5 at.%) loosen the structure of the glass and cause the increase of ionic conductivity σ_i by 3-4 times. It has been found a non-monotonous σ_i alteration is stipulated by the change of silver ion mobility, and is connected with the change of excess volume of the glass. It should be pointed out, that for Cu-doped Ag-As-Se vitreous alloys some densification of the structure of the glasses and corresponding σ_i decrease were observed (1).

The lineary increase of $\log \sigma_p$ and the lineary decrease of activation energy with tellurium concentration growth have been found for semiconducting alloys ($x > 20$ at.% Te). The additive composition dependence of σ_p has been observed for the glasses investigated, in spite of σ_i oscillations.

(1) Yu.G.Vlasov and E.A.Bychkov, Solid State Ionics, 14 (1984).

(2) S.K.Novosyolov and V.L.Vaninov, Fiz.Khim.Stekla, 3 (1977) 181.

ON THE HETEROGENEOUS DOPING OF IONIC CONDUCTORS

Joachim Maier

Max-Planck-Institut für Festkörperforschung
Heisenbergstr.1,D-7000 Stuttgart 80, W.Germany

The method of enhancing the ionic conductivity of a matrix ionic conductor (Li-,Cu-,Ag-halides) (1-4) by admixtures of an insulating oxide (Al_2O_3 , SiO_2 , etc.) has been shown to be an interesting phenomenon of great scientific and technical importance. An analogous enhancement effect has been found in systems of two coexisting ionic conductors.

In the cases of ionic conductors where the necessary data are reliably available, the author has shown that the effect can be quantitatively understood by space charges if and only if the relevant contact processes are taken into account: surface interactions in the case of the system ionic conductor /insulator and distribution equilibria of the mobile ions in the case of two ionic conductors (4-6).

As the quantitative treatment shows and the activation energy in all other cases suggests, the oxide is able to stabilize the mobile cation by nucleophilic surface groups and to increase the concentration of vacancies in the space charge regions.

Experiments on AgCl, AgBr, CuCl and TlCl using pure and chemically modified oxides as second phases are discussed and experiments from the literature are taken into the discussion, too. Theoretical treatments of the space charge layer contribution are given for different cases (dispersions, thin films etc.) and consequences such as vacancy-interstitial-junctions are taken account of. Analogous mechanisms can be assumed to give rise to enhanced extrinsic conductance in many pure polycrystalline materials.

References:

1. C. C. Liang, J. Electrochem. Soc. 120 (1973) 1289
2. J. B. Wagner, Mater. Res. Bull. 15 (1980) 1691
3. K. Shahi, J. B. Wagner, J. Electrochem. Soc. 126 (1979) 1963
4. J. Maier, Ber. Bunsenges. Phys. Chem. 88 (1984) 1057
5. J. Maier, J. Phys. Chem. Solids, in press
6. J. Maier, Ber. Bunsenges. Phys. Chem., in press

SYNTHESIS OF AND TRANSPORT IN $\text{LaF}_3: \text{O}^{2-}$ AND Li_2SO_4

C S Sunandana
School of Physics,
University of Hyderabad
HYDERABAD 500 134 INDIA

From among the factors that influence efficient fast-ion conduction in solids viz..

- (1) structural-structures that provide for a metal like framework and a near-linear path for ion-movement;
- (2) microstructural-existence of grain boundaries with low activation barriers;
- (3) polymorphism-co-existence of more than one structural form - realized in solid solutions (eg. Li_4SiO_4 - Li_3PO_4 (1:1 (1));
- (4) thermodynamic - stabilization of metastable structures (either high temperature crystalline or amorphous forms) with appreciable quenched-in disorder (eg. $\text{Li}_{3.6}\text{Ce}_{0.6}\text{V}_{0.4}\text{O}_4$ (2)),

the first and the last deserve to be explored further in view of the new possibilities they offer.

Among the "frameworks", a rhombohedral structure with the conducting species positioned along the 3-fold axis results in a near-linear path for conduction. Furthermore, creation of anion vacancies or substitution of smaller anion/cation is expected to increase the conductivity. Another attractive possibility is to quench (from melt) a solid which exhibits a structural phase transformation at high temperatures, so that it is obtained at room temperature either in the glassy-phase or high temperature crystalline phase - the latter one being usually responsible for fast-ion conduction.

The above ideas are tested with the systems (1) $\text{LaF}_3: \text{La}_2\text{O}_3 (r_{\text{O}^{2-}} = r_{\text{F}^-})$ and (2) Li_2SO_4 - which exhibits a monoclinic to cubic transformation at 846K.

- (1) A Khorassani, G. Izquierdo & A.R. West, Mat. Res. Bull. 16 1561 (1981).
- (2) J. Kuwano & A.R. West, Mat. Res. Bull. 15 1661 (1980).

ENHANCEMENT OF IONIC CONDUCTIVITY OF SrCl_2 BY Al_2O_3 DISPERSION

Saturo FUJITSU, Kunihito KOUMOTO and Hiroaki YANAGIDA

Department of Industrial Chemistry,
Faculty of Engineering,
University of Tokyo
7-3-1 Hogo Bunkyo-ku Tokyo 113, JAPAN

Abstract

Strontium chloride is a typical Cl^- conductor with fluorite structure and it has conductivity of $2 \times 10^{-4} \text{Scm}^{-1}$ and $5 \times 10^{-2} \text{Scm}^{-1}$ at 500°C and 700°C, respectively. Usually the enhancement of ionic conductivity is due to the increase of vacancy or interstitial ions by resulting of the addition of MCl ($\text{M}=\text{Na}, \text{K}$) or $\text{M}'\text{Cl}$ ($\text{M}'=\text{Y}, \text{Ga}, \text{La}$).

In some materials (LiI , AgI , CuCl , CaF_2 , LiBrH_2O and so on), the enhancement of ionic conductivity was observed by the addition of Al_2O_3 , which is typical insulator. In this case, X-ray diffraction measurements showed there were no phases present other than the ionic conductor and Al_2O_3 . The same results were observed in the SrCl_2 and Al_2O_3 system. The ionic conductivity increased about 1 order of magnitude by 25mol% dispersion of $2.6 \mu\text{m}$ Al_2O_3 at 500°C. The conductivity of the dispersed system strongly depended on the particle size and the concentration of Al_2O_3 , which suggested that high ionic conductivity layer were formed at the interface between ionic conductor matrix and Al_2O_3 particles. This consideration was also supported by the fitness with Wagner's model which was proposed in his work of CuCl .

The effective thickness and electrical conductivity of the interface layer were calculated by using two simple mixing models. In first step of this calculation, Maxwell's equation was used to obtain the conductivity of Al_2O_3 surrounded by the high ionic conductive layer using the observed conductivity of the sample, the conductivity of pure SrCl_2 and the volume fraction. In the next step, the Tiku's equation was used to estimate the relation between the effective thickness and conductivity of the interface layer using the result of the first step and the particle radii of Al_2O_3 measured by the sedimentation method. By applying this calculation to many samples with different composition and different particle size of Al_2O_3 , the adequate effective thickness and conductivity were estimated. From this calculation, the conductivity is about 2 orders of magnitude higher than pure SrCl_2 and the thickness of the ionic conductive layer is 0.1-0.6 μm and decreases with an increase in temperature. This result adequately explain the composition and particle size dependencies for Al_2O_3 particles dispersed in a SrCl_2 matrix.

NEUTRON DIFFRACTION STUDY OF THE DISTRIBUTION AND THERMAL MOTION OF SILVER IONS IN ALPHA- AND BETA- Ag_3SI J. J. Didisheim¹, R. K. McMullan² and B. J. Wuenesch¹

¹Department of Materials Science and Engineering, Massachusetts Institute of Technology, Cambridge, Mass. 02139, U.S.A. and ²Chemistry Department, Brookhaven National Laboratory, Upton, Long Island, N.Y. 11973, U.S.A.

Fast-ion conducting Ag_3SI , intermediate to AgI and Ag_2S , is of interest in establishing the role of bonding and mobile ion concentration on the Ag distribution and transport properties of these phases. Previous powder diffraction studies and a single-crystal x-ray analysis had established the existence of three phases: α ($T > 240^\circ\text{C}$), space group $\text{Im}\bar{3}\text{m}$, having a disordered bcc anion array and cations disordered among tetrahedral sites; β ($-116^\circ < T < 240^\circ\text{C}$), space group $\text{Pm}\bar{3}\text{m}$, having an ordered CsCl-type anion array and cations disordered in tetrahedral sites; and γ ($T < -116^\circ\text{C}$), space group $\text{R}\bar{3}$, with cations ordered in a subset of available tetrahedral sites. The present single-crystal neutron-diffraction study was undertaken to characterize the Ag distribution more precisely, capitalizing upon the higher resolution afforded by the lack of decrease of scattering length with angle and the fact that, as opposed to x-ray data, Fourier synthesis provides the probability distribution for the cation nucleus, rather than a convolution of the probability with a distribution of orbital electrons of comparable spatial extent. The structures were also examined as a function of temperature for the first time to permit distinction between time-averaged anharmonic thermal vibration and positional disorder.

The β phase was examined at temperatures of 23, 95, 168 and 232°C using Be-monochromated thermal neutrons of 1.05099 \AA wavelength at the High Flux Beam Reactor at Brookhaven National Laboratory. Three to six sets of symmetry-equivalent reflections for $\sin\theta/\lambda < 0.78 \text{ \AA}^{-1}$ were recorded to provide 72 independent intensities of which 61 to 55, depending upon temperature were $> \sigma$; internal agreement in I ranged 3.7% to 1.9% for the individual data sets. Refinement indicated partial positional disorder of S and I. Models examined included anharmonic temperature for Ag ions and/or partial occupancy of the octahedral site. The most successful model employed Ag ions solely in a tetrahedral site coordinated by 2S and 2I and anisotropic harmonic temperature factors. The temperature factors were found to vary linearly with temperature. Final weighted residuals, $R_w(F^2)$, including unobserved reflections, ranged 3.9-5.9%.

The anion-disordered α -phase was investigated at 323, 380, 442 and 475°C and 18 to 20 independent structure factors $> \sigma$ were obtained from averages of symmetry-equivalent intensities ranging 26-37 in number, depending on temperature. Final weighted residuals $R_w(F^2)$, including unobserved reflections, vary between 3.3 and 4.5%. The Ag probability density is highly delocalized compared to that in β , being elongated along [100] in a fashion qualitatively similar to α - Ag_2S . Significant differences relative to the sulfide, however, are evidence for occupancy of a site at $\frac{1}{2}\frac{1}{2}\frac{1}{2}$ and fine structure in the probability density. Rather than representing anharmonic effects, the latter features may be explained to satisfaction in terms of positional disorder of the Ag ions which depends on the local configuration of S and I about the site.

VAPOR SPECIES FROM FUSED $\text{Li}_2\text{O}-\text{B}_2\text{O}_3$, $\text{Li}_2\text{O}-\text{SiO}_2$ and $\text{Li}_2\text{O}-\text{P}_2\text{O}_5$ SYSTEMS FOR THIN FILM MANUFACTURING BY PVD

By Li-Wei Zhang, M. Yahagi, and K.S. Goto
Tokyo Institute of Technology
Meguro-ku, Ookayama 2-12
Tokyo, Japan

The identification of vapor species is very important for thin film of superionic-conductors manufacturing by PVD, CVD and any other elegant processes.

The intention of the present work is to estimate the vapor species and the equilibrium vapor pressure, which will be evaporated from fused $\text{Li}_2\text{O}-\text{B}_2\text{O}_3$, $\text{Li}_2\text{O}-\text{SiO}_2$ and $\text{Li}_2\text{O}-\text{P}_2\text{O}_5$ systems. The estimation was made from the thermodynamic data.

Furthermore, using the kinetic theory of gas molecules, the deposition rate and composition of thin film will be predicted in relation to temperature and composition of evaporation source.

PROTON CONDUCTION IN AMMONIUM ZEOLITES. EFFECTS OF DEAMMONIATION AND THERMAL TREATMENT

Erik Krogh Andersen, Inger Grete Krogh Andersen and Eivind Skou

Department of Chemistry, Odense University,
Campusvej 55, DK-5230 Odense M

Steen Yde-Andersen

Energy Research Laboratory, Niels Bohrs Allé 25,
DK-5230 Odense M

Abstract

Synthetic sodium and calcium zeolites (4A, 5A, 13X, Y) were exchanged to the ammonium form. The ac and dc conductivities have been measured from 25-300 °C. The dc conductivities measured with water vapour saturated hydrogen electrodes prove that protons move across the cell. During the dc experiments an amount of ammonia corresponding to the charge passed is liberated. The proton conduction in fully hydrated ammonium zeolites is therefore based on an ammonia vehicle. Electrolytic deammoniated zeolites are also proton conductors but with a lower conductivity than the corresponding ammonium zeolites. Thermally deammoniated zeolites show a similar behaviour. The ammonium zeolites loose ammonia, water and conductivity at high temperature (300 °C). This indicates that vehicles are necessary for proton conduction in zeolites.

STUDY ON THE PHYSICAL PROPERTIES OF AN AMORPHOUS
Ag₂SiF₆ AT LOW TEMPERATURE

Wen-Hai Yu and Qing Zheng
Department of Physics
University of Science and Technology of China
Hefei, Anhui
The People's Republic of China

An amorphous silver fast ionic conductor (AgI)_{0.79}(Ag₂O·B₂O₃)_{0.21} has been prepared by quenching the mixed raw materials in the composition from the melting point to the liquid-nitrogen temperature, and has been examined by DTA and XRD. It has determined that T_g = 160°C and T_c = 340°C.

The ionic conductivities of specimens within the temperature range of 100-300K have been measured by a.c. bridge method. The room temperature ionic conductivity $\sigma(25^\circ\text{C})$ is equal to $2.45 \times 10^{-2} \Omega^{-1} \text{cm}^{-1}$. The dependence of the ionic conductivity on temperature is in keeping with the Arrhenius relation very well for $T > 150\text{K}$ and the activation energy $E = 0.198 \text{ eV}$. In addition, a plus deviation of the conductivities was revealed for $T < 150\text{K}$. The lower the temperature and the higher the measuring frequency, the larger the deviation.

The electronic conductivities of the specimens have been measured within the temperature range of 170-270K. At room temperature the order of magnitude of its value is $10^{-3} \Omega^{-1} \text{cm}^{-1}$. The linear relation of $\ln \sigma_e \sim 1/T$ has been discovered, and the activation energy $E_c = 0.300 \text{ eV}$. Therefore, the ionic transport number is unity in the investigated temperature range.

The thermoelectric power θ of the specimens at 100-300K has been measured, and the formula

$$\theta = 0.216 + 0.124 \times 10^3 / T \text{ (mVK}^{-1}\text{)}$$

has been obtained. From this it was found that Ag⁺ transport heat $Q_{\text{Ag}^+} = 2.6 \text{ kcal/mol}$.

The influence of the magnetic fields of 3000-10000 Gauss on the longitudinal a.c. impedance, the transverse a.c. and d.c. impedance and the thermoelectric power have been studied, but no effect has been detected. According to the sensitivity of the instruments, we are sure that the effects of such magnetic fields on the above-mentioned physical properties must be below 1/1000.

INVESTIGATION OF THE TELLURIUM-RICH PART OF THE TERNARY SYSTEM Ag-Nb-Te USING A SOLID SILVER ELECTROLYTE

W. SITTE, I. BEGSTEIGER, and H. P. FRITZER

Institut für Physikalische und Theoretische Chemie
Technische Universität Graz
A-8010 Graz, AUSTRIA

In spite of the great technological importance (superconductivity, structure, magnetic properties) of the binary system Nb-Te numerous investigations showed both contradictory and inconsistent results with respect to the existence and range of composition of various phases (e.g., Nb_5Te_4 , $NbTe$, Nb_3Te_4 (?), Nb_3Te_7 (?), Nb_5Te_8 (?), $NbTe_3$ (?), and $NbTe_4$) below 600 K.

In contrast, the binary system Ag-Te is well known. At 600 K three compounds exist: $Ag_{2.0}Te$, $Ag_{1.9}Te$, and Ag_5Te_3 .

Only two ternary compounds have been reported in the system Ag-Nb-Te: Ag_2NbTe_3 and $Ag_2Nb_3Te_6$.

The aim of this work was the investigation of the tellurium-rich part of the System Ag-Nb-Te (reaching up to the compound $NbTe_2$ on the binary line Nb-Te) using AgI as solid electrolyte. The cell



has been chosen for coulometric titrations at 600 K (i.e. ca. 30 K below the melting point of the eutectic system Ag_5Te_3 -Te). In particular the investigation of the ternary system should give essential informations about the binary system Nb-Te at that temperature.

Binary and ternary samples have been prepared from high grade purity Ag_2Te and $NbTe_2$, as well as $NbTe_3$ and Te by solid state reaction in evacuated quartz ampoules at 670 K. Silver has been titrated into (and/or out of) the samples by the use of a precision current source. The open cell voltage has been measured as a function of the silver content by a high-impedance electrometer (galvanostatic intermittent titration technique). Typical current densities were in the region 0,02 - 0,4 mA/cm². The time necessary to achieve equilibrium after each titration step varied between 1 - 12 hours.

The binary system Ag-Te has been reinvestigated in accordance with the results of Valverde (1). In the present study the solubility limit of silver in pure Te has a value of about 2 mole-%. In the ternary system Ag-Nb-Te constant cell voltages were measured within large three-phase areas consisting of Ag_5Te_3 , Te, and $NbTe_3$, as well as Ag_5Te_3 , other Nb-Te-compounds, and $Ag_{1.9}Te$, respectively. The results showed no compound formation for higher Te-contents than $NbTe_3$ at 600 K. The ranges of composition as well as thermodynamic properties (e.g. ΔG_f^0 and ΔS_f^0) obtained from the emf-data, will be reported for various Nb-Te-compounds.

(1) N. Valverde, Z. Phys. Chem. (N.F.) 70 (1970) 113-127

APPLICATION OF FAST IONIC CONDUCTORS IN SOLID STATE GALVANIC CELLS FOR GAS SENSORS.

G. Hötzel and W. Weppner

Max-Planck-Institut für Festkörperforschung
D-7000 Stuttgart 80, Fed. Rep. Germany

The application of fast ionic conductors for measuring partial gas pressures of the transferred ionic species in the electrolyte, e.g., the determination of oxygen activities with the help of doped zirconia is well established and commercialized. There is, however, a large number of important species for which no solid electrolyte is available at the present time. Examples are Cl_2 , CO , CO_2 , NO , and SO_2 . Gas sensitive thin film mixed conductors were employed for these cases, which relate the activities of the gaseous species to the transferred ionic species in the fast solid electrolyte according to Duhem-Margules' equation. The measuring range is between room temperature and 473 K. These all solid state sensors may be miniaturized and integrated into electronic circuits.

Galvanic cells of the type

reference electrode	fast solid electrolyte	gas sensitive mixed conductor
---------------------	------------------------	-------------------------------

were constructed. Preferably, α -alumina, Ag_4RbI_5 or AgI were used as solid electrolytes. The gas sensitive mixed conductors consist of AgCl (for Cl_2 -partial pressure measurements), $AgNO_3$, Na_2CO_3 and others. Thin film AgCl on a AgI, Ag_4RbI_5 or α -alumina substrate shows Nernstian behavior with the correct change of potential with the variation of the chlorine partial gas pressure. A sometimes observed deviation from the absolute value according to Nernst's equation has been attributed to chemical variations of the reference electrode. Similar experimental responses using the other substrates as mixed conductors have been observed for the other gas components.

The applied technique has considerably expanded the application of solid state galvanic cells for monitoring gas partial pressures of a variety of chemical species.

ELECTROCHEMICAL BEHAVIOUR OF STABILIZED ZIRCONIA
USING THICK FILMS TECHNOLOGY

M. GOGÉ , K. HEGGESTAD , M. GOUET ,

Laboratoire de thermodynamique et électrochimie
des matériaux

Université Paris XII

avenue du Général de Gaulle - 94010 CRETEIL CEDEX-
FRANCE -

ABSTRACT :

Thick films technology is used to prepared cermets
set on a substrate .

The electrolyte is made of platinum and yttria
stabilized zirconia ; two or three electrodes of
platinum are set by the same process as the
electrolyte .

These samples are investigated by means of ac and
dc electrochemical methods between 200 and 500°C
and in a range of oxygen partial pressure from
10⁻⁴ to 1 atm .

The current - polarization curves are presented .
Interfacial O₂ /Pt/YSZ and bulk properties are
observed by means of complex admittance diagrams
obtained in a large range of frequencies :
10⁻² to 10⁶ Hz .

All the results are discussed . They show that
this kind of cells can be used as polarographic
oxygen sensors in these ranges of temperature and
oxygen partial pressure .

A STUDY ON THE EFFECT OF SILICON UPON THE ACTIVITY
COEFFICIENT OF NIOBIUM IN LIQUID IRON WITH THE
SOLID ELECTROLYTE OXYGEN CELL TECHNIQUE

TONG Ting, WEI Shoukun, ZHANG Shengbi & JI Mingfu

Beijing University of Iron and Steel Technology
Beijing, People's Republic of China

As a further investigation on the thermodynamic behaviour
of Nb in liquid iron, solid electrolyte oxygen cell technique
was used to study the effect of Si upon the activity coefficient
of Nb in liquid iron at three temperatures 1823, 1853 and 1883K.
In contrast to the previous researches on $a_{\text{Nb}}^{\text{Si}}$ and $a_{\text{Nb}}^{\text{Fe}}$ reported
elsewhere and with a view to preventing the reduction of NbO₂
by Si, liquid iron containing Nb and Si was equilibrated with
SiO₂ under purified Ar atmosphere in quartz crucible, the follow-
ing cell assembly being adopted:

Mo|Mo, MoO₂||ZrO₂(MgO)||[Si], SiO₂|Mo+ZrO₂ cermet, Mo

The chemical reactions involved were:



The error caused by the electronic conductivity of the MgO-doped
zirconia solid electrolyte tube was corrected with the Schmalz-
fried formula. With the a_{O} values experimentally ascertained,
the interaction coefficients $e_{\text{Nb}}^{\text{Si}}$ at three temperatures could be
evaluated both on the same concentration as well as the same
activity basis. The corresponding values of $e_{\text{Nb}}^{\text{Fe}}$ were calculated
with the conventional method, with results given as below:

K	Same concentration method	Same activity method
1823	1.38	1.02
1853	0.98	0.88
1883	0.72	0.52

$$e_{\text{Nb}}^{\text{Si}} = \frac{37763}{T} - 19.36 \quad (r=0.994) \quad e_{\text{Nb}}^{\text{Fe}} = \frac{28545}{T} - 14.60 \quad (r=0.967)$$

Values of $a_{\text{Nb}}^{\text{Si}} \cdot a_{\text{O}}^2$ for every experiment were found to be less
than the equilibrium constant for the reaction $\text{NbO}_2(\text{s}) = [\text{Nb}] + 2[\text{O}]$,
so that no formation of NbO₂ was assured.

References:

- (1) WEI Shoukun et al: Rare Metals (1983) (1983), No. 1, 10.
- (2) ZHANG Shengbi et al: Acta Metallurgical Sinica 20 (1984), 344.

**ION-SELECTIVE ELECTROCHEMICAL SENSORS BASED ON
ION-CONDUCTING CHALCOGENIDE GLASSES**

Yu. G. Vlasov and E. A. Bychkov

Department of Chemistry, Leningrad
University, Leningrad 199164, USSR

Silver ion conducting chalcogenide glasses are promising membrane materials for solid-state ion-sensitive electrodes - electrochemical sensors for selective determination of different ions in liquid media.

Sensors based on Ag-As-S and Ag-As-Se glasses provide the direct potentiometric determination of silver ions in strong acid and corrosive media, such as 6 M nitric acid.

Silver ion conducting chalcogenide glasses containing lead iodide or sulfide are highly sensitive to lead ions, 10-100 times more stable for active oxidizing treatment, and 10-20 times more selective to cadmium ions in comparison with crystalline ion-selective membranes.

Copper ion-selective electrodes based on copper-silver-arsenic-selenium glasses are 10-30 times more sensitive in strong acid media.

Cadmium chalcogenide glass sensors are 10-30 times more selective to alkali and some divalent cations, their acid stability and stability to oxidation being higher as well.

Different types of ion-selective electrochemical sensors based on chalcogenide glasses are described and ion sensing mechanism is discussed on the basis of investigation of solid-state properties of membranes.

**CORRELATION BETWEEN STRUCTURE AND TRANSPORT
PROPERTIES IN ION CONTAINING NETWORKS**

H. CHERADAME, A. GANDINI, J.F. LE NEST

Ecole Française de Papeterie (INPG), BP 65,
38402 Saint Martin d'Hères cedex, France

Various polyether-urethane networks containing several alkali metal salts have been shown to exhibit high ionic conductivity above their glass transition temperature (1). This situation reflects the fact that transport properties are dependant on the mobility of chain segments. For instance dynamic mechanical properties and ionic conductivity follow the same temperature dependance explained by free volume variations (2). Electrochemical studies based on the determination of the ionic transport numbers and by voltamperometry have confirmed the high anionic conductivity in agreement with the high local anionic mobility already detected by spin-spin relaxation (T_2) measurements (3). The interactions between the cations, such as lithium ions, and the oxygen atoms belonging to ether bonds deserved a special study which aimed at explaining the unusual high conductivity observed at constant segmental mobility at high salt concentration. A detailed study of the glass transition temperature of various networks possessing macromolecular chains between crosslinks of variable length and of different lithium perchlorate content shows that the ions are regularly dispersed in the amorphous material without phase segregation up to relatively high salt concentration. Equilibrium swelling measurements support the assumption that the salt is under the form of ion pairs or quadrupoles within a large salt concentration range.

REFERENCES

- (1) A. KILLIS, J.F. LE NEST, A. GANDINI, H. CHERADAME
Macromolecules, 17 (1984), 63 and ref. therein
- (2) A. KILLIS, J.F. LE NEST, A. GANDINI, H. CHERADAME, J.P. COHEN ADDAD
Solid State Ionics, 14 (1984), 231
- (3) A. KILLIS, J.F. LE NEST, A. GANDINI, H. CHERADAME, J.P. COHEN ADDAD
Polym. Bull., 6 (1982), 351

CONDUCTIVITY, DR, DSC, and NMR STUDIES OF POLY(VINYL ACETATE) COMPLEXED WITH ALKALI METAL SALTS*

M. C. Wintersgill, J. J. Fontanella, J. P. Calame, M. K. Smith
Physics Department
U.S. Naval Academy
Annapolis, Md 21402, USA

S. G. Greenbaum
Physics Department,
Hunter College, CUNY
New York, NY

C. G. Andeen
Physics Department,
Case Western Reserve University
Cleveland, Oh 44106, USA.

Electrical conductivity, dielectric relaxation (DR), differential scanning calorimetry (DSC) and nuclear magnetic resonance (NMR) studies have been carried out on poly(vinyl acetate) (PVAc) complexed with a variety of lithium and sodium salts including perchlorates, triflates and iodides. The electrical conductivity and dielectric relaxation measurements were carried out using a fully automated complex impedance bridge operating at seventeen frequencies over the range $10-10^5$ Hz. The conductivity varies with the concentration of the salt. For example, at 102°C the conductivity for 8:1 PVAc-lithium perchlorate is about 10^{-7} (ohm-cm)⁻¹ while that for 4:1 material is about 5 times greater. The variation of the conductivity with temperature is also described. The electrical relaxation spectrum for pure PVAc consists of four peaks. Significant differences are seen in the complexed material. For example, for 8:1 PVAc-lithium perchlorate most peaks are similar to those observed in pure PVAc while for 8:1 PVAc-sodium perchlorate, the spectrum is strongly affected. The spectra for PVAc-lithium iodide and PVAc-lithium triflate are extremely simple. The DSC studies were carried out using a DuPont 990 DSC and show three thermal features which are dependent upon the salt and the thermal history of the samples. Finally, new NMR studies are presented. The results are considered in the light of previous work on PVAc complexed with lithium perchlorate (1) and a model similar to that for an ionic elastomer.

1. M. C. Wintersgill, J. J. Fontanella, J. P. Calame, S. G. Greenbaum, and C. G. Andeen, *J. Electrochem. Soc.*, 131, 2208 (1984).

*This work was supported in part by the Office of Naval Research.

POLYMER SOLID ELECTROLYTE PHOTOELECTROCHEMICAL CELLS WITH n-Si POLYPYRROLE PHOTOELECTRODES

O. Inganas and T.A. Skotheim

Brookhaven National Laboratory
Department of Applied Science
Upton, New York 11973

We have developed a new type of photoelectrochemical cell (PEC) based on rectifying junctions between semiconductor electrodes and thin film polymer solid electrolytes. This holds out the hope of being able to manufacture all thin film solid state PEC's without the semiconductor surface corrosion problems associated with liquid electrolyte PEC's.

Our present study has focussed on surface modification techniques for improving the rates of charge transfer between semiconductor electrodes and redox ion couples in polymer solid electrolytes. Specifically, we have shown that surface modifications of n-Si electrodes with thin films of polypyrrole can dramatically reduce the large activation energy barrier against efficient charge transfer between bare semiconductor electrodes and polymer solid electrolytes.

The n-Si surface modifications we have studied include the following: (i) bare n-Si (etched in HF only); (ii) n-Si coated with 200-400 Å polypyrrole.BF₄; (iii) n-Si coated with 10-20 Å electron beam evaporated Pt; (iv) n-Si coated with 10-20 Å Pt followed by deposition of polypyrrole.BF₄; (v) n-Si with 10-20 Å Pt followed by deposition of polypyrrole.iodide. The n-Si was always etched in HF before the surface modification. The polypyrrole films were grown on the n-Si surface with the technique of photoassisted electrochemical oxidation.

A thin coating of polypyrrole.BF₄ greatly improves the charge transfer characteristics of the interface. 10-20 Å of Pt improves the electronic coupling further between the polypyrrole and the Si leading to more efficient hole scavenging. A Pt coating alone without polypyrrole produced slightly less efficient charge transfer.

The most efficient interfaces incorporate iodide as the anion in the polypyrrole, synthesized from MeCN solution containing tetraethylammonium iodide. With the polypyrrole.iodide coating the charge transfer characteristics relative to bare n-Si are improved by about three orders of magnitude, resulting in energy conversion efficiencies in the 3-4% range based on 100 mW/cm² incident white light.

The efficiency of the present interfaces are limited by high surface recombination velocities on the n-Si surface. This is shown by the poor spectral response in the high photon energy region of the spectrum.

Acknowledgement

This work was supported by the Division of Chemical Sciences, U.S. Department of Energy, Washington, D.C., under Contract No. DE-AC02-76CH00016.

ION CONDUCTION MECHANISM IN NETWORK POLYMERS FROM POLY(ETHYLENE OXIDE)
AND POLY(PROPYLENE OXIDE) CONTAINING LITHIUM PERCHLORATE

Masayoshi Watanabe, Satoshi Nagano, Kohei Sanui, and Naoya Ogata
Department of Chemistry, Sophia University, 7-1 Kioi-cho, Chiyoda-ku,
Tokyo 102, Japan

Ion conduction mechanism in network polymers from poly(ethylene oxide) (PEO) and poly(propylene oxide) (PPO) containing lithium perchlorate (LiClO₄) was clarified in terms of carrier generation and transport processes. The network polymers were prepared by a crosslinking reaction of triol-type PEO and PPO (number average mol.wt.=3000) with tolylene-2,4-diisocyanate. LiClO₄ was dissolved in the network polymers by an immersing method. The degree of crystallinity for the PEO networks was considerably lower than that of linear PEO. With increasing LiClO₄ concentration, the degree of crystallinity decreased still more, whereas the structure of the crystallites was similar to that of the salt-free PEO. Melting points of the crystallites were at around 20 °C. The PEO complexes with the LiClO₄ concentrations higher than [LiClO₄]/[EO unit]=0.05 were completely amorphous. In contrast, the PPO networks and the PPO-LiClO₄ complexes were completely amorphous, independent of the LiClO₄ concentrations. In the both complexes glass transition temperatures (T_g) increased with increasing the LiClO₄ concentrations. Ionic conductivity, estimated from complex impedance measurements, reached 10⁻³ Scm⁻¹ at 30 °C for the PEO complexes and at 70 °C for the PPO complexes. Arrhenius plots of the ionic conductivity for the partially crystalline PEO complexes deviated positively from a straight line above the melting points and obeyed a straight line function with larger temperature dependence below those temperatures. The amorphous PEO and PPO complexes deviated positively from the Arrhenius eq. in terms of the temperature dependence of conductivity. Ionic mobility of the both complexes in amorphous state (40-100 °C), measured by transient ionic current method, was changed from 10⁻⁶-10⁻³ cm² V⁻¹s⁻¹ in this temperature range, almost independent of the polymer structure. The Nernst-Einstein eq. correlated the ionic mobility with the ionic diffusion coefficient. The Williams-Landel-Ferry eq. with C₁=5-9 and C₂=30-70 held with a temperature dependence of the diffusion coefficient in the order of 10⁻⁸-10⁻⁷ cm²s⁻¹, when T_g was used as a reference temperature. The change in the number of carrier ions with temperature obeyed the Arrhenius eq. The degree of dissociation for LiClO₄ was more facilitated and the activation energy for carrier generation was lower for the PEO complexes, in comparison with those of the PPO complexes. The activation energy increased with increasing LiClO₄ concentrations in the both complexes. Thus, the carrier transport and generation processes were explained by the free volume and Arrhenius activation mechanisms, respectively. The temperature dependence of ionic conductivity in amorphous and rubbery state could be expressed by the following eq.

$$\sigma = \frac{e^2 D_+ N_+}{kT} \exp\left[-\left(\frac{U/2\varepsilon}{kT} + \frac{\gamma V_1^*}{V_f}\right)\right]$$

where e is elementary electric charge, N_+ and D_+ are constants, U is dissociation energy for the ion pair, ε is relative dielectric constant, γ is a numeric factor, V_1^* is a critical volume required for ion migration, and V_f is a free volume. Higher ionic conductivity in the PEO complexes was mainly based on the larger number of ionic carriers and the lower activation energy for carrier generation. The large decrease in the conductivity below the melting points of crystallites in the PEO complexes may be attributed to the condensed LiClO₄ concentrations in the amorphous region, which increased the activation energy for carrier generation and decreased the carrier mobility due to the increase in T_g.

THE KINETICS OF THE ELECTROCHEMICAL DOPING PROCESSES
OF POLYACETYLENE

B.Scrosati

Dipartimento di Chimica, University of Rome 'La Sapienza',
Piazzale A.Moro 5, 00185 Rome, Italy.

and

M.Lazzari

Dipartimento di Chimica Fisica Applicata, Polytechnic of Milan,
Milan, Italy.

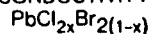
Polyacetylene is a very interesting polymer which has been proposed as an improved electrode material in rechargeable lithium batteries(1). However, this use may be somewhat limited by the kinetics of the electrochemical doping processes (2) which are characterized by a slow diffusion of the dopant species throughout the bulk of the polymer(3).

In this work we report a study of the electrochemical processes at the polyacetylene-electrolyte interface, with particular concern to the reversibility of the charge-transfer reaction and to the diffusion of the dopant species. This study has been carried out by cyclic voltammetry and a.c. impedance measurements.

REFERENCES.

- 1)-D.Mac Innes, M.A.Druy, R.J.Nigrey, D.P.Nairns, A.G.MacDiarmid and A.J.Heeger, J.Chem.Soc., Chem.Comm., 317 (1981).
- 2)-G.C.Farrington, B.Scrosati, D.Frydrych and J.DeNuzzio, J.Electrochem.Soc., 131, 7 (1984).
- 3)-A.Padula, B.Scrosati, M.Schwarz and U.Pedretti, J.Electrochem.Soc., 131, 2761 (1984).

STRUCTURE AND IONIC CONDUCTIVITY OF MIXED LEAD HALIDES



M. Lumberas, J. Protas*, S. Jebbari*,
G. D. Dirksen** and J. Schoonman**
Laboratoire de Genie Physique-CLOES
Universite de Metz
57045 Metz Cedex
France

*Laboratoire de Cristallographie
Universite de Nancy I
P. O. Box 239
54506 Vandoeuvre-les-Nancy
France

**Solid State Department
Utrecht University
P. O. Box 80.000
3508 TA Utrecht
The Netherlands

Lead chloride and lead bromide exhibit Schottky disorder and anion conductivity. They show complete mutual solid solubility. Mixed lead halide crystals have been grown by the Bridgeman technique in order to elucidate relations between structural and electrical properties. Microprobe analysis has been used to establish the anion ratio Cl/Br. All solid solutions adopt the orthorhombic PbCl_2 structure (Pnma). In this structure, two anion sites can be discerned. Preferential anion site occupancy has been observed for $\text{PbCl}_{0.5}\text{Br}_{1.5}$ and $\text{PbCl}_{1.5}\text{Br}_{0.5}$, while PbClBr is completely ordered.

The ionic conductivity of several compositions in the system $\text{PbCl}_2\text{-PbBr}_2$ has been studied by impedance spectroscopy as a function of composition and temperature. A simple equivalent circuit appears to fit all the data. Analysis of the bulk parameters reveals a maximum in the ΔH_m (migration enthalpy) vs. x relation. The concomitant ΔH_f (formation enthalpy) vs. x relation reveals a decrease for x ranging from 0 to ~0.5 and 1 to ~0.5, with a pronounced maximum at x=0.5 due to the complete ordering of the anion array. Isothermal conductivities decrease with x and reveal a minimum for x=0.5. Usually, cation conducting Schottky or Frenkel-type solid solutions obtained by homovalent anion doping reveal substantial conductivity enhancements (e.g., $\text{K}(\text{Cl},\text{Br})$, $\text{Ag}(\text{Cl},\text{Br})$). The present anion conducting Schottky-type solid solutions show the opposite behavior. This will be discussed in relation to ordering effects, along with homovalent dopant-induced lattice distortions on the number and mobility of the conducting defects.

Diffuse Neutron Scattering Study of
Antifluorite Type Cu_{2-x}Se

R. J. Cava[†], N. Hessel Andersen^{*}, K. Clausen^{*},
E. A. Rietman[†], and J. K. Kjems^{*}

[†]AT&T Bell Laboratories
Murray Hill, New Jersey 07974
U.S.A

^{*}Riso National Laboratory
Riso, Denmark

ABSTRACT

We have synthesized single crystals of Cu_2Se and $\text{Cu}_{1.8}\text{Se}$ by Bridgeman growth from the melt. The basic structure of these materials in their highly conducting β phase is that of the much studied fluorites except that the cations are the mobile species. Charge compensation in the non-stoichiometric case occurs through the introduction of a mixture of Cu^{2+} with the Cu^{1+} , unlike the case of the fluorites where nonstoichiometry in the mobile fluorine sublattice is accommodated by aliovalent dopant ions in the immobile cation sublattice. A highly cooperative motion is expected for Cu_2Se where for a normal antifluorite structure no vacant tetrahedral sites are expected to occur without accompanying interstitial ions. We have investigated the diffuse scattering intensity in the hol zone in the fast ion conducting phase for both $\text{Cu}_{1.8}\text{Se}$ and Cu_2Se . Maps of the diffuse scattering indicate a short-range ordering of the mobile ions which is significantly different from that in the fluorite structure compounds. The short-range order extends over several unit cells and the details of the ordering depend on the mobile ion stoichiometry. The diffuse scattering is quasielastic in nature and indicates that the short-range order is of dynamic origin. We have studied the energy widths of the principal diffuse scattering features as a function of position in reciprocal space and temperature.

DIFFUSION AND PRESSURE EFFECTS IN THE SUPERIONIC CONDUCTOR Ag_3SBr
STUDIED BY NMR

H. Huber, M. Mali, J. Roos, and D. Brinkmann

Physik-Institut, University of Zurich, 8001 Zurich, Switzerland

$\beta\text{-Ag}_3\text{SBr}$ exhibits an ionic conductivity of about $0.002 (\Omega \text{ cm})^{-1}$ at room temperature (1). In order to obtain detailed information on the microscopic processes involved in conduction, we have measured as a function of temperature the NMR relaxation times T_1 and T_2 of the mobile silver ions ^{107}Ag and ^{109}Ag and the self-diffusion coefficient D of ^{109}Ag by employing the NMR pulsed magnetic gradient technique.

The value of D at room temperature is $2.9 \cdot 10^{-12} \text{ m}^2/\text{s}$ with an activation energy of 0.19 eV in good agreement with conductivity data (1). Our results will be discussed in terms of the number of mobile Ag ions and their hopping rates.

The spin-lattice relaxation of the Ag nuclei is caused by fluctuating magnetic fields arising from anisotropic chemical shifts when Ag ions diffuse among inequivalent sites. Between 160 K and 550 K the T_1 data are analyzed in terms of two diffusion processes: (i) hopping with an activation energy of 0.14 eV, (ii) vacancy induced diffusion with a 0.19 eV vacancy enthalpy of formation and a 0.13 eV energy of migration, the underoccupancy of Ag sites being 1.2 % at room temperature.

By monitoring the ^{81}Br NMR signal as a function of pressure and temperature the boundaries of the high conducting β and the low conducting γ phase in the temperature-pressure phase diagram were determined similar to our previous studies in RbAg_4I_5 . (2).

Investigations of the influence of pressure on the relaxation times T_1 and T_2 are in progress.

- (1) G. Chiodelli, A. Magistris, A. Schiraldi, *Zeit.f.phys. Chemie* 118 (1979) 177.
(2) H. Huber, M. Mali, J. Roos, D. Brinkmann, *Rev. Sci. Instruments* 55 (1984) 1325.

INVESTIGATIONS ON THE FORCES OF INERTIA OF THE MOBILE IONS IN
SOLID IONIC CONDUCTORS - MEASUREMENTS ON RbAg_4I_5

Manfred Betsch, Hans Rickert and Rainer Wagner

University of Dortmund, Chair for Physical Chemistry I, P.O. Box 500 500,
D-4600 Dortmund 50

The forces of inertia of electrons in metallic conductors were already measured by Tolman [1] in 1916. By decelerating a metallic conductor a voltage pulse occurs between its two ends, which is proportional to the ratio mass/electrical charge of the electrons. This ratio is for example in the case of silver ions about 10^5 times greater than in the case of electrons. Therefore we have measured the forces of inertia of ions on solid ion conductors.

After having made investigations on $\alpha\text{-AgI}$ as a first model substance at a temperature of 170°C [2], we have investigated in further measurements the solid ion conductor RbAg_4I_5 at 25°C and 120°C.

In our experiments rods of RbAg_4I_5 with silver electrodes at both ends were decelerated by letting them drop from different heights to a plastic material on the ground. In the moment of striking the ground the forces of inertia of the mobile silver ions caused voltage pulses, which were proportional to the velocity before striking and to the length of the RbAg_4I_5 -rods but independent of the temperature which is in accordance to theoretical considerations. Using the mass and the electrical charge of the silver ions the voltage pulses could be calculated. Calculated and measured values were in agreement within the accuracy of measurement of 1%.

As the voltage is built up very quickly it is practically an exact measure for the acceleration at any time and therefore solid ion conductors may be of interest for the construction of accelerometers [3].

- [1] R.C. Tolman, T.D. Stewart, *Phys. Rev.* 8, 97 (1916)
[2] M. Betsch, H. Rickert and R. Wagner, *Ber. Bunsenges. Phys. Chem.*, accepted for publication
[3] H. Rickert; Patent Application in Germany under number Nr. 3346447.2 at 22.12.1984 and further ones in different countries

Bulk Interaction Between AgI and α -Fe₂O₃ in their Composite Electrolyte

Chen Li-quan, Zhao Zong-yuan and Dai Sou-yu
Institute of Physics, Chinese Academy of Sciences, P.O.Box 603, Beijing, China.

(Abstract)

We have found recently that not only the conductivity of β -AgI(α -Al₂O₃) composite electrolyte was increased substantially but also the α -phase to β -phase transition temperature was decreased obviously by the existence of DSPP α -Al₂O₃. It means that the bulk property of matrix phase β -AgI was influenced by the DSPP α -Al₂O₃. In this paper we will show that the bulk property of DSPP α -Fe₂O₃ is also effected by the mother phase AgI in AgI(α -Fe₂O₃) composite electrolyte.

The low temperature conductivity and susceptibility of composite electrolyte AgI(α -Fe₂O₃) have been investigated. It is noticed that the $\log \sigma$ vs. $1/T$ curve have a turning-point. The temperatures correspond to the turning-point are continuously decrease from 256K to 147K with the AgI content increasing from 0 to 90m/o. The susceptibility measurement coincide quite well with the results of electrical experiments.

The Mössbauer spectral studies of AgI(40m/o α -Fe₂O₃) have been performed at different temperatures. Each spectral is composed of three sub-spectra which corresponds to two interfacial states between AgI and α -Fe₂O₃ and one bulk state in α -Fe₂O₃. The hyperfine internal magnetic field(H_{in}) and quadrupole splitting (SQ) in α -Fe₂O₃ has abrupt change at about 190K.

Form above results it seems clear that the Morin transition temperature α -Fe₂O₃ is influenced by the existence of AgI. therefore the bulk properties of the two phases in composite electrolyte are interacted each other.

AN NMR STUDY OF Li₂Ti₃O₇

M. EL-GEMAL and R. DUPREE

Physics Department, University of Warwick, Coventry, U.K.

In view of its potential for providing information about activation energies, correlation times etc NMR is often used as a tool to investigate fast ion conductors. In many cases however the behaviour is anomalous in that the activation energy obtained from NMR is much less than that from the conductivity and the attempt frequencies anomalously low. One example of such a system is Li₂Ti₃O₇ for which Huberman and Boyce obtained an activation energy from $T_2 = 0.2$ eV, compared with 0.45 eV from σ , and an attempt frequency of $\sim 4 \times 10^7$ Hz. Various explanations were proposed for this behaviour including "the break-down of absolute rate theory", and 1d ionic motion. We have remeasured T_1 and T_2 for Li in very pure highly stoichiometric material and also in off stoichiometric material. We obtain a T_1 and T_2 more than an order of magnitude longer than observed by Huberman and Boyce over most of the temperature range and an activation energy for T_2 much closer to that measured in conductivity studies. Small departures from stoichiometry rapidly reduce the relaxation times. The results will be discussed in terms of the presence of paramagnetic ions in this material.

IONIC CONDUCTIVITY AND CRYSTAL STRUCTURE OF $\text{Li}_{(1-x)}\text{Ti}_{(2-x)}\text{In}_x\text{P}_3\text{O}_{12}$

H. HAMDOUNE and D. TRAN QUI
Laboratoire de Cristallographie, C.N.R.S., associé à l'U.S.M.G.,
166 X, 38042 Grenoble Cedex (France)

E.J.L. SCHOUER
Laboratoire d'Energétique Electrochimique, ENSEEG, B.P. 75,
38042 Saint Martin d'Hères Cedex (France)

It has been reported that for moderate substitution of Ti^{4+} ($x < 0.4$) by In^{3+} in $\text{Li}_{(1+x)}\text{Ti}_{(2-x)}\text{In}_x\text{P}_3\text{O}_{12}$, R3C Nasicon like structure was formed in this solid solution and high ionic conductivity was observed in these compounds. Further substitution ($x > 0.4$) of trivalent In has distorted the rhombohedral lattice parameters leading presumably to lower monoclinic symmetry (1).

Attempts to identify the presumed monoclinic phases by X-ray powder diffraction patterns were inconclusive.

In order to overcome this difficulty we have tried and recently succeeded to grow single crystals of phases with $x = 0.0, 0.6$ and 2.0 and straightforwardly determined their space groups and lattice parameters. Using these parameters the X-ray powder diffraction diagrams of the whole system, x ranging from 0.0 to 2.0 , are successfully indexed.

In this paper we describe :

- The experimental method used to grow the single crystals
- The crystal structure of two monoclinic phases : $\text{Li}_{1.6}\text{Ti}_{1.4}\text{In}_{0.6}\text{P}_3\text{O}_{12}$ and monoclinic $\text{Li}_3\text{In}_2\text{P}_3\text{O}_{12}$ and present the results of :
- Phase identification by X-ray powder diffraction, space group and unit cell constants, for $x = 0.0, 0.1, 0.2, 0.3, 0.4, 0.6, 1.0, 1.2, 1.4, 1.5, 1.6, 1.8, 1.9$ and 2.0 .
- Conductivity measurements versus temperature (from room temperature to 500°C).

It is also showed in this study that the conductivity of these phases, at 300°C , increases drastically with In concentration to reach a maximum value as high as $2 \cdot 10^{-2} (\Omega\text{cm})^{-1}$ for $x = 0.3$ and then decreases down to $\sim 10^{-3} (\Omega\text{cm})^{-1}$ for $x = 1.0$.

Finally correlations between conductivity behaviour of the $\text{Li}_{(1+x)}\text{Ti}_{(2-x)}\text{In}_x\text{P}_3\text{O}_{12}$ phases versus x and their structure deviation from Nasicon type structure are discussed.

(1) Li Shi-Chun and Lin Zu-Xiang, Solid State Ionics 9 and 10 (1983) 835-838.

RELATION BETWEEN ALKALI ION CONCENTRATION AND APPARENT GLASS BASICITY:
CONDUCTIVITY MAXIMUM IN GLASS

Steve W. Martin
Department of Chemistry
Purdue University
West Lafayette, Indiana 47907

ABSTRACT

Utilizing the wide glass-forming range of pseudo-binary system $x\text{Na}_2\text{O}(1-x)[\text{B}_2\text{O}_3 \cdot n\text{Al}_2\text{O}_3]$, to $72.5 \text{ mol}\% \text{Na}_2\text{O}$, the dependence of the ionic conductivity in glass on mobile ion fraction and apparent glass basicity has been examined in detail. At very high mobile ion fractions the increasing basicity of the glass, discussed in terms of the amount of charge residing on anionic sites, plays an increasing role in increasing the activation energy for ion migration and also reducing the number of "free" mobile charge carriers. These combined effects are seen to produce clearly observable maximum in the conductivity/mobile ion fraction curves. For systems where large anions are introduced into the glass, viz. $x = 1^-$, conductivity maximum are not observed and these results are compared to the present observations.

ION CONDUCTING GLASSES IN THE $\text{Na}_2\text{O}-\text{Y}_2\text{O}_3-\text{SiO}_2$ AND $\text{Li}_2\text{O}-\text{Y}_2\text{O}_3-\text{SiO}_2$ SYSTEMS

M. Grayson Alexander and Brian Riley

Technology Development Dept.
 Combustion Engineering, Inc.
 1000 Prospect Hill Rd.
 Windsor, CT 06095
 U.S.A.

We have synthesized and measured the ionic conductivity of glasses in the $\text{M}_2\text{O}-\text{Y}_2\text{O}_3-\text{SiO}_2$ (M= Na, Li) systems. The Na glasses, in particular, have potential applications, such as electrolytes in Na/S cells. Glass samples were formed by melting together the component materials, then pour-quenching the melts onto a room temperature refractory brick. Na-based compositions consisted of 20 to 50 m/o Na_2O , 1 to 20 m/o Y_2O_3 and 39 to 67 m/o SiO_2 . Li-based compositions consisted of 30 to 50 m/o Li_2O , 5 to 20 m/o Y_2O_3 and 39 to 60 m/o SiO_2 . Glass formation occurred in both the Na and Li systems for compositions with 10 or less mol percent Y_2O_3 . All glasses were clear. Those containing more than 30 m/o M_2O were light green, while others were colorless.

AC conductivity (σ) was measured with blocking electrodes at 10 kHz, between 25 and 400°C. For the Na glasses, σ increased with increasing ratio of Na to Y, reaching a maximum for the composition 39.1 Na_2O - 7.5 Y_2O_3 - 53.4 SiO_2 ($3.4 \times 10^{-3} (\Omega \text{cm})^{-1}$ at 300°C), then decreased with further increase in Na_2O content. The activation energy, E_a , reached a minimum (0.58 eV) for the same composition. For the Li glasses, σ also increased with increasing ratio of Li to Y, reaching a final maximum for 45 Li_2O - 6 Y_2O_3 - 49 SiO_2 ($3.0 \times 10^{-3} (\Omega \text{cm})^{-1}$ at 300°C). E_a was also lowest (0.60 eV) for this composition.

Preliminary results of tests of compatibility with Na or Li and S at 200 to 350°C are favorable. Although some discoloration of the glasses resulted from several days immersion in molten alkali metal or sulfur, observation by SEM and energy dispersion analysis showed that this was due to surface coating of alkali metal or sulfur on the sample and not to chemical reactions.

INTERRELATION BETWEEN THE GLASS TRANSITION AND IONIC CONDUCTIVITY

Steve W. Martin
 Department of Chemistry
 Purdue University
 West Lafayette, Indiana 47907

ABSTRACT

Recently the importance of the location of the glass transition relative to the working temperature of the ionically conducting electrolyte has been pointed out. Hence it was shown that for the widely different systems $\text{AgI} + \text{AgPO}_3$ and $\text{Na}_2\text{O} + \text{SiO}_2$ that both have essentially the same value of conductivity at their respective glass transitions. To examine this relationship between glass transition and working temperature further, the system $\text{Li}_2\text{O} + \text{P}_2\text{O}_5$ has been studied since our new measurements show that this system exhibits, for constant composition, a glass transition which can be varied systematically from 170°C to 350°C by thermal treatments of the liquid. Initial results indicate that the conductivity decreases with decreasing glass transition. These entirely new and unexpected results are discussed in terms of the relationships between the location of the glass transition and the long range connective bonding in the liquid.

Author Index

Abrantes, Teresa	Session 4-C	P20/P-13	page 56
Akridge, J.R.	Session 5-A	P7/B-7	page 63
Alcacer, Luis	Session 4-C	P20/P-13	page 56
Alden, Maggie	Session 7-A	P5/BA-21	page 92
Aldrovandi, S.	Session 6-C	P19/G-19	page 85
Alexander, M. Grayson	Session 9-C	P14/G-30	page 126
Allcock, H. R.	Session 1-B	P9/P-2	page 5
Almond, D.P.	Session 6-D	P24/EG-3	page 88
Andeen, C.G.	Session 1-B	P8/P-1	page 4
Andeen, C.G.	Session 9-A	P2/P-16	page 120
Andersen, N. Hessel	Session 9-B	P7/OC-9	page 122
Andersen, N.H.	Session 2-D	P30/ET-6	page 29
Andersen, N.H.	Session 7-C	P20/ET-12	page 100
Anderson, Erik Krogh	Session 8-C	P20/OC-6	page 116
Anderson, Inger Grete Krogh	Session 8-C	P20/OC-6	page 116
Anderson, R.L.	Session 7-A	P3/BA-19	page 91
Andreani, R.	Session 4-C	P17/P-10	page 54
Angell, C.A.	Session 3-A	P3/TH-10	page 32
Angell, C.A.	Session 6-B	P12/AC-19	page 82
Angell, C.A.	Session 8-B	P8/G-22	page 110
Angell, C.A.	Session 8-B	P10/G-24	page 111
Armand, M.	Session 4-C	P15/P-8	page 53
Armand, M.	Session 4-C	P17/P-10	page 54
Austin, P.	Session 1-B	P9/P-2	page 5
Avogadro, A.	Session 6-C	P19/G-19	page 85
Badwal, S.P.S.	Session 4-D	P22/I-1	page 57
Badwal, S.P.S.	Session 4-D	P28/I-7	page 60
Bajars, G.E.	Session 7-D	P29/OA-2	page 104
Baldini, Primo	Session 6-C	P17/G-17	page 84
Barj, M.	Session 3-C	P17/NA-3	page 40
Barrie, J.D.	Session 7-A	P2/BA-18	page 91
Barsoum, Michel W.	Session 3-D	P23/G-9	page 43
Basu, A.	Session 3-B	P12/AC-12	page 37
Basu, Anjali	Session 2-D	P31/ET-7	page 30
Bates, J.B.	Session 4-D	P26/I-5	page 59
Bates, J.B.	Session 7-A	P3/BA-19	page 91
Bates, J.B.	Session 8-a	P1/TH-29	page 106
Battle, P. D.	Session 2-B	P13/O-5	page 21
Baur, W.H.	Session 3-C	P15/NA-1	page 39
Bean, P.	Session 3-D	P25/G-11	page 44
Beech, F.	Session 1-D	P26/AC-5	page 13
Beech, F.	Session 5-B	P11/O-10	page 65
Begsteiger, I.	Session 8-D	P22/S-1	page 117
Bell, M.F.	Session 7-A	P1/BA-17	page 90
Bell, Michael	Session 7-A	P6/BA-22	page 93
Benders, J.A.	Session 7-D	P29/OA-2	page 104
Bentzon, M.D.	Session 2-D	P30/ET-6	page 29
Berthier, C.	Session 4-C	P17/P-10	page 54
Besenhard, J.O.	Session 5-C	P22/EM-14	page 71
Bets, V.V.	Session 7-D	P29/OA-2	page 104
Betsch, Manfred	Session 9-B	P9/OC-11	page 123
Betz, G.	Session 5-A	P9/B-9	page 64
Bhattacharja, Sankar	Session 4-C	P19/P-12	page 55
Bjorkstam, J. L.	Session 1-A	P6/TH-6	page 3
Bjorkstam, J.L.	Session 6-B	P10/AC-17	page 81
Blakanski, M.	Session 7-B	P14/EM-21	page 97

Blender, R.	Session 8-A	P6/TH-34	page 108
Blonsky, P. M.	Session 1-B	P9/P-2	page 5
Boatner, L.A.	Session 4-B	P8/PC-1	page 50
Boehm, H.	Session 4-A	P5/TH-19	page 48
Boehm, H.	Session 6-B	P9/AC-16	page 80
Boilot, J.P.	Session 3-C	P20/NA-6	page 41
Boilot, J.P.	Session 5-D	P29/BA-14	page 75
Boivin, J.C.	Session 2-B	P14/O-6	page 21
Boivin, J.C.	Session 5-B	P14/O-13	page 67
Bonino, F.	Session 4-B	P12/PC-5	page 52
Bonino, F.	Session 4-D	P27/I-6	page 59
Bonnat, M.	Session 8-B	P13/G-27	page 112
Borey, Bruce K.	Session 6-A	P3/TH-24	page 77
Borjesson, L.	Session 6-B	P14/AC-21	page 83
Borjesson, L.	Session 6-C	P18/G-18	page 85
Borjesson, L.	Session 3-A	P3/TH-10	page 32
Borsa, F.	Session 6-C	P19/G-19	page 85
Bose, M.	Session 3-B	P12/AC-12	page 37
Bose, Monisha	Session 2-D	P31/ET-7	page 30
Boughaleb, Y.	Session 4-A	P3/TH-17	page 47
Boukamp, Bernard A.	Session 3-A	P2/TH-9	page 31
Bouridah, A.	Session 4-C	P15/P-8	page 53
Breiter, M.W.	Session 5-D	P28/BA-13	page 74
Bretey, E.	Session 1-D	P24/AC-3	page 12
Brinkmann, D.	Session 6-B	P10/AC-17	page 81
Brinkmann, D.	Session 6-C	P16/G-16	page 84
Brinkmann, D.	Session 9-B	P8/OC-10	page 123
Brodwin, M.E.	Session 3-C	P21/NA-7	page 42
Brown, Scott H.	Session 4-B	P13/PC-6	page 52
Bruce, James A.	Session 3-D	P27/G-13	page 45
Bruce, James A.	Session 6-D	P28/EG-7	page 90
Bruce, P.G.	Session 2-C	P23/EM-7	page 27
Brun, Torben O.	Session 7-B	P13/EM-20	page 96
Bunde, A.	Session 3-A	P4/TH-11	page 32
Bunde, A.	Session 4-A	P2/TH-16	page 47
Bunshah, R.F.	Session 5-C	P20/EM-12	page 70
Burggraaf, A.J.	Session 4-D	P23/I-2	page 57
Burggraaf, A.J.	Session 5-C	P18/EM-10	page 69
Bychkov, E.A.	Session 8-B	P14/G-28	page 113
Bychkov, E.A.	Session 8-D	P26/S-5	page 119
Calame, J. P.	Session 1-B	P8/P-1	page 4
Calame, J.P.	Session 9-A	P2/P-16	page 120
Canfield, S.	Session 7-A	P7/BA-23	page 93
Canova, E.	Session 6-D	P26/EG-5	page 89
Cao, Wun-ying	Session 2-B	P15/O-7	page 22
Carini, G.	Session 8-B	P11/G-25	page 111
Carrillo-Cabrera, Wilder	Session 5-D	P26/BA-11	page 73
Catlow, C.R.A.	Session 1-A	P4/TH-4	page 2
Catlow, C.R.A.	Session 2-B	P13/O-5	page 21
Catlow, C.R.A.	Session 3-A	P5/TH-12	page 33
Catlow, C.R.A.	Session 5-B	P11/O-10	page 65
Catlow, C.R.A.	Session 6-A	P2/TH-23	page 77
Catlow, C.R.A.	Session 7-D	P25/FC-2	page 102
Catlow, C.R.A.	Session 1-D	P26/AC-5	page 13
Catti, M.	Session 4-B	P12/PC-5	page 52
Cava, R.J.	Session 2-C	P24/EM-8	page 26
Cava, R.J.	Session 7-B	P12/EM-19	page 96
Cava, R.J.	Session 9-B	P7/OC-9	page 122

Cazzanelli, E.	Session 2-D	P27/ET-3	page 28
Cazzanelli, Enzo	Session 1-D	P22/AC-1	page 11
Chadwick, A. V.	Session 1-D	P26/AC-5	page 13
Chadwick, A.V.	Session 7-D	P25/FC-2	page 102
Chaklanabish, N.C.	Session 5-A	P4/B-4	page 62
Champarnaud-Mesjard, J.C.	Session 2-B	P14/O-6	page 21
Chandra, S.	Session 6-D	P22/EG-1	page 87
Chandra, s.	Session 4-B	P11/PC-4	page 51
Chen, C.J.	Session 7-B	P11/EM-18	page 95
Chen, Li-quan	Session 7-D	P30/OA-3	page 105
Chen, Li-quan	Session 9-B	P10/OC-12	page 124
Chen, S.	Session 2-A	P4/BA-4	page 16
Chen, S.	Session 7-A	P8/BA-24	page 94
Cheradame, H.	Session 9-A	P1/P-15	page 119
Chiang, C.K.	Session 4-C	P18/P-11	page 55
Chiang, C.K.	Session 4-C	P21/P-14	page 56
Chiodelli, G.	Session 4-C	P16/P-9	page 54
Chiodelli, Gaetano	Session 1-C	P17/G-3	page 9
Chiodelli, Gaetano	Session 3-D	P22/G-8	page 42
Chou, Kuo-chieh	Session 2-D	P32/ET-8	page 30
Chowdari, B.V.R.	Session 1-A	P7/TH-7	page 4
Ciacchi, F.T.	Session 4-D	P22/I-1	page 57
Ciacchi, F.T.	Session 4-D	P28/I-7	page 60
Clausen, K.	Session 9-B	P7/OC-9	page 122
Clearfield, A.	Session 6-B	P11/AC-18	page 81
Collin, G.	Session 3-C	P20/NA-6	page 41
Collin, G.	Session 5-D	P29/BA-14	page 75
Colomban, Ph.	Session 3-C	P20/NA-6	page 41
Colomban, Ph.	Session 5-D	P29/BA-14	page 75
Comes, R.	Session 5-D	P29/BA-14	page 75
Conflant, P.	Session 5-B	P14/O-13	page 67
Cooper, E.I.	Session 6-B	P12/AC-19	page 82
Cormack, A.N.	Session 3-A	P6/TH-13	page 34
Cormack, A.N.	Session 1-A	P4/TH-4	page 2
Croce, F.	Session 5-B	P13/O-12	page 66
Curelaru, Irina M.	Session 8-A	P7/TH-35	page 109
Cutroni, M.	Session 6-C	P15/G-15	page 83
Cutroni, M.	Session 8-B	P11/G-25	page 111
Dai, Sou-yu	Session 9-B	P10/OC-12	page 124
Dalard, F.	Session 4-A	P1/TH-15	page 46
Dalard, F.	Session 4-C	P15/P-8	page 53
Dalba, G.	Session 7-C	P22/ET-14	page 101
Davies, Peter	Session 7-A	P5/BA-21	page 92
Davies, Peter K.	Session 2-A	P7/BA-7	page 18
Davies, Peter K.	Session 6-D	P27/EG-6	page 89
Davies, Peter K.	Session 7-A	P7/BA-23	page 93
Davis, G.T.	Session 4-C	P18/P-11	page 55
Davis, G.T.	Session 4-C	P21/P-14	page 56
DeNuzzio, J.D.	Session 5-D	P30/BA-15	page 75
DeNuzzio, John	Session 5-D	P25/BA-10	page 73
Dejus, R.	Session 6-A	P6/TH-27	page 79
Delmas, C.	Session 3-C	P17/NA-3	page 40
Deroo, D.	Session 4-A	P1/TH-15	page 46
Deroo, D.	Session 4-C	P15/P-8	page 53
Deshpande, V.H.	Session 1-C	P21/G-7	page 11
Deublein Gerhard	Session 6-D	P25/EG-4	page 88
Devaud, M.	Session 1-C	P16/G-2	page 8
Dianoux, A.J.	Session 3-C	P17/NA-3	page 40

Dianoux, A.J.	Session 1-C	P20/G-6	page 10
Dianoux, A.J.	Session 2-A	P3/BA-3	page 16
Dickens, P.G.	Session 2-C	P20/EM-4	page 24
Didisheim, J.J.	Session 3-C	P16/NA-2	page 34
Didisheim, J.J.	Session 8-C	P18/OC-4	page 115
Dieterich, W.	Session 3-A	P4/TH-11	page 32
Dieterich, W.	Session 4-A	P2/TH-16	page 47
Dietrich, W.	Session 8-A	P6/TH-34	page 108
Dirksen, G.J.	Session 9-B	P6/OC-8	page 122
Dou, S.	Session 2-B	P16/O-8	page 22
Dou, Shixue	Session 5-B	P16/O-15	page 68
Druger, Stephen D.	Session 1-A	P3/TH-3	page 2
Dudney, N. J.	Session 1-A	P5/TH-5	page 3
Dunn, B.	Session 2-A	P2/BA-2	page 15
Dunn, B.	Session 5-C	P20/EM-12	page 70
Dunn, B.	Session 5-D	P28/BA-13	page 74
Dunn, B.	Session 7-A	P2/BA-18	page 91
Dupree, R.	Session 9-C	P11/AC-22	page 124
Dye, J.L.	Session 2-C	P24/EM-8	page 26
Dygas, J.R.	Session 3-C	P15/NA-1	page 39
Dygas, J.R.	Session 3-C	P21/NA-7	page 42
Ebbsjoe, I.	Session 4-A	P4/TH-17	page 47
Ebbsjoe, T.	Session 6-A	P6/TH-27	page 79
El-Gemal, M.	Session 9-C	P11/AC-22	page 124
Eriksson, Anders	Session 2-A	P5/BA-5	page 17
Esaka, T.	Session 4-B	P10/PC-3	page 51
Faber, J.	Session 3-C	P15/NA-1	page 39
Faber, Jr. John	Session 7-B	P13/EM-20	page 96
Farrington, G.C.	Session 4-C	P16/P-9	page 54
Farrington, G.C.	Session 5-D	P30/BA-15	page 75
Farrington, G.C.	Session 7-A	P2/BA-18	page 91
Federico, M.	Session 6-C	P15/G-15	page 83
Federico, M.	Session 8-B	P11/G-25	page 111
Feist Thomas	Session 6-D	P27/EG-6	page 89
Ferloni, Paola	Session 1-B	P10/P-3	page 5
Findl, E.	Session 4-B	P9/PC-2	page 50
Fontana, A.	Session 2-D	P27/ET-3	page 28
Fontana, A.	Session 7-C	P22/ET-14	page 101
Fontanella, J.J.	Session 9-A	P2/P-16	page 120
Fontanella, J.J.	Session 1-B	P8/P-1	page 4
Forestier, M.	Session 2-D	P29/ET-5	page 29
Fornasini, P.	Session 7-C	P22/ET-14	page 101
Franceschetti, Donald R.	Session 1-A	P1/TH-1	page 1
Franco, J.I.	Session 5-A	P6/B-6	page 63
Frase, K. G.	Session 2-A	P1/BA-1	page 15
Frech, Roger	Session 1-B	P11/P-4	page 6
Frech, Roger	Session 1-D	P22/AC-1	page 11
Frech, Roger	Session 4-B	P13/PC-6	page 52
Frech, Roger	Session 6-B	P8/AC-15	page 80
Frit, B.	Session 2-B	P14/O-6	page 21
Fritzer, H.P.	Session 8-D	P22/S-1	page 117
Fujiki, Y.	Session 1-D	P25/AC-4	page 13
Fujiki, Y.	Session 2-D	P26/ET-2	page 27
Fujiki, Y.	Session 3-B	P10/AC-10	page 36
Fujitsu, Satoru	Session 8-C	P17/OC-3	page 114
Funke, K.	Session 4-A	P7/TH-21	page 49
Gandini, A.	Session 9-A	P1/P-15	page 119
Garbarczyk, J.	Session 5-D	P27/BA-12	page 74

Garini, G.	Session 6-C	P15/G-15	page 83
Garzon, Fernando	Session 6-D	P27/EG-6	page 89
Gavarri, J.R.	Session 2-A	P3/BA-3	page 16
Glasse, M.D.	Session 5-A	P1/B-1	page 60
Glasse, M.D.	Session 5-A	P8/B-8	page 64
Gobron, T.	Session 8-A	P4/TH-32	page 107
Godshall, Ned A.	Session 2-C	P22/EM-6	page 25
Goge, M.	Session 8-D	P24/S-3	page 118
Goldman, A.I.	Session 6-D	P26/EG-5	page 89
Goodenough, J.B.	Session 2-C	P23/EM-7	page 26
Gopalan, G.P.S.	Session 3-B	P13/AC-13	page 37
Gorecki, W.	Session 4-C	P17/P-10	page 54
Goto, K.S.	Session 5-B	P10/O-9	page 65
Goto, K.S.	Session 8-C	P19/OC-5	page 115
Gouet, M.	Session 8-D	P24/S-3	page 118
Gouyet, J.F.	Session 8-A	P3/TH-31	page 107
Gouyet, J.F.	Session 8-A	P4/TH-32	page 107
Gozzi, D.	Session 4-D	P25/I-4	page 58
Graia, T.	Session 5-B	P14/O-13	page 67
Greaves, C.	Session 2-C	P17/EM-1	page 23
Greaves, G.N.	Session 7-D	P25/FC-2	page 102
Greenbaum, S.G.	Session 9-A	P2/P-16	page 120
Greenblatt, M.	Session 7-B	P11/EM-18	page 95
Gregorkiewicz, M.	Session 3-B	P11/AC-11	page 36
Grins, J.	Session 6-B	P13/AC-20	page 82
Guitton, J.	Session 2-D	P29/ET-5	page 29
Halperin, W.P.	Session 7-A	P4/BA-20	page 92
Hammerberg, J. E.	Session 1-A	P2/TH-2	page 1
Hammou, A.	Session 5-C	P19/EM-11	page 70
Handoune, H.	Session 9-C	P12/AC-23	page 125
Hansen, H.E.	Session 2-D	P30/ET-6	page 29
Harder, H.	Session 4-A	P2/TH-16	page 47
Harding, C.A.	Session 4-C	P18/P-11	page 55
Harding, C.A.	Session 4-C	P21/P-14	page 56
Hardy, L.C.	Session 1-B	P9/P-2	page 5
Hariharan, K.	Session 6-C	P21/G-21	page 86
Harris, Caroline S.	Session 3-A	P7/TH-14	page 34
Harris, Kenneth D.M.	Session 7-B	P9/EM-16	page 94
Hartmann, E.	Session 3-B	P9/AC-9	page 35
Hashmi, S.A.	Session 4-B	P11/PC-4	page 51
Hatzikraniotis, E.	Session 7-B	P14/EM-21	page 97
Hayes, T.G.	Session 5-A	P5/B-5	page 62
Heggestad, K.	Session 8-D	P24/S-3	page 118
Heitjans, Paul	Session 7-C	P19/ET-11	page 99
Hoetzel, H.	Session 8-D	P23/S-2	page 117
Hooper, A.	Session 5-A	P8/B-8	page 64
Horne, Frederick H.	Session 6-A	P3/TH-24	page 77
Houttemane, C.	Session 2-B	P14/O-6	page 21
Hu, Mingfu	Session 8-D	P25/S-4	page 118
Huber, H.	Session 9-B	P8/OC-10	page 123
Hug, R.	Session 4-C	P16/P-9	page 54
Huggins, R.A.	Session 5-C	P23/EM-15	page 72
Huggins, R.A.	Session 7-D	P28/OA-1	page 104
Huggins, Robert A.	Session 6-D	P25/EG-4	page 88
Ikeda, Y.	Session 5-A	P2/B-2	page 61
Inganas, O.	Session 9-A	P3/P-17	page 120
Ingram, Malcolm D.	Session 3-D	P27/G-13	page 45
Ingram, Malcolm D.	Session 6-D	P28/EG-7	page 90

Ishigame, M.	Session 7-C	P18/ET-10	page 99
Ishii, T.	Session 6-A	P7/TH-28	page 79
Ishii, Tadao	Session 6-A	P1/TH-22	page 76
Ito, Yoshiaki	Session 2-B	P10/O-2	page 19
Ito, Yoshiaki	Session 7-D	P24/FC-1	page 102
Ito, Yukio	Session 1-B	P12/P-5	page 6
Ito, Yukio	Session 5-C	P21/EM-13	page 71
Iwahara, H.	Session 2-B	P12/O-4	page 20
Iwahara, H.	Session 4-B	P10/PC-3	page 51
Jacobs, P.W.M.	Session 6-A	P4/TH-25	page 78
Jain, H.	Session 1-C	P18/G-4	page 9
Jakubowski, W.	Session 5-D	P27/BA-12	page 74
Jebbari, S.	Session 9-B	P6/OC-8	page 122
Johnson, W.B.	Session 3-D	P24/G-10	page 44
Joo, S-K.	Session 7-D	P28/OA-1	page 104
Jorgensen, Jens-Erik	Session 7-B	P13/EM-20	page 96
Josowicz, M.	Session 5-C	P22/EM-14	page 71
Jourdaine, L.	Session 8-B	P13/G-27	page 112
Julien, J.	Session 7-B	P14/EM-21	page 97
Kahil, H.	Session 2-D	P29/ET-5	page 29
Kalia, R.K.	Session 4-A	P4/TH-18	page 48
Kanehori, Keiichi	Session 5-C	P21/EM-13	page 71
Kanno, R.	Session 5-A	P2/B-2	page 61
Kao, Y.H.	Session 6-D	P26/EG-5	page 89
Kennedy John, H.	Session 1-C	P19/G-5	page 10
Khandkar, A.C.	Session 6-D	P23/EG-2	page 87
Kilner, J.A.	Session 4-D	P23/I-2	page 57
Kirimo, Fumiyoshi	Session 5-C	P21/EM-13	page 71
Kjems, J.K.	Session 9-B	P7/OC-9	page 122
Kjems, Jorgen	Session 2-A	P5/BA-5	page 17
Knutz, Boye	Session 2-C	P21/EM-5	page 25
Kobayashi, M.	Session 5-B	P10/O-9	page 65
Komenda, P.	Session 5-C	P22/EM-14	page 71
Kone, A.	Session 8-B	P12/G-26	page 112
Koto, Kichiro	Session 2-B	P10/O-2	page 19
Koto, Kichiro	Session 7-D	P24/FC-1	page 102
Koumoto Kunihiro	Session 8-C	P17/OC-3	page 114
Kudo, Tetsuichi	Session 1-B	P12/P-5	page 6
Kulesa, F.	Session 4-B	P9/PC-2	page 50
Kuo, Chu-kun	Session 7-C	P23/ET-15	page 101
Kuo, Chu-kun	Session 8-A	P5/TH-33	page 108
Kuo, Zhuokun	Session 2-B	P9/O-1	page 19
Kutner, R.	Session 8-A	P2/TH-30	page 106
Latham, R.J.	Session 5-A	P1/B-1	page 60
Lazzari, M.	Session 9-A	P5/P-19	page 121
Le Nest, J.F.	Session 9-A	P1/P-15	page 119
Lee, Wing-Kit	Session 4-B	P8/PC-1	page 50
Lewis, J.B.	Session 2-A	P4/BA-4	page 16
Li, Shi-chun	Session 3-B	P14/AC-14	page 38
Li, Xiafei,	Session 2-B	P9/O-1	page 19
Li, Xiang-ting	Session 7-C	P23/ET-15	page 101
Liaw, Boryann	Session 5-C	P23/EM-15	page 72
Lin, Zu-xiang	Session 3-B	P14/AC-14	page 38
Linderoth, S.	Session 2-D	P30/ET-6	page 29
Linford, R.G.	Session 5-A	P1/B-1	page 60
Lingord, R.G.	Session 5-A	P8/B-8	page 64
Listerud, J.	Session 1-A	P6/TH-6	page 3
Liu, Changle	Session 8-B	P10/G-24	page 111

Liu, Q.G.	Session 3-B	P8/AC-8	page 35
Ljungmark, Hakan	Session 1-D	P27/AC-6	page 14
Lucazeau, G.	Session 2-A	P3/BA-3	page 16
Lucazeau, G.	Session 3-C	P17/NA-3	page 40
Lukacevic, E.	Session 7-C	P21/ET-13	page 100
Lumbreras, M.	Session 9-B	P6/OC-8	page 122
Lunden, Arnold	Session 1-D	P27/AC-6	page 14
Lusis, A.R.	Session 7-D	P29/OA-2	page 104
MacDiarmid, A.G.	Session 1-B	P13/P-6	page 7
MacDonaill, D.A.	Session 6-A	P4/TH-25	page 78
Magistris, Aldo	Session 1-B	P10/P-3	page 5
Magistris, Aldo	Session 1-C	P17/G-3	page 9
Maier, Joachim	Session 3-C	P19/NA-5	page 41
Maier, Joachim	Session 8-C	P15/OC-1	page 113
Maiti, H.S.	Session 5-A	P4/B-4	page 62
Mali, M.	Session 4-C	P17/P-10	page 54
Mali, M.	Session 6-B	P10/AC-17	page 81
Mali, M.	Session 6-C	P16/G-16	page 84
Mali, M.	Session 9-B	P8/OC-10	page 123
Malugani, J.P.	Session 1-C	P20/G-6	page 10
Maly-Schreiber, M.	Session 5-D	P28/BA-13	page 74
Mannari, I.	Session 6-A	P7/TH-28	page 79
Mari, C.M.	Session 4-B	P12/PC-5	page 52
Mariotto, G.	Session 2-A	P6/BA-6	page 17
Mariotto, G.	Session 2-D	P27/ET-3	page 28
Mariotto, G.	Session 5-D	P24/BA-9	page 72
Marple, B.	Session 2-B	P16/O-8	page 22
Martin, S.W.	Session 3-A	P3/TH-10	page 32
Martin, Steve W.	Session 6-C	P16/G-16	page 84
Martin, Steve W.	Session 9-C	P13/G-29	page 125
Martin, Steve W.	Session 9-C	P15/G-31	page 126
Mason, David M.	Session 4-D	P24/I-3	page 58
Masson, C.R.	Session 2-B	P16/O-8	page 22
Masson, C.R.	Session 5-B	P16/O-15	page 68
Matsui, Noboru	Session 2-D	P28/ET-4	page 28
Mazzacurati, V.	Session 2-D	P27/ET-3	page 28
Mbaeyi, Peter Nwoye O.	Session 6-A	P5/TH-26	page 78
McGhie, A.R.	Session 4-C	P16/P-9	page 54
McGhie, A.R.	Session 1-B	P13/P-6	page 7
McHale, A.E.	Session 4-D	P23/I-2	page 57
McIntyre, G.	Session 1-D	P26/AC-5	page 13
McIntyre, J.	Session 5-D	P25/BA-10	page 73
McMullan, R.K.	Session 8-C	P18/OC-4	page 115
Mehrotra, G.M.	Session 5-B	P12/O-11	page 66
Meng, Guang-yao	Session 2-B	P15/O-7	page 22
Meng, Guang-yao	Session 5-B	P15/O-14	page 67
Mercier, R.	Session 1-C	P20/G-6	page 10
Mercurio, D.	Session 2-B	P14/O-6	page 21
Miyauchi, Katsuki	Session 1-B	P12/P-5	page 6
Miyauchi, Katsuki	Session 5-C	P21/EM-13	page 71
Montagna, M.	Session 5-D	P24/BA-9	page 72
Montoneri, E.	Session 4-B	P9/PC-2	page 50
Mori, Haruki	Session 2-B	P10/O-2	page 19
Moroney, L.M.	Session 2-B	P13/O-5	page 21
Moroney, L.M.	Session 7-D	P25/FC-2	page 102
Munshi, M.Z.A.	Session 7-A	P1/BA-17	page 90
Munshi, Zafar	Session 7-A	P6/BA-22	page 93
Murch, G.E.	Session 6-A	P2/TH-23	page 77

Murphy, D.W.	Session 2-C	P24/EM-8	page 26
Murphy, D.W.	Session 7-B	P12/EM-19	page 96
Murray, A.D.	Session 6-A	P2/TH-23	page 77
Murugesamoorthi, K.A.	Session 3-D	P28/G-14	page 46
Murugesamoorthi, K.A.	Session 6-C	P21/G-21	page 86
Nagai, Masayuki	Session 3-C	P18/NA-4	page 40
Nagai, Masayuki	Session 7-A	P6/BA-22	page 93
Nagamo, Satoshi	Session 9-A	P4/P-18	page 121
Neat, R.J.	Session 5-A	P8/B-8	page 64
Newton-Howes, J.H.	Session 3-A	P6/TH-13	page 34
Ngai, K.L.	Session 1-C	P18/G-4	page 9
Nguyen, Bang C.	Session 4-D	P24/I-3	page 58
Nicholson, P.S.	Session 7-A	P1/BA-17	page 90
Nicholson, Patrick S.	Session 7-A	P6/BA-22	page 93
Nishino, Tasashi	Session 3-C	P18/NA-4	page 40
Nitzan, A.	Session 1-A	P3/TH-3	page 2
Nitzan, A.	Session 3-A	P1/TH-8	page 31
Nitzan, A.	Session 3-A	P7/TH-14	page 34
Noelting, J.	Session 2-B	P11/O-3	page 20
Nowick, A.S.	Session 4-B	P8/PC-1	page 50
Ogaki, K.	Session 4-B	P10/PC-3	page 51
Ogata, Naoya	Session 9-A	P4/P-18	page 121
Ohachi, T.	Session 1-D	P25/AC-4	page 13
Ohachi, T.	Session 2-D	P26/ET-2	page 27
Ohachi, Tadashi	Session 7-D	P24/FC-1	page 102
Onoda, Y.	Session 1-D	P25/AC-4	page 13
Onoda, Y.	Session 2-D	P26/ET-2	page 27
Onoda, Y.	Session 3-B	P10/AC-10	page 36
Otsuka, N.	Session 7-A	P8/BA-24	page 94
Oumari, J.	Session 5-C	P19/EM-11	page 70
Ouwerkerk, M.	Session 7-C	P20/ET-12	page 100
Owen, J.R.	Session 5-A	P3/B-3	page 61
Pacey, P.D.	Session 2-B	P16/O-8	page 22
Pacey, P.D.	Session 5-B	P16/O-15	page 68
Pasinetti, R.	Session 4-B	P12/PC-5	page 52
Patrick, A.J.	Session 5-A	P1/B-1	page 60
Paxinos, A.	Session 5-C	P22/EM-14	page 71
Pechenik, A.	Session 3-D	P26/G-12	page 45
Pechenik, A.	Session 8-B	P9/G-23	page 110
Pedone, D.	Session 4-A	P1/TH-15	page 46
Peng, Ding-kun	Session 2-B	P15/O-7	page 22
Peng, Ding-kun	Session 5-B	P15/O-14	page 67
Pentyush, E.V.	Session 7-D	P29/OA-2	page 104
Perissinotti, L.	Session 5-A	P6/B-6	page 63
Petersen, K.	Session 2-D	P30/ET-6	page 29
Petford, Amanda	Session 2-A	P5/BA-5	page 17
Petrucci, L.	Session 4-D	P25/I-4	page 58
Pezzati, Elisabetta	Session 6-C	P17/G-17	page 84
Pfeiffer G.	Session 7-A	P7/BA-23	page 93
Phipps, J.B.	Session 5-A	P5/B-5	page 62
Phipps, J.B.	Session 6-B	P10/AC-17	page 81
Picciotto De, L.A.	Session 2-C	P19/EM-3	page 24
Pintard-Screpel, M.	Session 1-D	P24/AC-3	page 12
Pizzini, S.	Session 4-B	P12/PC-5	page 52
Pradel, Annie	Session 1-C	P15/G-1	page 8
Prieur, J.-Y.	Session 1-C	P16/G-2	page 8
Prince, E.	Session 3-C	P16/NA-2	page 39
Protas, J.	Session 9-B	P6/OC-8	page 122

Radhakrishma, S.	Session 6-C	P21/G-21	page 86
Radhakrishna, S.	Session 3-D	P28/G-14	page 46
Raistrick, I.D.	Session 7-D	P28/OA-1	page 104
Raistrick, Ian D.	Session 5-C	P23/EM-15	page 72
Ratner, M.A.	Session 3-A	P1/TH-8	page 31
Ratner, M.A.	Session 3-D	P26/G-12	page 45
Ratner, M.A.	Session 4-A	P3/TH-17	page 47
Ratner, M.A.	Session 8-B	P9/G-23	page 110
Ratner, Mark A.	Session 1-A	P3/TH-3	page 2
Ratner, Mark A.	Session 3-A	P7/TH-14	page 34
Reddy, K. Narasimha	Session 7-D	P26/FC-3	page 103
Redman, William A.	Session 6-B	P8/AC-15	page 80
Rhyne, K.	Session 2-C	P24/EM-8	page 26
Ribes, Michel	Session 1-C	P15/G-1	page 8
Ricken, M.	Session 2-B	P11/O-3	page 20
Rickert, Hans	Session 9-B	P9/OC-11	page 123
Riess, I.	Session 4-A	P7/TH-21	page 49
Rietman, E.A.	Session 9-B	P7/OC-9	page 122
Robinson, W. R.	Session 2-A	P4/BA-4	page 16
Rocca, F.	Session 2-D	P27/ET-3	page 28
Rocca, F.	Session 7-C	P22/ET-14	page 101
Rogers, Michael D.	Session 7-B	P9/EM-16	page 94
Rokade, S.	Session 1-C	P21/G-7	page 11
Roman, E.	Session 3-A	P4/TH-11	page 32
Roos, J.	Session 4-C	P17/P-10	page 54
Roos, J.	Session 6-B	P10/AC-17	page 81
Roos, J.	Session 6-C	P16/G-16	page 84
Roos, J.	Session 9-B	P8/OC-10	page 123
Rosenberg, R.O.	Session 3-A	P1/TH-8	page 31
Rossi, F.	Session 5-D	P24/BA-9	page 72
Rosso, M.	Session 8-A	P3/TH-31	page 107
Roth, G.	Session 4-A	P5/TH-19	page 48
Roth, G.	Session 6-B	P9/AC-16	page 80
Roth, R.S.	Session 2-C	P24/EM-8	page 26
Roth, R.S.	Session 7-B	P12/EM-19	page 96
Roth, R.S.	Session 7-C	P21/ET-13	page 100
Roth, R.S.	Session 2-A	P1/BA-1	page 15
Roth, W.L.	Session 6-D	P26/EG-5	page 89
Roth, W.L.	Session 2-A	P2/BA-2	page 15
Rudkin, R.D.	Session 5-A	P3/B-3	page 61
Ruocco, G.	Session 2-D	P27/ET-3	page 28
Sahami, Saeed	Session 1-C	P19/G-5	page 10
Salzano, F.J.	Session 4-B	P9/PC-2	page 50
Sanesi, Manlio	Session 1-B	P10/P-3	page 5
Sankararaman, M.	Session 2-A	P4/BA-4	page 16
Santoro, A.	Session 2-A	P1/BA-1	page 15
Santoro, A.	Session 5-B	P11/O-10	page 65
Santoro, A.	Session 7-B	P12/EM-19	page 96
Santoro, A.	Session 7-C	P21/ET-13	page 100
Sanui, Kohei	Session 9-A	P4/P-18	page 121
Sapoval, B.	Session 8-A	P3/TH-31	page 107
Sato, H.	Session 2-A	P4/BA-4	page 16
Sato, H.	Session 4-A	P6/TH-20	page 49
Sato, H.	Session 7-A	P8/BA-24	page 94
Sayer, M.	Session 7-A	P1/BA-17	page 90
Sayer, Michael	Session 7-A	P6/BA-22	page 93
Schiraldi, Alberto	Session 6-C	P17/G-17	page 84
Schleitzweiler, P.M.	Session 3-D	P24/G-10	page 44

Schoch, B.	Session 3-B	P9/AC-9	page 35
Schooman, J.	Session 9-B	P6/OC-8	page 122
Schoonman, J.	Session 7-C	P20/ET-12	page 100
Schouler, E.J.L.	Session 2-D	P29/ET-5	page 29
Schouler, E.J.L.	Session 5-C	P19/EM-11	page 70
Schouler, E.J.L.	Session 9-C	P12/AC-23	page 125
Scrosati, B.	Session 4-D	P27/I-6	page 59
Scrosati, B.	Session 9-A	P5/P-19	page 121
Seleznev, B.L.	Session 8-B	P14/G-28	page 113
Sen, B.K.	Session 4-B	P14/PC-7	page 53
Sen, S.	Session 4-B	P14/PC-7	page 53
Senapati, Hemlata	Session 6-C	P20/G-20	page 86
Sequeira, C.A.C.	Session 7-B	P10/EM-17	page 95
Sequeira, Cesar	Session 4-C	P20/P-13	page 56
Shahi, K.	Session 3-B	P13/AC-13	page 37
Shakushiro, Kiyooki	Session 1-B	P12/P-5	page 6
Shea, Steven W.	Session 1-C	P19/G-5	page 10
Shibata, Y.	Session 3-B	P10/AC-10	page 36
Shinar, J.	Session 7-C	P17/ET-9	page 98
Shishkin, A.	Session 2-D	P30/ET-6	page 29
Shriver, D. F.	Session 1-B	P9/P-2	page 5
Shriver, D.F.	Session 3-A	P7/TH-14	page 34
Signorelli, G.	Session 2-D	P27/ET-3	page 28
Silver, B.L.	Session 7-C	P17/ET-9	page 98
Singh, B.	Session 6-D	P22/EG-1	page 87
Singh, Govind	Session 7-A	P6/BA-22	page 93
Singh, K.	Session 1-C	P21/G-7	page 11
Singh, N.	Session 6-D	P22/EG-1	page 87
Sisko, J.	Session 1-B	P9/P-2	page 5
Sitte, W.	Session 8-D	P22/S-1	page 117
Skaarup, S.	Session 2-D	P30/ET-6	page 29
Skaarup, Steen	Session 2-C	P21/EM-5	page 25
Skarstad, P.M.	Session 5-A	P5/B-5	page 62
Skarstad, P.M.	Session 6-B	P10/AC-17	page 81
Skotheim, T.A.	Session 9-A	P3/P-17	page 120
Skou, Eivind	Session 8-C	P20/OC-6	page 116
Smith, M.K.	Session 9-A	P2/P-16	page 120
Smith, M.K.	Session 1-B	P8/P-1	page 4
Smoot, S.W.	Session 4-C	P19/P-12	page 55
Smoot, S.W.	Session 7-A	P4/BA-20	page 92
Somasiri, N.L.D.	Session 1-B	P13/P-6	page 7
Sood, D.K.	Session 4-D	P22/I-1	page 57
Souquet, J.L.	Session 8-B	P12/G-26	page 112
Souquet, J.L.	Session 8-B	P13/G-27	page 112
Speed, A.M.	Session 2-C	P17/EM-1	page 23
Stafsudd, O.M.	Session 7-A	P2/BA-18	page 91
Staikov, G.	Session 2-A	P8/BA-8	page 18
Stancovschi, Victor	Session 5-D	P31/BA-16	page 76
Steele, B.C.H.	Session 4-D	P23/I-2	page 57
Steele, B.C.H.	Session 5-A	P3/B-3	page 61
Steele, B.C.H.	Session 5-B	P11/O-10	page 65
Subramanian, M.A.	Session 6-B	P11/AC-18	page 81
Subramanian, R.	Session 6-B	P11/AC-18	page 81
Suemoto, T.	Session 3-B	P10/AC-10	page 36
Sunandana, C.S.	Session 8-C	P16/OC-2	page 114
Sundar, H.G.K.	Session 8-B	P8/G-22	page 110
Suominen, Eero	Session 8-A	P7/TH-35	page 109
Susman, S.	Session 3-D	P26/G-12	page 45

Susman, S.	Session 8-B	P9/G-23	page 110
Susman, Sherman	Session 7-B	P13/EM-20	page 96
Suzuki, A.	Session 4-A	P6/TH-20	page 49
Suzuki, S.	Session 2-B	P12/O-4	page 20
Suzuki, S.	Session 3-B	P10/AC-10	page 36
Suzuki, S.	Session 7-C	P18/ET-10	page 99
Tachez, M.	Session 1-C	P20/G-6	page 10
Tairi, A.	Session 2-B	P14/O-6	page 21
Takahashi, K.	Session 6-A	P6/TH-27	page 79
Takahashi, T.	Session 4-C	P18/P-11	page 55
Takahashi, Toru	Session 4-C	P21/P-14	page 56
Takeda, Y.	Session 5-A	P2/B-2	page 61
Tanaka, M.	Session 2-B	P12/O-4	page 20
Tanaka, M.	Session 3-B	P10/AC-10	page 36
Tanaka, M.	Session 7-C	P18/ET-10	page 99
Taniguchi, I.	Session 1-D	P25/AC-4	page 13
Taniguchi, I.	Session 2-D	P26/ET-2	page 27
Tannhauser, D.S.	Session 7-C	P17/ET-9	page 98
Tarascon, J.M.	Session 2-C	P18/EM-2	page 23
Tarascon, J.M.	Session 5-C	P17/EM-9	page 69
Tare, V.B.	Session 5-B	P12/O-11	page 66
Teeters, Dale	Session 1-B	P11/P-4	page 6
Tegenfeldt, J.	Session 5-D	P30/BA-15	page 75
Terekhov, V.I.	Session 7-B	P15/EM-22	page 97
Thackeray, M.M.	Session 2-C	P19/EM-3	page 24
Thomas, D.	Session 2-B	P14/O-6	page 21
Thomas, D.	Session 5-B	P14/O-13	page 67
Thomas, John O.	Session 2-A	P5/BA-5	page 17
Thomas, John O.	Session 5-D	P25/BA-10	page 73
Thomas, John O.	Session 7-A	P5/BA-21	page 92
Thomas, M.A.	Session 2-C	P17/EM-1	page 23
Thomas, M.G.S.R.	Session 2-C	P23/EM-7	page 26
Tian, Shun-bao	Session 3-B	P14/AC-14	page 38
Tinglian, Wen	Session 2-B	P9/O-1	page 19
Tolpadi, S.K.	Session 4-B	P11/PC-4	page 51
Tomellini, M.	Session 4-D	P25/I-4	page 58
Tomozawa, M.	Session 3-D	P25/G-11	page 44
Torell, L.	Session 3-A	P3/TH-10	page 32
Torell, L.M.	Session 6-B	P14/AC-21	page 83
Torell, L.M.	Session 6-C	P18/G-18	page 85
Torgenson, D.	Session 3-B	P12/AC-12	page 37
Tran Qui, D.	Session 9-C	P12/AC-23	page 125
Tributsch, H.	Session 5-A	P9/B-9	page 64
Tripodo, G.	Session 6-C	P15/G-15	page 83
Tripodo, G.	Session 8-B	P11/G-25	page 111
Tuller, Harry L	Session 3-D	P23/G-9	page 43
Tung, Ting	Session 8-D	P25/S-4	page 118
Uchida, H.	Session 4-B	P10/PC-3	page 51
Unterekar, D.F.	Session 5-A	P5/B-5	page 62
Vashishta, P.	Session 4-A	P4/TH-18	page 48
Vashishta, P.	Session 6-A	P6/TH-27	page 79
Veldkamp, F.F.	Session 7-C	P20/ET-12	page 100
Villa, M.	Session 1-A	P6/TH-6	page 3
Villa, Marco	Session 3-D	P22/G-8	page 42
Villa, Marco	Session 1-C	P17/G-3	page 9
Vincent, Colin A.	Session 7-B	P9/EM-16	page 94
Vlasov, Yu. G.	Session 8-B	P14/G-28	page 113
Vlasov, Yu. G.	Session 8-D	P26/S-5	page 119

Volin, Kenneth J.	Session 7-B	P13/EM-20	page 96
Vourlis, H.	Session 5-A	P7/B-7	page 63
Wada, K.	Session 4-A	P6/TH-20	page 49
Wagner Rainer	Session 9-B	P9/OC-11	page 123
Wagner, Jr., J.B.	Session 5-B	P12/O-11	page 66
Wagner, Jr., J.B.	Session 6-D	P23/EG-2	page 87
Wallace, W. D.	Session 1-C	P16/G-2	page 8
Walsoec de Reca, N.W.	Session 5-A	P6/B-6	page 63
Wang, J. C.	Session 1-A	P5/TH-5	page 3
Wang, J.C.	Session 4-D	P26/I-5	page 59
Wang, J.C.	Session 8-A	P1/TH-29	page 106
Wang, Nanmeng	Session 7-B	P16/EM-23	page 98
Wang, Shu Yun	Session 7-D	P31/OA-4	page 105
Warhus, Udo	Session 3-C	P19/NA-5	page 41
Wasiucioneck, M.	Session 5-D	P27/BA-12	page 74
Watanabe, M.	Session 1-D	P25/AC-4	page 13
Watanabe, Masayoshi	Session 9-A	P4/P-18	page 121
Wei, Shoukun	Session 8-D	P25/S-4	page 118
Weller, M.T.	Session 2-C	P20/EM-4	page 24
Weppner, W.	Session 2-B	P9/O-1	page 19
Weppner, W.	Session 3-B	P9/AC-9	page 35
Weppner, W.	Session 8-D	P23/S-2	page 117
Weppner, Werner	Session 2-D	P25/ET-1	page 27
West, A.R.	Session 6-D	P24/EG-3	page 88
White, D.R.	Session 2-A	P4/BA-4	page 16
Whitmore, D.B.	Session 3-C	P15/NA-1	page 39
Whitmore, D.H.	Session 4-C	P19/P-12	page 55
Whitmore, D.H.	Session 7-A	P4/BA-20	page 92
Whitmore, D.W.	Session 3-D	P26/G-12	page 45
Whitmore, D.W.	Session 8-B	P9/G-23	page 110
Wintersgill, M.C.	Session 9-A	P2/P-16	page 120
Wintersgill, M.C.	Session 1-B	P8/P-1	page 4
Wolf, M.L.	Session 3-A	P5/TH-12	page 33
Wong, R.	Session 2-A	P2/BA-2	page 15
Wong, R.	Session 6-D	P26/EG-5	page 89
Worrell, W.L.	Session 3-B	P8/AC-8	page 35
Wuensch, B.J.	Session 3-C	P16/NA-2	page 39
Wuensch, B.J.	Session 8-C	P18/OC-4	page 115
Xue, Rong-jian	Session 7-D	P30/OA-3	page 105
Yahag, M.	Session 8-C	P19/OC-5	page 115
Yamamoto, O.	Session 5-A	P2/B-2	page 61
Yamashita, Kimihiro	Session 7-A	P6/BA-22	page 93
Yamauchi, T.	Session 4-B	P10/PC-3	page 51
Yan, Yi-min	Session 8-A	P5/TH-33	page 108
Yanagida, Hiroaki	Session 8-C	P17/OC-3	page 114
Yang, L.L.	Session 4-C	P16/P-9	page 54
Yang, Yuan	Session 1-D	P28/AC-7	page 14
Yoshikado, S.	Session 1-D	P25/AC-4	page 13
Yoshikado, S.	Session 2-D	P26/ET-2	page 27
Yoshikado, Shinzo	Session 7-D	P24/FC-1	page 102
Yoshimura Masahiro	Session 7-D	P27/FC-4	page 103
Yu, Hui-jin	Session 3-B	P14/AC-14	page 38
Yu, Wen-hai	Session 1-D	P28/AC-7	page 14
Yu, Wen-hai	Session 8-C	P21/OC-7	page 116
Yushina, L.D.	Session 7-B	P15/EM-22	page 97
Zaharescu, Maria	Session 5-D	P31/BA-16	page 76
Zahurak, S.M.	Session 2-C	P24/EM-8	page 26
Zang, Shengbi	Session 8-D	P25/S-4	page 118

Zehnder, D.A.	Session 5-C	P20/EM-12	page 70
Zhang, Li Wei	Session 5-B	P10/O-9	page 65
Zhang, Li Wei	Session 8-C	P19/OC-5	page 115
Zhang, Z.	Session 1-C	P19/G-5	page 10
Zhao, Zong-quan	Session 9-B	P10/OC-12	page 124
Zheng, Qing	Session 8-C	P21/OC-7	page 116
Zhou, Ming	Session 5-B	P15/O-14	page 67
d' Yvoire, F.	Session 1-D	P24/AC-3	page 12
de Leeuw, S.W.	Session 4-A	P4/TH-18	page 48
de Vries, K.J.	Session 5-C	P18/EM-10	page 69
van Beijeren, H.	Session 8-A	P2/TH-30	page 106
van Dijk, M.P.	Session 5-C	P18/EM-10	page 69
van Hemert, M.	Session 4-D	P23/I-2	page 57

This report was done with support from the Department of Energy. Any conclusions or opinions expressed in this report represent solely those of the author(s) and not necessarily those of The Regents of the University of California, the Lawrence Berkeley Laboratory or the Department of Energy.

Reference to a company or product name does not imply approval or recommendation of the product by the University of California or the U.S. Department of Energy to the exclusion of others that may be suitable.

TECHNICAL INFORMATION DEPARTMENT
LAWRENCE BERKELEY LABORATORY
UNIVERSITY OF CALIFORNIA
BERKELEY, CALIFORNIA 94720